DOI: 10.2478/v10208-011-0014-4

Bakkestuen, V., Aarrestad, P.A., Stabbetorp, O.E., Erikstad, L. & Eilertsen, O. 2010. Vegetation composition, gradients and environment relationships of birch forest in six reference areas in Norway. - Sommerfeltia 34: 1-223. Oslo. ISBN 82-7420-048-9. ISSN 0800-6865.

Terrestrial Monitoring of boreal birch forest ecosystems (TOV) was initiated in 1989 by the Directorate for Nature Management. The programme has a multidisciplinary approach and integrates studies of precipitation, soil water, soil, understorey vegetation composition, lichens on birch trunks, population studies of birds and mammals and environmental pollutants in plants and animals. Here we present studies of forest floor vegetation at establishment, which supplements and complements two studies established in boreal coniferous forests in 1988: 'The effect of acid precipitation on forest and forest understorey vegetation in Gjerstad, South Norway' and 'Vegetational and environmental monitoring of boreal spruce forest in ten reference areas', the latter initiated by the Norwegian Institute of Land Inventory (NIJOS) as part of a forest health monitoring programme.

The reference areas were selected to span regional gradients in climatic conditions and deposition of airborne pollutants, in old-growth bilberry-dominated birch forest in Norway. Ten macro plots in each reference area were located to span differences in nutrient and soil moisture conditions, terrain features, etc. by a sampling design similar to the one used in coniferous forests. Fifty 1×1 m meso sample plots, randomly chosen within the ten macro plots, were subjected to vegetation analysis, using frequency in subplots as well as percent cover as species abundance measures.

The main vegetational gradients were found by parallel use of DCA and GNMDS ordination methods; the results of which were subjected to environmental interpretation by means of non-parametric correlation and split-plot GLM analyses. Both ordination methods gave to large degree similar, interpretable, vegetation gradients. The most important ecoclines were related to variation in nutrient conditions, best expressed by pH, Ca, K and S. Tree influence, topographic (un)favourability, soil moisture and soil depth were other factors which were correlated with one of the two main vegetation gradients (ecoclines).

The main vegetational gradients and environmental/climatic/geographical complex gradients in the total data set were found by DCA and subsequent interpretation of the axes. The main complex gradient corresponded to the variation in the vegetation from sites with low pH and low content of nutrients (low concentrations of macro nutrients like C, Ca, Mn, S and Total N) and high loss on ignition to vice versa. The second gradient corresponded to variation in the vegetation from sites with high effective temperature sums at low latitudes and high soil concentrations of Mn and S, to sites with opposite characteristics. Most of the variation (> 80%) in the vegetation compositions could be ascribed to the between macro plots scale level, leaving a small residual variation on the between area and in the plots within macro plot scale level.

Keywords: *Betula*; Biodiversity; Boreal birch forest; Bryophyte; Climate; DCA; Ecology; Environment, Gradient; Lichens; Monitoring; Norway; Ordination; PCA; Permanent plots; Vascular plants; Vegetation.

Vegar Bakkestuen. Dept. of Botany, Natural History Museum, University of Oslo, P.O. Box 1172 Blindern, NO–0318 Oslo, Norway.

Vegar Bakkestuen, Odd Egil Stabbetorp and Lars Erikstad. Norwegian Institute for Nature Research, Gaustadalléen 21, NO-0349 Oslo, Norway.

Per Arild Aarrestad. Norwegian Institute for Nature Research, Tungasletta 2, NO-7485 Trondheim, Norway.

Odd Eilertsen, Norwegian Forest and Landscape Institute, Postboks 115, NO-1431 Ås.

INTRODUCTION

Acid rain has been one of the major impact factors on the South Norwegian environment since the 1970s (Anonymous 2006). The problem has for a large part been linked to deposition of long distance airborne sulphur, to which areas in south-western Norway dominated by Precambrian rocks with low buffer capacity have been regarded as the most vulnerable. In the 1970s and 1980s the main focus was on freshwater systems and fish populations, but concern for terrestrial systems originated soon after. In later years, airborne sulphur pollution has declined and some improvement of the environmental status has been reported for Norwegian ecosystems (http://www.miljostatus.no).

There has been an ongoing discussion regarding what impact acid rain has had on understorey vegetation and soil conditions. Possible damages to forest vegetation were first addressed around 1985 when vegetation changes that might be related to 'acid rain' were first recorded (Wittig & Neite 1985, Falkengren-Grerup 1986). As a response to this, several Norwegian projects were initiated with the aim to study possible changes in forest floor vegetation composition and chemical variables, like OPS (*'Overvåkingsprogram for skogskader',* [Norwegian monitoring programme for forest damage]) (Hylen & Larsson 2007) and ICP Forest (Intensive forest monitoring) (Andreassen et al. 2006). The first projects addressing ground vegetation in Norwegian boreal forests were 'The effect of acid precipitation on forest and forest understorey vegetation in Gjerstad, South Norway' (R. Økland & Eilertsen 1993) and 'Vegetational and environmental monitoring of boreal spruce forest' (T. Økland 1996). These monitoring projects were both initiated in 1988 and are still running (Framstad 2008).

The main methodological framework for vegetation monitoring in Norway (Lawesson et al. 2000) and also for this study (see Bakkestuen & Erikstad 2002) was established during the initial phases of ground vegetation monitoring. The framework was designed for early detection of vegetation changes related to long-distance airborne pollutants and other broad-scale impact factors, such as climatic change. A few important success factors were assumed to be: (1) Selection of reference areas that were minimally influenced by successions after local disturbances, e.g. wildfire, previous timber harvests and burn-and-slash cultivation. Such successions tend to obscure changes due to regional impact factors such as deposited airborne pollutants and climatic change. (2) Establishment of plots in each reference area along the main local complex gradients in a standardized way that ensured a comparable range of variation due to local environmental factors to be included from all areas. (3) Comprehensive sampling of environmental variables that in some way might have an effect on the species composition (R. Økland 1990). In practice collection of environmental variables was restricted to measurements of chemical characteristics in soil, e.g. organic matter content (humus) and chemical properties such as pH, C, N and exchangeable cations and physical characteristics such as relative elevation, soil depth, inclination, slope etc. Furthermore, data on biological characteristics such as e.g. the cover of different vegetation layers and species richness of different groups were also collected. (4) Use of two different species abundance measurements, subplot frequency and percentage cover, which ensured that demands for observer independence were fulfilled (by the subplot frequency method) while at the same time facilitating detection of temporal changes for frequent species (with high subplot frequency; see Aarrestad et al. 2008). (5) A sampling scheme that facilitated analysis of univariate as well as multivariate patterns of change. (6) Supplementary plant demography studies conducted in permanent vegetation plots, e.g. a parallel demography study (see R. Økland 1995, 2000).

The monitoring project 'TOV' (terrestrial monitoring) was initiated one year after the corresponding activities in boreal coniferous forests, i.e. in 1989, with focus on birch forest ecosystems as a supplement to the two monitoring programmes in coniferous forests (Løbersli 1989). Unlike the coniferous forest investigations, TOV is a larger multidisciplinary project that integrates studies of precipitation, soil water, soil chemical and physical properties, ground vegetation species composition, lichens on birch trunks, population studies of birds and mammals, and direct monitoring of environmental pollutants in plants and animals, into one monitoring approach.

Six reference areas for intensive monitoring of ground vegetation in birch forest were established between 1990 and 1993 (five of these in mountain birch forests). The first four reference areas, established in 1990–1992, were designed to cover a small part of the local floristic variation in the vegetation. Only species-poor bilberry-dominated birch forests sites were included, and the vegetation gradients identified by ordination methods were accordingly short in terms of compositional turnover (Brattbakk et al. 1991, 1992, Brattbakk 1993). However, the first results from the boreal coniferous forests monitoring projects indicated that changes due to airborne pollutants mainly occurred in more species-rich bilberry-dominated vegetation types (R. Økland 1994). It was thus decided to change the design of birch forest monitoring to cover roughly the same amount of variation in vegetation and environmental factors as in coniferous forests (i.e. include variation along a nutrient gradient from oligotrophic to medium eutrophic vegetation and a soil moisture gradient from dry to moist soil), and hence to make adjustments to the sampling design of the first four reference areas. The two areas established in 1993 were established according to the new protocol. The three long-term monitoring studies in Norwegian boreal forests were then thus methodologically co-ordinated with respect to: (1) the range of within-area environmental conditions sampled; (2) selection of areas with few and/or small signs of human-induced successions; (3) plot size; (4) interval between re-analyses; (5) species abundance measures; (6) environmental variables recorded at the start; and (7) analysis of vegetation-environment relationships at establishment (see T. Økland et al. 2001, 2004).The focus of this publication is to present the results of the baseline investigations of vegetation-environment relationships in the six reference areas after adjustment of methodology in 1993, i.e. results of field work performed in the period 1993–1997.

Even if TOV, as well as the two sister projects in coniferous forests, as a monitoring program, was basically designed to reveal effects of acid rain, the design and the long duration of the program underpins it importance in a more general monitoring context. In addition, the results from these studies have contributed, and will continue to contribute to increased understanding of the most important structuring processes in boreal forests (R. Økland & Eilertsen 1993, T. Økland 1996). The sub-alpine vegetation types between the boreal spruce forest and the alpine region have a considerable vertical distribution in Fennoscandia (Hämet-Ahti 1963, Wielgolaski 1997), and they are considered to be of great importance for biodiversity with high conservation value (Odland et al. 1992). It is a national task for Norway, due to its geographical position, to monitor the eventual change of these ecosystems, which are unique in a European context. The last years focus on biodiversity and climate change issues makes these birch forest investigations even more interesting because the monitoring concept makes it possible to study possible changes in amount and cover of field- and ground layer species along the zonal and sectional (i.e. regional) gradients (see Moen 1999).

The aims of this study is to identify variation in ground vegetation composition (‘ecoclines’) in six birch forests in Norway by use of multivariate statistical methods; and to interpret these ecoclines in terms of environmental variation. These two aims serve the main objective to understand the vegetation-environment relationships of boreal birch forests. This knowledge will be foundation for interpretation of eventually vegetation changes in the ongoing monitoring project.

THE STUDY AREAS

The six reference areas for monitoring boreal birch forest vegetation in Norway are Lund, Møsvatn, Gutulia, Åmotsdalen, Børgefjell and Dividalen, listed from south to north in Norway (Fig. 1 and Table 1). They were all located in areas protected by law (except Lund). The areas were selected in order to span the gradient in deposition of long-range transboundary air pollutants from south-southwest to the north of the country. The six areas cover the main climatic and geographical variation of (middle) and north boreal birch forest in Norway. Most of the reference areas are situated in forests developed by natural regeneration with minor human influence ('naturskog' according to Rolstad et al. 2002). However, grazing pressure by sheep and domestic reindeer have, in some areas, brought about vegetation changes in direction of semi-natural vegetation. The reference areas comprise a comparable range of variation in natural vegetation, e.g. lichen-dominated, bilberry dominated, small fern and tall herb dominated vegetation, related to local variation in soil moisture and soil richness.

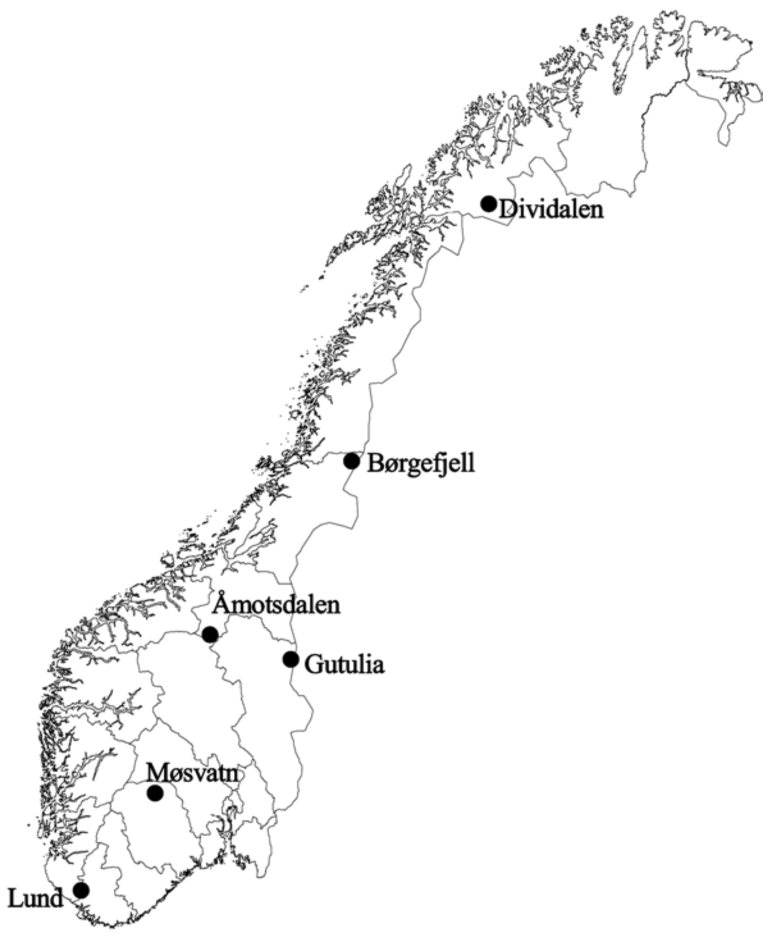

Fig. 1. Map of Norway showing the localisation of the 6 monitoring reference areas.

Tab 1. Monitoring areas: geographical position, climate and background information. UTM (Universal Transverse Mercator) is according to the World Geodetic System (WGS84). The monitoring areas of Lund, Møsvatn and Åmotsdalen belong to zone 32W, Gutulia and Børgefjell belong to 33W and Dividalen is situated in zone 34W. Vegetation zones, sections and terminology are according to Moen (1999). Mean annual precipitation is estimated from 1961–90 normals (Førland 1993) for stations close to each study area, also taking topographic position and altitude (cf. Sjørs 1948, Førland 1979) into account. Temperature is based upon 1961–90 normals (Aune 1993) for stations close to each area, adjusted for altitude according to Laaksonen (1976). * refers to month with lowest mean normal temperature 1961–90 (January in most cases, occasionally February).

Reference area	County	Munici-pality	Lat. (EN)	Long. (EE)	UTM grid reference	Vegetation zone	Vegetation section	Altitude (m)	Area (km^2)	Annual precipi-tation (mm)	Temperature			First ana-lyzed (year)
											Year	Jan.*	Jul.	
Lund	Rogaland	Lund	58°33′	6°26′	LK 50,92	Middle Boreal	Western (O2)	350–420	0.1	2100	6.4	–1.1	14.7	1996
Møsvatn	Telemark	Tinn	59°51–52′	8°17′	MM 60,35	Northern Boreal	Slightly western (O1)	1000–1050	0.3	810	0.8	–8.4	11.4	1997
Gutulia	Hedmark	Engerdal	62°01–03′	12°09–11′	UJ 48–53,80–87	Northern Boreal	Transitional (OC)	770–865	5	700	–0.3	–12.0	11.4	1993
Åmotsdalen	Sør-Trøndelag	Oppdal	62°28′	9°28′	NQ 21–23,25–27	Northern Boreal	Transitional (OC)	900–925	1	500	0.7	–8.0	10.5	1996
Børgefjell	Nord-Trøndelag	Røyrvik	65°01–7′	12°44–56′	VN 44–45,15	Northern Boreal	Slightly western (O1)	520–580	0.8	1100	1.4	–8.3	12.1	1995
Dividalen	Troms	Målselv	68°40–45′	19°36–49′	DB 50–51,22	Northern Boreal	Kontinental (C)	385–615	2	300	0.8	–9.4	12.8	1993

The reference area in Børgefjell was established in 1990 (Brattbakk et al. 1991) and methodically revised in 1995 (Eilertsen & Stabbetorp 1997). Lund was established in 1991 (Brattbakk et al. 1992) and the sampling revised in 1996 (Stabbetorp et al. 1999). Åmotsdalen was established in 1991 (Brattbakk et al. 1992), revised in 1994/96 (Bakkestuen et al. 1999a). Møsvatn was established in 1992 (Brattbakk 1993) and revised in 1994/97 (Bakkestuen et al. 1999b). Gutulia and Dividalen were established in 1993 (Eilertsen & Often 1994, Eilertsen & Brattbakk 1994).

GEOLOGY

Precambrian bedrock dominates in all reference areas, however, to variable extents influenced by tectonic movements and metamorphosis linked to the Caledonian mountain formations (Sigmond et al. 1984).

In the Lund area the bedrock consists of gneiss rich in biotite (mica), which give rise to soils relatively poor in mineral nutrients, while the bedrock in the Møsvatn area consists of metarhyolite and metamorphic tuffs belonging to the Rjukan group, which give rise to soils slightly richer in mineral nutrients (Dons & Jorde 1978, Dons et al. 1990).

In Åmotsdalen the Precambrian rocks consist of metamorphic shales rich in quartzitic and granitic materials, feldspar and with elements of deformed basal conglomerates (Krill 1987). The bedrock of Gutulia belongs to the Kvitvola nappe unit (Nystuen & Trømborg 1972, Nystuen 1979), which consists of deformed and metamorphic sandstones rich in quartz and feldspar, normally producing nutrient poor soils. Locally more mica-rich rocks outcrops give rise.to soils somewhat richer in mineral nutrients.

In the Børgefjell area the bedrock is dominated by granites and granitic gneisses poor in mineral nutrients, but with some gneisses richer in feldspar minerals. The investigation area in Dividalen has a higher geodiversity, situated on three main geological units (Osland 1974). The lowest lying part consists of an autochtonous, locally metamorphic granite or granitic gneiss with veins of dark mica and amphibole. The steep intermediate area consists of conglomerate, clay schists and sandstones, in some places with thin zones of limestone. At higher altitudes, the bedrock belongs to a nappe complex, locally with zones with shattered mica rich rocks and marble. The Dividalen reference area is thus very different from the other areas with bedrocks that give rise to soils richer in base minerals, i.e. with high values of pH, Ca and Mg.

QUATERNARY DEPOSITS, LANDFORMS AND TOPOGRAPHY

The Lund reference area is situated 320–420 m a.s.l. in a relatively steep mountain side facing northeast. One of the investigated sites is situated on a gravel deposit between two small lakes. The mountain side varies between even slopes and small gully-like depressions with periodic small streams. In the upper parts, where the terrain is less steep, small fens occur, but most of the mountain side is well drained with a thin layer of till, often with a high block content and with considerable variation in the size of the stone blocks.

The Møsvatn reference area is situated between the high mountains on the Hardangervidda mountain plateau and the deep valleys south of this. The monitoring area (1000–1050 m a.s.l.) is located on the north and east slopes of a small hill, above a mire surrounded by a mountain meadow landscape. The till deposits are thin and discontinuous and contain several bedrock outcrops. In the northern low-lying parts of this reference area the till has a very high content of blocks, compared with the rest of the area.

The Åmotsdalen reference area (900–925 m a.s.l.) is situated on kame terraces and till deposits on the south facing slopes of the valley. Glacifluvial sandy deposits dominate the lower parts of the area. The glacifluvial deposits are linked to a glacier directed drainage system which extends up the valley to passpoints to the west and north-west in the mountains (Sollid et al. 1980a, 1980b). At higher altitudes, thin and discontinuous deposits of till dominate together with mires and bedrock outcrops.

In the Gutulia reference area (770–865 m a.s.l.) till dominates with variable thickness, normally thin at higher altitudes and thicker in the mountain slopes and the valleys. The till contains some limestone and dolomite erratics, originating from sedimentary rocks found between the Precambrian basement and the nappe rocks above.

The Børgefjell reference area is situated between 520 and 580 m a.s.l. A coarse till deposit dominates the area, which contains few bedrock outcrops partly situated on the east slopes of a U-shaped valley, one on weakly convex terrain in between mires and the other on a medium steep valley side.

The Dividalen reference area extents across a wide U-shaped valley in the lower part of the valley side, between 385 and 615 m a.s.l. Glacifluvial deposits are found at middle levels in the valley side. These are linked to a glacier directed drainage system going up the valley to pass points towards the east. Block-rich tills dominate the valley floor. The till is also rich in clay and consolidated, which does not favour drainage. The terrain is therefore locally paludified. At higher elevations the till cover is thin and discontinuous.

CLIMATE

The reference areas span a geographical gradient from south to north Norway with major differences in tempeartures and precipitation (Table 1). The southernmost area, Lund, differed strongly from the other areas (Table 1). Lund has the highest summer temperature (> 11.5 °C) and the winter temperature is rather mild (> –1.4 °C) (Førland 1993). The other areas have lower summer temperatures, ranging between 11.4 and 8.0 °C. Gutulia has the lowest winter temperature (–11.4 °C). Lund is also the area with far the highest precipitation, while Dividalen to the north has the lowest mean annual precipitation.

VEGETATION ZONES AND SECTIONS

The six reference areas span natural climatic and geographical gradients of Norwegian birch forests (Table 1, Fig. 1) as well as gradients in deposition of major long-distance airborne pollutants (Tørseth & Semb 1997, Aas et al. 2002). The areas span almost the entire oceanicity gradient from the markedly oceanic section (O2) at Lund to the slightly continental section (C1) at Dividalen (terminology of vegetation zones and sections in accordance with Moen 1999). All areas are situated in the north boreal vegetation zone, except Lund which is situated in the lower part of the middle boreal zone, close to the more termophilous south boreal zone (Table 1).

HISTORICAL BACKGROUND OF BOREAL BIRCH FOREST INVESTIGATIONS

Boreal birch forests have been described from central and southern parts of Norway by e.g. Nordhagen (1928, 1943), Mork & Heiberg (1936), Dahl (1957), Aune (1973) and Moen (1990). Several associations in the hierarchical plant sociological system (Braun-Blanquet 1928, 1965, Dierschke 1994) have been proposed by Nordhagen (1943), Kielland-Lund (1972, 1973, 1981) and Aune (1973). Overviews of the relations of birch forests to syntaxonomy have been given by Vevle (1986), Dahl (1986), Kielland-Lund (1994) and Fremstad (1997). Relevés and vegetation descriptions from birch forests spread over Norway have been used to classify the boreal birch forests into vegetation types by Fremstad (1997). These vegetation types are, to a large extent, based on environmental gradients (climate, soil related and long-term human impact). R. Økland & Bendiksen (1985) classified upper boreal and middle boreal vegetation types on poor soils in the Grunningsdalen area in Telemark according to positions along the complex gradient topographic moisture–snow cover into xeric, subxeric, submesic and mesic series. This accord with Finnish studies, e.g. Kalela (1961), Hämet Ahti (1963) and Kielland Lund (1967, 1973, 1981). However, counting the mentioned studies above as well, hardly any environment-vegetation relationships studies using gradient analyses techniques (sensu R. Økland 1990) has been performed in Fennoscandian boreal birch forests. This knowledge gap has been one of the main drivers to complete this monograhy.

AREA HISTORY AND INFLUENCE OF GRAZING

Lund

The Lund reference area is not protected by law, but privately owned. It is situated just outside the Førland/Sletthei landscape Protection area (Fig. 2). The investigated area is located far from built-up areas and only to a small degree influenced by human activity (Brattbakk et al. 1992, Stabbetorp et al. 1999). A sheepwalk occurs in the main valley, Urdalen, and heathland has periodically been burnt on ridges in the vicinity of the reference area until recently. The sheep have access to the investigated area. However, no visual signs of grazing have been recorded from the reference area. The area is used for hunting elk and deer, but it is not heavily used for recreation.

Møsvatn

The reference area is situated on Merakkhaugen on privately owned land within the Møsvatn-Austfjell Landscape Protection Area, protected by law since 1993 (Fig. 3). Summer farming has earlier been common in the area, but at the time of establishment summer farming only took place in Hjerdalen (Brattbakk 1993). Today there is a weak grazing pressure by cattle and sheep in and around the investigated plots, and frequent cutting of woods have been observed. Merakkhaugen is visited by some hikers, and in autumn the area is often used by people collecting berries, especially cloudberry. However, it is assumed that the investigated area, due to its position in the north facing slope away from the main pathways, is more protected from grazing, wood cutting and human trampling than the surrounding areas (Bakkestuen et al. 1999a, Bakkestuen & Erikstad 2002).

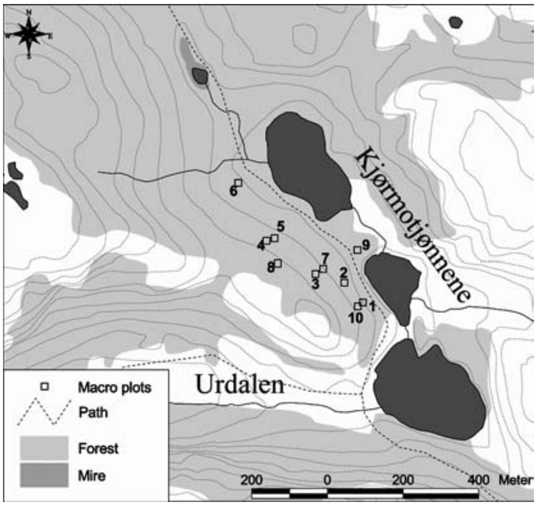

Fig. 2. Map of the reference area Lund with positions of macro plots 1–10. Based on digital N50 maps from the Norwegian Mapping Authority. Map sheet Ørsdalsvatnet 1312 III.

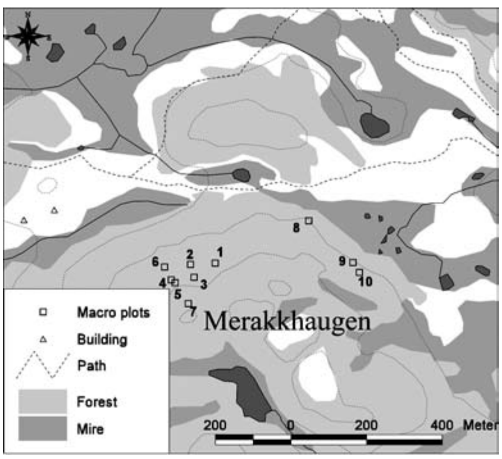

Fig. 3. Map of the reference area Møsvatn with positions of macro plots 1–10. Based on digital N50 maps from the Norwegian Mapping Authority. Map sheet Frøystul 1514 I.

Gutulia

The investigated area (Fig. 4) is state owned land, protected as a part of the Gutulia National Park since 1968. Summer farming was performed regularly in Gutulia until 1949 (Kielland-Lund 1972, Wold 1989). Later on, to restore some of the original mountain dairy farming environment, the pasture has been grazed again by cattle for some years. Only a small area within the investigation area is considered to be influenced by grazing for the last hundred years (O. Vangen pers. medd, Eilertsen & Often 1994). However, the influence from grazing by domestic reindeer was at the time of analysis significant in the whole area, particularly above the tree limit, where also the trampling effect is largest. The national park is also much visited by tourists and hikers, but these mainly follow the main tracks outside the reference area. According to Godal & Hauge (1964) and Ø. Aas (1989) there has been some wood cutting in Gutulia, and at least four forest fires have occurred in historical times (Wold 1989). However, traces of forest fires were most abundant in pine forests in the area.

Two other vegetation monitoring projects have been established in Gutulia. Boreal coniferous forests are monitored in Gutulia as one of the ten reference areas in 'Vegetational and environmental monitoring of boreal spruce forest' by the Norwegian forest and landscape institute (formerly NIJOS; T. Økland 1993, 1996). The coniferous forest sites are situated just to the south-east of the birch forest reference area. In 1992, NIJOS also established a monitoring project within low alpine vegetation in Gutulia (Rydgren 1994) which has, however, so far not been re-analysed.

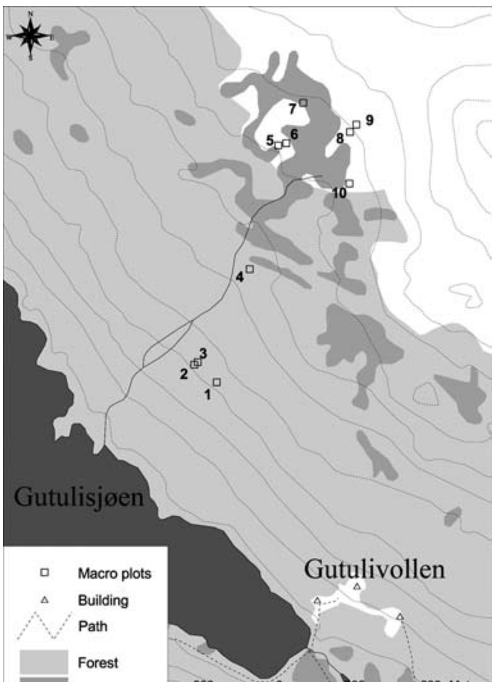

Fig. 4. Map of the reference area Gutulia with positions of macro plots 1–10. Based on digital N50 maps from the Norwegian Mapping Authority. Map sheet Elgå 1719 IV.

Åmotsdalen

The investigated area is privately owned, but from 2002 included in the Åmotsdalen Landscape Protection Area (Fig. 5). Five summer farms have occured in the vicinity of the reference area, while none of these were still in active use at the time of the establishment of the reference area (Brattbakk et al. 1992). The forests close to the summer farms have earlier been considerably affected by grazing by cattle and sheep, and by removal of shrubs to improve the grazing land. Furthermore they have been affected by wood cutting and hay harvesting. However, the reference area is situated in the least affected parts of the forests, and at the time of analysis the vegetation appeared only slightly affected by grazing. A tourist path runs through the area, but it is not much in use. Some sheepwalks were observed in the investigation area during fieldwork in 1996 (Bakkestuen et al. 1999b).

Børgefjell

The investigated area (Fig. 6) is state owned land and protected as a part of Børgefjell National Park since 1963. A sámi camp is situated close to the reference area, and the whole area was influenced by summer grazing by domestic reindeer. By 1996 the number of reindeer was estimated to be approximately two thousand individuals (Eilertsen & Stabbetorp 1997), and the vegetation in the reference

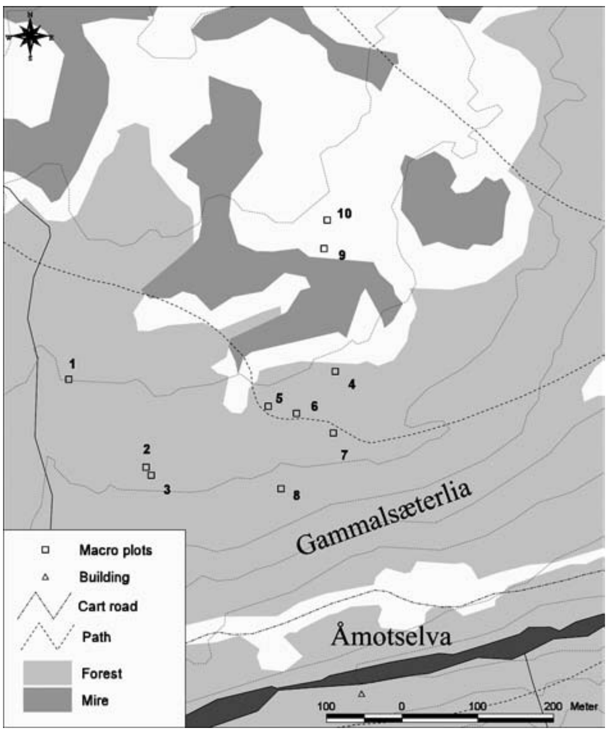

Fig. 5. Map of the reference area Åmotsdalen with positions of macro plots 1–10. Based on digital N50 maps from the Norwegian Mapping Authority. Map sheet Snøhetta 1519 IV.

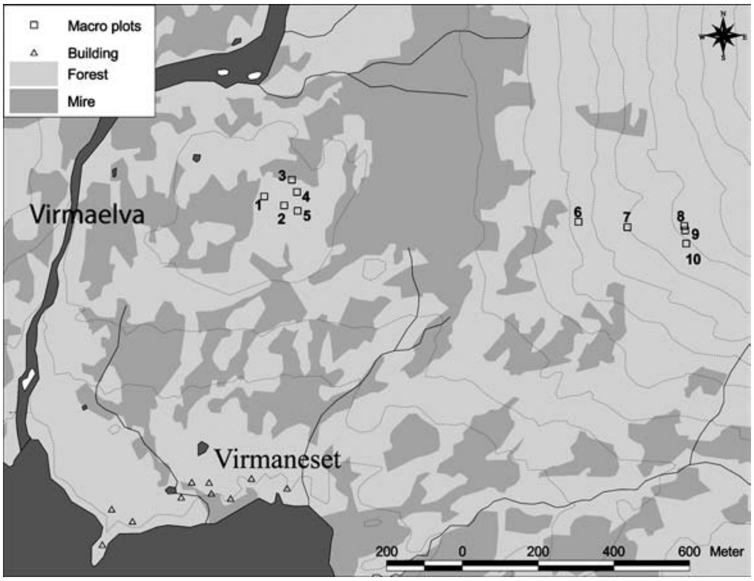

Fig. 6. Map of the reference area Børgefjell with positions of macro plots 1–10. Based on digital N50 maps from the Norwegian Mapping Authority. Map sheet Børgefjellet 1925 IV.

area was likely to be affected by the grazing pressure. Snow scooters were extensively used also within the borders of the national park. Few signs of wood cutting occurred in the area, and no signs of hay harvesting and grazing of farm animals could be observed. No summer farms exist (or have existed) in the area; just some privately owned cottages and a tourist cottage were present. Hikers get access to the area by a taxi boat across the lake Store Namsvatn. This has resulted in a low but continuous flow of hikers into the area, but this activity seemed not to have any significant influence on the vegetation in the monitored area.

Dividalen

The investigated area is state owned land and is protected as a part of Dividalen National Park since 1971. The National Park is used in the summer by the Swedish sámi villages (sidas) of Lainiovouma and Saarivuoma (Eilertsen & Brattbakk 1994). The area south of Skaterdalen have been utilized by the reindeer management of Saarivuoma (Kalstad 1974). No summer farms have existed in the area and the only traces of fellings in the investigation area occurred along Hagembekken (Fig. 7). Three hiker cabins were situated in the national park, and the area was much visited by locals and tourists. Some human impact occurred along the main tracks, but the major part of the national park is little affected by trampling. Previously there has been military activity in the area (Munch 1974).

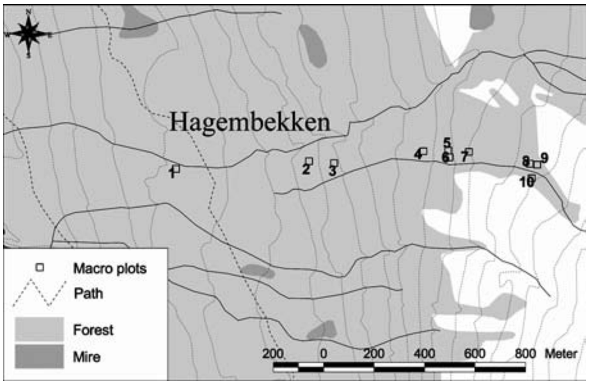

Fig. 7. Map of the reference area Dividalen with positions of macro plots 1–10. Based on digital N50 maps from the Norwegian Mapping Authority. Map sheet Altevatn 1532 II.

MATERIAL AND METHODS

Data were collected from Gutulia and Dividalen in 1993 (soil data for Dividalen sampled 1998), from Børgefjell in 1995, from Lund and Åmotsdalen in 1996 and from Møsvatn in 1997. These data represents the first analyses of each of the six reference areas with common methodology (see below).

SAMPLING DESIGN

Early phase methodology

When the first four reference areas (Børgefjell in 1990, Lund in 1991, Åmotsdalen in 1991, and Møsvatn in 1992) were established, sites of slightly variable shape and size (approximately 50 m^2) were placed subjectively in homogenous bilberry-dominated birch forests. The vegetation was at that time analysed in sample plots subjectively distributed along transects within each site. At Børgefjell 10 sites were established, with ten 0.5×0.5 m sample plots in each site, 100 in total (Brattbakk et al. 1991). At Lund six sites were established with six to ten 1×1 m sample plots in each site, 50 sample plots in total (Brattbakk et al. 1992), while at Åmotsdalen and Møsvatn 10 sites each containing five 1×1 m sample plots were established (Brattbakk et al. 1992, Brattbakk 1993). All sample plots were permanently marked.

New methodology

In 1993 it was decided to include vegetation over a wider range of variation in soil moisture, soil mineral nutrient richness and microclimate within each reference area. In Gutulia and Dividalen, established in 1993, a restricted random sampling procedure was used.

Ten macro plots, each 5×10 m, were placed subjectively in each reference area in order to represent the main floristical and ecological gradients within the birch forest. Five meso plots for vegetation analysis, each 1×1 m, were randomly distributed within each of the macro plots. A meso plot was rejected if containing a tree taller than 2 m or if more than 20% of the plot was covered by stones or fallen tree logs. All plots were placed at least one meter from to the nearest plot to avoid trampling destruction of the vegetation within the plots. The corners of the macro plots and the lower left corner of each meso plot were marked by wooden poles. All corners of the meso plot were permanently marked with subterranean eloxed aluminium tubes. This restricted random sampling procedure is regarded as an optimal compromise between objectivity and time consumption in vegetation monitoring (cf. R. Økland 1990, T. Økland 1996).

Adjustment of early methodology

The field sampling design used in Børgefjell, Lund, Åmotsdalen and Møsvatn reference areas 1990–92 was changed before first re-analysis (in Børgefjell in 1995, in Lund and Åmotsdalen in 1996, and in Møsvatn in 1997).

Thirty of the original sample plots from each reference area were retained, while 20 new 1×1 m sample plots (meso plots) were established within four new macro plots, using the same methods as described for Gutulia and Dividalen. The new macro plots were subjectively positioned within the birch forest of each reference area, to ensure that all 1×1 m sample plots together represented the main floristical and ecological gradients within the reference area.

At Børgefjell the original 0.5×0.5 m sample plots were expanded to 1×1 m plots. After adjustment all reference area contains fifty 1×1 m sample plots (meso plots) for vegetation analyses distributed within ten macro plots (or sites). The total number of meso plots within the TOV birch forest monitoring programme is therefore 300.

RECORDING OF VEGETATION IN THE SAMPLE PLOTS

Each of the 300 meso plots (50 in each reference area) was divided into 16 equally large 0.0625 m^2 subplots. Presence/absence of all species of vascular plants, bryophytes and macrolichens was

Table 2. Environmental variables; abbreviation, unit of measurement and potential range of scale. Mmol: millimoles, ddu: day-degree unit.

Abbrev.	Variable	Unit	Pot. range
Local macro plot variables			
Ma Slo	Macro plot slope	°	0–90
Ma Asp	Macro plot aspect unfavourability	°, recalc	0–180
Ma HI	Macro plot heat index		-∞ – +∞
Ma Ter	Macro plot terrain form		-2 – +2
Ma Une	Macro plot terrain unevenness		0–5
TBA	Tree basal area	m^3/ha	0–∞
Local meso plot variables			
Me Slo	Meso plot slope	°	0–90
Me Asp	Meso plot aspect unfavourability	°, recalc	0–180
Me HI	Meso plot heat index		-∞ – +∞
Me Ter	Meso plot terrain form		-2 – +2
Me Une	Meso plot terrain unevenness		1–5
Smi	Minimum soil depth	cm	0–105
Sme	Medium soil depth	cm	0–105
Sma	Maximum soil depth	cm	0–105
Mme	Soil moisture	%	0–100
LOI	Loss-on-ignition	%	0–100
Total N	Kjeldahl nitrogen	mmol(+)/kg/LOI	0–∞
pH_{H_2O}	pH (H_2O – extraction)		0–14

recorded in each subplot and frequency in subplots calculated as a measure of abundance. A species was recorded as present when any part of the plant was positioned within (over) the subplot. The percentage cover of every species was estimated within each 1×1 m meso plot as an additional measure of abundance. An aluminium frame of 1×1 m was used for exact delineation of subplots.

RECORDING OF ENVIRONMENTAL VARIABLES

A total of 38 explanatory variables including local topography, forest structure, soil properties and regional climatic and geographic variables, were measured or calculated for each of the 300 plots. A summary of explanatory variables with abbreviations is given in Table 2. The term ‘explanatory’ is used in the statistical meaning of the word to indicate the variables’ potential for explaining variation in other data sets (e.g. R. Økland et al. 2001). Causal relationships are discussed *a posteriori* by taking correlations with the explanatory variables as well as other relevant material into account.

Table 2 (continued). Environmental variables; abbreviation, unit of measurement and potential range of scale. Mmol: millimoles, ddu: day-degree unit.

Abbrev.	Variable	Unit	Pot. range
pH_{CaCl_2}	pH ($CaCl_2$ – extraction)		0–14
H	Exchangeable hydrogen	mmol/kg/LOI	0–∞
Al	NH_4NO_3 extractable aluminium	mmol/kg/LOI	0–∞
C	NH_4NO_3 extractable carbon	mmol/kg/LOI	0–∞
Ca	NH_4NO_3 extractable calsium	mmol/kg/LOI	0–∞
Fe	NH_4NO_3 extractable iron	mmol/kg/LOI	0–∞
K	NH_4NO_3 extractable potassium	mmol/kg/LOI	0–∞
Mg	NH_4NO_3 extractable magnesium	mmol/kg/LOI	0–∞
Mn	NH_4NO_3 extractable manganese	mmol/kg/LOI	0–∞
Na	NH_4NO_3 extractable sodium	mmol/kg/LOI	0–∞
P	NH_4NO_3 extractable phosphorous	mmol/kg/LOI	0–∞
S	NH_4NO_3 extractable sulphour	mmol/kg/LOI	0–∞
Zn	NH_4NO_3 extractable zink	µmol/kg/LOI	0–∞
Regional parameters			
Prec.	Annual precipitation	mm	0–∞
T	Mean annual temperature	°C	0–∞
ETS	Effective temperature sum	ddu	0–∞
Tamm’s H	Tamm’s humidity index mm 0-∞		
Lat.	Latitude	°	-90 – 90
Long.	Longitude	°C	-180 – 180
Alt.	Altitude	m	

Thirty-one local environmental variables were recorded in each reference area at specific scales (macro or meso plot). A local macro plot variable is considered to represent the entire area around (and encompassing) a meso plot, recorded for a 5×5 m around each plot or for the entire macro plot. Meso plot variables represent the area within the 1×1 m plot.

Local macro plot variables

All macro plot variables, except tree basal area, were measured for each meso plot in a 5×5 m area with the meso plot in the centre. *Macro plot slope* (Ma Slo), representative for the 5×5 m area, was measured by a clinometer The aspect of the 5×5 m area was measured by a 360 ° compass; values were read off to nearest degree. *Macro plot aspect unfavourability* (Ma Asp) expressed as deviation from SSW [202.5 °, cf. T. Økland (1990, 1996), R. Økland & Eilertsen (1993)], was calculated from the aspect measurements. SSW is considered to be the most favourable aspect (Dargie 1984, Heikkinen 1991) due to high incoming radiation at times of day with high temperatures. The *Macro plot heat index* (Ma HI), similar to Parker's index (Parker 1988) was calculated by the following formula:

$$\text{Ma Hi} = \tan(\text{Ma Slo}) \times \cos(\text{Ma Asp})$$

Increasing Ma Hi values reflects increasing solar radiation.

Macro plot terrain form (Ma Ter) was estimated subjectively on a scale from –2 to +2; where –2 indicates a distinctly concave recession in the terrain, –1 indicates a weak concavity, 0 corresponds to an even surface or a balance between concave and convex micro-forms (at scales considerably finer than the macro plot), +1 indicates a weak convexity and +2 indicates a distinct convex ridge or protruding land form at the relevant scale. *Macro plot unevenness* (Ma Une) was estimated subjectively on a scale from 1 to 5, where 1 represents an even surface and 5 represents a surface with many convex and/or concave parts, with high relative altitude differences.

Tree basal area (TBA) was measured at breast height at each meso plot by means of a relascope. The basal area expresses the tree density (m^2/ha) around the plot and thus reflects the supply of light to the understorey vegetation.

Local meso plot variables

Meso plot slope (Me Slo) was measured by placing a clinometer on the metal frame, adjusted to fit the slope of the terrain. The aspect was measured by a 360 ° compass. *Meso plot aspect unfavourability* (Me Asp) was calculated in the same way as for macro plot unfavourability (see above). *Meso plot heat index* (Me HI) was calculated as for macro plot heat index:

$$\text{Me HI} = \tan(\text{Me Slo}) \times \cos(\text{Me Asp})$$

Increasing Me Hi values reflects increasing solar radiation.

Microtopographic indices were calculated from assessments within each of the 16 subplots within the meso plot. The terrain form was assessed on the scale from –2 to +2 for each subplot, where –2 represents a distinct concave terrain and +2 a distinct convex terrain (on the rekevant scale). The mean value for the 16 subplots was termed *meso plot terrain form* (Me Ter), while the variance provides an estimation of the unevenness in the meso plot, *the meso plot terrain unevenness* (Me Une).

Meso plot soil depth was measured by recording the soil depth at eight fixed sites; two on each side of the meso plot approximately ten cm outside the plot. The following three variables were derived: *Minimum soil depth* (Smi), *median soil depth* (Sme) and *maximum soil depth* (Sma).

Soil moisture (Mme) was determined in a volumetric bulk sample collected from the upper 5 cm of the soil, 10 cm outside the meso plot, using a 100 cm^3 metallic soil corer with a lower cutting egde. All samples from one reference area were collected on the same day, after a period of some days without rainfall, with the aim of representing median soil moisture conditions (cf. T. Økland 1990, R. Økland & Eilertsen 1993). The samples were stored in tightly sealed polythene bags. The samples were weighed fresh and oven-dried at 110°C to constant weight, and the water content was calculated as weight percentage of fresh soil and used as a measure for soil moisture.

Soil samples were collected from the upper 5 cm of the humus layer (Oh) for chemical analyses. If the humus layer was less than 5 cm thick, the whole layer was sampled. Several subsamples were collected outside the border of each meso plot and the subsamples were mixed in order to counteract fine-scale spatial variation in physical and chemical properties of the humus. All samples from one reference area were collected on the same day and oven-dried at 25°C as soon as possible after sampling.

The soil samples were analysed at the Norwegian Forest and Landscape Institute according to methods described in Ogner et al. (1991). *Loss-on-ignition* (LOI) was determined by ignition in muffle furnace at 590°C and expressed as weight percentage of dry soil. Digestible organic nitrogen and NH_4 was analysed by the *Kjeldahl-nitrogen* method (Total N). *pH* was analysed by H_2O extraction, (pH_{H_2O}) and $CaCl_2$ extraction (pH_{CaCl_2}). *Ammonium nitrate extractable elements* (Al, C, Ca, Fe, K, Mg, Mn, Na, P, S, Zn) were analysed by a simultaneous ICP technique (Inductively-Coupled Plasma Emission Spectroscopy) and *exchangeable acidity/hydrogen* (H) by titration of an ammonium nitrate extract. The concentrations of extractable elements and Kjeldahl nitrogen were expressed as fractions of loss on ignition as recommended by T. Økland (1988).

Regional climatic and geographical variables

Seven region-scale, climatic and geographical variables (regional variables) were used in the numerical and statistical analyses of the total dataset, comparing the reference areas. *Mean annual precipitation* (Prec.) [normal period 1961–90; Førland (1993)] and *mean annual temperature* (T) [Aune (1993), corrected for altitude according to Laaksonen (1976)] were taken from the nearest weather observation stations. For some reference areas, several weather stations were combined to produce an integrated estimate of precipitation and temperature. *Effective temperature sum* (ETS) according to Laaksonen (1979) and *Tamm's index of humidity* (Tamm's H) (Tamm 1959) were calculated for each macro plot. *Latitude* (Lat.) and *longitude* (Long.) for each reference area and *altitude* (Alt.) for each macro plot were taken from digital N50 maps from the Norwegian Mapping Authority.

NUMERICAL AND STATISTICAL ANALYSES OF DATA SETS FROM EACH REFERENCE AREA

Data manipulation: transformation of variables

For all variables (Tables 2), skewness and kurtosis standardised by division with their expected standard deviations, $(6/n)^{0.5}$ (Sokal & Rohlf 1995), were calculated. Acceptable homogeneity of variances (homoscedasticity) was achieved by transforming all variables to zero skewness [transformation formulae of R. Økland *et al,* (2001) were used]:

$$y'_{kj} = e^{c_k x_{kj}} \quad (1)$$

$$y'_{kj} = \ln(c_k + x_{kj}) \quad (2)$$

$$y'_{kj} = \ln[c_k + \ln(c_k + x_{kj})] \quad (3)$$

where x_{kj} is the original value of variable k in plot j and c_k is a variable-specific parameter determined so that the transformed variable $Y' = \{y_{kj}'\}$ has zero skewness. Eq. (1) was applied to left-skewed variables (standardised skewness < 0), eq. (2) to right-skewed variables and eq. (3) was applied to right-skewed variables for which no value of c_k could be found by eq. (2) that resulted in standardised skewness = 0. After transformation, all variables Y' were ranged to obtain new variables $Y = \{y_{kj}\}$ on a 0–1 scale:

$$\mathrm{y}_{\mathrm{kj}} = [y'_{kj} - \min(y'_{kj})]/[\max(y'_{kj}) - \min(y'_{kj})] \quad (4)$$

Ordination of vegetation-sample plot matrices

Detrended Correspondence Analysis (DCA; Hill 1979, Hill & Gauch 1980) ordination was used to extract the main gradients of the frequency in subplot abundance data sets from the six reference areas. The calculations were performed by means of CANOCO 4.5 (ter Braak 1987b, 1990, ter Braak & Smilauer 1998, 2002). Detrending by segments and non-linear rescaling options were used to avoid arch and edge effects of corresponding correspondence analysis (CA) ordinations (R. Økland 1990). The DCA ordination axes are scaled in standard deviation (S.D.) units.

Global Non-metric Multidimensional Scaling, GNMDS (Kruskal 1964a, 1964b) was used to ordinate frequency in subplots data sets from each reference area. GNMDS were run using R Version 2.4.1 (Anonymous 2004a), including packages *vegan* Version 1.9–13 (Oksanen 2007, Oksanen et al. 2007) and *MASS*, the latter included in package cluster *stats* (Anonymous 2004b), using functions *vegdist*, *initMDS*, *isoMDS* and *postMDS*, with options: dimensionality = 2; dissimilarity measure = percentage dissimilarity (Bray-Curtis), standardized by division with species maxima: minimum number of starting configurations = 100, of which one was the DCA; maximum number of iterations = 1000; stress reductions ratio for stopping iteration procedure = 0.99999. Solutions were not accepted unless reached from at least two different starting configurations.

The degree of correspondence between the axes obtained by DCA and GNMDS was tested by calculating Kendall's rank correlation coefficients between scores along the first two DCA axes and the two GNMDS axes. The GNMDS ordination axes were overall very strongly correlated (see results from each reference area) with the corresponding DCA axes. We therefore present only the DCA ordination results which have advantage (over GNMDS) that the ordination axes are scaled in standard deviation (S.D.) units (e.g. R. Økland 1990).

All ordination diagrams were made by ArcView 3.2 (Anonymus1999a).

Methods for correlating ordination axis with environmental data and interpretation of ordination results

DCA ordinations were interpreted by split-plot GLM analysis (Crawley 2002) combined with Kendall's rank correlation coefficient τ calculated between plot scores along DCA axes and environmental variables. Parallel use of these two methods has proved useful because scale-dependent vegetation-environment relationships are revealed and relationships are evaluated by use of appropriate degrees of freedom (Auestad et al. 2008, Liu et al. 2008).

GLM was chosen because it allows flexible handling of data over a wide range of statistical properties (Venables & Ripley 2002). By split-plot analysis each axis, the ordination plot score was used as response variable and one or more environmental variables were used as predictors. The aov function of R version 2.4.1 was used with identity link function and normal errors (Anonymous 2004a). Statistical inference was obtained by considering species (plot) as nested within macro plot. The parameters of SSexpl/SSmacro plot (fraction of variation explained by variable at the macro plot), model coefficient r, F (measurement of fit between predictor and response variables at a given hierarchical level) and P value for F (for a test of no relationship against the two-tailed alternative) were used to determine the contributions of the measured environmental variables to explaining variation in species composition.

Correlation analyses were performed between pairs of local explanatory variables and between these variables and the DCA-ordination sample plot scores. Kendall's τ was used as a measure of correlation in both analyses (Conover 1980). Kendall's τ is a non-parametric measure (it only takes the ranks of variables into account), recommended by Fenstad et al. (1977) whenever the underlying distribution is unknown (or conditions of homogeneous variances and normal distribution of errors not expected to be satisfied). Kendall's τ and the corresponding statistical test of deviation from 0 were performed in SPSS 11.0 (Anonymous 1999b).

Ordination of environmental data by means of PCA

PCA (Principal Component Analysis) ordination (Pearson 1901, ter Braak & Prentice 1988) was run on a correlation matrix (on centred and standardised transformed variables and conjugate variables), using the 31 local variables from each reference area. Correlation biplot scaling of axes was used to optimise the fit of angles between variable vectors to inter-variable correlations. The resulting PCA axes summarise the correlation structure between the environmental variables. All PCA analyses were performed by means of CANOCO 4.5

Distributions of species abundances in the DCA ordination

Frequencies in subplots for species that occur in more than 5 meso plots were plotted onto the meso plot positions in the DCA ordination diagram for each reference area. This gives valuable information about the autecology of each species (T. Økland 1996). The resulting diagrams were used to make isoline diagrams for environmental variables. Isolines were constructed by block kriging interpolation using kriging interpolation version 3.2 for ArcView 3.2 (Anonymous 1999a). Plot scores in the two-dimensional space spanned by ordination axes 1 and 2 were used as geographic co-ordinates and an isotropic semi-variance analysis of the transformed explanatory variable was performed, using an active lag of 4 S.D. units and steps of 0.25 S.D. units. Interpolation was performed from a grid with cell size of 0.25×0.25 S.D. units. Goodness-of-fit of the three-dimensional surface (and the isolines) was assessed by a cross-validation, jackknifing procedure (Anonymous 1998) whereby r^2 was calculated between the original and the predicted values for the variable. Interpolations were made by use of 12 neighbouring plots. After analysis, the fitted values for the explanatory variable were de-ranged and back transformed to the original scale. De-ranging was performed by solving

$$y_{kj} = \frac{y'_{kj} - \min(y'_{kj})}{\max(y_{kj}) - \min(y_{kj})}$$

for y_{kj}', and back-transformation was performed by solving (1)–(3) for y_{kj}:

$$y'_{kj} = e^{c_k x_{kj}} \;;\; z_{kj} = \frac{\ln(y'_{kj})}{c_k} \tag{5}$$

$$y'_{kj} = \ln(c_k + x_{kj})\;;\; z_{kj} = e^{y'_{kj}} - c_k \tag{6}$$

$$y'_{kj} = \ln[c_k + \ln(c_k + x_{kj})]\;;\; z_{kj} = e^{e^{y'_{kj}} - c_k} - c_k \tag{7}$$

Isolines were smoothed by using a B-spline function (Pavlidis 1982) and visualised as a line theme in ArcView 3.2 (Anonymous 1999a) to fit the de-ranged and back-transformed interpolated values.

NUMERICAL AND STATISTICAL ANALYSES OF THE TOTAL DATA SET FROM ALL REFERENCE AREAS

DCA ordination of the total data set

DCA was performed on the total data set consisting of 300 meso plots from the six reference areas. The same options were used as in the DCA of the data from each reference area.

A second DCA ordination of the total data set was also performed, using 7 covariables for the regional climatic/geographical environmental variables not shared with the local environmental variables (C | E in the terminology used for variation partitioning; see below). These covariables were found as follows:

A Canonical Correspondence Analyses, CCA (ter Braak 1986, 1987a), with the 31 local environmental variables as covariables and the seven regional environmental variables as explanatory variables, was performed on the total data set. The resulting (maximally constrained) seven CCA axes (with sample scores that are linear combinations of the environmental variables, cf. Palmer 1993) sort the variation in species composition that is exclusively attributable to climatic/geographical variables ({C | E}) on axes of decresing importance for variation in species composition.

DCA ordinations of the total data set were interpreted by split-plot GLM analysis (Crawley 2002) combined with Kendall's rank correlation coefficient τ calculated between plot scores along DCA axes and environmental variables.

The DCA ordination with covariables was used to study regional variation in the response of vegetation to main complex-gradients, cf. T. Økland (1996). For selected species, occurrences were plotted at meso-plot positions by using different symbols for each reference area.

NOMENCLATURE

The nomenclature of vascular plants follows Lid & Lid (2005). *Alchemilla* spp. may include several species of the genus, except *A. alpina*. *Dryopteris expansa* agg. may include *Dryopteris expansa* (C.Presl.) Fraser-Jenk. & Jermy, *D. dilatata* (Hoffm.) A. Gray, and *D. carthusiana* (Vill.) H.P.Fuchs. *Euphrasia* spp. and *Taraxacum* spp. may include several species. *Hieracium* is identified to the section level.

The nomenclature of bryophytes follows Frisvoll et al. (1995). *Bryum* spp. is determined to the genus level. *Dicranum fuscescens* agg. may include *D. flexicaule* Brid. and *D. fuscescens* Sm. *Hypnum cupressiforme* agg. may include *H. andoi* A.J.E.Sm., *H. cupressiforme* Hedw., *H. jutlandicum* Holmen & Warncke and *H. resupinatum* Spruce. *Plagiothecium laetum* includes also *P. denticulatum* (Hedw.) Schimp. and *P. laetum* var. *secundum* (Lindb.) Frisv. et al. (= *P. curvifolium* Schlieph.). *Rhytidiadelphus squarrosus* agg. includes *R. squarrosus* (Hedw.) Warnst. and *R. subpinnatus* (Lindb.) T.Kop. *Chiloscyphus coadunatus* refers to *C. coadunatus* var. *rivularis* (Raddi) Frisv. et al. (= *Lophocolea bidentata* (L.) Dum.). *Scapania* spp. may include several species of the genus. *Lophozia ventricosa* agg. may include *L. silvicola* Buch, *L. ventricosa* (Dicks.) Dum. and *L. longiflora* (Nees) Schiffn.

The nomenclature of lichens follows Krog et al. (1994). *Cladonia arbuscula* agg. may include *C. arbuscula* (Wallr.) Flot. and *C. mitis* Sandst. *Cladonia chlorophaea* agg. may include *C. chlorophaea* (Flörke ex Sommerf.) Spreng., *C. cryptochlorophaea* Asah., *C. grayi* Merr. ex Sandst., *C. fimbriata* (L.) Fr., *C. merochlorophaea* Asah., and *C. pyxidata* (L.) Hoffm. *Cladonia coccifera* agg. may include *C. borealis* S.Stenroos, *C. coccifera* (L.) Willd., and *C. pleurota* (Flörke) Schaer. *Cladonia coniocraea* agg. may include *C. coniocraea* (Flörke) Spreng. and *C. ochrochlora* Flörke.

RESULTS

LUND REFERENCE AREA

Correlations between environmental variables

There were strong pairwise correlations between several of the topographical variables, between topographical and chemical variables and between soil chemical variables (Table 3).

Macro and meso plot slope and heat indices were negatively correlated. Macro and meso plot aspect unfavourability were negatively correlated with heat indices and positively with macro plot terrain unevenness and meso plot slope. Macro plot slope was further positively correlated with median and maximum soil depth. The topographical variables terrain unevenness and terrain form and tree basal area, however, hardly showed significant correlations with other variables.

Macro and meso plot slope and the macro plot heat index were also positively correlated to pH, C and Mn and negatively correlated with Ca, Mg, Zn, P and soil moisture.

Soil moisture was positively correlated with LOI, Ca, Mg and Na and negatively correlated with pH. LOI was positively correlated with Ca, Mg, P and Zn.

pH showed an unexpected, positive, correlation with variables reflecting soil acidity such as exchangeable hydrogen (H) and extractable Fe and Al concentrations, and was negatively correlated with concentrations of elements that are typically abundantly present in base-rich soils, such as Ca and Mg. Ca, Mg, P and Zn were, however, positively correlated with each other and negatively correlated with H.

PCA ordination of environmental variables

The first PCA axis accounted for 31.6 % (eigenvalue of 0.316) of the variance in the matrix of standardised transformed environmental variables, and the second axis for 15.5 % (eigenvalue of 0.155).

pH_{H_2O}, pH_{CaCl_2}, extractable Al, S, Fe and C, exchangeable H and macro plot slope obtained high loadings on PCA axis 1 (Fig. 8). Low loadings were obtained by extractable Mg, P, Ca and Zn, LOI and macro- and meso plot heat indices. This negative correlation between the two groups of variables was consistent with the pairwise rank correlation values of the variables in Table 3. Several of the topographical variables that were significantly correlated with the variables mentioned above also had a similar distribution pattern in the PCA ordination duiagram.

Macro plot aspect unfavourablility, minimum soil depth and soil moisture obtained high loadings on PCA axis 2 while extractable K, Fe, Mn and C obtained low loadings.

DCA ordination

The gradient length of DCA axis 1 was 2.37 S.D. units, and the length of DCA axis 2 was 1.15 S.D. units. The eigenvalue of the first axis was 0.230. The next three axes had decreasing eigenvalues of 0.126, 0.073 and 0.046, respectively.

The sample plots were distributed relatively evenly in the DCA ordination diagram, although slightly more plots were located on the left hand side (Fig. 9). Two plots were somewhat separated

Table 3. Lund: Kendall's rank correlation coefficients τ between 31 environmental variables in the 50 meso plots (lower triangle), with significance probabilities (upper triangle). Statistically significant correlations (P<0.05) in bold face. Names of explanatory variables abbreviated in accordance with Table 2.

	1	2	3	4	5	6	7	8	9	10	11	12	13	14	15	16
01 Ma Slo	*	0.050	**0.000**	0.518	0.752	0.149	**0.000**	0.090	**0.000**	0.453	0.125	0.861	**0.032**	**0.009**	**0.012**	**0.003**
02 Ma Asp	0.201	*	**0.000**	0.588	**0.016**	0.633	**0.014**	**0.000**	**0.002**	0.092	0.833	0.073	**0.008**	**0.906**	**0.113**	**0.400**
03 Ma HI	**–0.815**	**–0.383**	*	0.697	0.611	0.160	**0.000**	**0.032**	**0.000**	0.620	0.319	0.827	**0.011**	**0.031**	**0.025**	**0.014**
04 Ma Ter	0.072	–0.061	–0.043	*	0.432	0.448	0.541	0.098	0.874	0.922	0.584	0.485	0.639	0.406	0.163	0.104
05 Ma Une	–0.035	**0.267**	–0.055	–0.095	*	0.887	0.765	**0.038**	0.297	0.597	0.478	0.205	0.357	0.693	0.281	0.297
06 TBA	–0.151	0.051	0.145	0.087	–0.016	*	0.172	0.617	0.201	0.385	0.741	0.081	0.339	0.980	0.754	0.754
07 Me Slo	**0.595**	**0.252**	**–0.545**	0.068	0.033	–0.142	*	**0.017**	**0.000**	0.853	0.113	0.707	0.161	0.237	**0.029**	**0.024**
08 Me Asp	0.169	**0.368**	**–0.211**	–0.182	**0.225**	0.052	**0.238**	*	**0.000**	0.249	0.639	0.253	**0.024**	0.416	0.052	0.292
09 Me HI	**–0.563**	**–0.315**	**0.552**	0.017	–0.113	0.131	**–0.807**	**–0.430**	*	0.788	0.092	0.924	**0.031**	0.209	0.207	0.062
10 Me Ter	–0.077	0.175	0.050	–0.011	–0.059	–0.092	0.019	0.117	–0.027	*	0.414	0.674	0.490	0.192	0.239	0.297
11 Me Une	0.153	0.021	–0.098	–0.060	0.077	–0.034	0.158	0.046	–0.165	–0.083	*	0.307	0.063	0.960	0.311	0.477
12 Smi	–0.019	0.193	–0.023	–0.082	0.147	–0.192	–0.040	0.120	–0.010	0.045	–0.107	*	**0.000**	0.076	0.066	**0.009**
13 Sme	**0.214**	**0.268**	**–0.251**	–0.051	0.100	–0.099	0.140	**0.222**	**–0.212**	0.070	–0.183	**0.416**	*	**0.000**	0.841	0.907
14 Sma	**0.262**	0.012	**–0.213**	0.092	0.043	0.003	0.118	–0.080	–0.124	–0.133	0.005	0.187	**0.397**	*	0.175	0.054
15 Mme	**–0.248**	0.159	**0.219**	–0.153	0.116	0.032	**–0.217**	0.191	0.123	0.119	0.099	0.192	0.020	–0.134	*	**0.000**
16 LOI	**–0.293**	0.085	**0.241**	–0.178	0.113	–0.032	**–0.224**	0.103	0.182	0.105	0.070	**0.274**	–0.011	–0.190	**0.527**	*
17 Total N	0.171	0.153	–0.174	0.048	–0.135	0.079	0.137	–0.039	–0.096	0.080	–0.029	–0.068	0.005	0.185	–0.136	–0.136
18 pH_{H_2O}	**0.355**	**0.381**	**–0.416**	0.007	0.021	–0.100	**0.366**	0.160	**–0.357**	0.138	0.087	–0.003	0.115	**0.200**	**–0.262**	**–0.316**
19 pH_{CaCl_2}	**0.318**	**0.357**	**–0.382**	–0.015	0.010	–0.096	**0.315**	0.172	**–0.328**	0.152	0.044	–0.066	0.114	0.165	**–0.228**	**–0.325**
20 H	0.168	0.115	–0.124	0.160	0.122	–0.063	0.087	–0.107	–0.035	0.107	–0.190	**0.263**	0.187	**0.297**	–0.073	–0.161
21 Al	**0.301**	**0.214**	**–0.306**	0.178	–0.046	–0.088	0.184	–0.053	–0.151	0.051	–0.099	0.121	0.181	**0.312**	**–0.218**	**–0.384**
22 C	**0.348**	0.002	**–0.305**	0.039	–0.063	0.093	**0.260**	–0.030	**–0.202**	–0.070	–0.002	**–0.278**	0.036	**0.228**	**–0.370**	**–0.517**
23 Ca	**–0.268**	–0.120	**0.255**	**–0.278**	0.080	–0.053	–0.164	0.095	0.096	–0.022	0.155	–0.127	–0.182	**–0.252**	**0.241**	**0.342**
24 Fe	**0.325**	–0.007	**–0.260**	**0.214**	0.014	0.098	0.185	–0.080	–0.158	–0.154	–0.096	–0.136	0.092	**0.280**	**–0.394**	**–0.616**
25 K	0.193	**–0.207**	–0.116	0.075	–0.179	0.096	0.157	–0.105	–0.086	–0.124	0.050	**–0.329**	–0.090	0.177	**–0.251**	**–0.270**
26 Mg	**–0.298**	–0.164	**0.290**	–0.124	0.094	–0.006	**–0.205**	–0.057	**0.210**	–0.039	0.129	–0.101	**–0.248**	**–0.280**	**0.264**	**0.433**
27 Mn	**0.396**	–0.014	**–0.388**	–0.108	–0.099	–0.081	**0.350**	0.145	**–0.344**	–0.181	0.118	**–0.252**	–0.036	–0.030	**–0.293**	**–0.296**
28 Na	–0.181	0.086	0.152	–0.029	–0.031	–0.022	–0.062	0.115	0.063	0.110	0.118	0.039	**–0.202**	**–0.285**	**0.283**	**0.430**
29 P	**–0.293**	–0.181	**0.285**	–0.106	–0.037	0.166	**–0.212**	–0.002	**0.205**	–0.029	0.091	**–0.205**	**–0.258**	**–0.297**	**0.197**	**0.318**
30 S	**0.413**	0.120	**–0.380**	0.091	–0.148	0.050	**0.343**	0.048	**–0.304**	0.034	–0.035	–0.148	0.103	**0.290**	**–0.300**	**–0.401**
31 Zn	**–0.311**	**–0.241**	**0.309**	–0.141	0.048	–0.025	**–0.205**	–0.066	**0.193**	–0.124	0.078	**–0.281**	**–0.197**	**–0.218**	0.104	**0.215**

Table 3 (continued). Lund: Kendall's rank correlation coefficients τ between 31 environmental variables in the 50 meso plots (lower triangle), with significance probabilities (upper triangle). Statistically significant correlations ($P<0.05$) in bold face. Names of explanatory variables abbreviated in accordance with Table 2.

	17	18	19	20	21	22	23	24	25	26	27	28	29	30	31
01 Ma Slo	**0.084**	**0.000**	**0.001**	0.090	**0.002**	**0.000**	**0.007**	**0.001**	0.052	**0.003**	**0.000**	0.068	**0.003**	**0.000**	**0.002**
02 Ma Asp	0.129	**0.000**	**0.000**	0.252	**0.034**	0.987	0.232	0.946	**0.002**	0.102	0.893	0.390	0.071	0.232	**0.017**
03 Ma HI	0.076	**0.000**	**0.000**	0.203	**0.002**	**0.002**	**0.009**	**0.008**	0.235	**0.003**	**0.000**	0.120	**0.004**	**0.000**	**0.002**
04 Ma Ter	0.659	0.951	0.895	0.143	0.104	0.724	0.011	0.050	0.491	0.258	0.322	0.791	0.331	0.406	0.197
05 Ma Une	0.210	0.847	0.930	0.258	0.668	0.557	0.456	0.895	0.098	0.386	0.357	0.772	0.732	0.169	0.655
06 TBA	0.441	0.334	0.352	0.537	0.393	0.365	0.606	0.339	0.347	0.953	0.431	0.832	0.106	0.629	0.806
07 Me Slo	0.167	**0.000**	**0.002**	0.379	0.064	**0.009**	0.099	0.062	0.113	**0.038**	**0.000**	0.530	**0.033**	**0.001**	**0.038**
08 Me Asp	0.688	0.104	0.082	0.277	0.592	0.763	0.332	0.412	0.284	0.558	0.141	0.241	0.987	0.627	0.503
09 Me HI	0.328	**0.000**	**0.001**	0.719	0.122	**0.039**	0.328	0.106	0.380	**0.032**	**0.000**	0.520	**0.036**	**0.002**	**0.047**
10 Me Ter	0.429	0.173	0.134	0.289	0.614	0.490	0.827	0.126	0.219	0.699	0.072	0.274	0.775	0.736	0.219
11 Me Une	0.770	0.379	0.657	0.053	0.311	0.980	0.114	0.327	0.610	0.189	0.231	0.231	0.353	0.719	0.427
12 Smi	0.513	0.979	0.530	**0.012**	0.246	**0.008**	0.226	0.194	**0.002**	0.333	**0.016**	0.708	**0.050**	0.155	**0.007**
13 Sme	0.960	0.241	0.248	0.056	0.066	0.713	0.063	0.349	0.357	**0.011**	0.713	**0.040**	**0.009**	0.292	**0.045**
14 Sma	0.061	**0.043**	0.095	**0.003**	**0.002**	**0.021**	**0.010**	**0.004**	0.073	**0.004**	0.763	**0.004**	**0.003**	**0.003**	**0.027**
15 Mme	0.162	**0.008**	**0.020**	0.457	**0.026**	**0.000**	**0.014**	**0.000**	**0.010**	**0.007**	**0.003**	**0.004**	**0.044**	**0.002**	0.288
16 LOI	0.162	**0.001**	**0.001**	0.099	**0.000**	**0.000**	**0.000**	**0.000**	**0.006**	**0.000**	**0.002**	**0.000**	**0.001**	**0.000**	**0.028**
17 Total N	*	**0.000**	**0.000**	**0.020**	**0.001**	**0.000**	**0.004**	0.189	**0.003**	**0.006**	0.587	0.345	0.110	**0.000**	**0.021**
18 pH_{H_2O}	**0.355**	*	**0.000**	**0.005**	**0.000**	**0.000**	**0.000**	**0.004**	0.808	**0.000**	**0.018**	**0.020**	**0.000**	**0.000**	**0.000**
19 pH_{CaCl_2}	**0.357**	**0.834**	*	**0.039**	**0.000**	**0.000**	**0.001**	**0.003**	0.621	**0.000**	**0.014**	**0.029**	**0.000**	**0.000**	**0.000**
20 H	**0.228**	**0.278**	**0.203**	*	**0.000**	0.106	**0.000**	**0.000**	0.345	**0.000**	**0.040**	0.162	**0.000**	**0.002**	**0.000**
21 Al	**0.314**	**0.527**	**0.495**	**0.629**	*	**0.003**	**0.000**	**0.000**	0.694	**0.000**	0.993	**0.004**	**0.000**	**0.000**	**0.000**
22 C	**0.345**	**0.342**	**0.390**	0.158	**0.290**	*	**0.010**	**0.000**	**0.000**	**0.001**	**0.000**	**0.001**	**0.021**	**0.000**	**0.042**
23 Ca	**–0.278**	**–0.367**	**–0.330**	**–0.577**	**–0.693**	**–0.251**	*	**0.000**	0.861	**0.000**	0.694	**0.005**	**0.000**	**0.000**	**0.000**
24 Fe	0.128	**0.283**	**0.288**	**0.358**	**0.504**	**0.558**	**–0.451**	*	**0.024**	**0.000**	**0.037**	**0.000**	**0.000**	**0.000**	**0.001**
25 K	**0.288**	0.024	0.048	–0.092	–0.038	**0.447**	–0.017	**0.220**	*	0.967	**0.032**	0.139	0.238	**0.001**	0.553
26 Mg	**–0.269**	**–0.498**	**–0.459**	**–0.450**	**–0.693**	**–0.316**	**0.703**	**–0.458**	–0.004	*	0.311	**0.000**	**0.000**	**0.000**	**0.000**
27 Mn	0.053	**0.232**	**0.242**	**–0.200**	0.001	**0.388**	0.038	**0.203**	**0.210**	–0.099	*	**0.034**	0.770	**0.017**	0.900
28 Na	–0.092	**–0.229**	**–0.214**	–0.136	**–0.278**	**–0.336**	**0.272**	**–0.389**	–0.144	**0.402**	**–0.207**	*	**0.002**	**0.007**	**0.029**
29 P	–0.156	**–0.547**	**–0.486**	**–0.546**	**–0.698**	**–0.226**	**0.561**	**–0.466**	0.115	**0.607**	–0.029	**0.296**	*	**0.000**	**0.000**
30 S	**0.546**	**0.500**	**0.517**	**0.300**	**0.445**	**0.597**	**–0.438**	**0.422**	**0.311**	**–0.471**	**0.233**	**–0.265**	**–0.378**	*	**0.001**
31 Zn	**–0.226**	**–0.442**	**–0.402**	**–0.496**	**–0.647**	**–0.198**	**0.602**	**–0.334**	0.058	**0.611**	0.012	**0.213**	**0.561**	**–0.337**	*

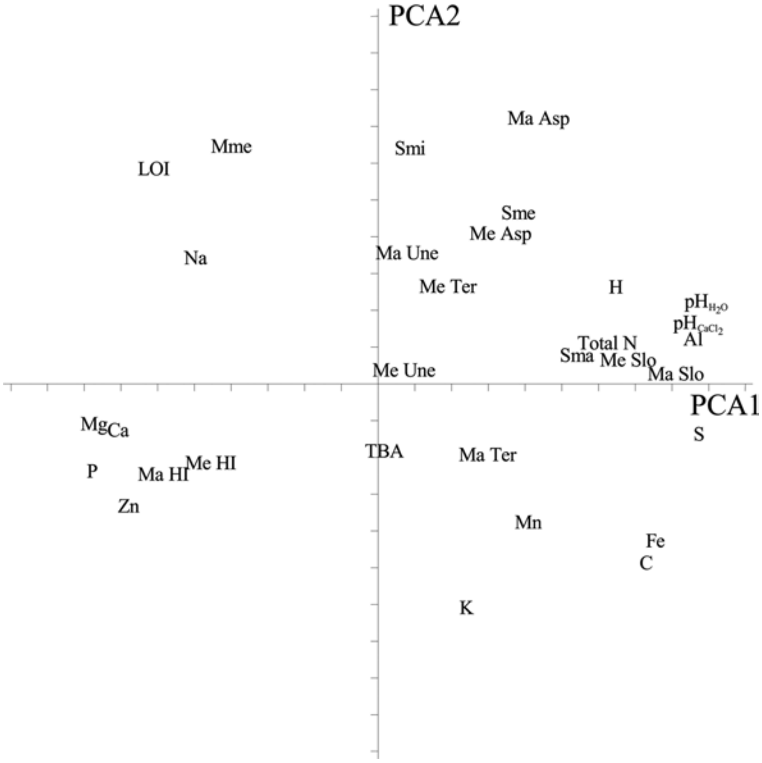

Fig. 8. Lund: PCA ordination of 31 environmental variables. Abbreviations in accordance with Table 2, axes 1 (horizontal) and 2 (vertical). Positions of variables in the ordination space give the head of variable vectors. Tickmarks indicate 0.1 units along both axes.

from the other plots on the right hand side of the diagram. These plots were removed, and a new DCA ordination was performed on the remaining 48 sample plots. As the new ordination did not change the overall distribution pattern of sample plots in the diagram, we decided to use the ordination of all sample plots for further analyses.

GNMDS ordination

The GNMDS ordination diagram (Fig. 10) was visually similar with the DCA diagram (Fig. 9b), although plot 43 obtained a higher score along axis 2 in the GNMDS ordination. The correlation between GNMDS axis 1 and DCA axis 1 was $\tau = 0.784$ and for GNMDS axis 2 and DCA axis 2 $\tau = 0.628$ (both $P < 0.001$).

Split-plot GLM analysis of relationships between ordination axes and environmental variables

Variation (in plot scores) along DCA axis 1 was partitioned with 84.49 % at the macro-plot scale (i.e. between macro plots) and 15.51 % at the (between) meso plot scale within macro plots (Table 4).

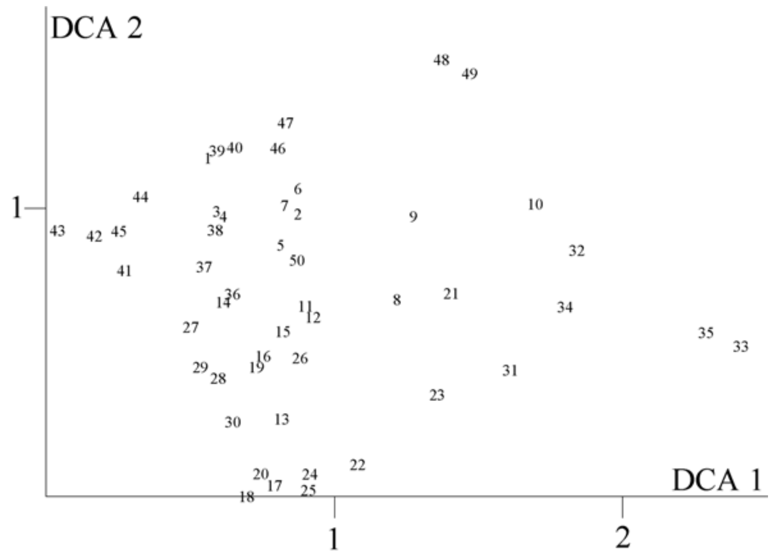

Fig. 9. Lund: DCA ordination diagram of 50 meso plots, axes 1 (horizontal) and 2 (vertical). Meso plot number are plotted just right of the sample plot positions. Scaling of axes in S.D. units.

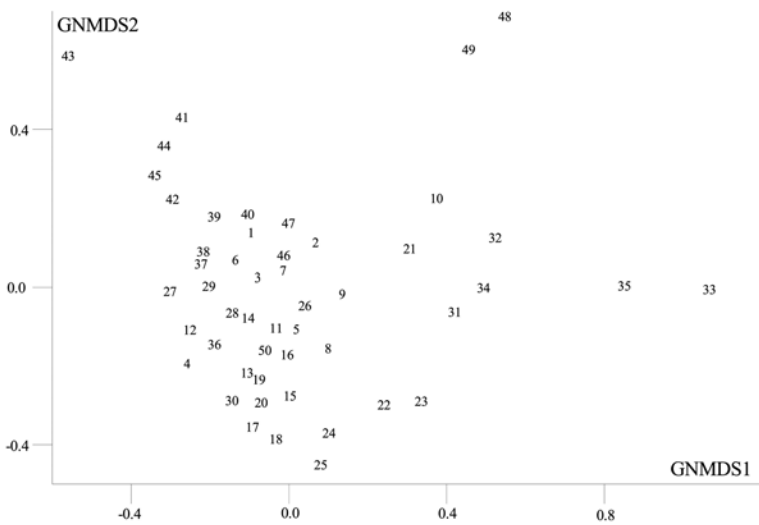

Fig. 10. Lund: GNMDS ordination biplot diagram of 50 meso plots (indicated by their number).

Table 4. Lund: Split-plot GLM analysis and Kendall's nonparametric correlation coefficient τ between DCA 1 and 31 environmental variables (predictor) in the 50 meso plots. df_{resid}: degrees of freedom for the residuals; *SS*: total variation; *FVE*: fraction of total variation attributable to a given scale (macro plot or meso plot); SS_{expl}/SS: fraction of the variation attributable to the scale in question, explained by a variable; *r*: model coefficient (only given when significant at the α = 0.05 level, otherwise blank); *F*: *F* statistic for test of the hypothesis that $r = 0$ against the two-tailed alternative. Split-plot GLM relationships significant at level α = 0.05, *P*, *F*, *r* and SS_{expl}/SS, and Kendall's nonparametric correlation coefficient $|\tau| \geq 0.30$ are given in bold face. Numbers and abbreviations for names of environmental variables are in accordance with Tab. 2.

Predictor	Dependent variable = DCA 1 (SS = 12.1733)								Correlation between predictor and DCA 1
	Error level								
	Macro plot $df_{resid} = 8$ $SS_{macro\ plot} = 10.2848$ $FVE = 0.8449$ of SS				Meso plot within macro plot $df_{resid} = 39$ $SS_{meso\ plot} = 1.88852$ $FVE = 0.1551$ of SS				Total
	$SS_{expl}/SS_{macro\ plot}$	*r*	*F*	*P*	$SS_{expl}/SS_{meso\ plot}$	*r*	*F*	*P*	τ
Ma Slo	0.2219		2.2815	0.1694	0.0084		0.3302	0.5688	0.270
Ma Asp	**0.4466**	**0.9461**	**6.4551**	**0.0346**	0.0098		0.3866	0.5377	**0.400**
Ma HI	0.2699		2.9570	0.1238	0.0105		0.4142	0.5236	–0.337
Ma Ter	0.0011		0.0084	0.9293	0.0208		0.8292	0.3681	–0.125
Ma Une	0.0367		0.3050	0.5958	0.0212		0.8430	0.3642	0.099
TBA	0.0214		0.1747	0.6870	0.0481		1.9706	0.1683	–0.086
Me Slo	0.2717		2.9843	0.1223	0.0033		0.1294	0.7210	**0.322**
Me Asp	0.2464		2.6161	0.1444	0.0107		0.4236	0.5190	0.294
Me HI	0.2440		2.5821	0.1467	0.0000		0.0003	0.9955	–0.293
Me Ter	**0.4894**	**3.0151**	**7.6669**	**0.0243**	0.0010		0.0382	0.8460	0.210
Me Une	0.0055		0.0441	0.8389	**0.1737**	**–0.3918**	**8.1997**	**0.0067**	–0.080
Smi	0.3257		3.8641	0.0849	0.0815		3.4594	0.0705	0.239
Sme	0.1569		1.4890	0.2571	**0.1256**	**0.4043**	**5.6031**	**0.0230**	0.218
Sma	0.1183		1.0738	0.3304	0.0352		1.4224	0.2402	0.056
Mme	0.0013		0.0102	0.9222	0.0022		0.0862	0.7706	–0.096
LOI	0.0008		0.0065	0.9379	0.0002		0.0076	0.9308	–0.053
Total N	**0.5568**	**2.0410**	**10.050**	**0.0132**	0.0001		0.0055	0.9410	0.273
pH_{H_2O}	**0.6956**	**2.2347**	**18.283**	**0.0027**	**0.1753**	**0.5774**	**8.2895**	**0.0064**	**0.511**
pH_{CaCl_2}	**0.7261**	**2.2714**	**21.208**	**0.0017**	**0.1588**	**0.5124**	**7.3636**	**0.0098**	**0.500**
H	**0.5077**	**2.3715**	**8.2486**	**0.0208**	**0.1406**	**0.4577**	**6.3826**	**0.0157**	–0.298
Al	**0.5783**	**1.9645**	**10.972**	**0.0107**	0.0706		2.9642	0.0931	**0.309**
C	0.0551		0.4670	0.5137	0.0092		0.3604	0.5518	0.184
Ca	**0.5188**	**–2.3164**	**8.6251**	**0.0188**	**0.0964**	**–0.3769**	**4.1628**	**0.0481**	–0.251
Fe	0.0015		0.0123	0.9146	0.0002		0.0061	0.9384	0.290
K	0.0193		0.1570	0.7023	**0.1399**	**–0.5058**	**6.3454**	**0.0160**	–0.082
Mg	**0.5321**	**–2.3242**	**9.0990**	**0.0167**	**0.1211**	**–0.4074**	**5.3728**	**0.0258**	–0.293
Mn	0.0117		0.0948	0.7660	0.0030		0.1187	0.7323	0.228
Na	0.0084		0.0682	0.8006	0.0421		1.7140	0.1981	–0.091
P	**0.4680**	**–1.9429**	**7.0384**	**0.0291**	**0.1497**	**–0.4073**	**6.8654**	**0.0125**	–0.298
S	0.3645		4.5884	0.0646	0.0433		1.7644	0.1918	**0.309**
Zn	**0.8342**	**–2.4589**	**40.254**	**0.0002**	0.0213		0.848	0.3628	**–0.339**

Table 5. Lund: Split-plot GLM analysis and Kendall's nonparametric correlation coefficient τ between DCA 2 and 31 environmental variables (predictor) in the 50 meso plots. df_{resid}: degrees of freedom for the residuals; *SS*: total variation; *FVE*: fraction of total variation attributable to a given scale (macro plot or meso plot); SS_{expl}/SS: fraction of the variation attributable to the scale in question, explained by a variable; *r*: model coefficient (only given when significant at the α = 0.05 level, otherwise blank); *F*: *F* statistic for test of the hypothesis that $r = 0$ against the two-tailed alternative. Split-plot GLM relationships significant at level α = 0.05, *P*, *F*, *r* and SS_{expl}/SS, and Kendall's nonparametric correlation coefficient $|\tau| \geq 0.30$ are given in bold face. Numbers and abbreviations for names of environmental variables are in accordance with Tab. 2.

Predictor	Dependent variable = DCA 2 (*SS* = 12.1733)								Correlation between predictor and DCA 2
	Error level								
	Macro plot $df_{resid} = 8$ $SS_{macro\ plot} = 5.5784$ $FVE = 0.7876$ of *SS*				Meso plot within macro plot $df_{resid} = 39$ $SS_{meso\ plot} = 1.50473$ $FVE = 0.2124$ of *SS*				Total
	$SS_{expl}/SS_{macro\ plot}$	*r*	*F*	*P*	$SS_{expl}/SS_{meso\ plot}$	*r*	*F*	*P*	τ
Ma Slo	0.1084		0.9730	0.3528	0.0303		1.2184	0.2764	0.170
Ma Asp	**0.4576**	**–0.7053**	**6.7504**	**0.0317**	0.0139		0.5497	0.4629	**–0.381**
Ma HI	0.0008		0.0068	0.9365	0.0298		1.1990	0.2802	–0.075
Ma Ter	0.1384		1.2846	0.2899	0.0070		0.2753	0.6028	0.133
Ma Une	0.2716		2.9830	0.1224	0.0086		0.3392	0.5637	–0.297
TBA	0.0186		0.1517	0.7070	0.0029		0.1128	0.7387	–0.051
Me slo	0.0774		0.6710	0.4364	**0.1128**	**–0.0650**	**4.9587**	**0.0318**	0.054
Me Asp	0.2764		3.0565	0.1185	0.0585		2.4240	0.1276	–0.255
Me HI	0.0055		0.0446	0.8380	**0.1966**	**0.5199**	**9.5450**	**0.0037**	0.053
Me Ter	0.0280		0.2301	0.6443	0.0037		0.1448	0.7056	–0.092
Me Une	0.0646		0.5526	0.4785	0.0060		0.2358	0.6300	0.019
Smi	0.1121		1.0100	0.3443	0.0045		0.1770	0.6763	–0.148
Sme	0.1349		1.2472	0.2965	0.0000		0.0011	0.9742	–0.158
Sma	0.2085		2.1079	0.1846	0.0013		0.0515	0.8217	0.135
Mme	**0.5780**	**–1.0537**	**10.958**	**0.0107**	0.0357		1.4454	0.2365	**–0.402**
LOI	**0.4372**	**–0.9283**	**6.2146**	**0.0376**	0.0394		1.6016	0.2132	–0.291
Total N	0.0303		0.2496	0.6308	0.0063		0.2455	0.6230	0.179
pH_{H_2O}	0.0164		0.1337	0.7241	0.0000		0.0000	0.9770	0.030
pH_{CaCl_2}	0.0040		0.0320	0.8625	0.0011		0.0430	0.8368	–0.012
H	0.0895		0.7867	0.4010	0.0023		0.0909	0.7646	0.063
Al	0.1066		0.9545	0.3572	0.0167		0.6642	0.4200	0.104
C	0.3010		3.4446	0.1006	0.0463		1.8942	0.1766	0.213
Ca	0.2323		2.4207	0.1584	0.0027		0.1039	0.7490	–0.149
Fe	0.3904		5.1225	0.0535	0.0406		1.6495	0.2066	0.179
K	**0.5131**	**1.6687**	**8.4307**	**0.0198**	0.0146		0.5776	0.4518	**0.358**
Mg	0.1925		1.9078	0.2046	0.0109		0.4315	0.5151	–0.215
Mn	0.0696		0.5981	0.4615	0.0041		0.1614	0.6900	0.136
Na	**0.4694**	**–1.6676**	**7.0773**	**0.0288**	0.0024		0.0928	0.7623	0.087
P	0.1185		1.0755	0.3300	0.0441		1.8010	0.1874	–0.040
S	0.2200		2.2570	0.1714	0.0362		1.4643	0.2335	–0.040
Zn	0.0566		0.4804	0.5079	0.0124		0.4916	0.4874	–0.064

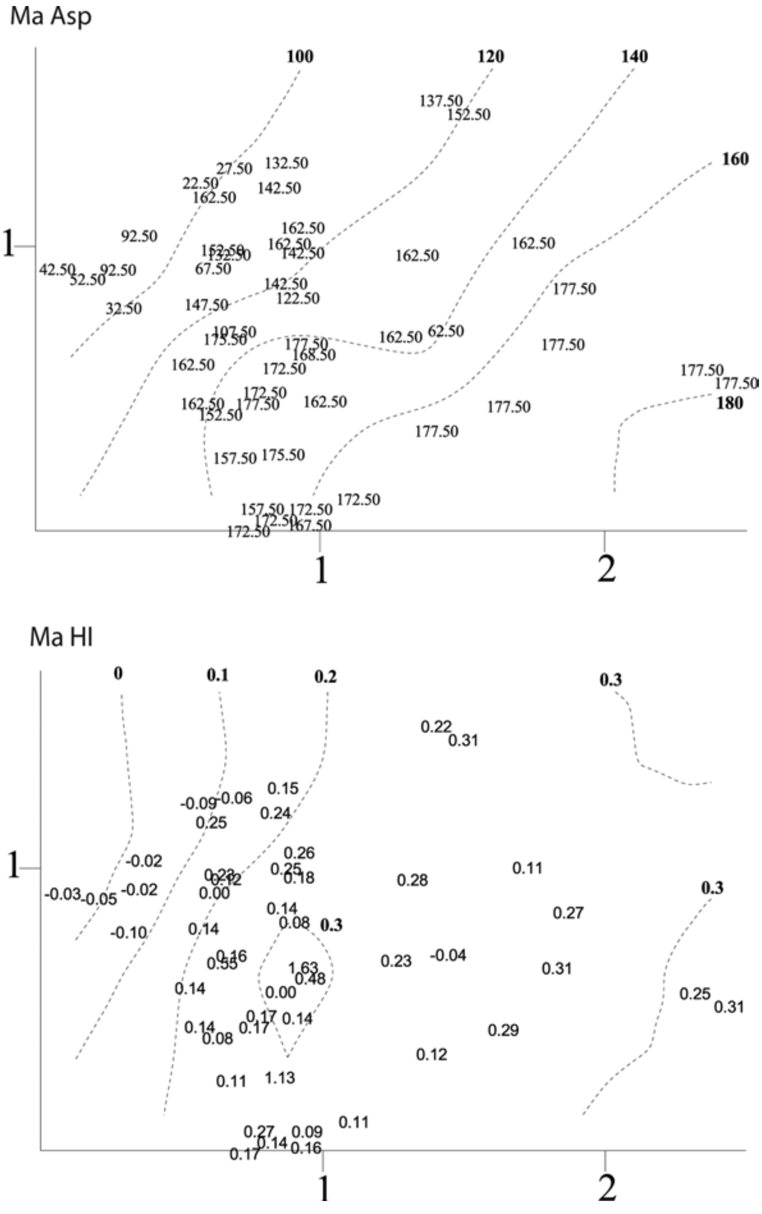

Figs 11-12. Lund: isolines for environmental variables in the DCA ordinations of 50 meso plots, axes 1 (horizontal) and 2 (vertical). Values for the environmental variables are plotted onto the meso plots' positions. Scaling in S.D. units. Fig. 11. Ma Asp ($R^2 = 0.491$). Fig. 12. Ma HI ($R^2 = 0.573$). R^2 refers to the coefficient of determination between original and smoothened values as interpolated from the isolines. Names of environmental variables in accordance with Table 2.

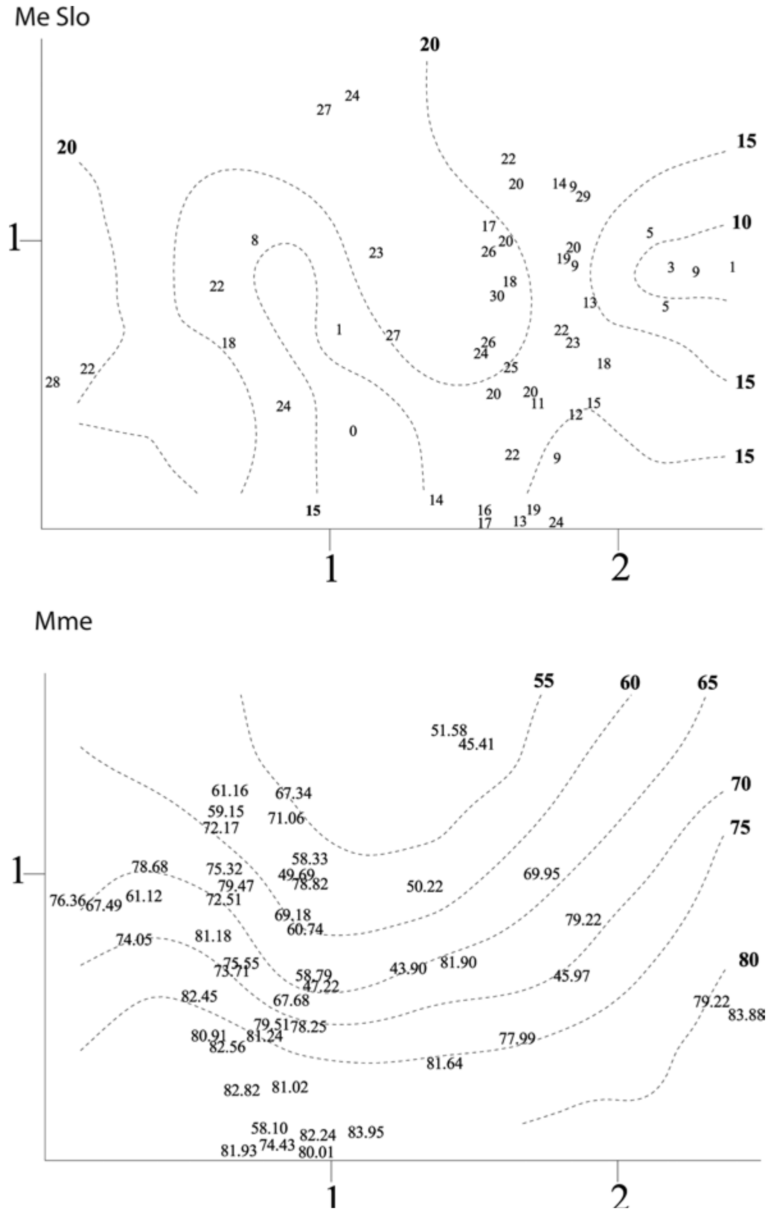

Figs 13-14. Lund: isolines for environmental variables in the DCA ordinations of 50 meso plots, axes 1 (horizontal) and 2 (vertical). Values for the environmental variables are plotted onto the meso plots' positions. Scaling in S.D. units. Fig. 13. Me Slo ($R^2 = 0.493$). Fig. 14. Mme (Soil moisture) ($R^2 = 0.503$). R^2 refers to the coefficient of determination between original and smoothened values as interpolated from the isolines. Names of environmental variables in accordance with Table 2.

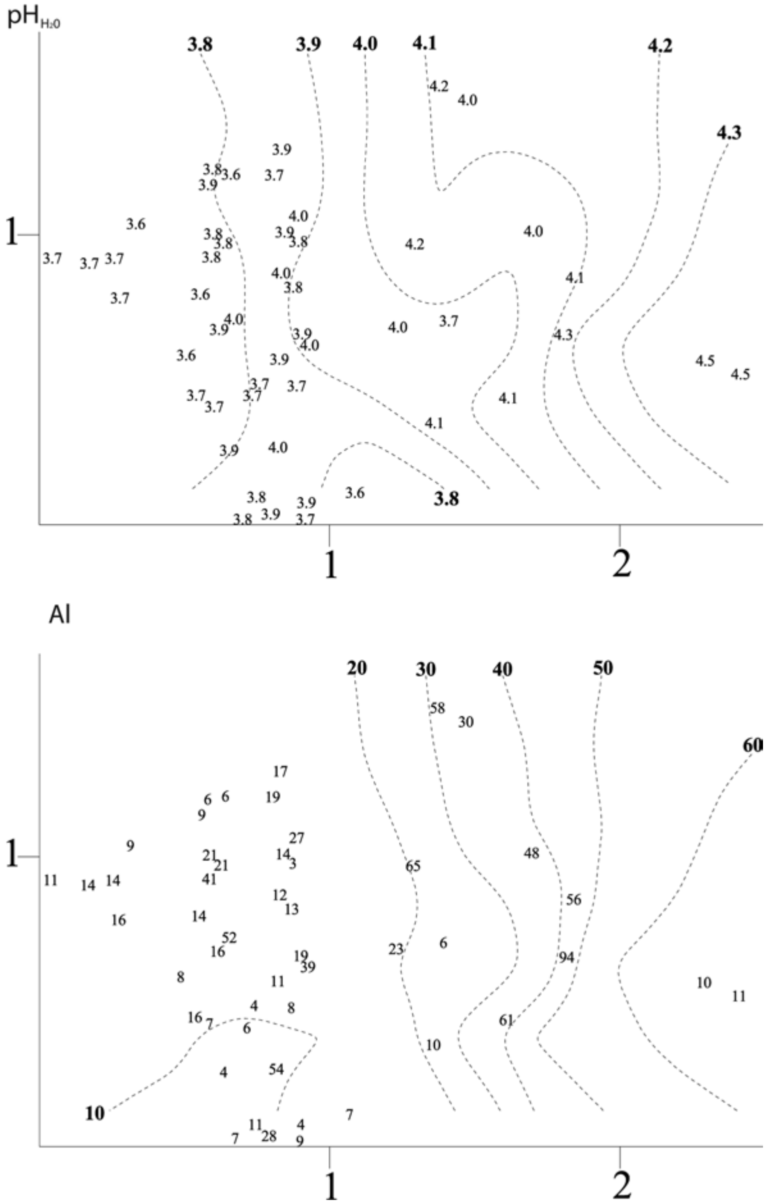

Figs 15-16. Lund: isolines for environmental variables in the DCA ordinations of 50 meso plots, axes 1 (horizontal) and 2 (vertical). Values for the environmental variables are plotted onto the meso plots' positions. Scaling in S.D. units. Fig. 15. pH_{H_2O} ($R^2 = 0.605$). Fig. 16. Al ($R^2 = 0.508$). R^2 refers to the coefficient of determination between original and smoothened values as interpolated from the isolines. Names of environmental variables in accordance with Table 2.

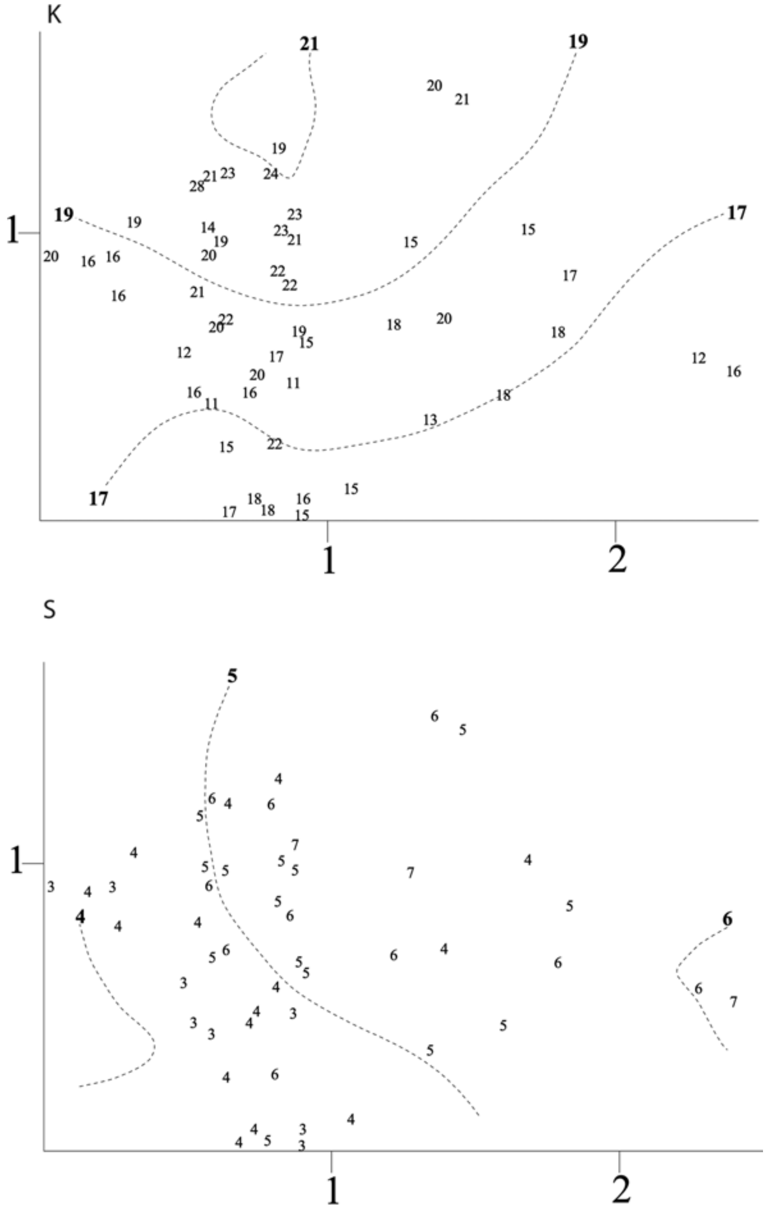

Figs 17-18. Lund: isolines for environmental variables in the DCA ordinations of 50 meso plots, axes 1 (horizontal) and 2 (vertical). Values for the environmental variables are plotted onto the meso plots' positions. Scaling in S.D. units. Fig. 17. K (R^2 = 0.437). Fig. 18. S (R^2 = 0.564). R^2 refers to the coefficient of determination between original and smoothened values as interpolated from the isolines. Names of environmental variables in accordance with Table 2.

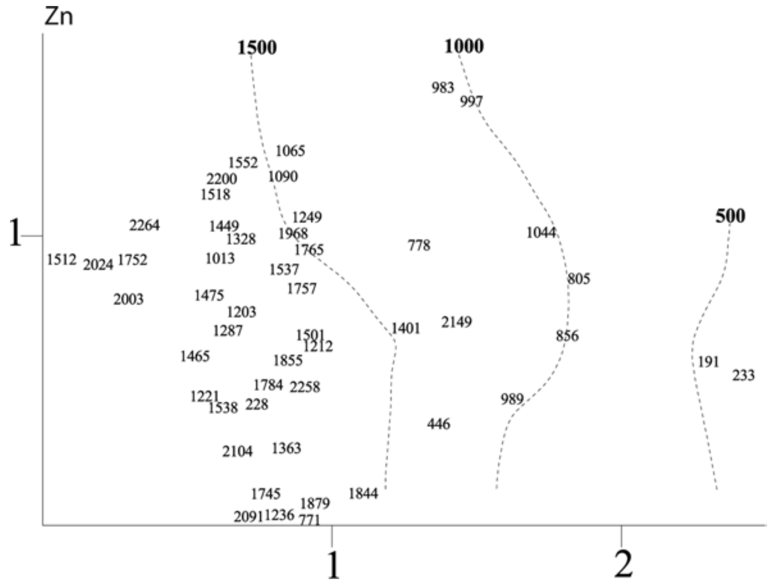

Fig. 19. Lund: isolines for environmental variables in the DCA ordinations of 50 meso plots, axes 1 (horizontal) and 2 (vertical). Values for the environmental variables are plotted onto the meso plots' positions. Scaling in S.D. units. Fig. 19. Zn ($R^2 = 0.585$). R^2 refers to the coefficient of determination between original and smoothened values as interpolated from the isolines. Names of environmental variables in accordance with Table 2.

For the second ordination axis, 78.76 % of the variation was explained at the macro plot scale and 21.24 % at the meso plot scale (Table 5).

At the macro plot scale, eleven environmental variables were significantly (at the $\alpha = 0.05$ level) related to DCA 1 while five variables (also at the $\alpha = 0.05$ level) were related to DCA 2. At the plot scale level, nine environmental variables were significantly related to DCA 1 and two variables to DCA 2 (Tables 4 and 5).

At the macro plot scale, soil concentrations of Ca, Mg, P and Zn decreased significantly along DCA 1 while pH and the concentrations of Total N, H and Al, macro plot aspect unfavourability and meso plot terrain form increased. At the meso plot scale, many of these variables showed the same tendencies. Predictors with additional significant relationship at the meso plot scale were meso plot unevenness which decreased (at the $\alpha = 0.05$ level) while medium soil depth (Sme) increased. Macro plot aspect unfavourability, meso plot terrain form and the concentration of Zn were, however, not significantly related to DCA 2 on the meso plot scale.

At the macro-plot scale, DCA 2 was positively related to the concentration of K and negatively related to aspect unfavourability, soil moisture, loss on ignition and the concentration of Na in soil. At the meso plot scale, DCA axis 2 was significantly negatively related to meso plot slope and significantly positively related to meso plot heat index (Table 5).

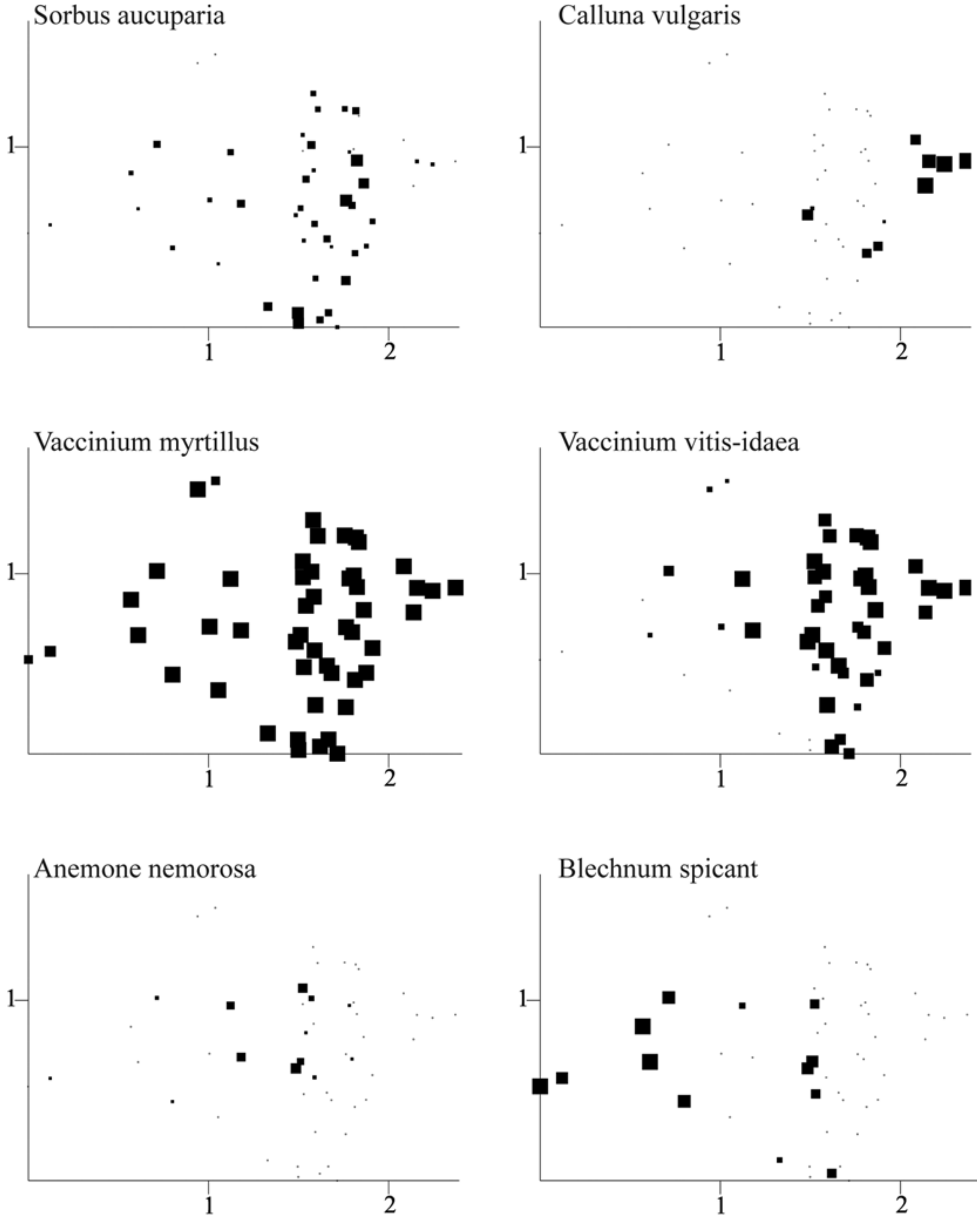

Figs 20-25. Lund: distributions of species abundances in the DCA ordination of 50 meso plots, axes 1 (horizontal) and 2 (vertical). Frequency in subplots for each species in each meso plot proportional to quadrate size. Scaling in S.D. units. Fig. 20. *Sorbus aucuparia*. Fig. 21. *Calluna vulgaris*. Fig. 22. *Vaccinium myrtillus*. Fig. 23. *Vaccinium vitis-idaea*. Fig. 24. *Anemona nemorosa*. Fig. 25. *Blechnum spicant*.

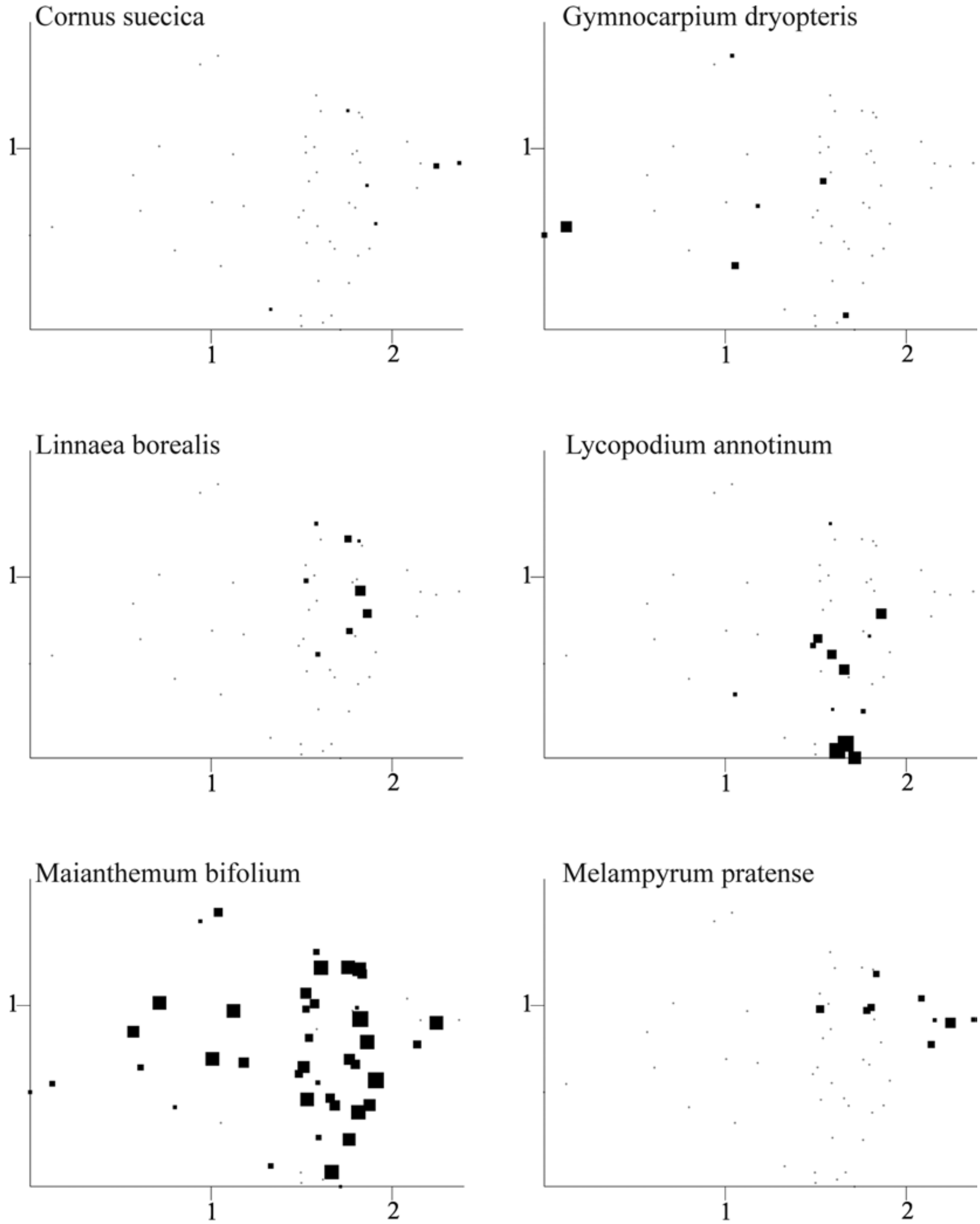

Figs 26-31. Lund: distributions of species abundances in the DCA ordination of 50 meso plots, axes 1 (horizontal) and 2 (vertical). Frequency in subplots for each species in each meso plot proportional to quadrate size. Scaling in S.D. units. Fig. 26. *Chamepericlymenum suecicum* (syn. *Cornus suecica*). Fig. 27. *Gynmocarpium dryopteris*. Fig. 28. *Linnaea borealis*. Fig. 29. *Lycopodium annotinum*. Fig. 30. *Maianthemum bifolium*. Fig. 31. *Melampyrum pratense*.

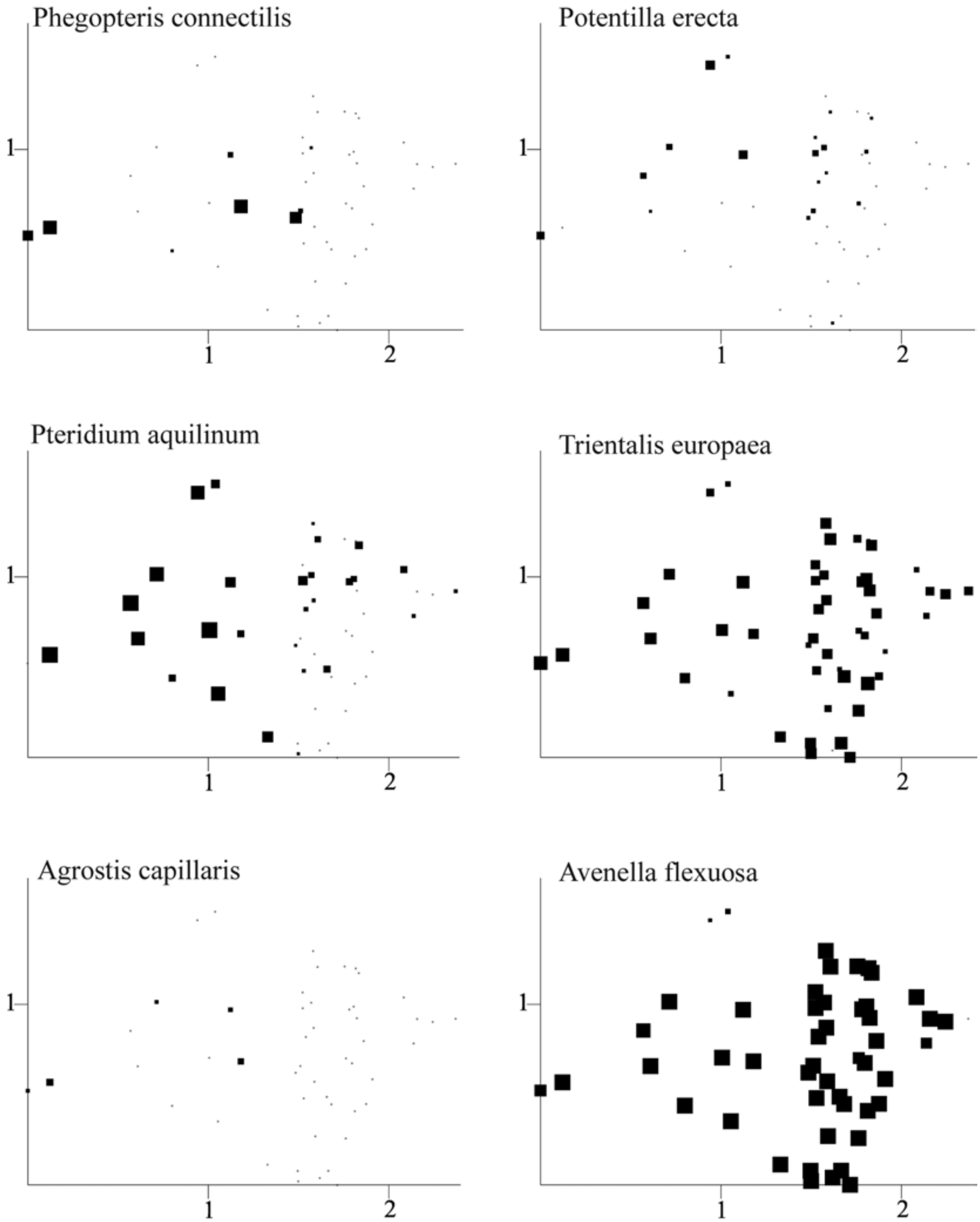

Figs 32-37. Lund: distributions of species abundances in the DCA ordination of 50 meso plots, axes 1 (horizontal) and 2 (vertical). Frequency in subplots for each species in each meso plot proportional to quadrate size. Scaling in S.D. units. Fig. 32. *Phegopteris connectilis*. Fig. 33. *Potentilla erecta*. Fig. 34. *Pteridium aquilinum*. Fig. 35. *Trientalis europaea*. Fig. 36. *Agrostis capillaris*. Fig. 37. *Avenella flexuosa*.

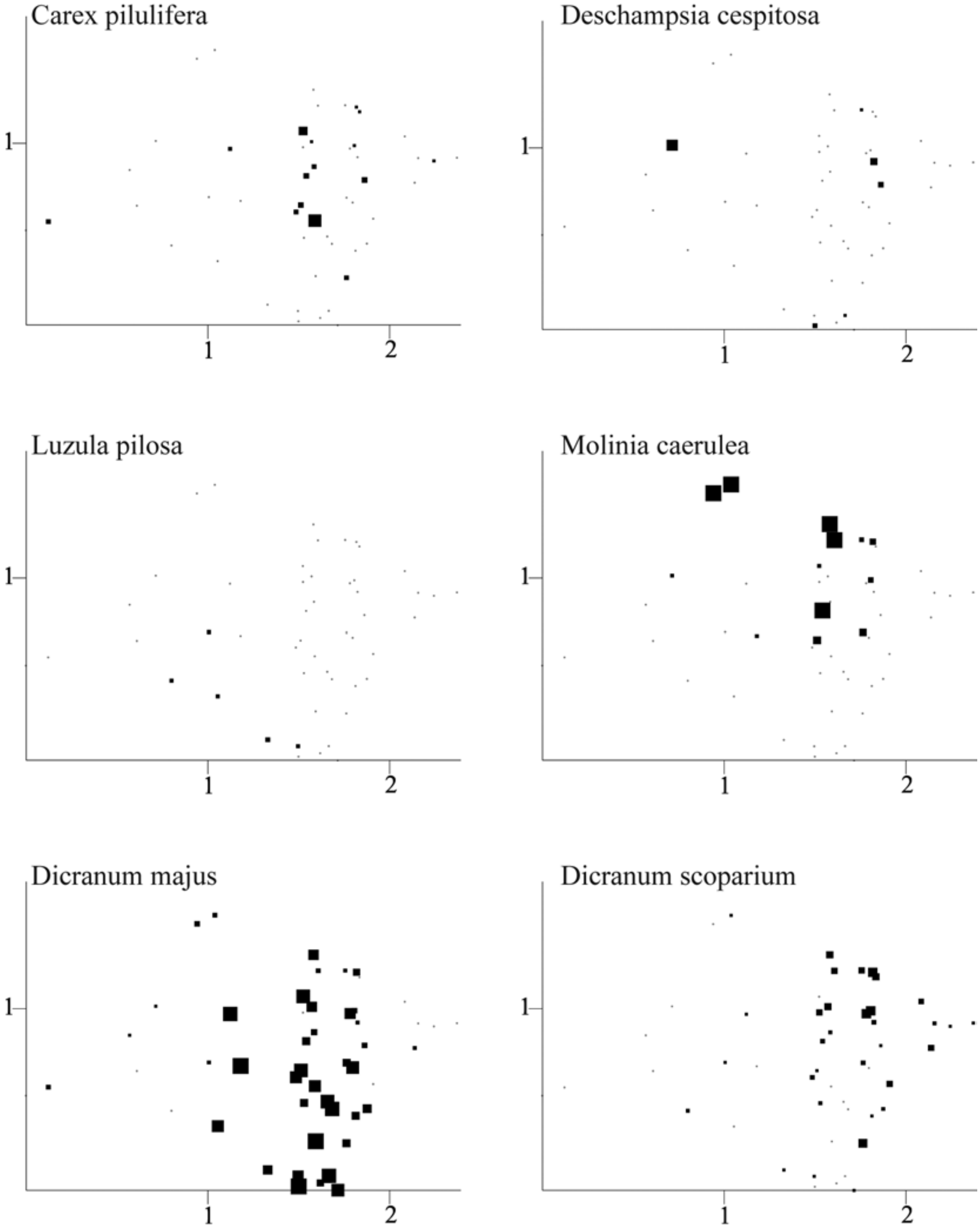

Figs 38-43. Lund: distributions of species abundances in the DCA ordination of 50 meso plots, axes 1 (horizontal) and 2 (vertical). Frequency in subplots for each species in each meso plot proportional to quadrate size. Scaling in S.D. units. Fig. 38. *Carex pilulifera*. Fig. 39. *Deschampsia cespitosa*. Fig. 40. *Luzula pilosa*. Fig. 41. *Molinia caerulea*. Fig. 42. *Dicranum majus*. Fig. 43. *Dicranum scoparium*.

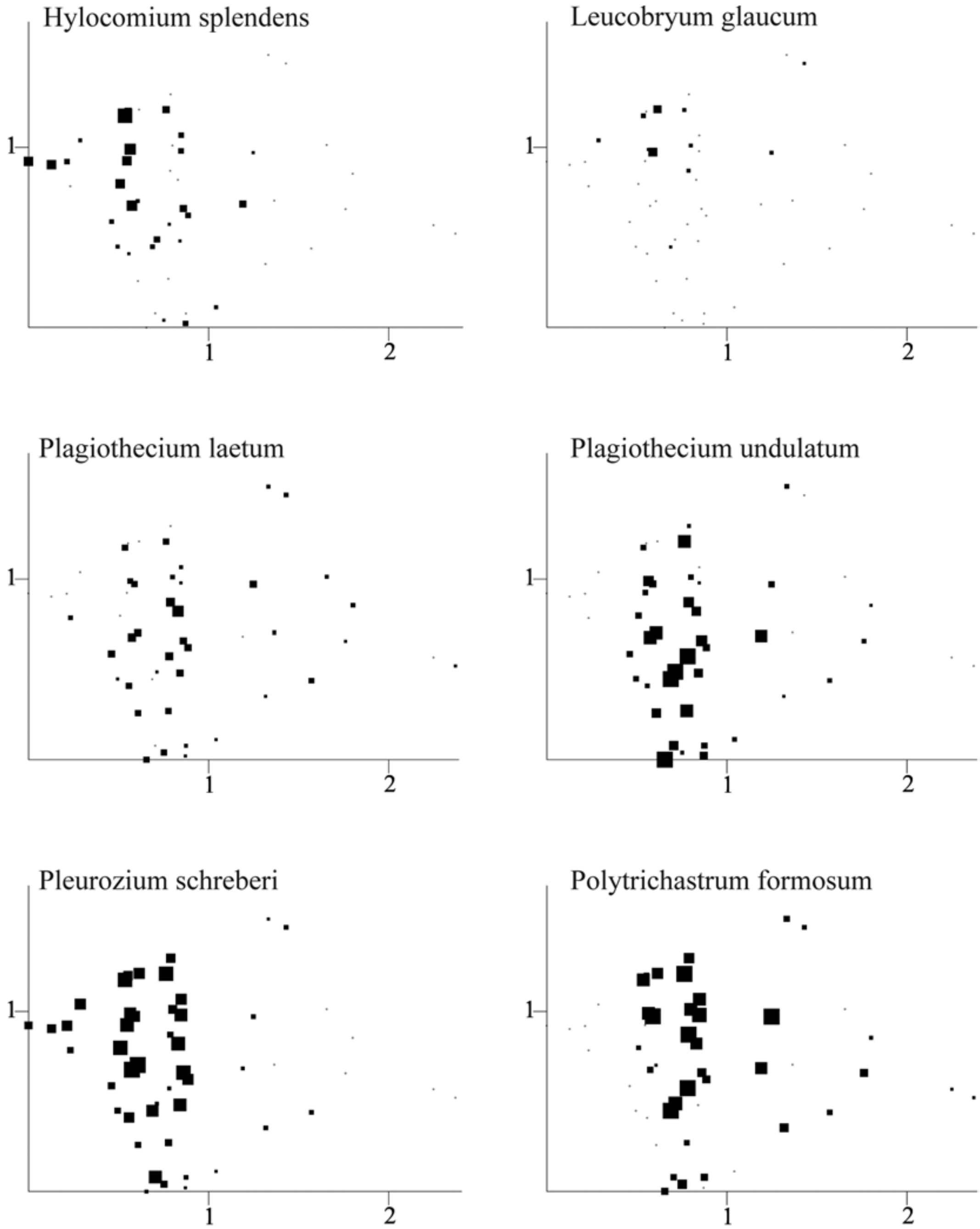

Figs 44-49. Lund: distributions of species abundances in the DCA ordination of 50 meso plots, axes 1 (horizontal) and 2 (vertical). Frequency in subplots for each species in each meso plot proportional to quadrate size. Scaling in S.D. units. Fig. 44. *Hylocomium splendens*. Fig. 45. *Leucobryum glaucum*. Fig. 46. *Plagiothecium laetum*. Fig. 47. *Plagiothecium undulatum*. Fig. 48. *Pleurozium schreberi*. Fig. 49. *Polytrichastrum formosum*.

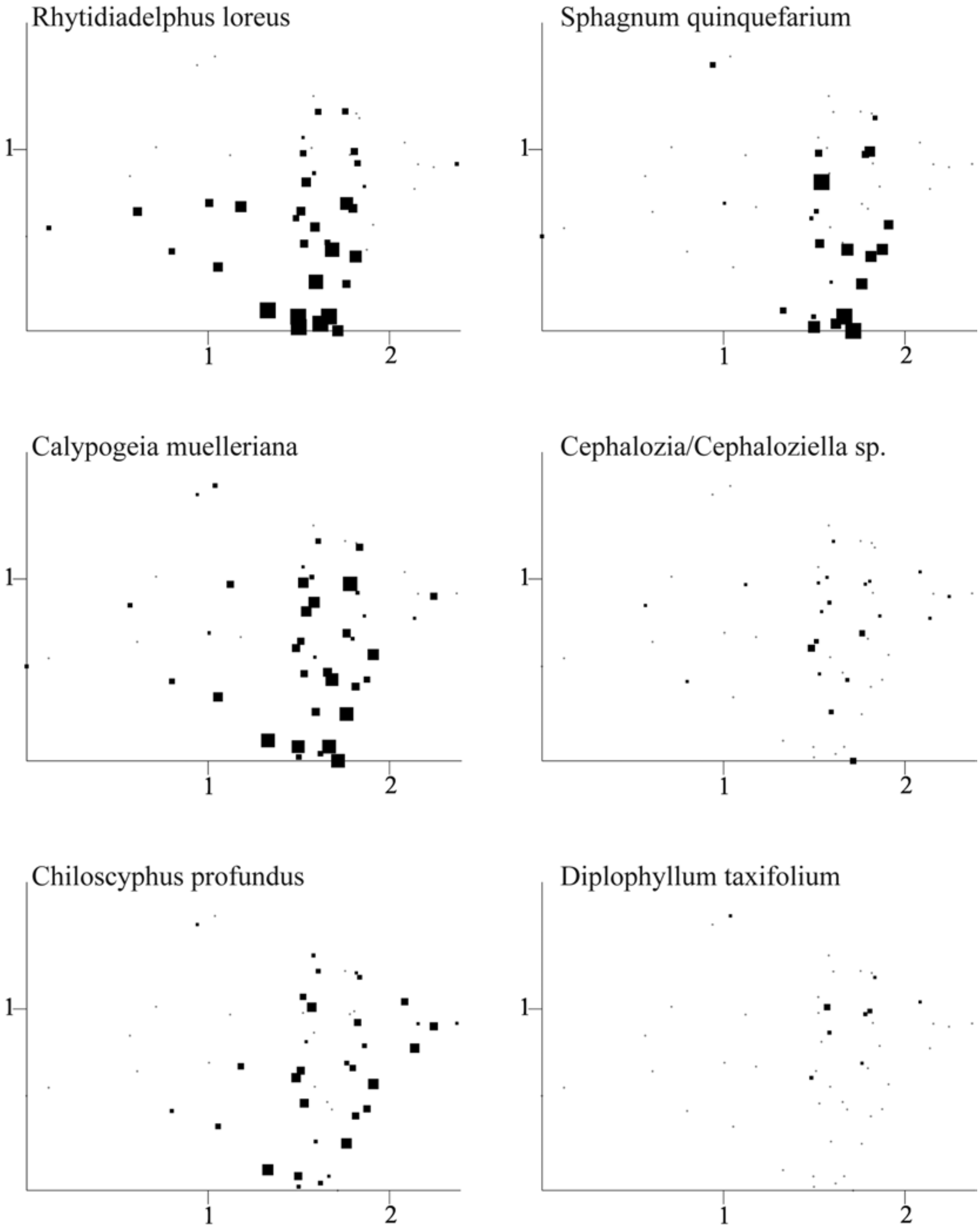

Figs 50-55. Lund: distributions of species abundances in the DCA ordination of 50 meso plots, axes 1 (horizontal) and 2 (vertical). Frequency in subplots for each species in each meso plot proportional to quadrate size. Scaling in S.D. units. Fig. 50. *Rhytidiadelphus loreus*. Fig. 51. *Sphagnum quinquefarium*. Fig. 52. *Calypogeia muelleriana*. Fig. 53. *Cephalozia*/*Cephaloziella* sp. Fig. 54. *Chiloscyphus profundus*. Fig. 55. *Diplophyllum taxifolium*.

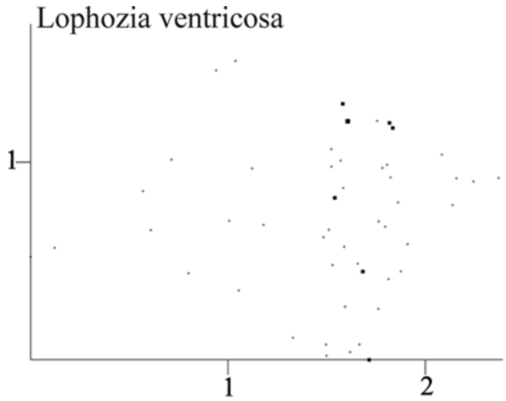

Fig. 56. Lund: distributions of species abundances in the DCA ordination of 50 meso plots, axes 1 (horizontal) and 2 (vertical). Frequency in subplots for each species in each meso plot proportional to quadrate size. Scaling in S.D. units. Fig. 56. *Lophozia ventricosa*.

Correlations between DCA ordination axes and environmental variables

Seven environmental variables had correlations with DCA axis 1 and three with DCA axis 2 at the $|\tau|$ > 0.3 level (Tables 4 and 5). The two measures of pH (pH_{H_2O}, τ = 0.511 and pH_{CaCl_2}, τ = 0.500) were best correlated with the first DCA axis (Fig. 15), while soil moisture (τ = –0.402) was the variable most strongly correlated with DCA 2 (Fig. 14).

Other strong correlations with DCA 1 and 2 at the $|\tau|$ > 0.3 level which are visualised in iso-diagram figures are macro plot aspect (τ = –0.400, Fig. 11), macro plot heat index (τ = –0.337, Fig. 12), meso plot slope (τ = –0.322, Fig. 13) and the concentrations of Al (τ = –0.303, Fig. 16), K (τ = 0.358 with DCA 2, Fig. 17), S (τ = 0.309, Fig. 18) and Zn (τ = –0.339, Fig. 19).

Frequent species

A total of 69 species were recorded within the fifty 1×1m meso plots: 35 vascular plants, 19 mosses, 15 liverworts (and no lichens). The most frequent species were (the sum of subplot frequencies in brackets): *Vaccinium myrtillus* (779 out of 800), *Avenella flexuosa* (744), *Vaccinium vitis-idaea* (543), *Trientalis europaea* (452), *Maianthemum bifolium* (386), *Pleurozium schreberi* (363), *Dicranum majus* (339), *Polytrichastrum formosum* (311), *Rhytidiadelphus loreus* (278), and *Plagiothecium undulatum* (271).

The distribution of species abundance in the DCA ordination

Common species with wide ecological amplitude were *Vaccinium myrtillus* (Fig. 22), *Maianthemum bifolium* (Fig. 30), *Trientalis europaea* (Fig. 35) and *Avenella flexuosa* (Fig. 37).

Species restricted to the left hand side of the ordination diagram and which hence showed optimum in sample plots with low pH values were *Calluna vulgaris* (Fig. 21), *Chamaepericlymenum suecicum* (Fig. 26), *Linnaea borealis* (Fig. 28), *Lycopodium annotinum* (Fig. 29) and *Melampyrum* *pratense* (Fig. 31). The mosses *Dicranium scoparium* (Fig. 43), *Hylocomium splendens* (Fig. 44) and *Pleurozium schreberi* (Fig. 48) also showed preference for low DCA axis 1 values.

Agrostis capillaris (Fig. 36), *Diplophyllum taxifolium* (Fig. 55) and to some extent *Blechnum spicant* (Fig. 25), *Phegopteris connectilis* (Fig. 32) and *Potentilla erecta* (Fig. 33), situated mainly at the right hand side of the DCA diagram, showed preferences for sites with higher pH.

Most of the other species had their optimum distribution at low to medium DCA axis 1 scores.

MØSVATN REFERENCE AREA

Correlations between environmental variables

There were strong pairwise correlations between several of the topographical variables, between soil chemical variables and between topographical and chemical variables related to soil richness (Table 6).

Macro and meso plot slopes and heat indices were negatively correlated, and slopes were positively correlated with meso plot terrain form. Tree basal area (tree biomass) was positively correlated with macro plot slope, macro plot heat index and macro plot aspect unfavourability.

LOI was negatively correlated with soil pH and with concentrations of all extractable elements, except P, and positively correlated with exchangeable H. In general, element concentrations were pairwise positively correlated, and all were negatively correlated with exchangeable H.

Tree basal area, macro plot and meso plot slope and heat indices were correlated with chemical variables that were related to a gradient in soil nutrient richness. They were positively (except heat indices) correlated with total nitrogen, extractable Ca, Mg, Na and K and with pH, and negatively

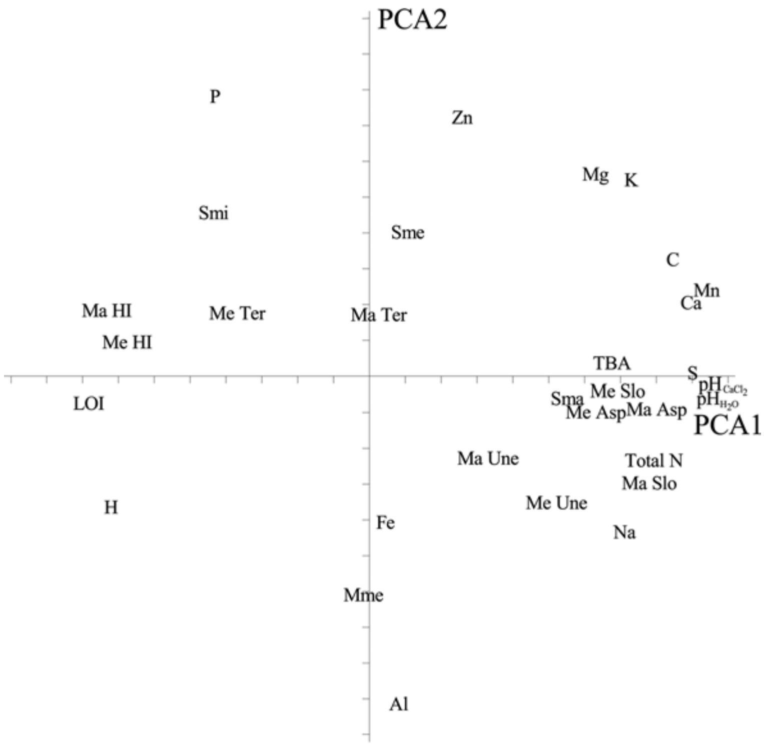

Fig. 57. Møsvatn: PCA ordination of 31 environmental variables. Abbreviations in accordance with Table 2. Positions of variables in the ordination space give the head of variable vectors. Tickmarks indicate 0.1 units along both axes.

Table 6. Møsvatn: Kendall's rank correlation coefficients τ between 31 environmental variables in the 50 meso plots (lower triangle), with significance probabilities (upper triangle). Statistically significant correlations (P<0.05) in bold face. Names of explanatory variables abbreviated in accordance with Table 2.

	1	2	3	4	5	6	7	8	9	10	11	12	13	14	15	16
01 Ma Slo	*	**0.004**	**0.000**	0.910	**0.028**	**0.007**	**0.000**	0.085	**0.000**	**0.000**	**0.038**	**0.014**	0.274	0.148	0.564	**0.011**
02 Ma Asp	**0.323**	*	**0.000**	0.415	0.177	**0.028**	**0.022**	**0.000**	**0.000**	**0.004**	0.091	0.657	0.345	**0.002**	0.515	**0.002**
03 Ma HI	**–0.713**	**–0.658**	*	0.524	0.052	**0.003**	**0.000**	**0.001**	**0.000**	**0.000**	0.081	0.141	0.953	**0.016**	0.880	**0.002**
04 Ma Ter	–0.012	–0.089	0.067	*	0.892	0.430	0.097	0.551	0.318	0.094	0.722	0.958	0.748	0.077	0.515	0.537
05 Ma Une	**0.238**	0.145	–0.200	0.014	*	0.195	0.113	0.118	**0.020**	0.489	**0.001**	0.084	0.100	0.880	0.177	0.445
06 TBA	**0.294**	**0.237**	**–0.308**	0.082	0.133	*	0.091	**0.046**	**0.007**	0.109	**0.028**	0.262	0.424	0.415	0.496	**0.010**
07 Me Slo	**0.585**	**0.247**	**–0.470**	–0.174	0.163	0.174	*	0.207	**0.000**	**0.000**	0.181	0.177	0.584	**0.001**	0.794	**0.001**
08 Me Asp	0.188	**0.589**	**–0.351**	0.063	0.161	**0.206**	0.131	*	**0.000**	0.352	**0.013**	0.727	0.349	0.077	0.953	**0.003**
09 Me HI	**–0.493**	**–0.439**	**0.503**	0.102	**–0.232**	**–0.268**	**–0.666**	**–0.489**	*	**0.002**	**0.016**	0.200	0.251	**0.003**	0.834	**0.000**
10 Me Ter	**–0.415**	**–0.312**	**0.420**	0.176	–0.071	–0.165	**–0.403**	–0.097	**0.317**	*	0.106	0.054	0.573	0.148	0.226	0.122
11 Me Une	**0.221**	0.179	–0.177	0.037	**0.321**	**0.222**	0.136	**0.254**	**–0.238**	–0.164	*	**0.002**	0.687	0.411	0.402	0.155
12 Smi	**–0.279**	–0.050	0.160	0.006	–0.186	–0.121	–0.146	–0.038	0.135	0.209	**–0.332**	*	**0.003**	0.302	0.206	**0.009**
13 Sme	–0.117	0.100	–0.006	–0.033	–0.166	0.081	0.056	0.095	–0.114	0.057	0.040	**0.318**	*	**0.018**	**0.033**	0.967
14 Sma	0.154	**0.323**	**–0.244**	–0.182	–0.015	0.082	**0.334**	0.180	**–0.295**	–0.147	0.082	–0.110	**0.237**	*	0.900	**0.002**
15 Mme	0.061	0.068	–0.015	–0.066	0.135	–0.068	0.026	–0.006	0.020	–0.122	0.082	–0.133	**–0.211**	–0.012	*	0.139
16 LOI	**–0.268**	**–0.318**	**0.311**	0.063	–0.076	**–0.258**	**–0.344**	**–0.305**	**0.406**	0.156	–0.140	**0.274**	0.004	**–0.311**	0.144	*
17 Total N	**0.244**	**0.423**	**–0.283**	0.001	0.141	**0.325**	0.133	**0.305**	**–0.303**	–0.146	**0.233**	–0.199	0.019	**0.270**	0.118	**–0.398**
18 pH_{H_2O}	**0.364**	**0.304**	**–0.357**	–0.026	0.101	**0.407**	**0.354**	**0.251**	**–0.411**	**–0.218**	**0.206**	**–0.369**	–0.066	**0.263**	–0.060	**–0.622**
19 pH_{CaCl_2}	**0.360**	**0.307**	**–0.357**	–0.045	0.116	**0.378**	**0.352**	**0.236**	**–0.400**	**–0.200**	**0.207**	**–0.368**	–0.076	**0.284**	–0.071	**–0.630**
20 H	**–0.323**	**–0.302**	**0.391**	–0.006	–0.069	**–0.345**	**–0.369**	–0.191	**0.369**	**0.240**	–0.106	0.186	0.024	–0.151	0.120	**0.453**
21 Al	**0.215**	0.076	–0.068	–0.073	0.061	0.043	–0.003	0.084	–0.012	–0.124	**0.211**	**–0.306**	**–0.251**	0.085	**0.360**	–0.048
22 C	**0.308**	**0.383**	**–0.359**	0.077	0.123	**0.290**	**0.256**	**0.250**	**–0.305**	–0.124	0.097	–0.146	0.039	0.179	–0.166	**–0.554**
23 Ca	**0.457**	**0.397**	**–0.499**	–0.015	0.115	**0.459**	**0.457**	**0.211**	**–0.429**	**–0.252**	0.107	–0.190	0.042	**0.215**	–0.089	**–0.510**
24 Fe	0.088	0.153	–0.032	0.058	0.118	–0.098	–0.062	0.162	0.034	–0.025	0.132	–0.053	–0.143	–0.037	0.148	–0.074
25 K	0.201	**0.351**	**–0.323**	0.097	0.100	**0.297**	**0.258**	**0.242**	**–0.262**	–0.073	0.023	–0.042	0.125	0.151	**–0.200**	**–0.471**
26 Mg	0.161	**0.288**	**–0.249**	0.190	0.044	**0.223**	**0.256**	**0.244**	**–0.264**	–0.127	0.035	0.078	0.108	0.021	–0.179	**–0.362**
27 Mn	**0.326**	**0.324**	**–0.376**	–0.004	0.076	**0.357**	**0.388**	0.194	**–0.385**	–0.196	0.109	**–0.246**	–0.011	**0.252**	–0.125	**–0.582**
28 Na	**0.515**	**0.394**	**–0.491**	–0.073	0.148	**0.291**	**0.340**	**0.227**	**–0.372**	**–0.344**	0.188	**–0.248**	–0.062	0.168	**0.223**	**–0.277**
29 P	**–0.382**	–0.174	**0.206**	0.013	–0.090	–0.125	–0.144	**–0.203**	**0.195**	**0.213**	**–0.269**	**0.419**	**0.267**	–0.123	**–0.326**	**0.216**
30 S	**0.422**	**0.516**	**–0.509**	–0.092	0.172	**0.354**	**0.332**	**0.347**	**–0.441**	**–0.212**	0.191	–0.197	0.054	**0.313**	–0.051	**–0.496**
31 Zn	–0.026	0.061	0.002	0.078	–0.003	–0.029	0.173	0.020	–0.076	–0.003	–0.089	0.184	0.117	0.019	**–0.254**	**–0.231**

Table 6 (continued). Møsvatn: Kendall's rank correlation coefficients τ between 31 environmental variables in the 50 meso plots (lower triangle), with significance probabilities (upper triangle). Statistically significant correlations (P<0.05) in bold face. Names of explanatory variables abbreviated in accordance with Table 2.

	17	18	19	20	21	22	23	24	25	26	27	28	29	30	31
01 Ma Slo	**0.021**	**0.001**	**0.001**	**0.002**	**0.042**	**0.004**	**0.000**	0.404	0.057	0.128	**0.002**	**0.000**	**0.000**	**0.000**	0.803
02 Ma Asp	**0.000**	**0.004**	**0.004**	**0.004**	0.471	**0.000**	**0.000**	0.145	**0.042**	**0.006**	**0.002**	**0.000**	0.096	**0.000**	0.560
03 Ma HI	**0.005**	**0.000**	**0.000**	**0.000**	0.501	**0.000**	**0.000**	0.749	**0.001**	**0.013**	**0.000**	**0.000**	**0.040**	**0.000**	0.987
04 Ma Ter	0.993	0.800	0.660	0.953	0.472	0.452	0.886	0.571	0.339	0.062	0.966	0.472	0.899	0.365	0.441
05 Ma Une	0.156	0.314	0.247	0.486	0.540	0.217	0.250	0.237	0.318	0.656	0.445	0.137	0.369	0.085	0.980
05 TBA	**0.001**	**0.000**	**0.000**	**0.001**	0.668	**0.004**	**0.000**	0.326	**0.003**	**0.026**	**0.000**	**0.004**	0.211	**0.000**	0.769
07 Me Slo	0.187	**0.000**	**0.000**	**0.000**	0.980	**0.011**	**0.000**	0.539	**0.010**	**0.011**	**0.000**	**0.001**	0.150	**0.001**	0.085
08 Me Asp	**0.003**	**0.013**	**0.020**	0.058	0.404	**0.013**	**0.036**	0.108	**0.016**	**0.016**	0.054	**0.025**	**0.044**	**0.001**	0.846
09 Me HI	**0.002**	**0.000**	**0.000**	**0.000**	0.900	**0.002**	**0.000**	0.732	**0.007**	**0.007**	**0.000**	**0.000**	**0.046**	**0.000**	0.437
10 Me Ter	0.148	**0.031**	**0.048**	**0.017**	0.220	0.220	**0.012**	0.801	0.470	0.207	0.051	**0.001**	**0.034**	**0.036**	0.973
11 Me Une	**0.018**	**0.037**	**0.036**	0.284	**0.032**	0.323	0.276	0.180	0.815	0.725	0.269	0.056	**0.006**	0.052	0.366
12 Smi	0.059	**0.000**	**0.000**	0.077	**0.004**	0.166	0.072	0.615	0.690	0.456	**0.019**	**0.018**	**0.000**	0.061	0.080
13 Sme	0.847	0.508	0.446	0.808	**0.011**	0.694	0.669	0.147	0.206	0.272	0.913	0.530	**0.007**	0.586	0.238
14 Sma	**0.006**	**0.008**	**0.004**	0.125	0.388	0.069	**0.029**	0.706	0.125	0.834	**0.011**	0.089	0.212	**0.002**	0.847
15 Mme	0.225	0.541	0.467	0.219	**0.000**	0.089	0.362	0.130	**0.040**	0.067	0.201	**0.022**	**0.001**	0.598	**0.009**
16 LOI	**0.000**	**0.000**	**0.000**	**0.000**	0.622	**0.000**	**0.000**	0.447	**0.000**	**0.000**	**0.000**	**0.005**	**0.027**	**0.000**	**0.018**
17 Total N	*	**0.000**	**0.000**	**0.003**	**0.011**	**0.001**	**0.000**	0.311	**0.049**	0.281	**0.000**	**0.001**	**0.000**	**0.000**	0.336
18 pH_{H_2O}	**0.502**	*	**0.000**	**0.000**	0.757	**0.000**	**0.000**	0.259	**0.000**	**0.001**	**0.000**	**0.001**	**0.001**	**0.000**	0.083
19 pH_{CaCl_2}	**0.492**	**0.946**	*	**0.000**	0.732	**0.000**	**0.000**	0.266	**0.000**	**0.001**	**0.000**	**0.001**	**0.002**	**0.000**	0.064
20 H	**–0.288**	**–0.614**	**–0.613**	*	**0.004**	**0.000**	**0.000**	**0.021**	**0.000**	**0.000**	**0.000**	**0.017**	0.670	**0.000**	**0.003**
21 Al	**0.249**	0.030	0.034	**0.280**	*	0.371	0.457	**0.000**	**0.016**	**0.000**	0.157	**0.002**	**0.000**	0.498	**0.000**
22 C	**0.334**	**0.512**	**0.517**	**–0.471**	–0.087	*	**0.000**	0.296	**0.000**	**0.000**	**0.000**	**0.013**	0.719	**0.000**	**0.000**
23 Ca	**0.404**	**0.657**	**0.645**	**–0.652**	–0.073	**0.535**	*	0.201	**0.000**	**0.000**	**0.000**	**0.000**	0.201	**0.000**	**0.033**
24 Fe	0.099	–0.111	–0.109	**0.224**	**0.442**	0.102	–0.125	*	0.477	0.732	0.080	0.178	**0.005**	0.940	0.993
25 K	**0.192**	**0.450**	**0.461**	**–0.473**	**–0.236**	**0.691**	**0.566**	–0.069	*	**0.000**	**0.000**	0.072	0.173	**0.000**	**0.000**
26 Mg	0.105	**0.334**	**0.333**	**–0.497**	**–0.345**	**0.517**	**0.502**	0.033	**0.558**	*	**0.000**	0.252	0.148	**0.004**	**0.000**
27 Mn	**0.355**	**0.750**	**0.767**	**–0.691**	–0.138	**0.587**	**0.683**	–0.171	**0.579**	**0.447**	*	**0.002**	0.139	**0.000**	**0.000**
28 Na	**0.334**	**0.330**	**0.319**	**–0.233**	**0.301**	**0.242**	**0.433**	0.131	0.176	0.112	**0.296**	*	**0.000**	**0.000**	0.118
29 P	**–0.378**	**–0.322**	**–0.307**	0.042	**–0.620**	–0.035	–0.125	**–0.273**	0.133	0.141	–0.144	**–0.450**	*	0.083	**0.005**
30 S	**0.425**	**0.529**	**0.535**	**–0.393**	0.066	**0.618**	**0.561**	0.007	**0.538**	**0.282**	**0.571**	**0.425**	-0.169	*	0.362
31 Zn	–0.094	0.170	0.181	**–0.295**	**–0.433**	**0.367**	**0.208**	0.001	**0.427**	**0.549**	**0.342**	–0.153	**0.275**	0.089	*

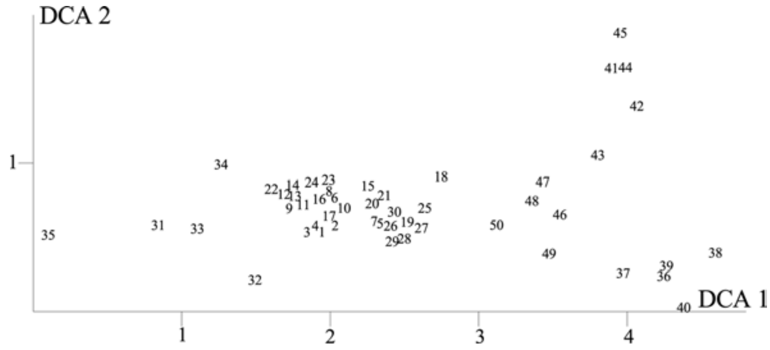

Fig. 58. Møsvatn: DCA ordination diagram of 50 meso plots, axes 1 (horizontal) and 2 (vertical). Meso plot number are plotted just right of the sample plot positions. Scaling of axes in S.D. units.

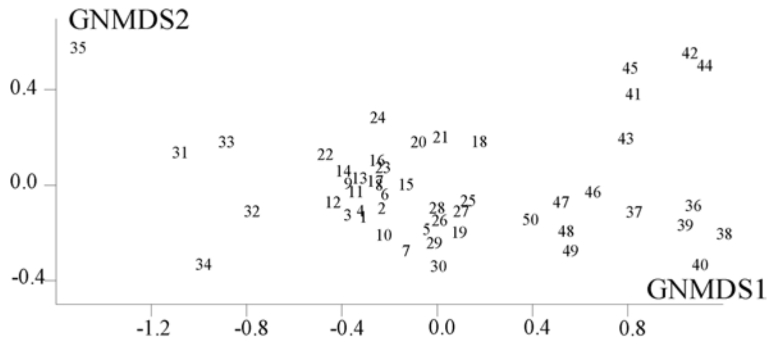

Fig. 59. Møsvatn: GNMDS ordination biplot diagram of 50 meso plots (indicated by their number).

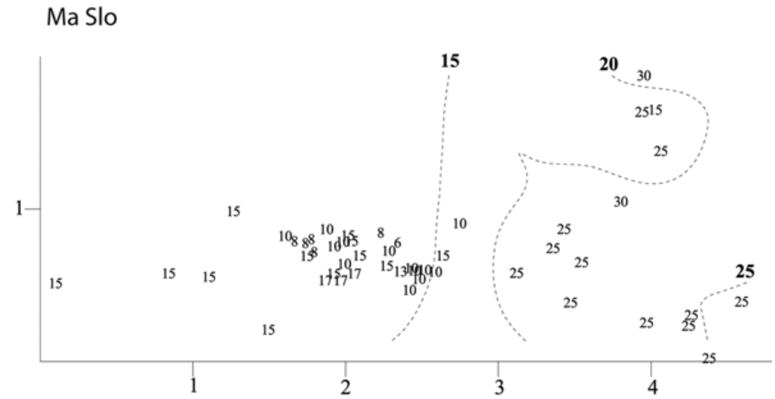

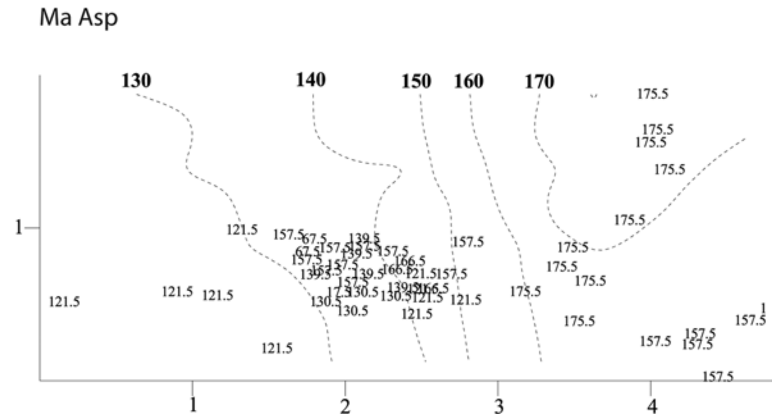

Figs 60-61. Møsvatn: isolines for environmental variables in the DCA ordinations of 50 meso plots, axes 1 (horizontal) and 2 (vertical). Values for the environmental variables are plotted onto the meso plots' positions. Scaling in S.D. units. Fig. 60. Ma Slo ($R^2 = 0.648$). Fig. 61. Ma Asp ($R^2 = 0.615$). R^2 refers to the coefficient of determination between original and smoothened values as interpolated from the isolines. Names of environmental variables in accordance with Table 2.

correlated (except heat indices) with LOI and exchangeable H. Minimum soil depth was positively correlated with soil acidity (H) and negatively correlated with pH while maximum soil depth was positively correlated with pH.

Macro plot terrain form and terrain unevenness showed no significant correlations with soil chemical variables. However, the meso plot terrain form was negatively correlated with soil pH and extractable concentrations of Ca and Na, while meso plot terrain unevenness was positively correlated with soil pH.

Soil moisture was not significantly correlated with topographical variables and heat index. However, it was positively correlated with extractable Na and Al and negatively correlated with extractable P, K and Zn.

Table 7. Møsvatn: Split-plot GLM analysis and Kendall's nonparametric correlation coefficient τ between DCA 1 and 31 environmental variables (predictor) in the 50 meso plots. df_{resid}: degrees of freedom for the residuals; *SS*: total variation; *FVE*: fraction of total variation attributable to a given scale (macro plot or meso plot); SS_{expl}/SS: fraction of the variation attributable to the scale in question, explained by a variable; *r*: model coefficient (only given when significant at the $\alpha = 0.05$ level, otherwise blank); *F*: *F* statistic for test of the hypothesis that $r = 0$ against the two-tailed alternative. Split-plot GLM relationships significant at level $\alpha = 0.05$, *P*, *F*, *r* and SS_{expl}/SS, and Kendall's nonparametric correlation coefficient $|\tau| \geq 0.30$ are given in bold face. Numbers and abbreviations for names of environmental variables are in accordance with Tab. 2.

Predictor	Dependent variable = DCA 1 (SS = 50.8559)								Correlation between predictor and DCA 1
	Error level								
	Macro plot $df_{resid} = 8$ $SS_{macro\ plot} = 47.6090$ $FVE = 0.9362$ of SS				Meso plot within macro plot $df_{resid} = 39$ $SS_{meso\ plot} = 3.24690$ $FVE = 0.0638$ of SS				Total
	$SS_{expl}/SS_{macro\ plot}$	*r*	*F*	*P*	$SS_{expl}/SS_{meso\ plot}$	*r*	*F*	*P*	τ
Ma Slo	**0.4611**	**2.6769**	**6.8448**	**0.0308**	0.0007		0.0273	0.8696	**0.388**
Ma Asp	**0.4985**	**2.6061**	**7.9514**	**0.0225**	0.0283		1.1350	0.2933	**0.441**
Ma HI	**0.7252**	**–4.6325**	**21.2480**	**0.0017**	0.0075		0.2942	0.5906	**–0.433**
Ma Ter	0.1041		0.9297	0.3632	0.0411		1.6733	0.2034	–0.128
Ma Une	0.1335		1.2323	0.2992	0.0065		0.2554	0.6161	0.131
TBA	**0.6836**	**4.0763**	**17.2840**	**0.0032**	0.0008		0.0310	0.8610	**0.617**
Me Slo	**0.5123**	**4.1573**	**8.4031**	**0.0199**	0.0386		1.5677	0.2180	**0.379**
Me Asp	0.0902		0.7930	0.3992	0.0213		0.8508	0.3620	0.035
Me HI	**0.7630**	**–4.7897**	**25.7500**	**0.0294**	0.0565		0.0291	0.8655	**–0.426**
Me Ter	**0.6624**	**–7.2123**	**15.6980**	**0.0042**	0.0026		0.1031	0.7499	–0.250
Me Une	**0.5105**	**6.6347**	**8.3436**	**0.0203**	0.0220		0.8777	0.3546	0.177
Smi	**0.5935**	**–4.3949**	**11.6790**	**0.0091**	0.0213		0.8494	0.3624	–0.297
Sme	0.0000		0.0000	0.9968	0.0168		0.6650	0.4198	–0.002
Sma	**0.6022**	**5.6671**	**12.1090**	**0.0083**	0.0009		0.0338	0.8551	**0.364**
Mme	0.0142		0.1150	0.7433	0.0643		2.6806	0.1096	0.047
LOI	**0.6560**	**–3.0244**	**15.2590**	**0.0045**	0.0002		0.0093	0.9237	**–0.499**
Total N	**0.8349**	**5.7496**	**40.4630**	**0.0002**	0.0043		0.1695	0.6829	**0.500**
pH_{H_2O}	**0.9084**	**4.0510**	**79.3780**	**0.0000**	0.0076		0.2995	0.5873	**0.716**
pH_{CaCl_2}	**0.9198**	**3.9279**	**91.7770**	**0.0000**	0.0027		0.1053	0.7473	**0.726**
H	**0.7214**	**–4.6122**	**20.7130**	**0.0019**	**0.1006**	**–0.6547**	**4.3636**	**0.0433**	**–0.536**
Al	0.0470		0.3944	0.5475	0.0500		2.0534	0.1598	0.105
C	**0.6319**	**3.5272**	**13.7320**	**0.0060**	0.0026		0.1011	0.7522	**0.491**
Ca	**0.8994**	**5.1352**	**71.5000**	**0.0000**	**0.0981**	**0.7604**	**4.2421**	**0.0462**	**0.675**
Fe	0.0238		0.1948	0.6706	0.0318		1.2798	0.2648	–0.045
K	**0.5455**	**4.2784**	**9.6034**	**0.0147**	**0.0987**	**0.5387**	**4.2692**	**0.0455**	**0.450**
Mg	0.2609		2.8233	0.1314	0.0432		1.7621	0.1921	**0.324**
Mn	**0.8145**	**3.2564**	**35.1220**	**0.0004**	**0.0989**	**0.6429**	**4.2791**	**0.0453**	**0.636**
Na	**0.7596**	**4.3704**	**25.2840**	**0.0010**	0.0018		0.0684	0.7950	**0.458**
P	**0.4529**	**–2.7878**	**6.6221**	**0.0330**	0.0335		1.3539	0.2517	**–0.313**
S	**0.9355**	**4.8181**	**116.130**	**0.0000**	0.0316		1.2736	0.2660	**0.602**
Zn	0.0003		0.0023	0.9626	0.0781		3.3024	0.0769	0.099

Table 8. Møsvatn: Split-plot GLM analysis and Kendall's nonparametric correlation coefficient τ between DCA 2 and 31 environmental variables (predictor) in the 50 meso plots. df_{resid}: degrees of freedom for the residuals; *SS*: total variation; *FVE*: fraction of total variation attributable to a given scale (macro plot or meso plot); SS_{expl}/SS: fraction of the variation attributable to the scale in question, explained by a variable; *r*: model coefficient (only given when significant at the α = 0.05 level, otherwise blank); *F*: *F* statistic for test of the hypothesis that *r* = 0 against the two-tailed alternative. Split-plot GLM relationships significant at level α = 0.05, *P*, *F*, *r* and SS_{expl}/SS, and Kendall's nonparametric correlation coefficient $|\tau| \geq 0.30$ are given in bold face. Numbers and abbreviations for names of environmental variables are in accordance with Tab. 2.

Predictor	Dependent variable = DCA 2 (*SS* = 5.8257)								Correlation between predictor and DCA 2
	Error level								
	Macro plot df_{resid} = 8 $SS_{macro\ plot}$ = 4.7768 *FVE* = 0.8200 of *SS*				Meso plot within macro plot df_{resid} = 39 $SS_{meso\ plot}$ = 1.04892 *FVE* = 0.1800 of *SS*				Total
	$SS_{expl}/SS_{macro\ plot}$	*r*	*F*	*P*	$SS_{expl}/SS_{meso\ plot}$	*r*	*F*	*P*	τ
Ma Slo	0.0033		0.0269	0.8737	0.0172		0.6837	0.4133	–0.170Ma
Asp	0.2392		2.5146	0.1515	0.0010		0.0373	0.8480	0.298
Ma HI	0.0582		0.4948	0.5018	0.0084		0.3337	0.5668	–0.122
Ma Ter	0.2876		3.2288	0.1101	0.0215		0.8554	0.3607	0.230
Ma Une	0.0942		0.8324	0.3882	0.0008		0.0320	0.8590	0.026
TBA	0.0075		0.0605	0.8118	0.0570		2.3596	0.1326	–0.066
Me slo	0.0118		0.0956	0.7651	0.0047		0.1859	0.6688	–0.102
Me Asp	0.0018		0.0145	0.9072	0.0215		0.8574	0.3602	0.151
Me HI	0.0010		0.0082	0.9299	0.0178		0.7071	0.4055	–0.148
Me Ter	0.0129		0.1049	0.7543	0.0127		0.5013	0.4831	–0.014
Me Une	0.0318		0.2628	0.6220	0.0035		0.1373	0.7130	0.051
Smi	0.0054		0.0433	0.8404	0.0009		0.0348	0.8530	0.140
Sme	0.0164		0.1331	0.7247	**0.0967**	**0.2233**	**4.1768**	**0.0478**	0.199
Sma	0.0264		0.2168	0.6539	0.0600		2.4888	0.1227	–0.035
Mme	0.0031		0.0253	0.8776	0.0236		0.9424	0.3377	–0.027
LOI	0.0002		0.0017	0.9680	0.0123		0.4863	0.4897	0.055
Total N	0.0001		0.0010	0.9758	0.0327		1.3171	0.2581	–0.001
pH_{H_2O}	0.0012		0.0098	0.9236	0.0068		0.2665	0.6086	–0.080
pH_{CaCl_2}	0.0036		0.0293	0.8683	0.0105		0.4145	0.5234	–0.096
H	0.1858		1.8250	0.2137	0.0000		0.0000	0.9978	–0.068
Al	0.1121		1.0102	0.3443	0.0011		0.0433	0.8363	–0.193
C	0.1594		1.5166	0.2531	0.0012		0.0471	0.8293	0.064
Ca	0.0819		0.7138	0.4227	0.0002		0.0063	0.9374	0.056
Fe	0.0512		0.4317	0.5296	0.0000		0.0005	0.9830	0.045
K	0.1305		1.2002	0.3052	0.0028		0.1094	0.7426	0.125
Mg	0.2825		3.1495	0.1139	0.0273		1.0937	0.3021	0.234
Mn	0.0370		0.3071	0.5946	0.0062		0.2422	0.6254	0.017
Na	0.0377		0.3137	0.5908	0.0733		3.0835	0.0869	0.035
P	0.0011		0.0088	0.9277	0.0025		0.0995	0.7541	0.127
S	0.0790		0.6866	0.4314	0.0080		0.3138	0.5786	0.035
Zn	0.2082		2.1031	0.1850	0.0330		1.3296	0.2559	0.172

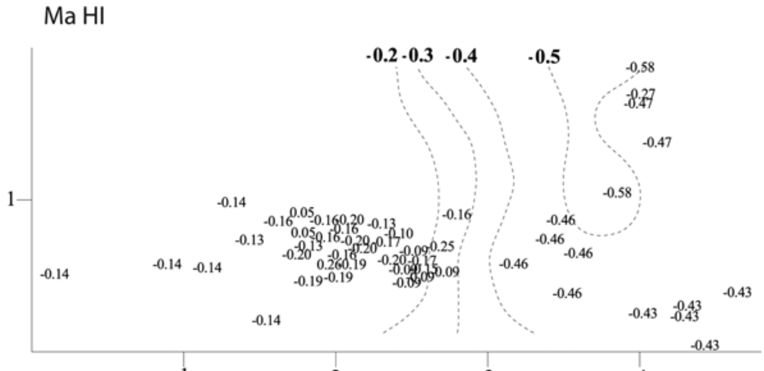

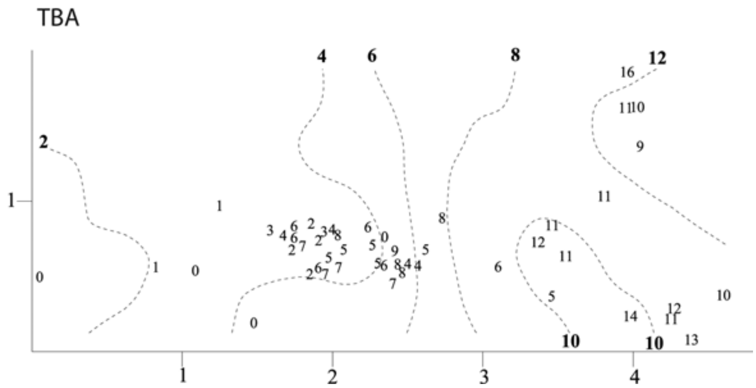

Figs 62-63. Møsvatn: isolines for environmental variables in the DCA ordinations of 50 meso plots, axes 1 (horizontal) and 2 (vertical). Values for the environmental variables are plotted onto the meso plots' positions. Scaling in S.D. units. Fig. 62. Ma HI (R^2 = 0. 684). Fig. 63. TBA (R^2 = 0.507). R^2 refers to the coefficient of determination between original and smoothened values as interpolated from the isolines. Names of environmental variables in accordance with Table 2.

PCA ordination of environmental variables

The first PCA axis accounted for 40.6 % (eigenvalue of 0.406) of the variance in the matrix of standardised transformed environmental variables, and the second axis accounted for 14.6 % (eigenvalue of 0.146).

pH_{H_2O}, pH_{CaCl_2} and extractable S, Mn, Ca and C obtained the highest loadings on PCA axis 1, while loss-on-ignition, exchangeable H and macro- and meso plot heat indices obtained low loadings (Fig. 57). Extractable Al and soil moisture obtained low loadings on PCA axis 2, while extractable P and Zn obtained high loadings.

The PCA results were consistent with the correlation matrix of the environmental variables,

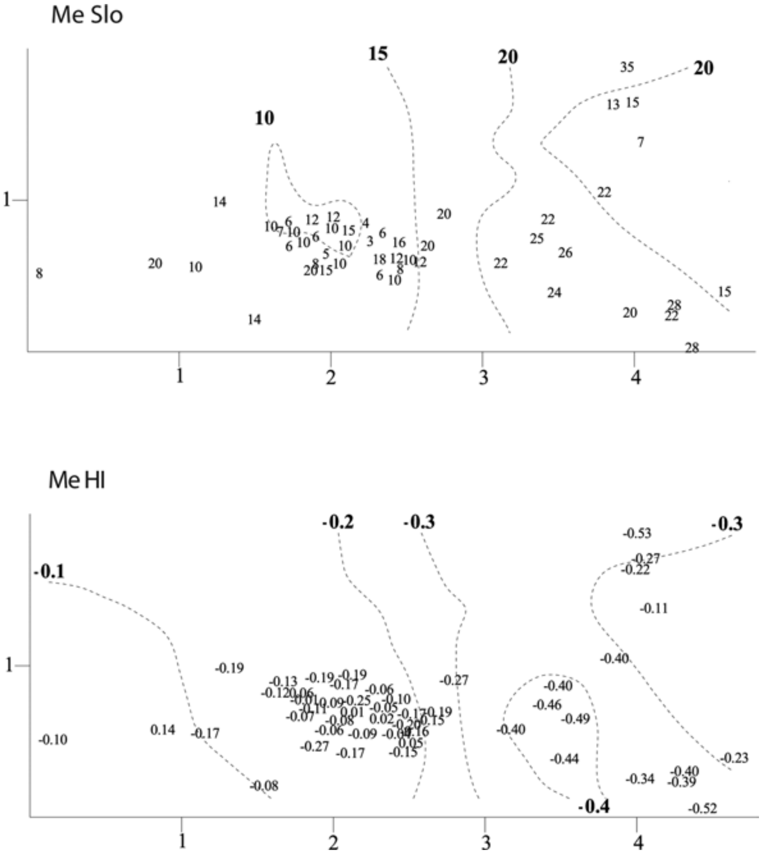

Figs 64-65. Møsvatn: isolines for environmental variables in the DCA ordinations of 50 meso plots, axes 1 (horizontal) and 2 (vertical). Values for the environmental variables are plotted onto the meso plots' positions. Scaling in S.D. units. Fig. 64. Me Slo (R^2 = 0.643). Fig. 65. Me HI (R^2 = 0.748). R^2 refers to the coefficient of determination between original and smoothened values as interpolated from the isolines. Names of environmental variables in accordance with Table 2.

showing that pH, Ca, Mn and several of the topgraphical indices (not heat indices) with high loadings on axis 1 were highly positively correlated, and that variables in this group was negatively correlated with loss on ignition, extractable H and heat indices. Thus the environmental data from the Møsvatn reference area reflects an important gradient in soil nutrient richness and base status.

DCA ordination

The gradient length of the two first DCA axes was 4.53 and 1.88 S.D. units, and the eigenvalues were 0.554 and 0.140, respectively. Meso plot 35 made up an outlier along the first axis. A second DCA

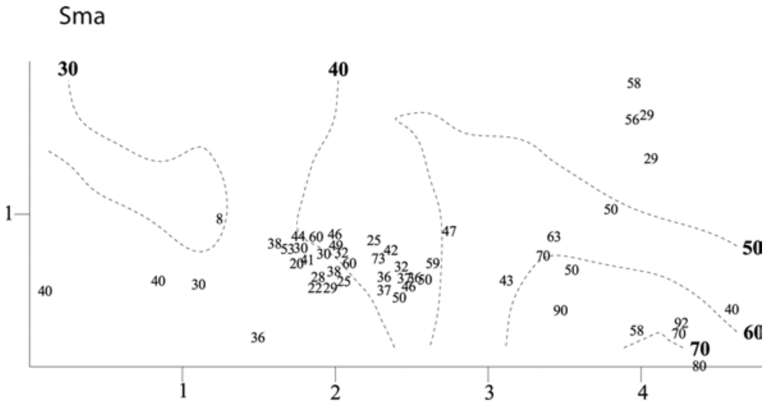

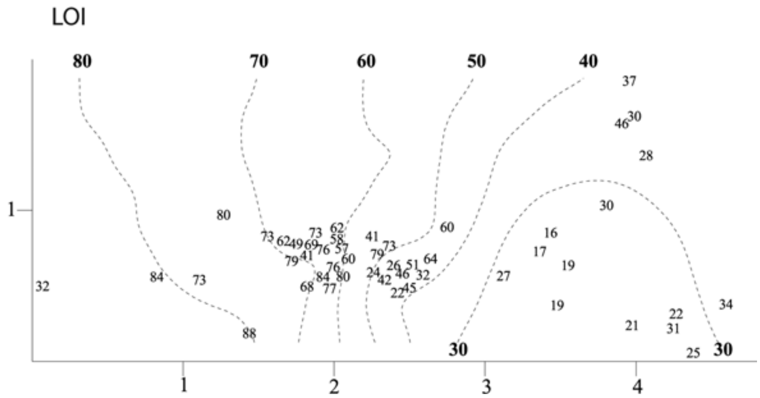

Figs 66-67. Møsvatn: isolines for environmental variables in the DCA ordinations of 50 meso plots, axes 1 (horizontal) and 2 (vertical). Values for the environmental variables are plotted onto the meso plots' positions. Scaling in S.D. units. Fig. 66. Sma ($R^2 = 0.583$). Fig. 67. LOI ($R^2 = 0.707$). R^2 refers to the coefficient of determination between original and smoothened values as interpolated from the isolines. Names of environmental variables in accordance with Table 2.

ordination was obtained by removing this plot from the analysis, and a new ordination was performed. However, the relative positions of the remaining plots in the diagram did not change, nor was the main pattern along the axes affected. All plots were therefore used in further analyses.

The first axis represented a high proportion of the structured variation in the material while, consequently, the remaining axes captured smaller amounts of variation. Variation along DCA axis 2 was mainly restricted to sample plots to the right in the ordination diagram, i.e. with high DCA 1 scores (Fig. 58).

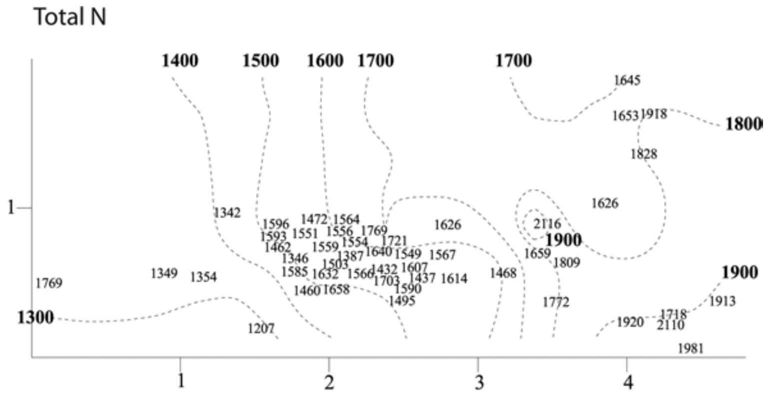

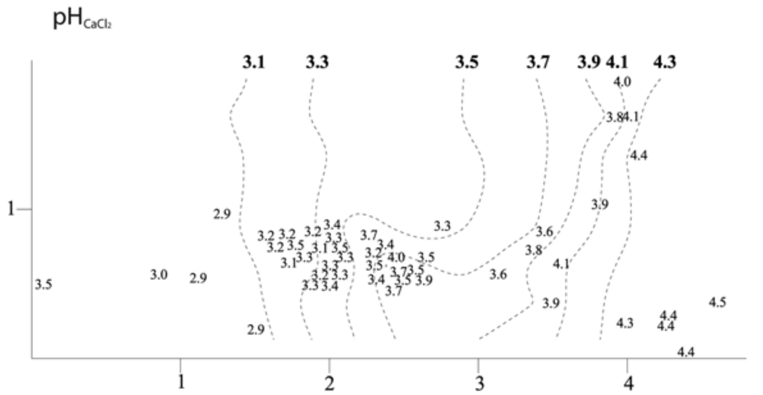

Figs 68-69. Møsvatn: isolines for environmental variables in the DCA ordinations of 50 meso plots, axes 1 (horizontal) and 2 (vertical). Values for the environmental variables are plotted onto the meso plots' positions. Scaling in S.D. units. Fig. 68. Total N (R^2 = 0.738). Fig. 69. pH$_{CaCl_2}$ (R^2 = 0.837). R^2 refers to the coefficient of determination between original and smoothened values as interpolated from the isolines. Names of environmental variables in accordance with Table 2.

GNMDS ordination

The GNMDS ordination diagram (Fig. 59) was visually similar to the DCA diagram (Fig. 58), although plot 35 was separated somewhat from all other plots both along the first and the second ordination axis. The correlation between GNMDS 1 and DCA 1 was $\tau = 0.953$, and the correlation between GNMDS 2 and DCA 2 was $\tau = 0.407$ (both $P < 0.001$).

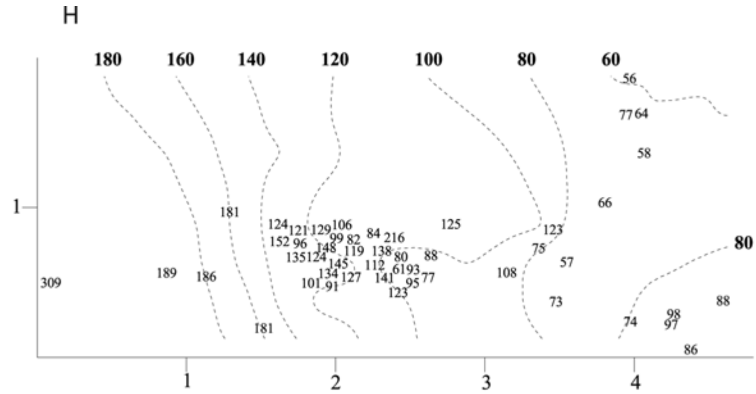

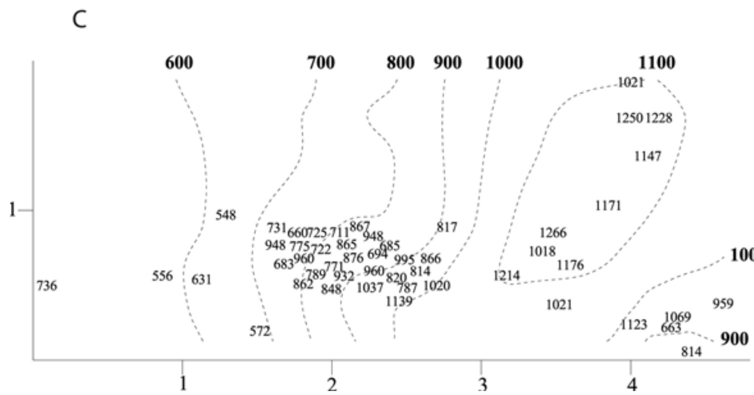

Figs 70-71. Møsvatn: isolines for environmental variables in the DCA ordinations of 50 meso plots, axes 1 (horizontal) and 2 (vertical). Values for the environmental variables are plotted onto the meso plots' positions. Scaling in S.D. units. Fig. 70. H (R^2 = 0.750). Fig. 71. C (R^2 = 0.753). R^2 refers to the coefficient of determination between original and smoothened values as interpolated from the isolines. Names of environmental variables in accordance with Table 2.

Split-plot GLM analysis of relationships between ordination axes and environmental variables

Variation (in plot scores) along DCA axis 1 was partitioned with 93.62 % at the macro plot scale (i.e. between macro plots) and 6.38 % at the (between) meso plot scale within macro plots (Table 7). For the second ordination axis, 82.00 % of the variation was explained at the macro plot scale and 18.00 % at the meso plot scale (Table 8)

At the macro plot scale, twenty-two environmental variables were significantly (at the $\alpha = 0.05$ level) related to DCA 1 while no variable (also at the $\alpha = 0.05$ level) was related to DCA 2. At the meso plot scale, four environmental variables were significantly related to DCA 1 and one variable to DCA 2 (Tables 7 and 8).

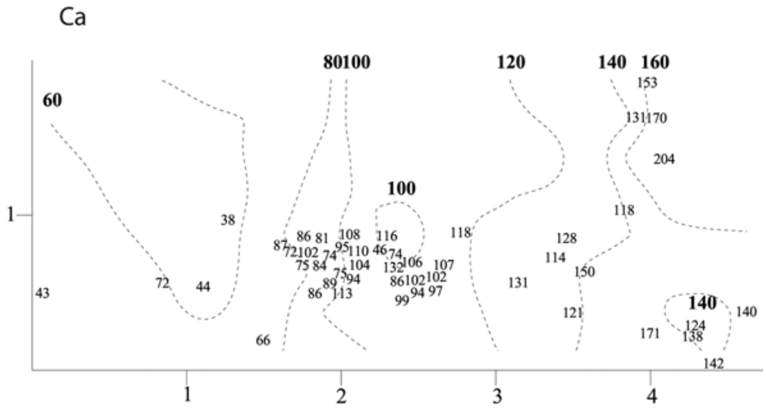

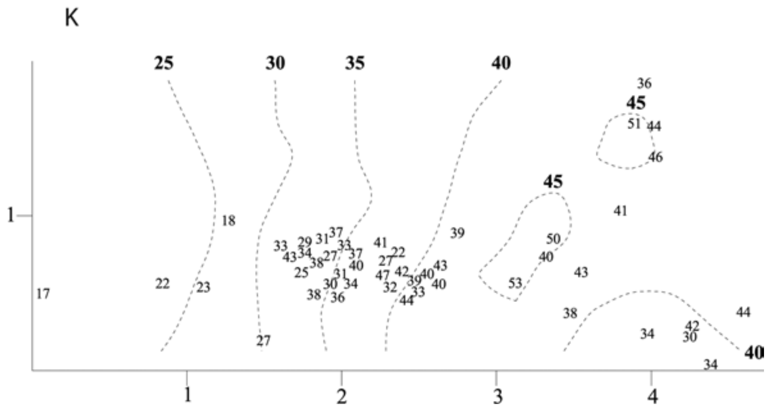

Figs 72-73. Møsvatn: isolines for environmental variables in the DCA ordinations of 50 meso plots, axes 1 (horizontal) and 2 (vertical). Values for the environmental variables are plotted onto the meso plots' positions. Scaling in S.D. units. Fig. 72. Ca ($R^2 = 0.803$). Fig. 73. K ($R^2 = 0.669$). R^2 refers to the coefficient of determination between original and smoothened values as interpolated from the isolines. Names of environmental variables in accordance with Table 2.

At the macro plot scale, most of the significant variables increased along DCA 1; exceptions were heat indices, meso plot terrain form, minimum soil depth, LOI and the concentrations of H and P in soil which decreased.

At the meso plot scale, DCA 2 was only significant positively correlated with median soil depth. No other significant relationships were detected (at the $\alpha = 0.05$ level) (Table 8).

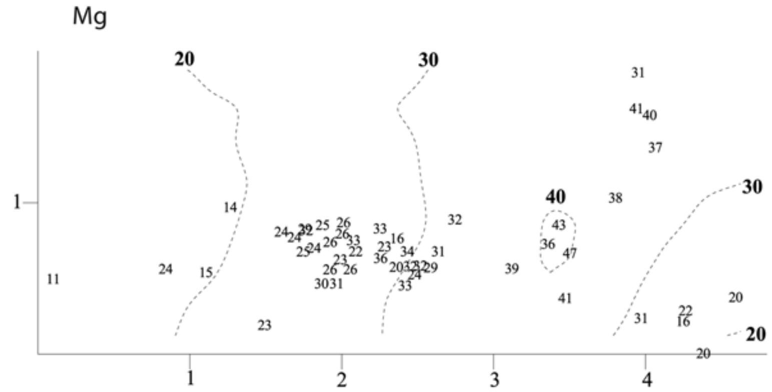

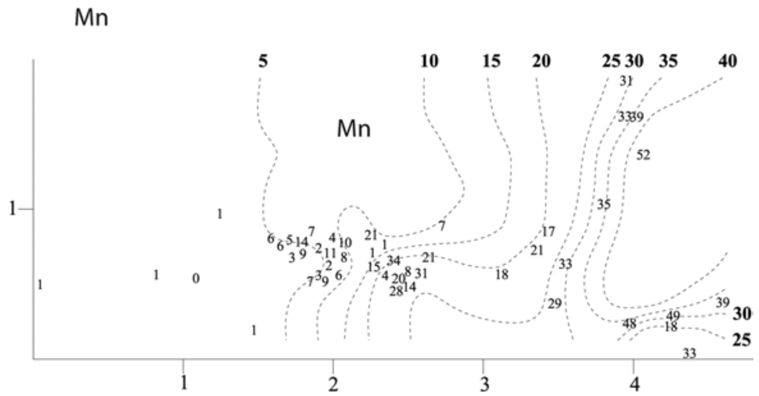

Figs 74-75. Møsvatn: isolines for environmental variables in the DCA ordinations of 50 meso plots, axes 1 (horizontal) and 2 (vertical). Values for the environmental variables are plotted onto the meso plots' positions. Scaling in S.D. units. Fig. 74. Mg (R^2 = 0.618). Fig. 75. Mn (R^2 = 0.771). R^2 refers to the coefficient of determination between original and smoothened values as interpolated from the isolines. Names of environmental variables in accordance with Table 2.

Correlations between DCA ordination axes and environmental variables

Twenty of the 31 measured variables were strongly correlated with DCA axis 1 ($|\tau| > 0.300$), while no variables were equally strongly correlated with DCA 2 (Table 7). pH_{CaCl_2} (τ = 0.726, Fig. 69), pH_{H_2O} (τ = 0.716), extractable Ca (τ = 0.675, Fig. 72) and Mn (τ = 0.636, Fig. 75) and tree basal area (τ = 0.617, Fig. 63) were best correlated with DCA axis 1, while meso plot aspect unfavourablility (τ = 0.298) was the variable most strongly correlated with DCA 2.

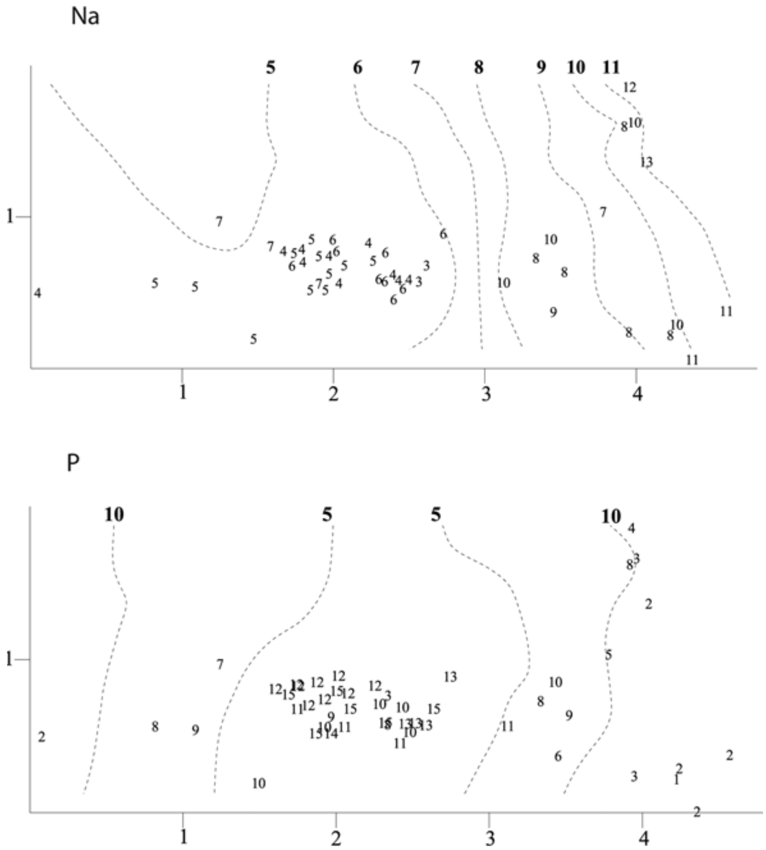

Figs 76-77. Møsvatn: isolines for environmental variables in the DCA ordinations of 50 meso plots, axes 1 (horizontal) and 2 (vertical). Values for the environmental variables are plotted onto the meso plots' positions. Scaling in S.D. units. Fig. 76. Na ($R^2 = 0.743$). Fig. 77. P ($R^2 = 0.569$). R^2 refers to the coefficient of determination between original and smoothened values as interpolated from the isolines. Names of environmental variables in accordance with Table 2.

Frequent species

A total of 124 species were recorded within the fifty 1×1 m meso plots: 61 vascular plants, 25 mosses, 19 liverworts and 19 lichens. The most frequent species were (the sum of subplot frequencies in brackets): *Avenella flexuosa* (717 out of 800), *Barbilophozia lycopodioides* (691), *Vaccinium myrtillus* (663), *Vaccinium vitis-idaea* (452), *Empetrum nigrum* (443), *Trientalis europaea* (376), *Pleurozium schreberi* (347), *Hylocomium splendens* (312), *Vaccinium uliginosum* (298), and *Brachythecium reflexum* (295).

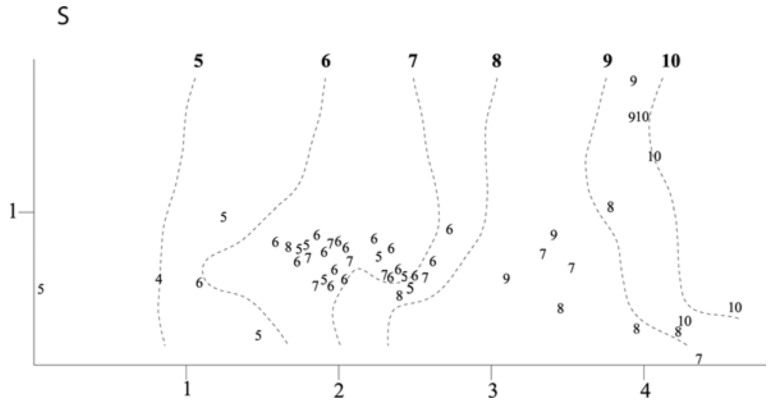

Fig. 78. Møsvatn: isolines for environmental variables in the DCA ordinations of 50 meso plots, axes 1 (horizontal) and 2 (vertical). Values for the environmental variables are plotted onto the meso plots' positions. Scaling in S.D. units. Fig. 78. S ($R^2 = 0.776$). R^2 refers to the coefficient of determination between original and smoothened values as interpolated from the isolines. Names of environmental variables in accordance with Table 2.

The distribution of species abundance in the DCA ordination

Forty seven of the total 124 species occurred in 5 or more of the meso plots (Figs 79-125).

Only *Vaccinium myrtillus* (Fig. 82) occurred abundantly in most of the meso plots, demonstrating a wide ecological amplitude. *Empetrum nigrum* (Fig. 81), *Vaccinium uliginosum* (Fig. 83) and *Vaccinium vitis-idaea* (Fig. 84) also had relatively wide ecological amplitudes, but were absent from the extreme right-hand situated plots in the DCA ordination diagram with favourable soil nutrient status. *Solidago virgaurea* (Fig. 97), *Trientalis europaea* (Fig. 98), *Avenella flexuosa* (Fig. 100), *Brachythecium reflexum* (Fig. 103) and *Barbilophozia lycopodioides* (Fig. 115) were only absent from plots with very low DCA 1 scores, i.e. the plots with the most acid and nutrient-poor soils.

Species with more narrow amplitudes in the material, which showed preferences for soils with higher pH and higher concentrations of nutrients, were *Geranium sylvaticum* (Fig. 85), *Phegopteris connectilis* (Fig. 94), *Ranunculus acris* (Fig. 95), *Rumex acetosa* (Fig. 96), *Milium effusum* (Fig. 102) and *Mnium spinosum* (Fig. 108).

Cladonia arbuscula (Fig. 119), *C. rangiferina* (Fig. 124) and *C. stellaris* (Fig. 125) were restricted to the left-hand side of the ordination diagram and thus occurred in sample plots with low slope, low tree basal area, low soil nutrient status and high LOI values (on ridges with scattered trees).

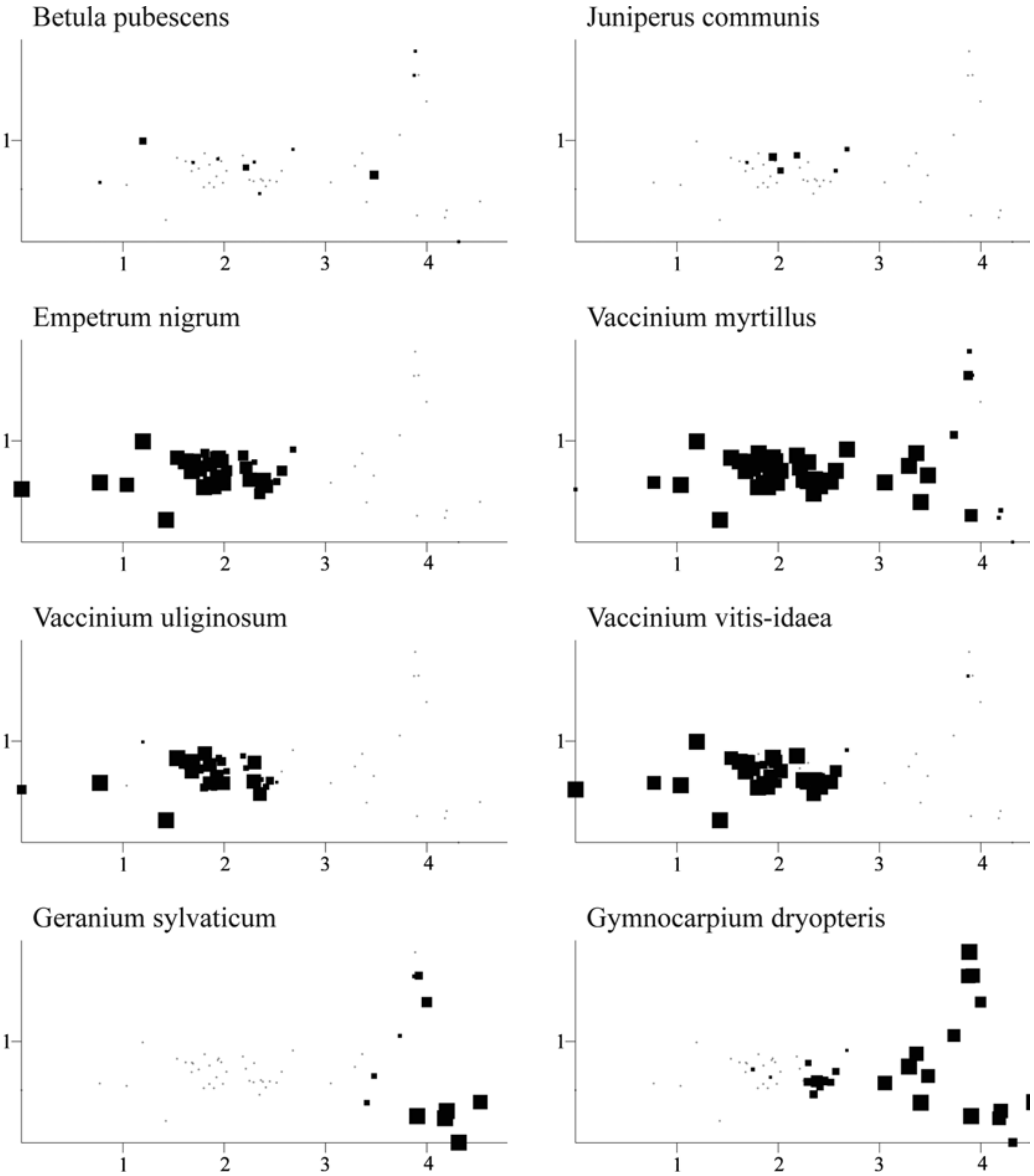

Figs 79-86. Møsvatn: distributions of species abundances in the DCA ordination of 50 meso plots, axes 1 (horizontal) and 2 (vertical). Frequency in subplots for each species in each meso plot proportional to quadrate size. Scaling in S.D. units. Fig. 79. *Betula pubescens*. Fig. 80. *Juniperus communis*. Fig. 81. *Empetrum nigrum*. Fig. 82. *Vaccinium myrtillus*. Fig. 83. *Vaccinium uliginosum*. Fig. 84. *Vaccinium vitis-idaea*. Fig. 85. *Geranium sylvaticum*. Fig. 86. *Gymnocarpium dryopteris*.

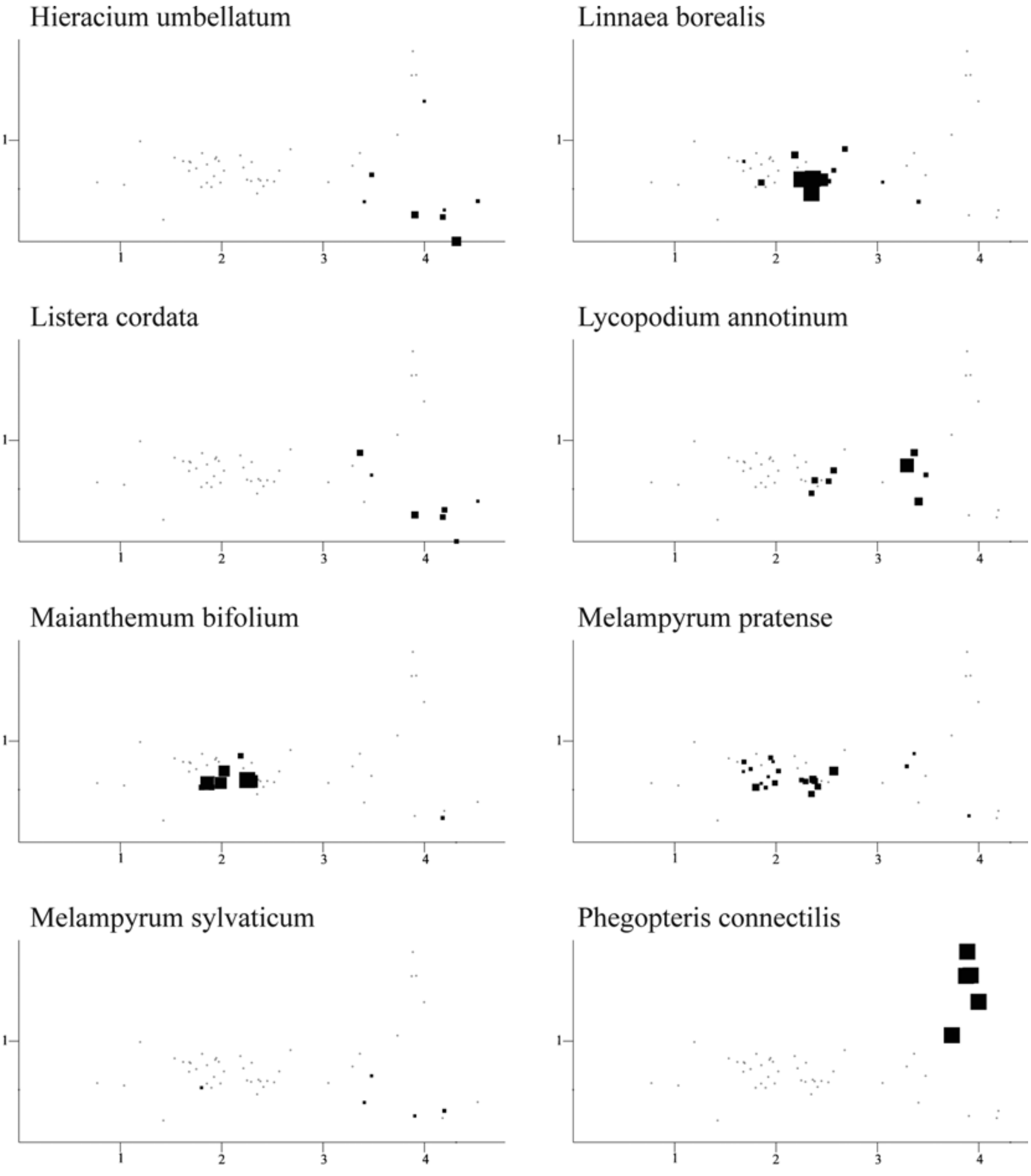

Figs 87-94. Møsvatn: distributions of species abundances in the DCA ordination of 50 meso plots, axes 1 (horizontal) and 2 (vertical). Frequency in subplots for each species in each meso plot proportional to quadrate size. Scaling in S.D. units. Fig. 87. *Hieracium umbellatum*. Fig. 88. *Linnaea borealis*. Fig. 89. *Listera cordata*. Fig. 90. *Lycopodium annotinum*. Fig. 91. *Maianthemum bifolium*. Fig. 92. *Melampyrum pratense*. Fig. 93. *Melampyrum sylvaticum*. Fig. 94. *Phegopteris connectilis*.

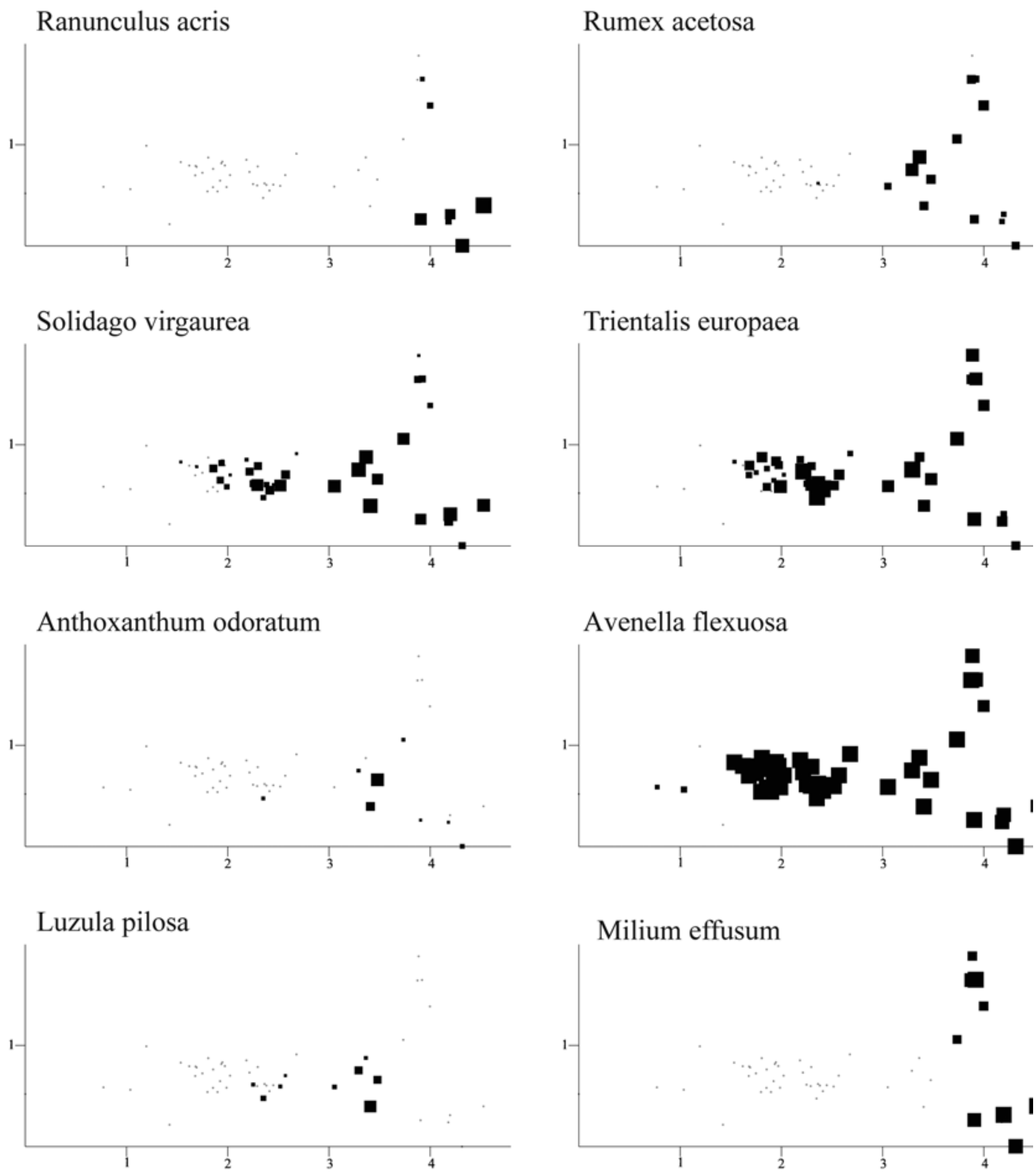

Figs 95-102. Møsvatn: distributions of species abundances in the DCA ordination of 50 meso plots, axes 1 (horizontal) and 2 (vertical). Frequency in subplots for each species in each meso plot proportional to quadrate size. Scaling in S.D. units. Fig. 95. *Ranunculus acris*. Fig. 96. *Rumex acetosa*. Fig. 97. *Solidago virgaurea*. Fig. 98. *Trientalis europaea*. Fig. 99. *Anthoxanthum odoratum*. Fig. 100. *Avenella flexuosa*. Fig. 101. *Luzula pilosa*. Fig. 102. *Milium effusum*.

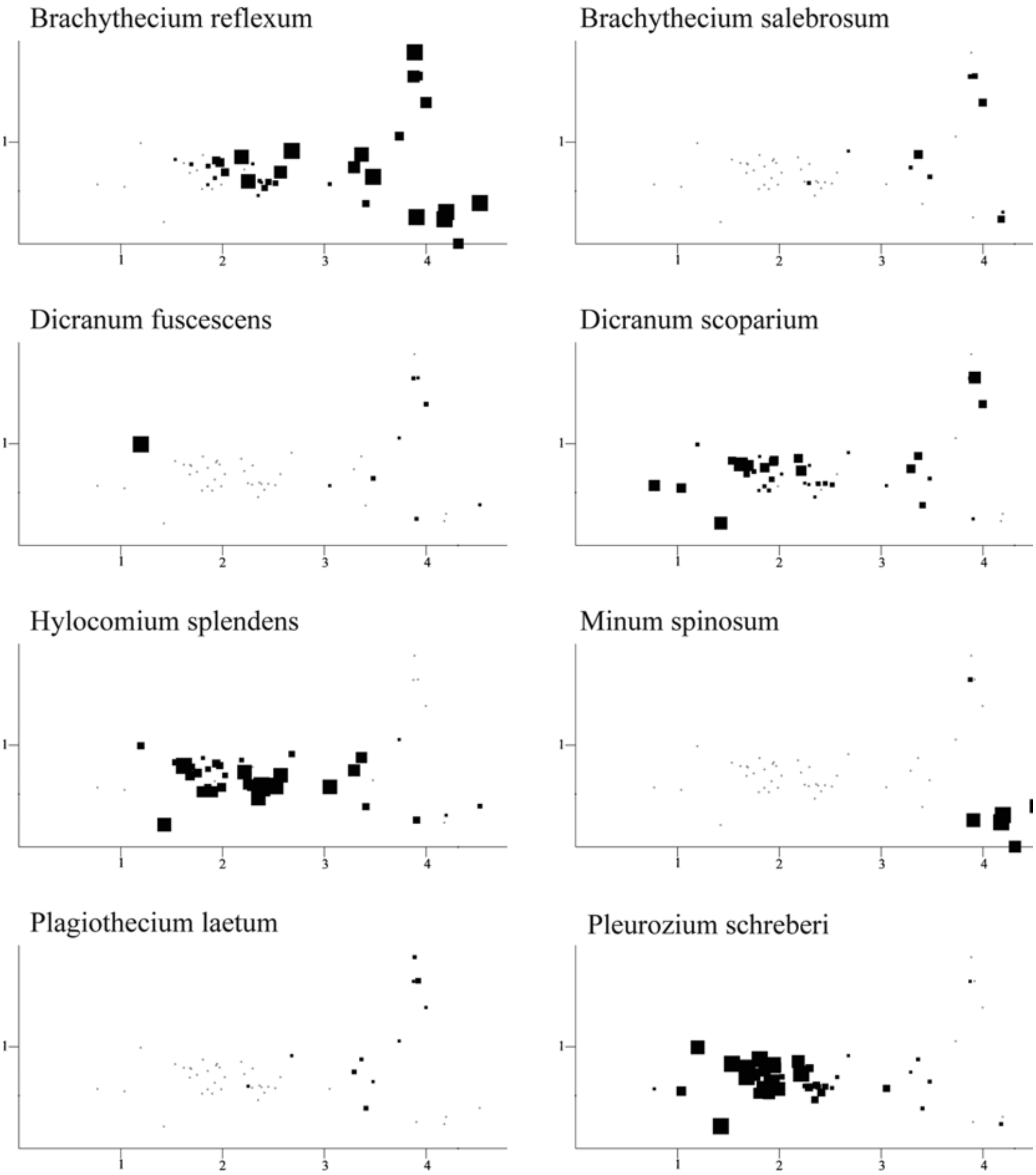

Figs 103-110. Møsvatn: distributions of species abundances in the DCA ordination of 50 meso plots, axes 1 (horizontal) and 2 (vertical). Frequency in subplots for each species in each meso plot proportional to quadrate size. Scaling in S.D. units. Fig. 103. *Brachythecium reflexum*. Fig. 104. *Brachythecium salebrosum*. Fig. 105. *Dicranum fuscescens*. Fig. 106. *Dicranum scoparium*. Fig. 107. *Hylocomium splendens*. Fig. 108. *Mnium spinosum*. Fig. 109. *Plagiothecium laetum*. Fig. 110. *Pleurozium schreberi*.

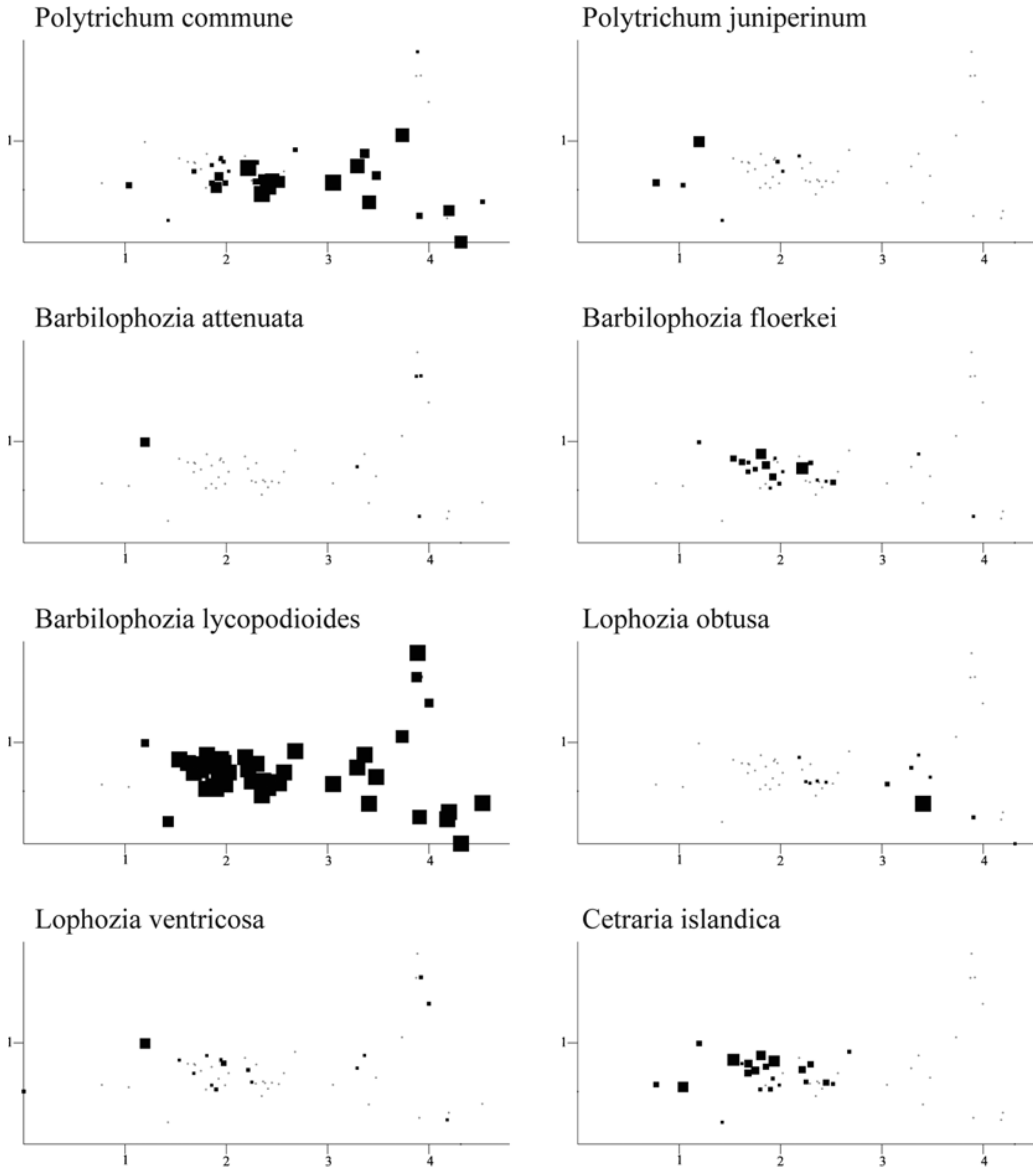

Figs 111-118. Møsvatn: distributions of species abundances in the DCA ordination of 50 meso plots, axes 1 (horizontal) and 2 (vertical). Frequency in subplots for each species in each meso plot proportional to quadrate size. Scaling in S.D. units. Fig. 111. *Polytrichum commune*. Fig. 112. *Polytrichum juniperinum*. Fig. 113. *Barbilophozia attenuata*. Fig. 114. *Barbilophozia floerkei*. Fig. 115. *Barbilophozia lycopodioides*. Fig. 116. *Lophozia obtusa*. Fig. 117. *Lophozia ventricosa*. Fig. 118. *Cetraria islandica*.

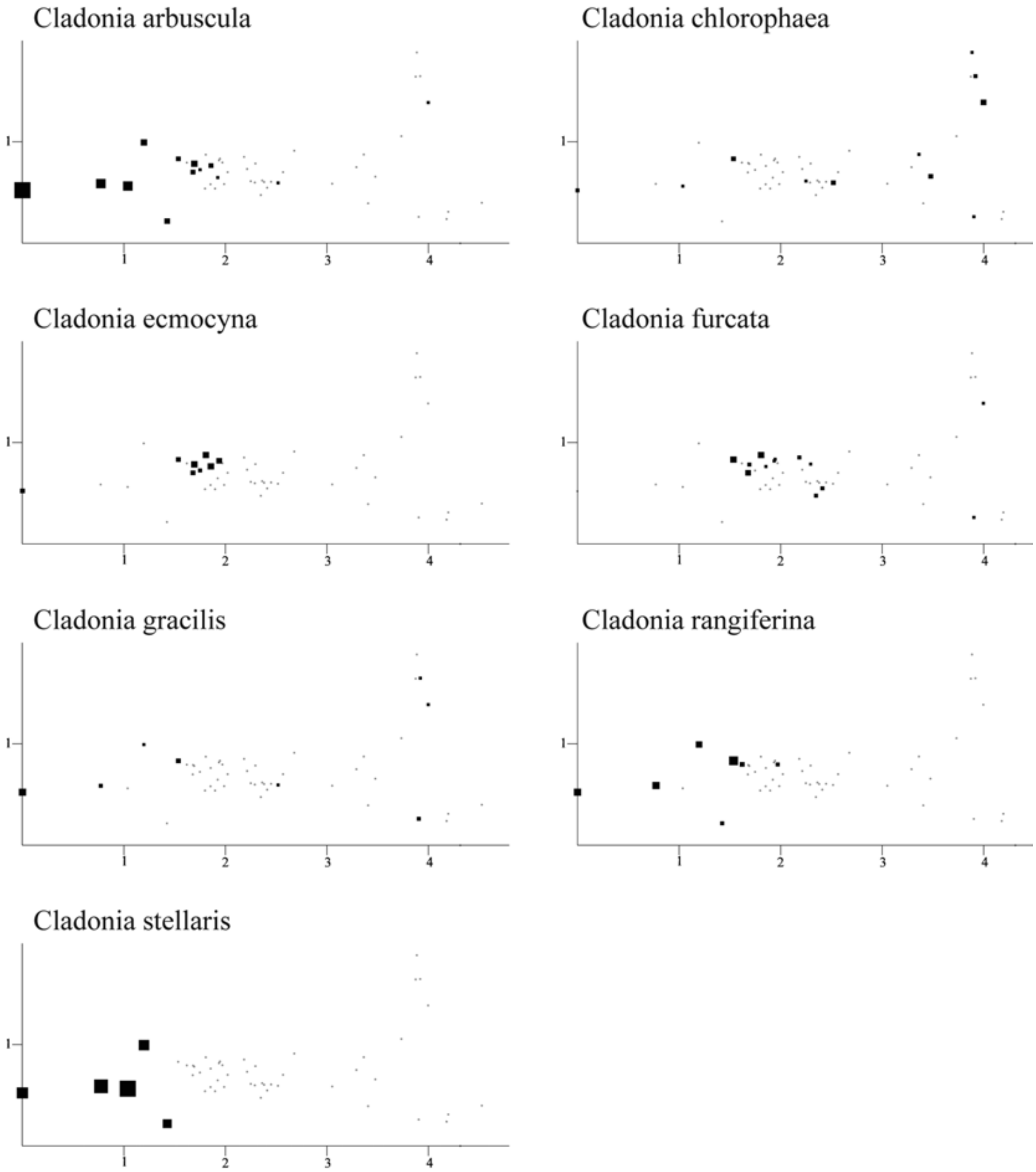

Figs 119-125. Møsvatn: distributions of species abundances in the DCA ordination of 50 meso plots, axes 1 (horizontal) and 2 (vertical). Frequency in subplots for each species in each meso plot proportional to quadrate size. Scaling in S.D. units. Fig. 119. *Cladonia arbuscula*. Fig. 120. *Cladonia chlorophaea*. Fig. 121. *Cladonia ecmocyna*. Fig. 122. *Cladonia furcata*. Fig. 123. *Cladonia gracilis*. Fig. 124. *Cladonia rangiferina*. Fig. 125. *Cladonia stellaris*.

GUTULIA REFERENCE AREA

Correlations between environmental variables

Macro and meso plot slope were negatively correlated with heat indices, tree basal area, soil moisture and soil pH, and negatively correlated with soil depth, loss-on-ignition and exchangeable H (Table 9). Tree basal area was positively correlated with soil pH. Soil depth (Smi, Sme and Sma) was, in general, negatively correlated with concentrations of extractable elements that reflected soil richness (e.g. Ca, Mg, K and Na) and with pH, and positively correlated with loss-on-ignition and soil acidity (exchangeable H).

Soil moisture was positively correlated with soil pH, extractable P, C, Ca, K, Mg, Mn and Zn and negatively correlated with loss on ignition and soil acidity. Loss-on-ignition was, in turn, positively correlated with soil acidity and negatively correlated with variables reflecting soil nutrient richness. Variables reflecting soil nutrient richness (pH, P, N, Ca, Mg, Na, K, Mn) were, in general, internally positively correlated, each of these were negatively correlated with soil acidity (exchangeable H and extractable Al). Thus the Gutulia reference area showed variation in soil nutrient richness and base status with the most acidic plots situated in rather flat areas with deeper soils characterized by high

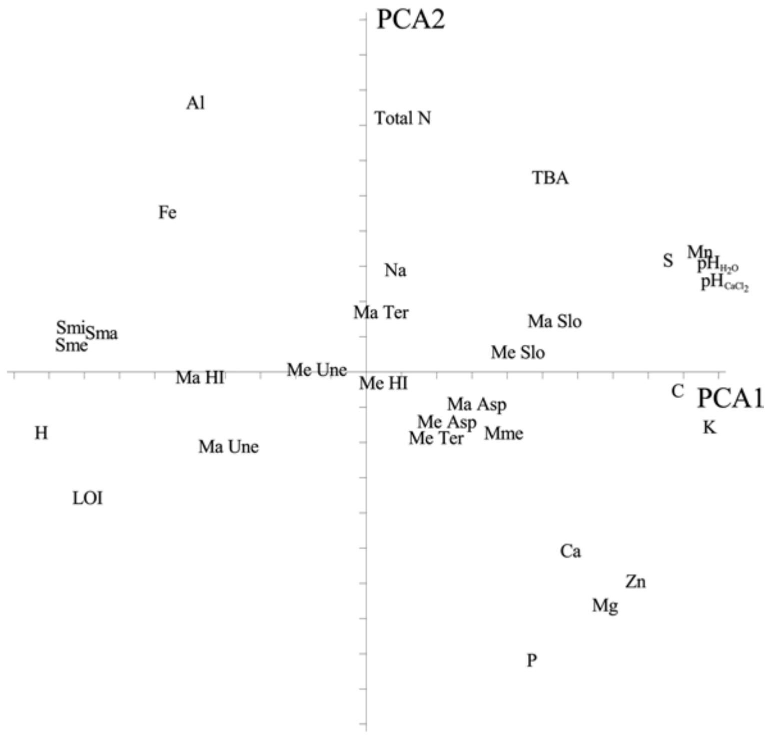

Fig. 126. Gutulia: PCA ordination of 31 environmental variables. Abbreviations in accordance with Table 2, axes 1 (horizontal) and 2 (vertical). Positions of variables in the ordination space give the head of variable vectors. Tickmarks indicate 0.1 units along both axes.

Table 9. Gutulia: Kendall's rank correlation coefficients τ between 31 environmental variables in the 50 meso plots (lower triangle), with significance probabilities (upper triangle). Statistically significant correlations (P<0.05) in bold face. Names of explanatory variables abbreviated in accordance with Table 2.

	1	2	3	4	5	6	7	8	9	10	11	12	13	14	15	16
01 Ma Slo	*	0.474	**0.000**	0.072	**0.001**	**0.019**	**0.000**	0.069	**0.000**	**0.003**	0.053	**0.027**	**0.009**	**0.022**	**0.023**	**0.000**
02 Ma Asp	0.073	*	**0.002**	0.104	0.599	0.743	0.170	**0.000**	**0.001**	0.190	0.978	0.338	0.187	0.580	0.175	0.841
03 Ma HI	**–0.789**	**–0.309**	*	0.326	**0.006**	**0.032**	**0.000**	**0.000**	**0.000**	**0.017**	0.167	**0.004**	**0.001**	**0.007**	**0.006**	**0.000**
04 Ma Ter	0.205	–0.182	–0.109	*	0.503	0.885	0.527	0.241	0.589	**0.000**	0.302	0.554	0.522	0.672	0.353	0.907
05 Ma Une	**–0.387**	0.058	**0.301**	–0.083	*	0.083	**0.000**	0.873	**0.011**	0.405	**0.000**	0.177	0.068	**0.033**	**0.012**	**0.002**
06 TBA	**0.241**	0.033	**–0.214**	0.016	–0.193	*	0.147	0.440	0.125	0.459	0.553	**0.030**	0.051	0.378	0.597	**0.000**
07 Me Slo	**0.693**	0.139	**–0.632**	0.072	**–0.393**	0.148	*	0.368	**0.000**	0.120	0.296	**0.044**	**0.009**	**0.013**	**0.034**	**0.001**
08 Me Asp	0.183	**0.707**	**–0.354**	–0.130	0.018	0.077	0.090	*	**0.000**	0.915	0.964	0.678	0.356	0.993	0.225	0.913
09 Me HI	**–0.648**	**–0.325**	**0.760**	–0.060	**0.279**	–0.153	**–0.662**	**–0.446**	*	0.076	0.365	0.168	0.058	0.104	0.072	**0.021**
10 Me Ter	**–0.415**	–0.312	**0.420**	**0.176**	–0.071	–0.165	–0.403	–0.097	0.317	*	0.106	0.054	0.573	0.148	0.226	0.122
11 Me Une	–0.219	0.003	0.152	–0.129	**0.566**	–0.067	–0.118	0.005	0.100	–0.052	*	0.677	1.000	0.957	0.139	0.164
12 Smi	**–0.232**	–0.099	**0.290**	0.068	0.154	**–0.226**	**–0.210**	–0.042	0.141	0.002	0.048	*	**0.000**	**0.000**	**0.000**	**0.000**
13 Sme	**–0.266**	–0.132	**0.323**	0.072	0.202	–0.197	**–0.263**	–0.092	0.187	–0.001	0.000	**0.792**	*	**0.000**	**0.000**	**0.000**
14 Sma	**–0.233**	–0.055	**0.264**	0.047	**0.234**	–0.089	**–0.252**	–0.001	0.160	–0.020	0.006	**0.706**	**0.728**	*	**0.000**	**0.000**
15 Mme	**0.229**	0.134	**–0.268**	–0.102	**–0.275**	0.053	**0.212**	0.119	–0.176	0.138	–0.163	**–0.437**	**–0.497**	**–0.504**	*	**0.000**
16 LOI	**–0.424**	–0.020	**0.368**	–0.013	**0.341**	**–0.455**	**–0.319**	–0.011	**0.225**	–0.082	0.153	**0.530**	**0.512**	**0.417**	**–0.365**	*
17 Total N	–0.100	–0.068	0.164	0.007	–0.108	**0.218**	–0.042	–0.104	0.094	**–0.222**	0.056	0.035	0.015	0.069	**–0.220**	–0.066
18 pH_{H_2O}	**0.376**	0.016	**–0.345**	0.039	**–0.367**	**0.435**	**0.293**	–0.002	**–0.207**	0.056	–0.192	**–0.587**	**–0.545**	**–0.466**	**0.343**	**–0.748**
19 pH_{CaCl_2}	**0.399**	0.017	**–0.351**	0.054	**–0.355**	**0.455**	**0.315**	0.003	**–0.220**	0.079	–0.178	**–0.592**	**–0.565**	**–0.472**	**0.326**	**–0.764**
20 H	**–0.357**	–0.041	**0.353**	0.023	**0.391**	**–0.380**	**–0.272**	–0.042	**0.202**	–0.078	0.204	**0.599**	**0.580**	**0.508**	**–0.407**	**0.667**
21 Al	–0.151	–0.048	**0.195**	0.094	0.186	0.145	–0.109	–0.076	0.094	–0.173	0.177	**0.249**	**0.268**	**0.275**	**–0.456**	0.112
22 C	**0.283**	0.051	**–0.250**	–0.102	**–0.275**	**0.267**	**0.198**	0.042	–0.120	0.055	–0.143	**–0.533**	**–0.535**	**–0.514**	**0.389**	**–0.453**
23 Ca	0.131	–0.065	–0.119	–0.029	–0.184	0.018	0.082	–0.022	–0.101	0.138	–0.084	**–0.304**	**–0.292**	**–0.313**	**0.215**	–0.102
24 Fe	**–0.286**	–0.073	**0.312**	–0.043	**0.372**	0.026	**–0.225**	–0.073	0.184	**–0.240**	**0.376**	**0.347**	**0.343**	**0.333**	**–0.512**	**0.298**
25 K	**0.296**	0.129	**–0.339**	–0.122	**–0.279**	**0.263**	**0.237**	0.078	–0.171	0.031	–0.188	**–0.671**	**–0.633**	**–0.595**	**0.473**	**–0.513**
26 Mg	0.165	0.089	**–0.219**	–0.126	–0.118	–0.033	0.124	0.108	–0.143	0.111	–0.044	**–0.418**	**–0.417**	**–0.435**	**0.396**	**–0.195**
27 Mn	**0.367**	0.128	**–0.430**	0.003	**–0.318**	**0.414**	**0.336**	0.075	**–0.269**	0.078	–0.137	**–0.589**	**–0.586**	**–0.463**	**0.319**	**–0.696**
28 Na	–0.058	–0.116	0.124	–0.146	0.071	0.119	–0.050	–0.108	0.099	–0.195	0.108	–0.046	–0.018	–0.021	–0.154	0.025
29 P	0.117	0.017	–0.115	–0.152	–0.168	–0.191	0.084	–0.016	–0.012	0.152	–0.171	**–0.270**	**–0.278**	**–0.293**	**0.456**	–0.105
30 S	**0.316**	0.075	**–0.294**	–0.051	**–0.314**	**0.380**	**0.267**	0.016	–0.176	–0.033	–0.102	**–0.494**	**–0.530**	**–0.458**	**0.228**	**–0.530**
31 Zn	0.149	0.146	**–0.236**	–0.170	–0.065	0.074	0.096	0.157	–0.119	0.041	–0.038	**–0.528**	**–0.512**	**–0.480**	**0.496**	**–0.295**

Table 9 (continued). Gutulia: Kendall's rank correlation coefficients τ between 31 environmental variables in the 50 meso plots (lower triangle), with significance probabilities (upper triangle). Statistically significant correlations (P<0.05) in bold face. Names of explanatory variables abbreviated in accordance with Table 2.

	17	18	19	20	21	22	23	24	25	26	27	28	29	30	31
01 Ma Slo	0.317	**0.000**	**0.000**	**0.000**	0.132	**0.005**	0.193	**0.004**	**0.003**	0.101	**0.000**	0.562	0.243	**0.002**	0.137
02 Ma Asp	0.492	0.873	0.860	0.675	0.627	0.603	0.513	0.461	**0.001**	0.365	0.197	0.241	0.867	0.451	0.140
03 Ma HI	0.094	**0.000**	**0.000**	**0.000**	**0.046**	**0.010**	0.222	**0.001**	**0.001**	**0.025**	**0.000**	0.203	0.241	**0.003**	**0.016**
04 Ma Ter	0.950	0.725	0.626	0.836	0.392	0.353	0.794	0.698	0.268	0.252	0.978	0.185	0.168	0.646	0.123
05 Ma Une	0.323	**0.001**	**0.001**	**0.000**	0.089	**0.012**	0.092	**0.001**	**0.011**	0.281	**0.004**	0.516	0.124	**0.004**	0.551
05 TBA	**0.029**	**0.000**	**0.000**	**0.000**	0.147	**0.007**	0.860	0.795	**0.008**	0.744	**0.000**	0.230	0.055	**0.000**	0.455
07 Me Slo	0.674	**0.004**	**0.002**	**0.006**	0.275	**0.047**	0.410	**0.024**	**0.018**	0.214	**0.001**	0.614	0.401	**0.008**	0.338
08 Me Asp	0.288	0.987	0.973	0.669	0.436	0.669	0.821	0.456	0.427	0.273	0.446	0.273	0.874	0.874	0.110
09 Me HI	0.336	**0.035**	**0.025**	**0.039**	0.336	0.219	0.303	0.060	0.080	0.143	**0.006**	0.311	0.900	0.072	0.225
10 Me Ter	**0.042**	0.612	0.471	0.476	0.113	0.618	0.206	**0.028**	0.776	0.310	0.476	0.075	0.165	0.762	0.708
11 Me Une	0.609	0.082	0.106	0.063	0.108	0.193	0.446	**0.001**	0.087	0.686	0.212	0.328	0.121	0.355	0.726
12 Smi	0.729	**0.000**	**0.000**	**0.000**	**0.014**	**0.000**	**0.003**	**0.001**	**0.000**	**0.000**	**0.000**	0.654	**0.008**	**0.000**	**0.000**
13 Sme	0.880	**0.000**	**0.000**	**0.000**	**0.007**	**0.000**	**0.003**	**0.001**	**0.000**	**0.000**	**0.000**	0.854	**0.005**	**0.000**	**0.000**
14 Sma	0.482	**0.000**	**0.000**	**0.000**	**0.005**	**0.000**	**0.001**	**0.001**	**0.000**	**0.000**	**0.000**	0.828	**0.003**	**0.000**	**0.000**
15 Mme	**0.024**	**0.000**	**0.001**	**0.000**	**0.000**	**0.000**	**0.028**	**0.000**	**0.000**	**0.000**	**0.001**	0.114	**0.000**	**0.020**	**0.000**
16 LOI	0.498	**0.000**	**0.000**	**0.000**	0.252	**0.000**	0.296	**0.002**	**0.000**	**0.046**	**0.000**	0.795	0.281	**0.000**	**0.003**
17 Total N	*	0.215	0.181	0.417	**0.000**	0.598	0.900	**0.010**	0.553	**0.006**	0.398	**0.001**	**0.001**	**0.022**	**0.005**
18 pH_{H_2O}	0.121	*	**0.000**	**0.000**	0.085	**0.000**	**0.008**	**0.001**	**0.000**	**0.004**	**0.000**	0.920	0.228	**0.000**	**0.000**
19 pH_{CaCl_2}	0.131	**0.942**	*	**0.000**	0.128	**0.000**	**0.008**	**0.001**	**0.000**	**0.005**	**0.000**	0.763	0.209	**0.000**	**0.000**
20 H	–0.079	**–0.834**	**–0.832**	*	**0.004**	**0.000**	**0.002**	**0.000**	**0.000**	**0.000**	**0.000**	0.927	**0.022**	**0.000**	**0.000**
21 Al	**0.381**	–0.169	–0.149	**0.285**	*	**0.003**	**0.000**	**0.000**	**0.000**	**0.000**	0.139	0.096	**0.000**	0.398	**0.000**
22 C	0.051	**0.584**	**0.606**	**–0.610**	–0.293	*	**0.001**	**0.004**	**0.000**	**0.000**	**0.000**	0.304	**0.001**	**0.000**	**0.000**
23 Ca	–0.012	**0.261**	**0.261**	**–0.304**	**–0.429**	**0.339**	*	**0.000**	**0.000**	**0.000**	0.051	0.477	**0.001**	0.069	**0.000**
24 Fe	**0.251**	**–0.340**	**–0.320**	**0.429**	**0.634**	**–0.283**	**–0.350**	*	**0.000**	**0.000**	**0.002**	**0.039**	**0.000**	0.139	**0.000**
25 K	–0.058	**0.638**	**0.626**	**–0.700**	**–0.399**	**0.711**	**0.396**	**–0.422**	*	**0.000**	**0.000**	0.834	**0.000**	**0.000**	**0.000**
26 Mg	**–0.269**	**0.282**	**0.275**	**–0.391**	**–0.646**	**0.406**	**0.603**	**–0.460**	**0.525**	*	**0.008**	0.707	**0.000**	**0.036**	**0.000**
27 Mn	0.082	**0.771**	**0.788**	**–0.729**	–0.144	**0.528**	0.190	**–0.301**	**0.624**	**0.260**	*	0.744	0.168	**0.000**	**0.000**
28 Na	**0.318**	0.010	0.029	0.009	0.162	0.100	0.069	**0.202**	0.020	–0.037	–0.032	*	0.207	0.060	0.795
29 P	**–0.316**	0.118	0.123	**–0.223**	**–0.736**	**0.316**	**0.337**	**–0.510**	**0.386**	**0.548**	0.135	–0.123	*	0.178	**0.000**
30 S	**0.223**	**0.635**	**0.651**	**–0.592**	–0.082	**0.633**	0.177	–0.144	**0.576**	**0.205**	**0.618**	0.184	0.131	*	**0.001**
31 Zn	**–0.277**	**0.343**	**0.357**	**–0.442**	**–0.569**	**0.584**	**0.419**	**–0.376**	**0.605**	**0.691**	**0.393**	–0.025	**0.546**	**0.334**	*

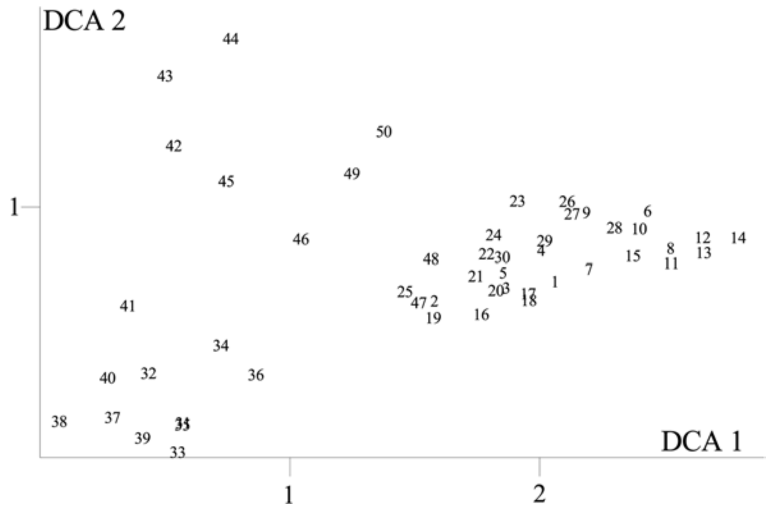

Fig. 127. Gutulia: DCA ordination diagram of 50 meso plots, axes 1 (horizontal) and 2 (vertical). Meso plot number are plotted just right of the sample plot positions. Scaling of axes in S.D. units.

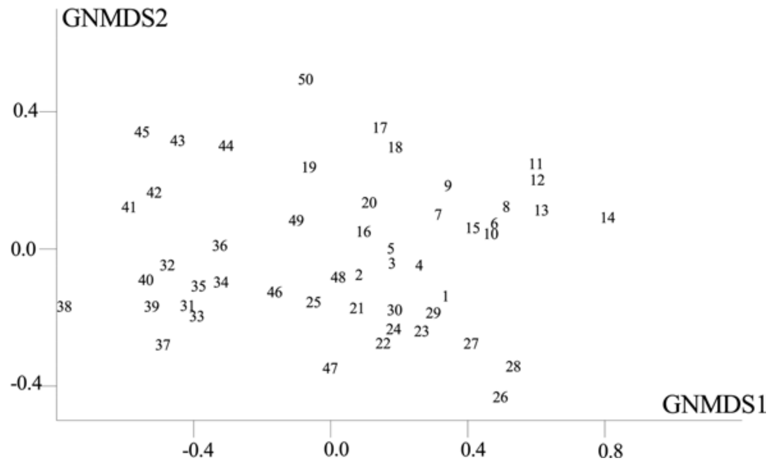

Fig.128. Gutulia: GNMDS ordination biplot diagram of 50 meso plots (indicated by their number).

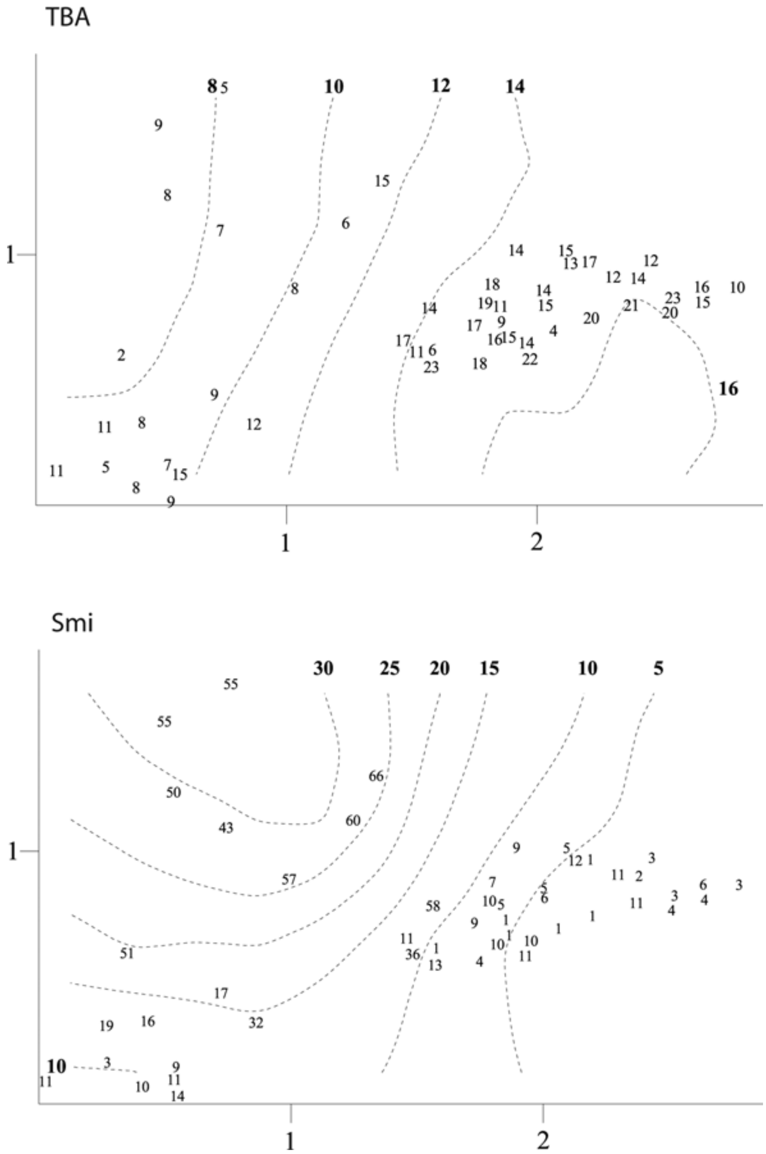

Figs 129-130. Gutulia: isolines for environmental variables in the DCA ordinations of 50 meso plots, axes 1 (horizontal) and 2 (vertical). Values for the environmental variables are plotted onto the meso plots' positions. Scaling in S.D. units. Fig. 129. TBA ($R^2 = 0.611$). Fig. 130. Smi ($R^2 = 0.658$). R^2 refers to the coefficient of determination between original and smoothened values as interpolated from the isolines. Names of environmental variables in accordance with Table 2.

Table 10. Gutulia: Split-plot GLM analysis and Kendall's nonparametric correlation coefficient τ between DCA 1 and 31 environmental variables (predictor) in the 50 meso plots. df_{resid}: degrees of freedom for the residuals; *SS*: total variation; *FVE*: fraction of total variation attributable to a given scale (macro plot or meso plot); SS_{expl}/SS: fraction of the variation attributable to the scale in question, explained by a variable; *r*: model coefficient (only given when significant at the α = 0.05 level, otherwise blank); *F*: *F* statistic for test of the hypothesis that *r* = 0 against the two-tailed alternative. Split-plot GLM relationships significant at level α = 0.05, *P*, *F*, *r* and SS_{expl}/SS, and Kendall's nonparametric correlation coefficient $|\tau| \geq 0.30$ are given in bold face. Numbers and abbreviations for names of environmental variables are in accordance with Tab. 2.

Predictor	Dependent variable = DCA 1 (*SS* = 29.2643)								Correlation between predictor and DCA 1
	Error level								
	Macro plot df_{resid} = 8 $SS_{macro\ plot}$ = 27.9043 *FVE* = 0.9535 of *SS*				Meso plot within macro plot df_{resid} = 39 $SS_{meso\ plot}$ = 1.36000 *FVE* = 0.0465 of *SS*				Total
	$SS_{expl}/SS_{macro\ plot}$	*r*	*F*	*P*	$SS_{expl}/SS_{meso\ plot}$	*r*	*F*	*P*	τ
Ma Slo	0.0553		0.4679	0.5133	0.0009		0.0347	0.8533	0.217
Ma Asp	0.0023		0.0181	0.8963	0.0002		0.0060	0.9387	–0.046
Ma HI	0.0619		0.5279	0.4882	0.0002		0.0077	0.9304	–0.188
Ma Ter	0.0047		0.0381	0.8500	0.0341		1.3776	0.2476	–0.049
Ma Une	0.2292		2.3785	0.1616	0.0147		0.5807	0.4506	–0.297
TBA	**0.5716**	**2.9582**	**10.6740**	**0.0114**	0.0008		0.0329	0.8571	**0.365**
Me Slo	0.0246		0.2016	0.6654	0.0510		2.0951	0.1558	0.133
Me Asp	0.0116		0.0937	0.7673	0.0195		0.7764	0.3836	0.024
Me HI	0.0844		0.7378	0.4154	0.0004		0.0176	0.8953	–0.102
Me Ter	0.0578		0.4910	0.5034	0.0084		0.3290	0.5695	–0.035
Me Une	0.0227		0.1855	0.6780	0.0901		3.8621	0.0565	–0.137
Smi	0.3935		5.1903	0.0522	0.0000		0.0006	0.9799	**–0.430**
Sme	**0.4095**	**–1.747**	**5.5481**	**0.0463**	0.0528		2.1723	0.1485	**–0.403**
Sma	0.3352		4.0344	0.0795	0.0217		0.8646	0.3582	–0.271
Mme	0.1321		1.2176	0.3019	0.0139		0.5497	0.4629	0.169
LOI	**0.5269**	**–1.873**	**8.9093**	**0.0175**	0.0003		0.0130	0.9099	**–0.451**
Total N	**0.4169**	**2.2566**	**5.7199**	**0.0437**	0.0041		0.1622	0.6893	0.295
pH_{H_2O}	**0.7113**	**2.1803**	**19.7090**	**0.0022**	0.0084		0.3288	0.5697	**0.568**
pH_{CaCl_2}	**0.7125**	**2.0798**	**19.8230**	**0.0021**	0.0024		0.0945	0.7601	**0.575**
H	**0.6636**	**–2.061**	**15.7810**	**0.0041**	0.0003		0.0102	0.9201	**–0.553**
Al	0.0054		0.0435	0.8400	0.0019		0.0755	0.7849	–0.053
C	**0.6654**	**2.7013**	**15.9080**	**0.0040**	0.0124		0.4908	0.4877	**0.558**
Ca	0.2347		2.4533	0.1559	0.0012		0.0451	0.8330	0.221
Fe	0.0180		0.1468	0.7116	0.0132		0.5204	0.4750	–0.112
K	**0.4409**	**2.2281**	**6.3085**	**0.0363**	0.0088		0.3466	0.5594	**0.487**
Mg	0.0773		0.6702	0.4367	0.0208		0.8285	0.3683	0.189
Mn	**0.5906**	**1.8420**	**11.5410**	**0.0094**	0.0001		0.0055	0.9413	**0.451**
Na	0.3533		4.3706	0.0700	0.0004		0.0156	0.9013	0.269
P	0.0025		0.0200	0.8910	0.0003		0.0105	0.9188	0.030
S	**0.8087**	**2.6093**	**33.8220**	**0.0004**	0.0101		0.3984	0.5316	**0.605**
Zn	0.1602		1.5260	0.2518	0.0019		0.0740	0.7870	0.288

Table 11. Gutulia: Split-plot GLM analysis and Kendall's nonparametric correlation coefficient τ between DCA 2 and 31 environmental variables (predictor) in the 50 meso plots. df_{resid}: degrees of freedom for the residuals; *SS*: total variation; *FVE*: fraction of total variation attributable to a given scale (macro plot or meso plot); SS_{expl}/SS: fraction of the variation attributable to the scale in question, explained by a variable; *r*: model coefficient (only given when significant at the α = 0.05 level, otherwise blank); *F*: *F* statistic for test of the hypothesis that *r* = 0 against the two-tailed alternative. Split-plot GLM relationships significant at level α = 0.05, *P*, *F*, *r* and SS_{expl}/SS, and Kendall's non-parametric correlation coefficient $|\tau| \geq 0.30$ are given in bold face. Numbers and abbreviations for names of environmental variables are in accordance with Tab. 2.

Predictor	Dependent variable = DCA 2 (*SS* = 6.0188)								Correlation between predictor and DCA 2
	Error level								
	Macro plot df_{resid} = 8 $SS_{macro\ plot}$ = 4.6643 *FVE* = 0.7750 of *SS*				Meso plot within macro plot df_{resid} = 39 $SS_{meso\ plot}$ = 1.35446 *FVE* = 0.2250 of *SS*				Total
	$SS_{expl}/SS_{macro\ plot}$	*r*	*F*	*P*	$SS_{expl}/SS_{meso\ plot}$	*r*	*F*	*P*	τ
Ma Slo	0.3389		4.1007	0.0774	0.0275		1.1011	0.3005	–0.102
Ma Asp	0.0472		0.3967	0.5464	0.0003		0.0099	0.9214	–0.109
Ma HI	0.2968		3.3759	0.1035	0.0142		0.5604	0.4586	0.159
Ma Ter	0.0342		0.2837	0.6088	0.0302		1.2132	0.2774	0.039
Ma Une	0.0231		0.1893	0.6750	0.0010		0.0409	0.8408	0.094
TBA	0.0021		0.0171	0.8992	0.0051		0.2015	0.6560	0.023
Me slo	0.3579		4.4591	0.0677	0.0334		1.3460	0.2530	–0.182
Me Asp	0.0718		0.6189	0.4541	0.0127		0.5003	0.4836	–0.042
Me HI	0.3162		3.6994	0.0906	0.0010		3.6994	0.0906	0.092
Me Ter	0.1452		1.3585	0.2774	0.0291		1.1710	0.2859	–0.057
Me Une	0.0245		0.2007	0.6660	0.0075		0.2954	0.5899	0.074
Smi	0.0295		0.2431	0.6352	0.0109		0.4303	0.5157	0.001
Sme	0.0342		0.2834	0.6089	0.0692		2.9001	0.0965	0.033
Sma	0.0869		0.7613	0.4083	0.0612		2.5422	0.1189	0.099
Mme	0.0264		0.2172	0.6536	0.0078		0.3070	0.5827	–0.200
LOI	0.0057		0.0456	0.8363	0.0142		0.5625	0.4578	0.032
Total N	**0.4236**	**0.9300**	**5.8802**	**0.0415**	0.0215		0.8551	0.3608	0.299
pH_{H_2O}	0.0006		0.0048	0.9464	0.0356		1.4406	0.2373	0.028
pH_{CaCl_2}	0.0005		0.0043	0.9493	0.0123		0.4852	0.4902	0.039
H	0.0017		0.0139	0.9090	0.0010		0.0373	0.8478	–0.017
Al	0.0316		0.2611	0.6232	0.0079		0.3106	0.5805	0.048
C	0.0013		0.0106	0.9207	0.0356		1.4410	0.2372	0.104
Ca	0.1056		0.9449	0.3595	0.0090		0.3557	0.5543	0.242
Fe	0.0555		0.4697	0.5125	0.0078		0.3046	0.5842	0.133
K	0.0307		0.2537	0.6280	0.0002		0.0069	0.9345	–0.006
Mg	0.0004		0.0028	0.9589	0.0297		1.1946	0.2811	0.048
Mn	0.0001		0.0009	0.9769	0.0135		0.5340	0.4693	–0.074
Na	**0.4173**	**1.4811**	**5.7294**	**0.0436**	0.0078		0.3071	0.5826	**0.367**
P	0.0146		0.1188	0.7392	0.0058		0.2268	0.6366	–0.074
S	0.0206		0.1681	0.6926	0.0003		0.0130	0.9096	0.056
Zn	0.0077		0.0617	0.8102	0.0079		0.3114	0.5800	0.020

loss on ignition, and the more base rich plots on steeper slopes with higher biomass of trees.

PCA ordination of environmental variables

The first two PCA axes accounted for 46.6% and 14.5% of the variance in the matrix of standardised transformed environmental variables, respectively (the corresponding eigenvalues were 0.466 and 0.145).

Lowest loadings on PCA axis 1 as well as loadings close to zero on PCA axis 2 were obtained by median, minimum and maximum soil depth, loss-on-ignition, and exchangeable H, S and Mn (Fig. 126). High loadings on this axis and loadings close to zero on PCA axis 2 were obtained by extractable C, K, P and Zn and pH_{H_2O} and pH_{CaCl_2}. Extractable Mg and Ca obtained relatively high loadings on PCA axis 1 together with macro and meso plot slope, while soil concentrations of Fe, macro plot heat index and macro plot unevenness obtained low loadings.

Total N and extractable Al obtained high loadings on PCA axis 2, while extractable P and Mg obtained low loadings.

The PCA ordination results were thus consistent with the correlation matrix in Table 9, emphasising importance of soil nutrient richness and topography for the environmental structure in the Gutulia reference area.

DCA ordination

The gradient length of the two first DCA axes was 2.76 and 1.62 S.D. units with eigenvalues of 0.404 and 0.136 respectively, showing that the first axis was particularly important.

The sample plots were relatively evenly distributed along DCA axis 1, but dispersion along DCA axis 2 was largest among plots with DCA axis 1 values less than 1.4 S.D. units (Fig. 127).

GNMDS ordination

The GNMDS ordination diagram (Fig. 128) showed good visual similarity to the DCA diagram (Fig. 127). The correlation between GNMDS axis 1 and DCA axis 1 was $\tau = 0.917$ and between GNMDS axis 2 and DCA axis 2 $\tau = 0.342$.

Split-plot GLM analysis of relationships between ordination axes and environmental variables

Variation (in plot scores) along DCA axis 1 was partitioned with 95.35 % at the macro plot scale (i.e. between macro plots) and 4.65 % at the (between) meso plot scale within macro plots (Table 10). For the second ordination axis, 77.50 % of the variation was explained at the macro plot scale and 22.50 % at the meso plot scale (Table 11).

At the macro plot scale, eleven environmental variables were significantly (at the $\alpha = 0.05$ level) related to DCA 1 while two variables (also at the $\alpha = 0.05$ level) were related to DCA 2. At the meso plot scale level, no environmental variables were significantly related to both DCA 1 and DCA 2 (Tables 10 and 11).

At the macro plot scale, tree basal area and both pH measures and soil concentrations of Total N, C, K, Mn and S increased significantly along DCA 1, while soil concentration of H, loss-on-ignition and median soil depth decreased (Table 10).

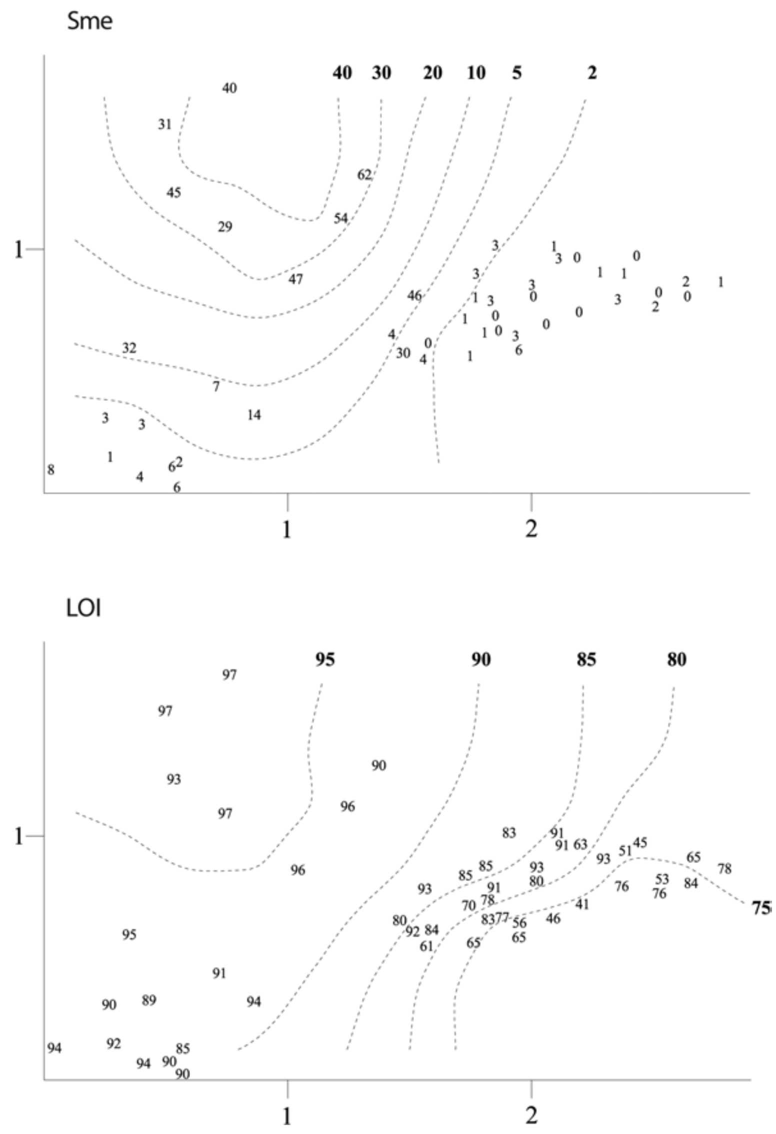

Figs 131-132. Gutulia: isolines for environmental variables in the DCA ordinations of 50 meso plots, axes 1 (horizontal) and 2 (vertical). Values for the environmental variables are plotted onto the meso plots' positions. Scaling in S.D. units. Fig. 131. Sme (R^2 = 0.691). Fig. 132. LOI (R^2 = 0.681). R^2 refers to the coefficient of determination between original and smoothened values as interpolated from the isolines. Names of environmental variables in accordance with Table 2.

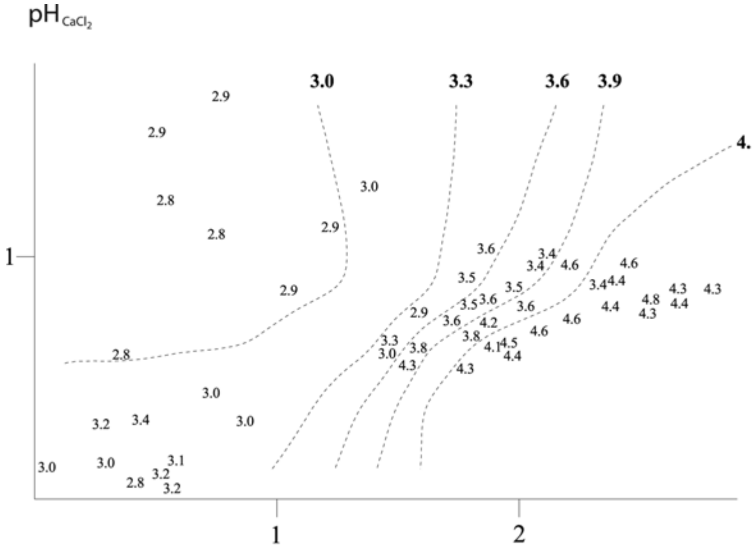

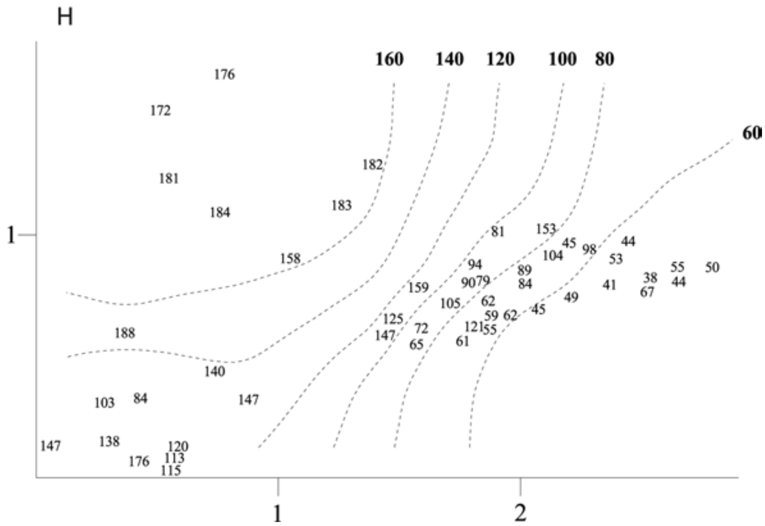

Figs 133-134. Gutulia: isolines for environmental variables in the DCA ordinations of 50 meso plots, axes 1 (horizontal) and 2 (vertical). Values for the environmental variables are plotted onto the meso plots' positions. Scaling in S.D. units. Fig. 133. pH_{CaCl_2} ($R^2 = 0.852$). Fig. 134. H ($R^2 = 0.785$). R^2 refers to the coefficient of determination between original and smoothened values as interpolated from the isolines. Names of environmental variables in accordance with Table 2.

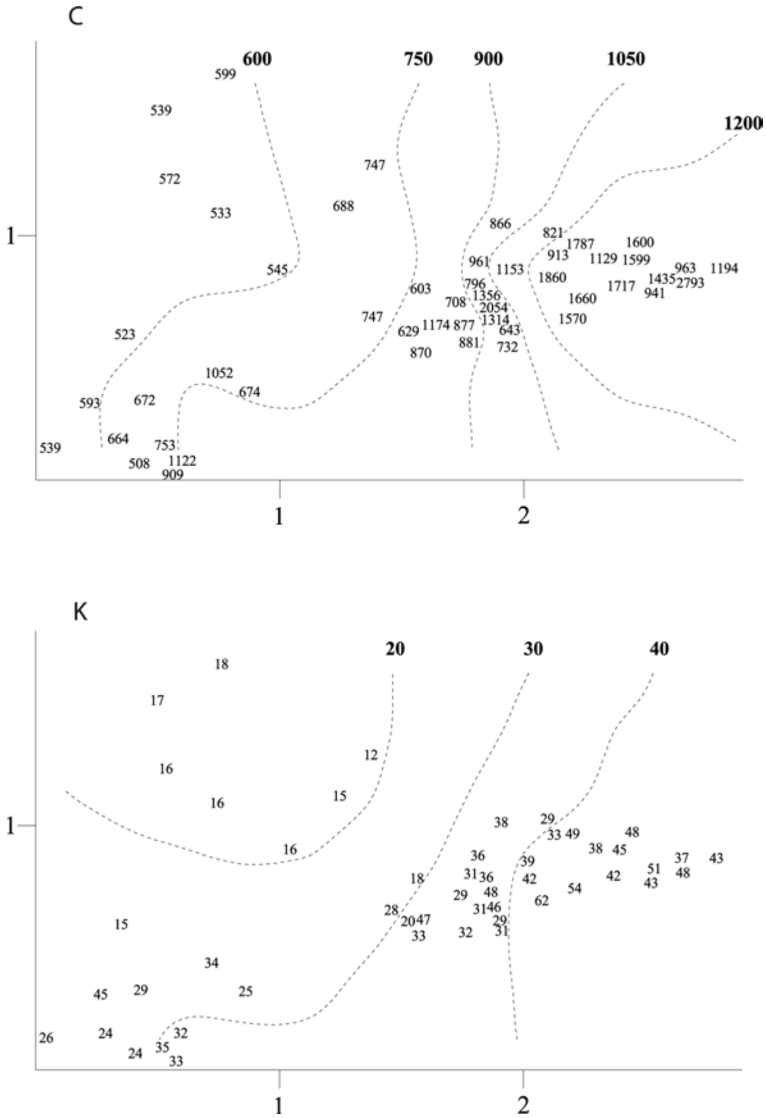

Figs 135-136. Gutulia: isolines for environmental variables in the DCA ordinations of 50 meso plots, axes 1 (horizontal) and 2 (vertical). Values for the environmental variables are plotted onto the meso plots' positions. Scaling in S.D. units. Fig. 135. C (R^2 = 0.714). Fig. 136. K (R^2 = 0.726). R^2 refers to the coefficient of determination between original and smoothened values as interpolated from the isolines. Names of environmental variables in accordance with Table 2.

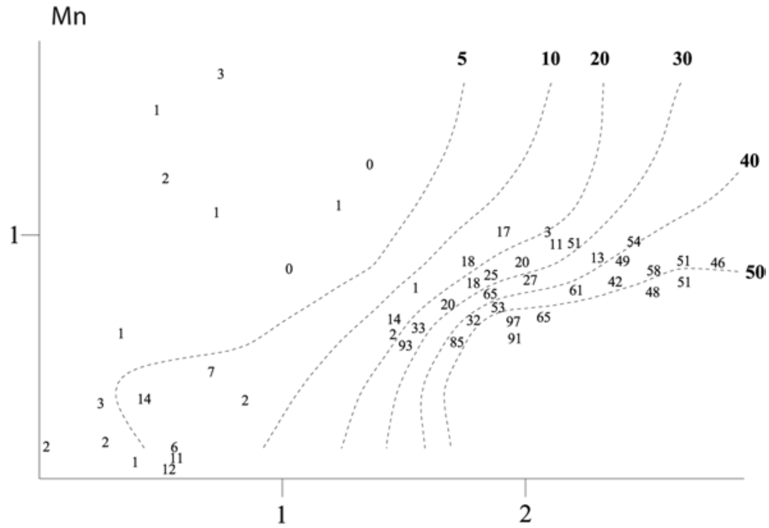

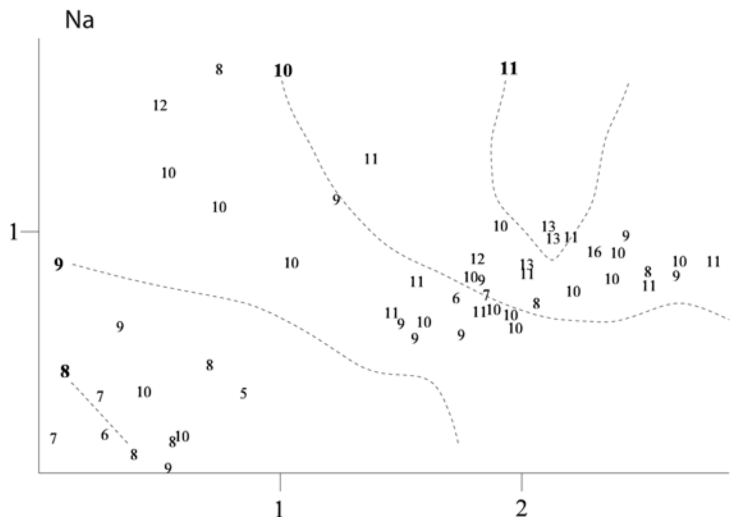

Figs 137-138. Gutulia: isolines for environmental variables in the DCA ordinations of 50 meso plots, axes 1 (horizontal) and 2 (vertical). Values for the environmental variables are plotted onto the meso plots' positions. Scaling in S.D. units. Fig. 136. Mn (R^2 = 0.812). Fig. 137. Na (R^2 = 0.666). R^2 refers to the coefficient of determination between original and smoothened values as interpolated from the isolines. Names of environmental variables in accordance with Table 2.

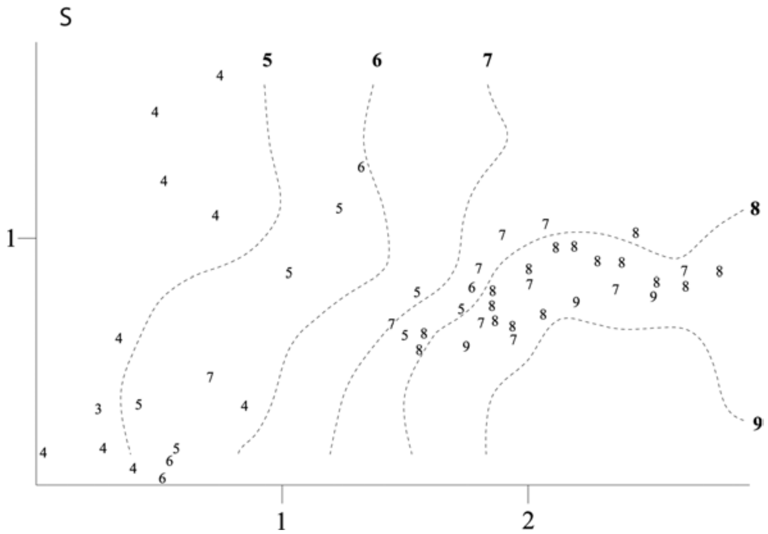

Fig. 139. Gutulia: isolines for environmental variables in the DCA ordinations of 50 meso plots, axes 1 (horizontal) and 2 (vertical). Values for the environmental variables are plotted onto the meso plots' positions. Scaling in S.D. units. Fig. 139. S ($R^2 = 0.815$). R^2 refers to the coefficient of determination between original and smoothened values as interpolated from the isolines. Names of environmental variables in accordance with Table 2.

At the macro plot scale, DCA 2 was only significant (positively) related to the concentration of Total N and Na (Table 11).

Correlations between DCA axes and environmental variables

Extractable S (Fig. 139), pH measuresments [pH_{CaCl_2} (Fig. 133)], extractable C (Fig. 135) and exchangeable H (negatively related to the axis; Fig. 134) showed the highest correlations with DCA axis 1 (Table 15). A total of 11 out of 31 of the measured variables had a correlation $|\tau| > 0.300$ (Figs 129-139). Variables related to high soil nutrient richness were positively correlated while loss-on-ignition and exchangeable H were negatively correlated with this axis.

Only one variable, extractable Na (Fig. 138), had a correlation higher than $|\tau| > 0.300$ with DCA axis 2.

Frequent species

A total of 87 species were recorded within the fifty 1×1 m meso sample plots: 41 vascular plants, 19 mosses, 11 liverworts and 16 lichens. The most frequent species (the sum of subplot frequencies in brackets) are: *Vaccinium myrtillus* (786 out of 800), *Avenella flexuosa* (766), *Vaccinium vitis-idaea* (674), *Barbilophozia lycopodioides* (534), *Dicranum scoparium* (473), *Trientalis europaea* (352),

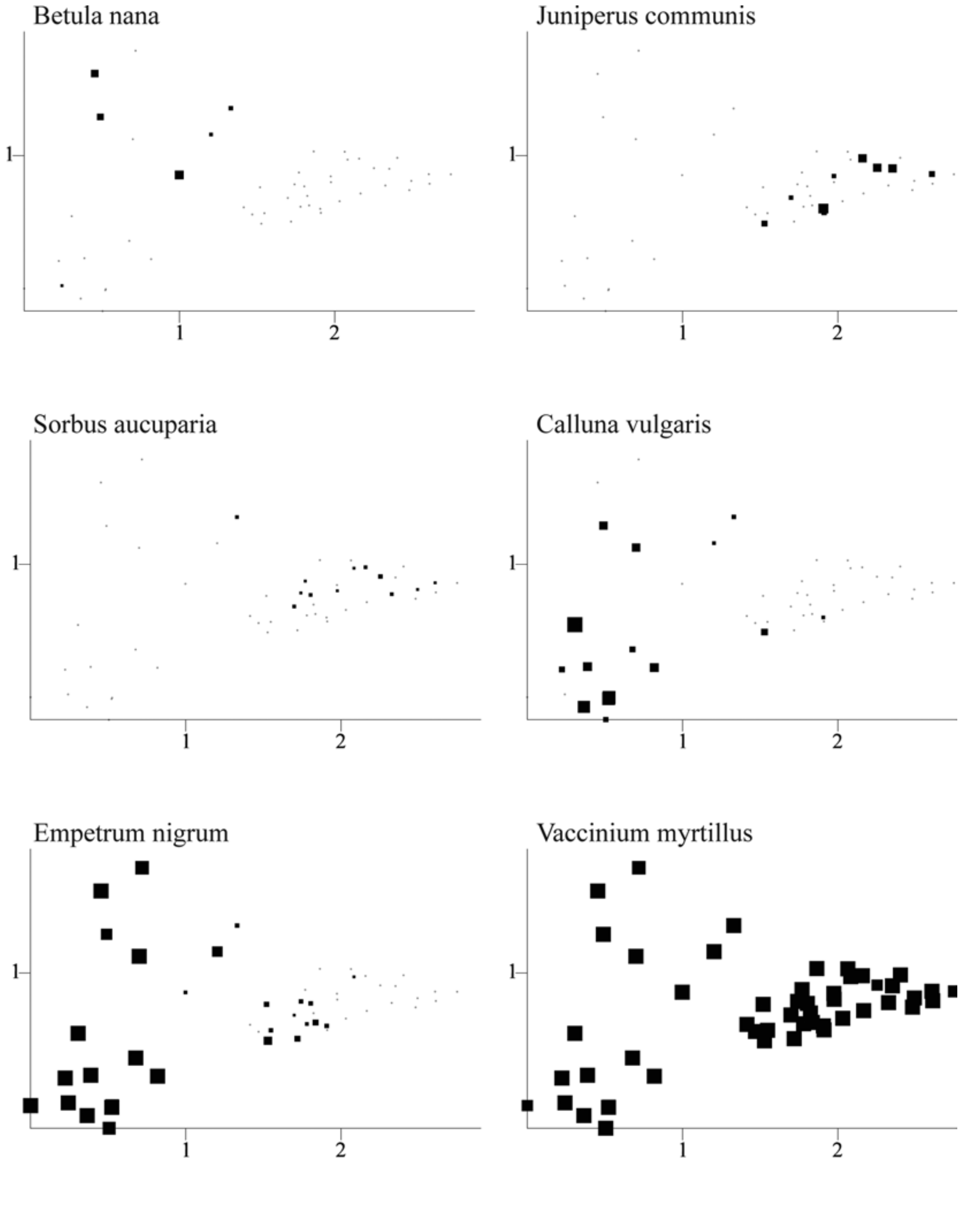

Figs 140-145. Gutulia: distributions of species abundances in the DCA ordination of 50 meso plots, axes 1 (horizontal) and 2 (vertical). Frequency in subplots for each species in each meso plot proportional to quadrate size. Scaling in S.D. units. Fig. 140. *Betula nana*. Fig. 141. *Juniperus communis*. Fig. 142. *Sorbus aucuparia*. Fig. 143. *Calluna vulgaris*. Fig. 144. *Empetrum nigrum*. Fig. 145. *Vaccinium myrtillus*.

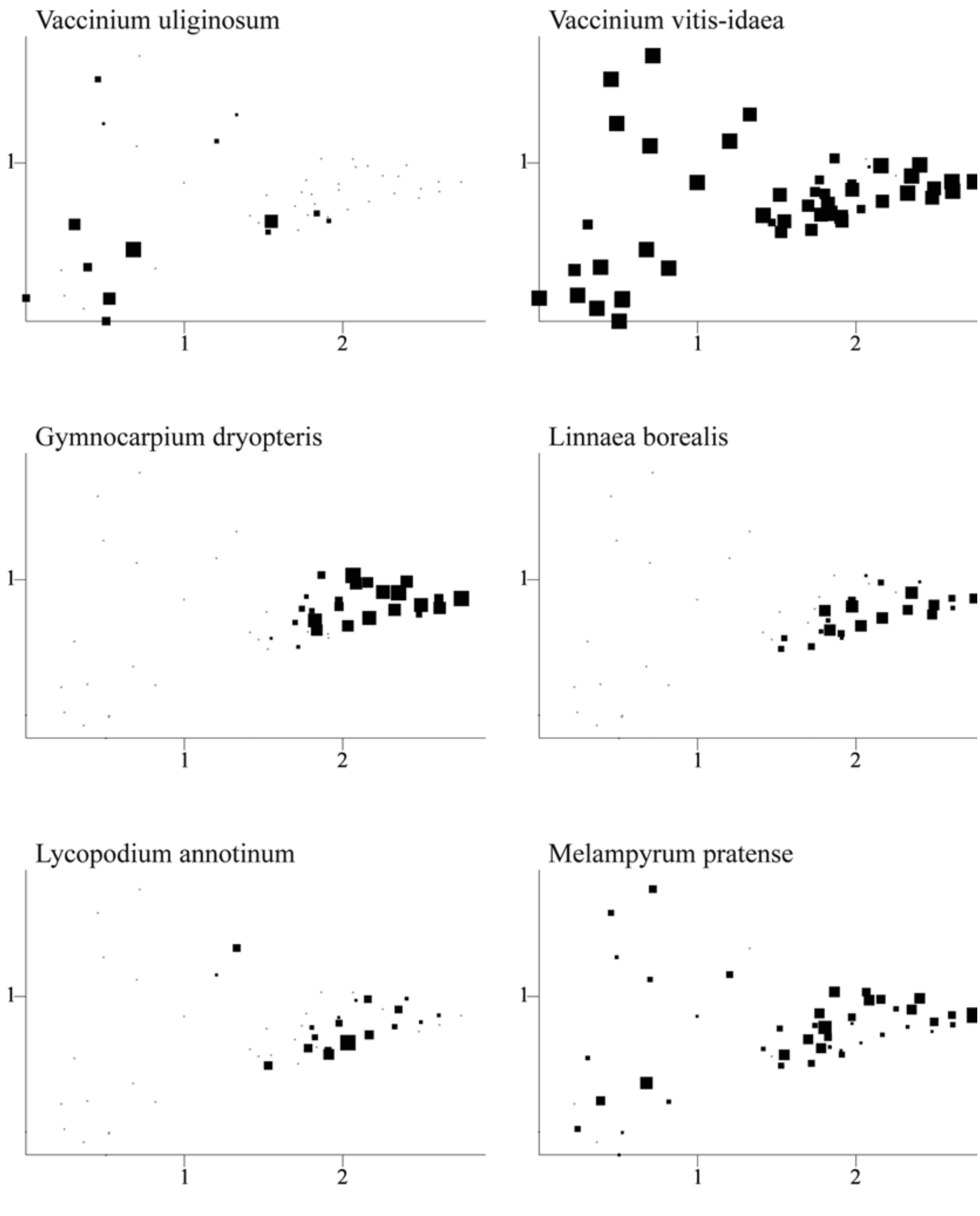

Figs 146-151. Gutulia: distributions of species abundances in the DCA ordination of 50 meso plots, axes 1 (horizontal) and 2 (vertical). Frequency in subplots for each species in each meso plot proportional to quadrate size. Scaling in S.D. units. Fig. 146. *Vaccinium uliginosum*. Fig. 147. *Vaccinium vitis-idaea*. Fig. 148. *Gymnocarpium dryopteris*. Fig. 149. *Linnaea borealis*. Fig. 150. *Lycopodium annotinum*. Fig. 151. *Melampyrum pratense*.

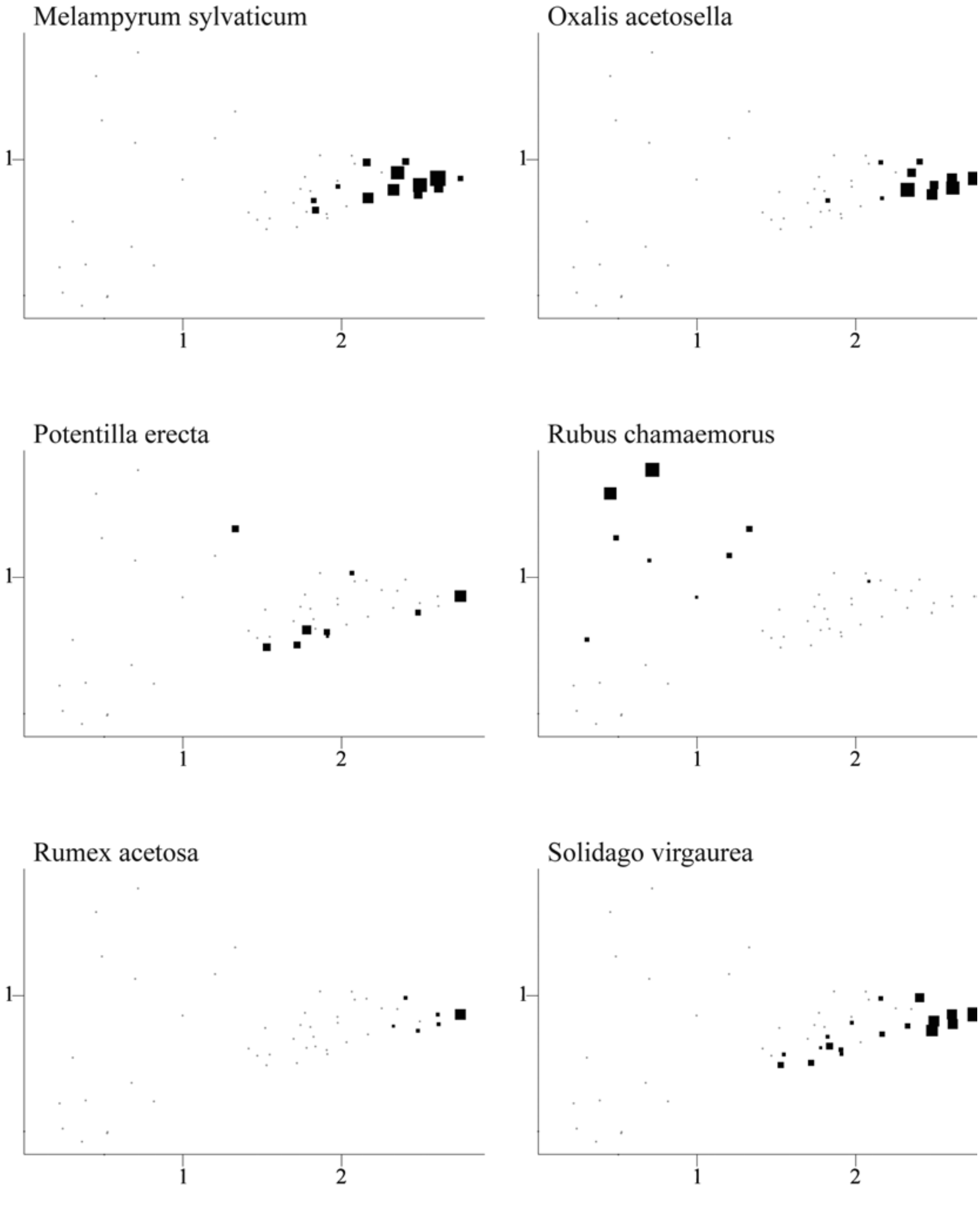

Figs 152-157. Gutulia: distributions of species abundances in the DCA ordination of 50 meso plots, axes 1 (horizontal) and 2 (vertical). Frequency in subplots for each species in each meso plot proportional to quadrate size. Scaling in S.D. units. Fig. 152. *Melampyrum sylvaticum*. Fig. 153. *Oxalis acetosella*. Fig. 154. *Potentilla erecta*. Fig. 155. *Rubus chamaemorus*. Fig. 156. *Rumex acetosa*. Fig. 157. *Solidago virgaurea*.

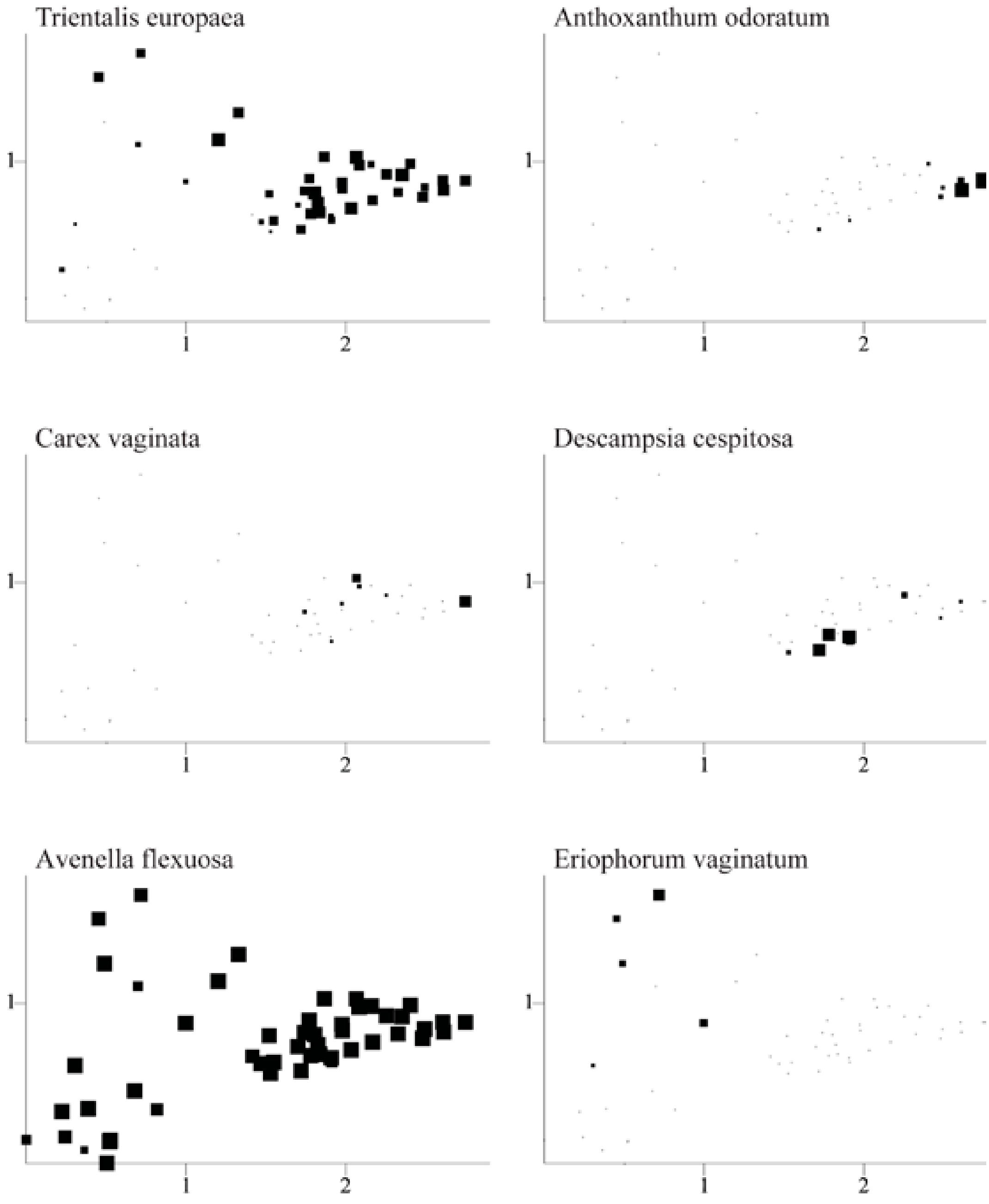

Figs 158-163. Gutulia: distributions of species abundances in the DCA ordination of 50 meso plots, axes 1 (horizontal) and 2 (vertical). Frequency in subplots for each species in each meso plot proportional to quadrate size. Scaling in S.D. units. Fig. 158. *Trientalis europaea*. 159. *Anthoxanthum odoratum*. Fig. 160. *Carex vaginata*. Fig. 161. *Deschampsia cespitosa*. Fig. 162. *Avenella flexuosa*. Fig. 163. *Eriophorum vaginatum*.

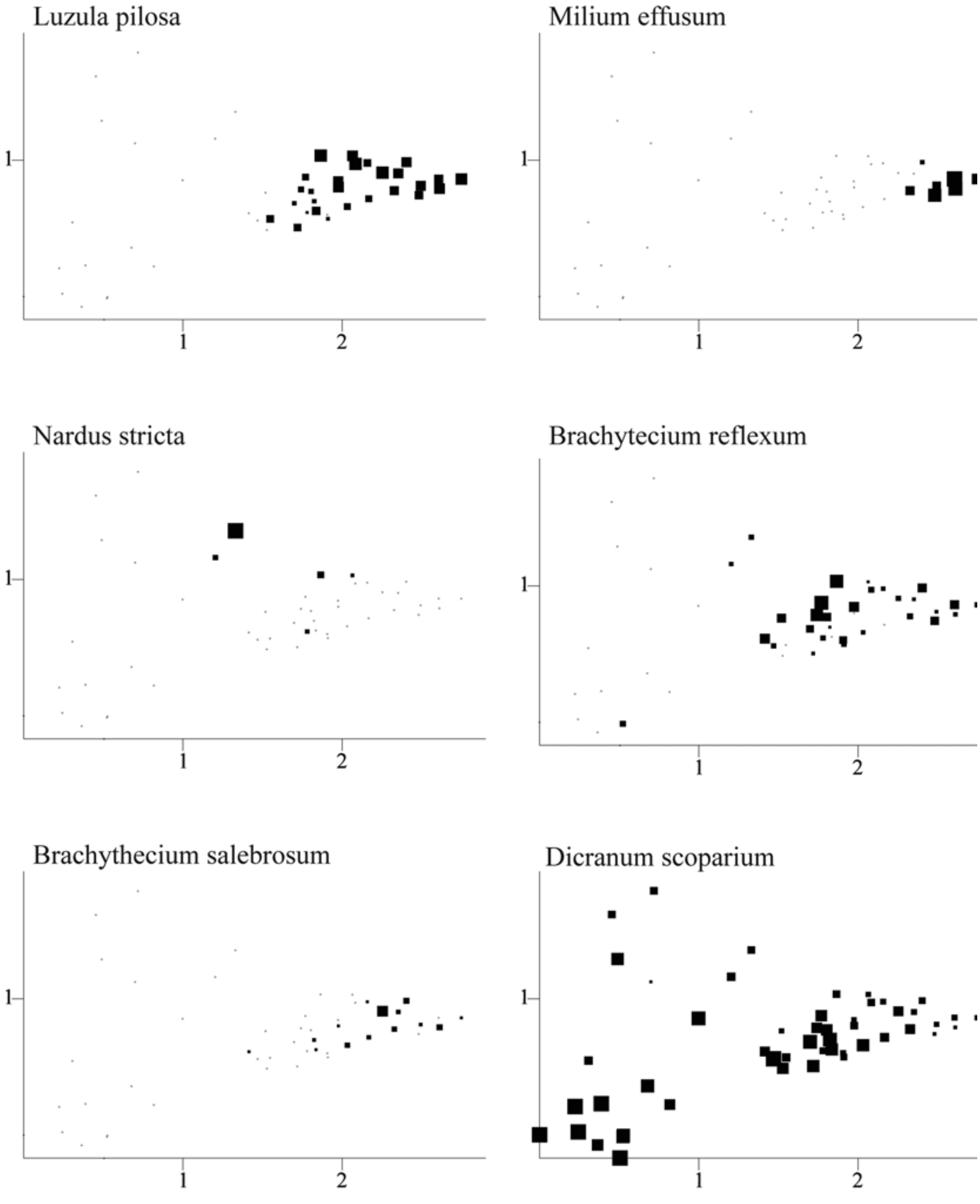

Figs 164-169. Gutulia: distributions of species abundances in the DCA ordination of 50 meso plots, axes 1 (horizontal) and 2 (vertical). Frequency in subplots for each species in each meso plot proportional to quadrate size. Scaling in S.D. units. Fig. 164. *Luzula pilosa*. Fig. 165. *Milium effusum*. Fig. 166. *Nardus stricta*. Fig. 167. *Brachythecium reflexum*. Fig. 168. *Brachythecium salebrosum*. Fig. 169. *Dicranum scoparium*.

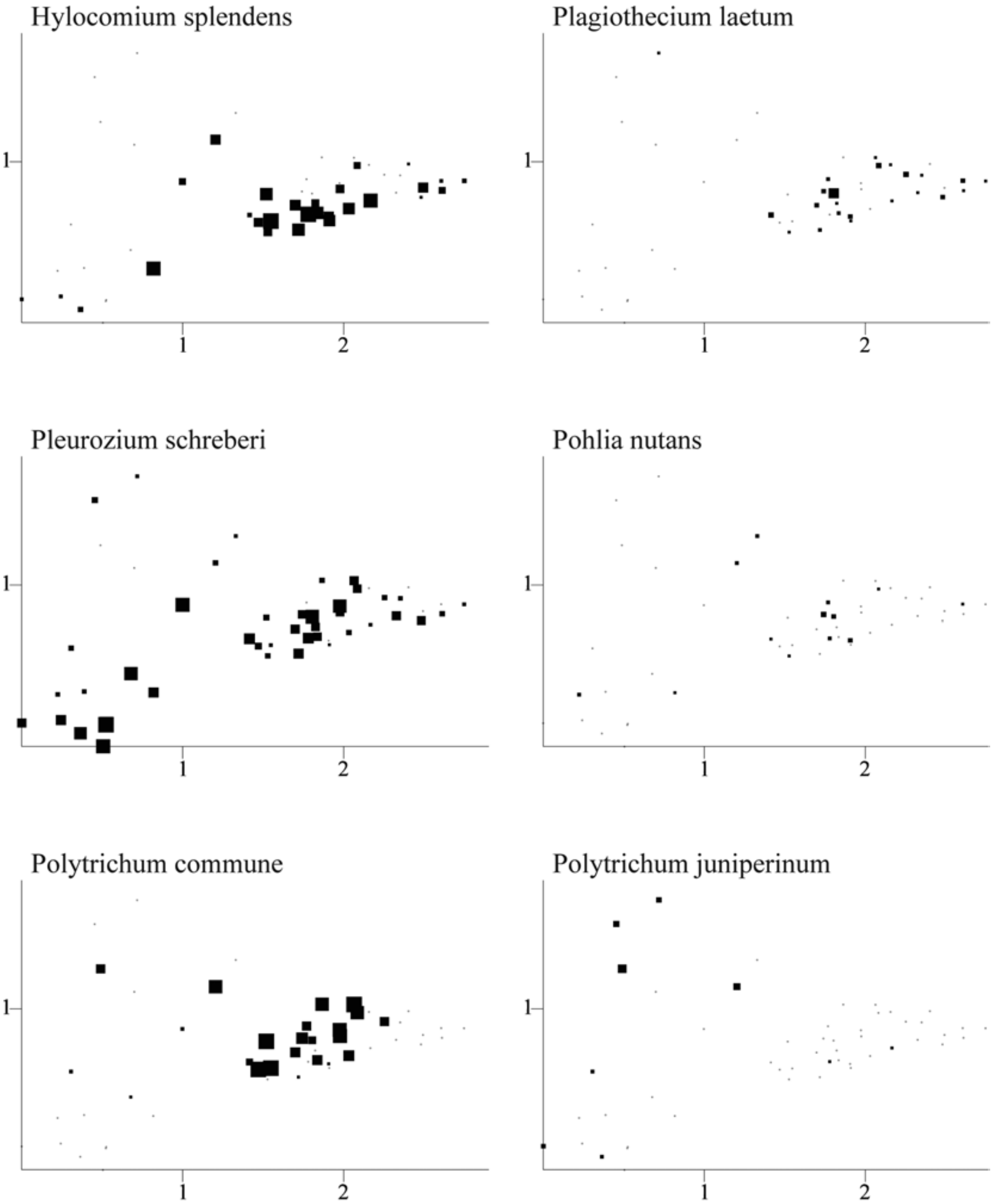

Figs 170-175. Gutulia: distributions of species abundances in the DCA ordination of 50 meso plots, axes 1 (horizontal) and 2 (vertical). Frequency in subplots for each species in each meso plot proportional to quadrate size. Scaling in S.D. units. Fig. 170. *Hylocomium splendens*. Fig. 171. *Plagiothecium laetum*. Fig. 172. *Pleurozium schreberi*. Fig. 173. *Pohlia nutans*. Fig. 174. *Polytrichum commune*. Fig. 175. *Polytrichum juniperinum*.

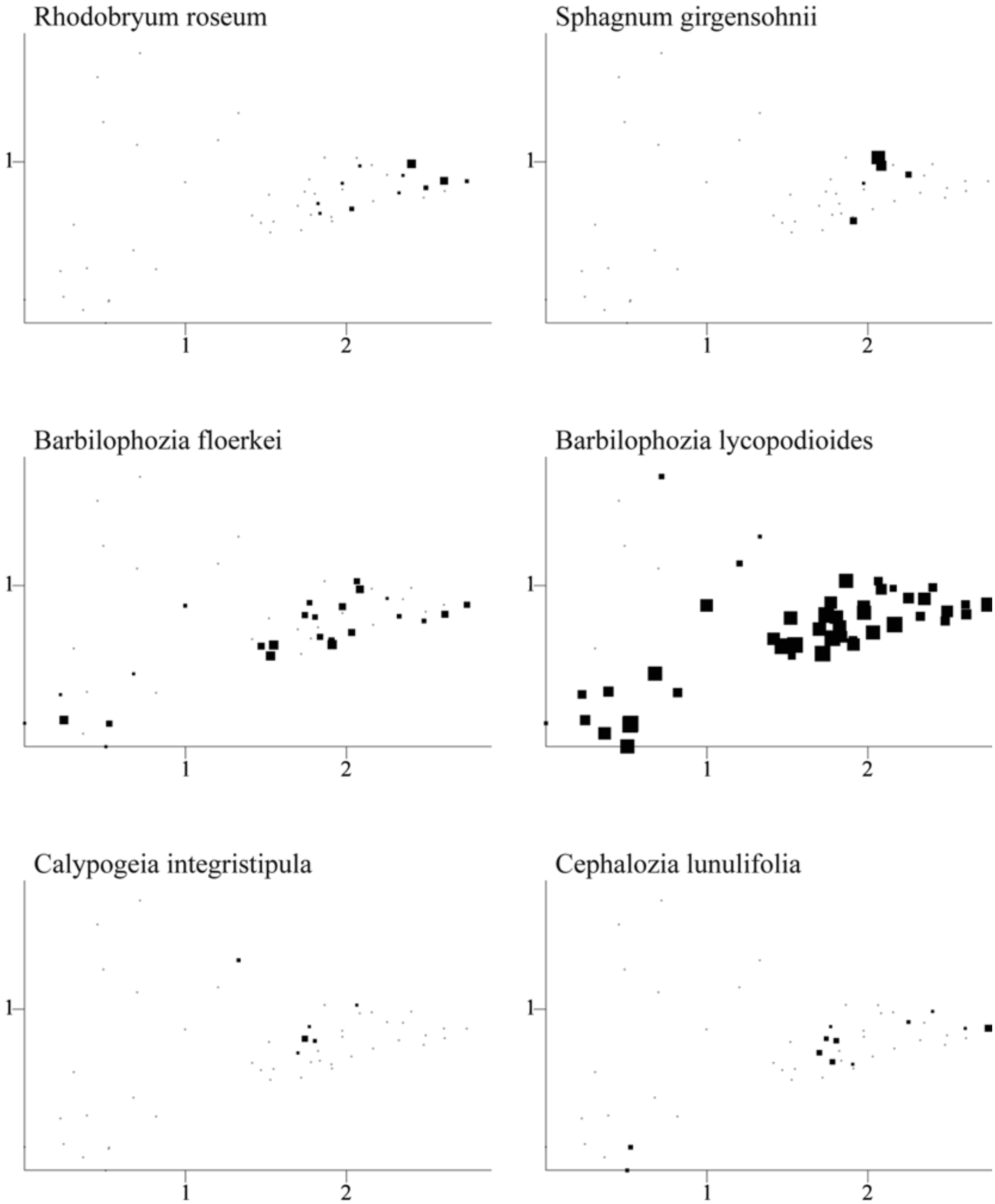

Figs 176-181. Gutulia: distributions of species abundances in the DCA ordination of 50 meso plots, axes 1 (horizontal) and 2 (vertical). Frequency in subplots for each species in each meso plot proportional to quadrate size. Scaling in S.D. units. Fig. 176. *Rhodobryum roseum*. Fig. 177. *Sphagnum girgensohnii*. Fig. 178. *Barbilophozia floerkei*. Fig. 179. *Barbilophozia lycopodioides*. Fig. 180. *Calypogeia integristipula*. Fig. 181. *Cephalozia lunulifolia*.

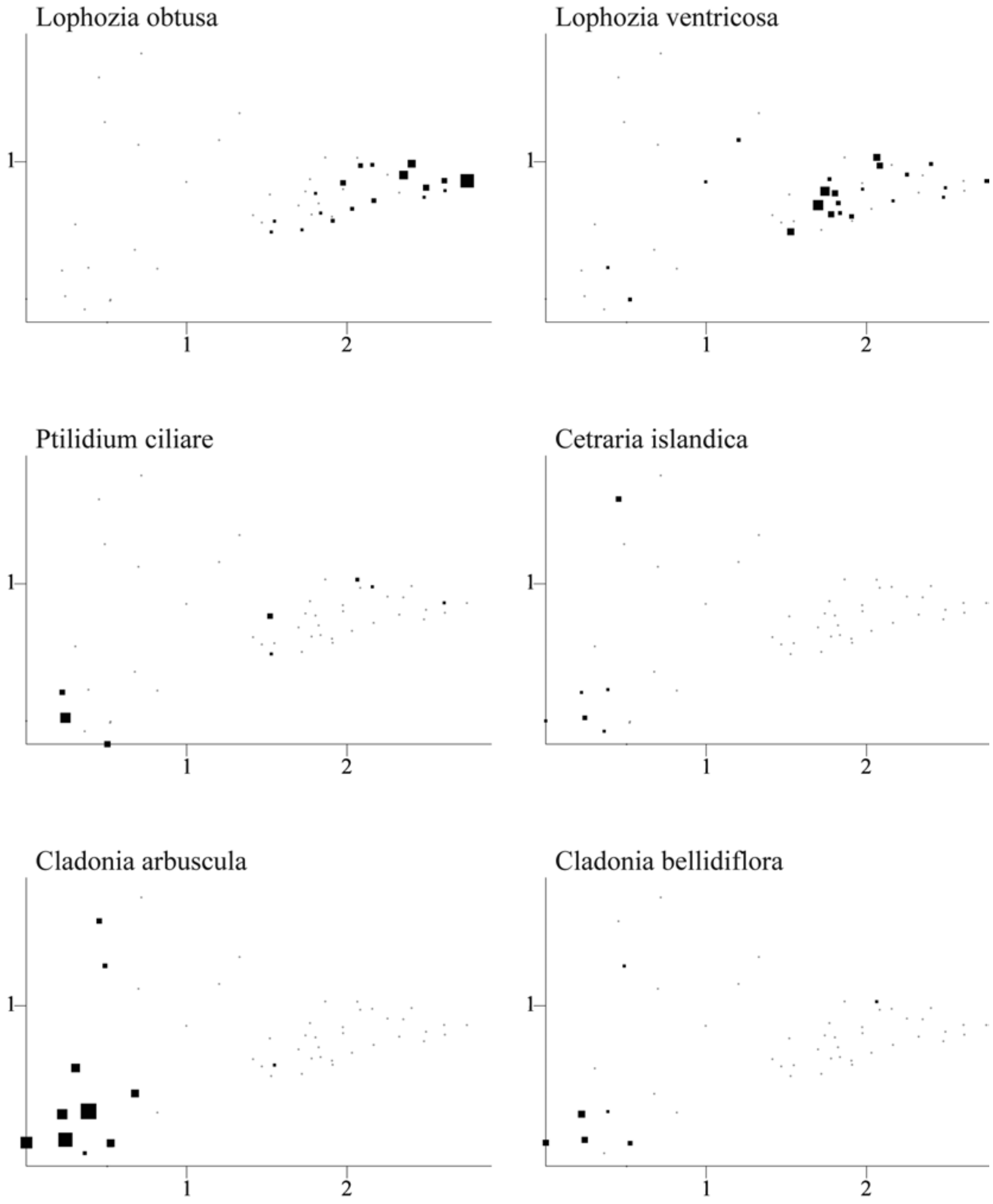

Figs 182-187. Gutulia: distributions of species abundances in the DCA ordination of 50 meso plots, axes 1 (horizontal) and 2 (vertical). Frequency in subplots for each species in each meso plot proportional to quadrate size. Scaling in S.D. units. Fig. 182. *Lophozia obtusa*. Fig. 183. *Lophozia ventricosa*. Fig. 184. *Ptilidium ciliare*. Fig. 185. *Cetraria islandica*. Fig. 186. *Cladonia arbuscula*. Fig. 197. *Cladonia bellidiflora*.

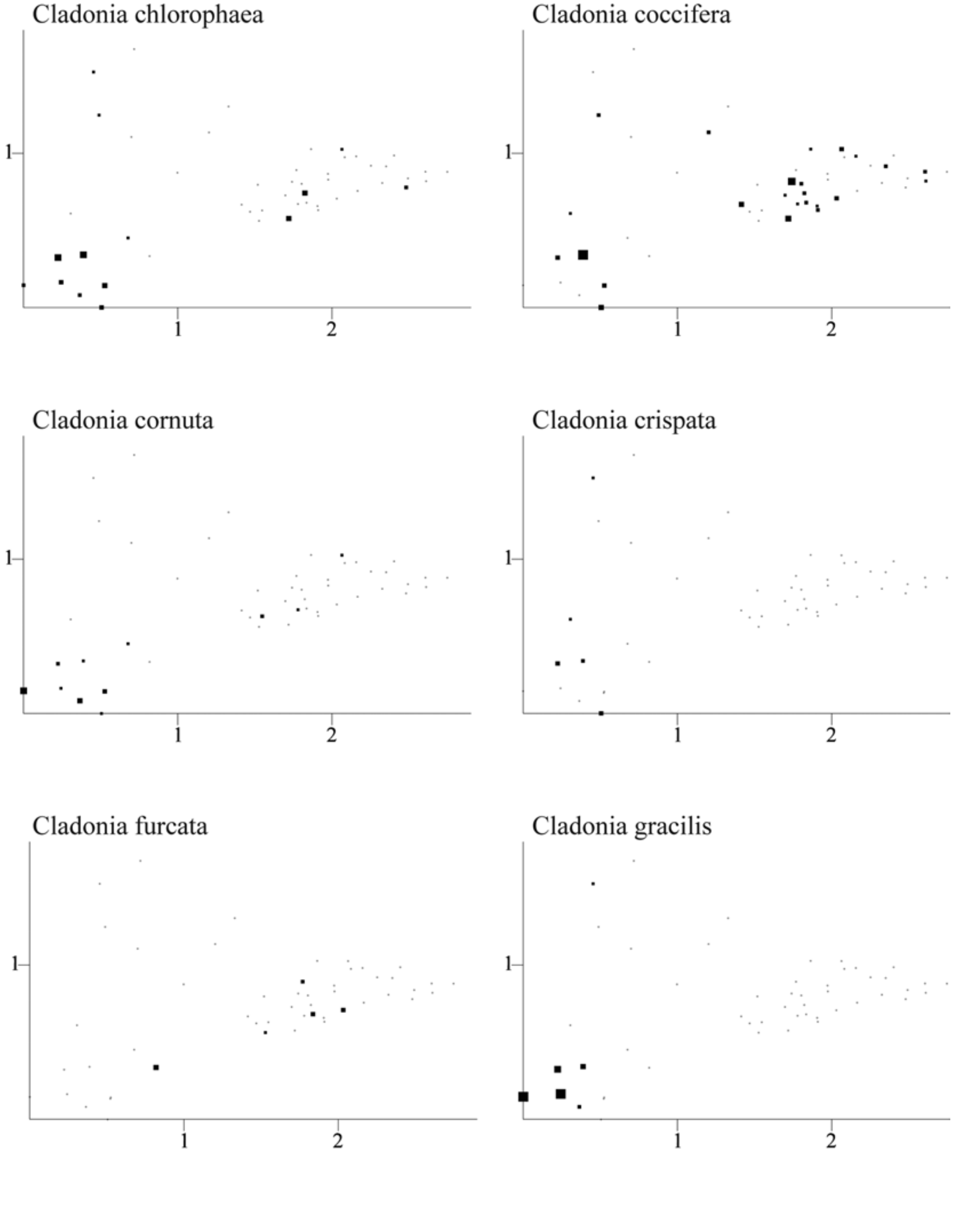

Figs 188-193. Gutulia: distributions of species abundances in the DCA ordination of 50 meso plots, axes 1 (horizontal) and 2 (vertical). Frequency in subplots for each species in each meso plot proportional to quadrate size. Scaling in S.D. units. Fig. 188. *Cladonia chlorophaea*. Fig. 189. *Cladonia coccifera*. Fig. 190. *Cladonia cornuta*. Fig. 191. *Cladonia crispata*. Fig. 192. *Cladonia furcata*. Fig. 193. *Cladonia gracilis*.

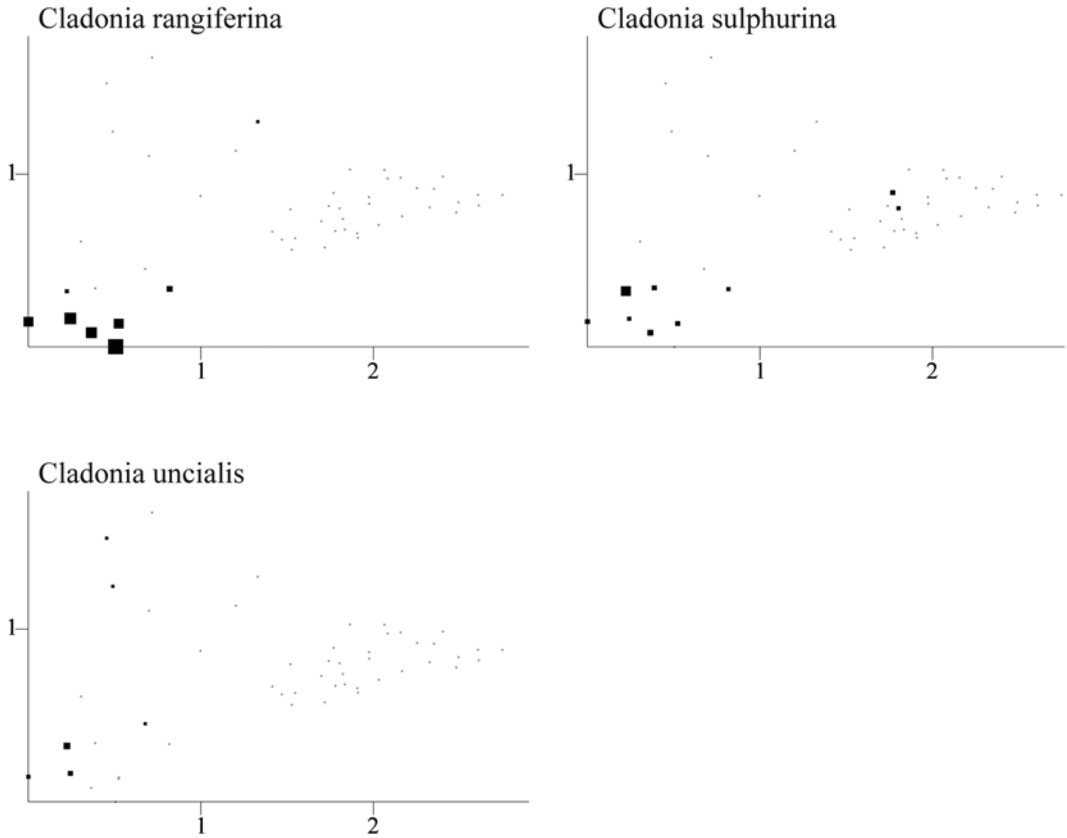

Figs 194-196. Gutulia: distributions of species abundances in the DCA ordination of 50 meso plots, axes 1 (horizontal) and 2 (vertical). Frequency in subplots for each species in each meso plot proportional to quadrate size. Scaling in S.D. units. Fig. 194. *Cladonia rangiferina*. Fig. 195. *Cladonia sulphurina*. Fig. 196. *Cladonia uncialis*.

Pleurozium schreberi (315), *Empetrum nigrum* (286), *Melampyrum pratense* (267) and *Gymnocarpium dryopteris* (251).

The distribution of species abundance in the DCA ordination

Fifty seven of the totally 87 species occurred in 5 or more of the sample plots (Figs 140–196). *Vaccinium myrtillus* (Fig. 145), *Vaccinium vitis-idaea* (Fig. 147), *Avenella flexuosa* (Fig. 162) and *Dicranum scoparium* (Fig. 169) had wide ecological amplitudes and were highly abundant in most of the sample plots. *Barbilophozia lycopodioides* (Fig. 179) also had a relatively wide distribution, although it was rather rare in plots with low axis 1 scores and high axis 2 scores that were poor in soil nutrients, acidic, and situated on relatively deep soils.

Species restricted to high DCA axis1 scores, preferring soils with high pH values and high concentrations of extractable C, Ca, K, Mn and S, were *Juniperus communis* (Fig. 141), *Gymnocarpium dryopteris* (Fig. 148), *Linnaea borealis* (Fig. 149), *Melampyrum sylvaticum* (Fig. 152), *Oxalis acetosella* (Fig. 153), *Rumex acetosa* (Fig. 156), *Solidago virgaurea* (Fig. 157*), Anthoxanthum odoratum* (Fig. 159), *Carex vaginata* (Fig. 160), *Deschampsia cespitosa* (Fig. 161), *Luzula pilosa* (Fig. 164), *Milium effusum* (Fig. 165), *Brachythecium salebrosum* (Fig. 168), *Plagiothecium laetum* (Fig. 171), *Rhodobryum roseum* (Fig. 176) and *Lophozia obtusa* (Fig. 182).

Species restricted to sample plots with lower soil pH and less nutrient-rich soils were *Betula nana* (Fig. 140), *Eriophorum vaginatum* (Fig. 163), *Cetraria islandica* (Fig. 185), *Cladonia arbuscula* (Fig. 186), *Cladonia bellidiflora* (Fig.187), *Cladonia crispata* (Fig. 191), *Cladonia gracilis* (Fig. 193), *Cladonia rangiferina* (Fig. 194) and *Cladonia uncialis* (Fig. 196). Of these *Betula nana* and *Eriophorum vaginatum* had their main occurrence at high DCA axis 2 scores, on deep soils, while the *Cladonia* species were restricted to low DCA 2 scores, preferring a thin soil layer.

Melampyrum pratense (Fig. 151) and *Trientalis europaea* (Fig. 158) seemed to occur irrespectively to pH and concentration of C, H, K, Mn, Na and S (cf. Fig. 133-139).

ÅMOTSDALEN REFERENCE AREA

Correlations between environmental variables

There were strong pairwise correlations between several of the topographical variables, between soil chemical variables and between topographical and chemical variables related to soil nutrient richness and soil moisture (Table 12).

Macro plot slope was positively correlated with macro and meso plot aspect unfavourability and negatively correlated with macro plot heat index and macro plot terrain form. Meso plot slope was positive correlated with macro plot aspect unfavourability and negative correlated with meso plot heat index. In general meso plot slope was positively correlated with soil chemical variables that reflected soil nutrient status (e.g. Ca concentrations and pH) and negatively correlated with soil acidity (H and Fe) and high LOI. Meso plot heat index was negatively correlated with soil variables related to a gradient in soil nutrient richness (e.g. pH, Ca and K).

Tree basal area was negatively correlated with LOI and H and positively correlated with pH and most extractable elements. Median, minimum and maximum soil depths were internally positively

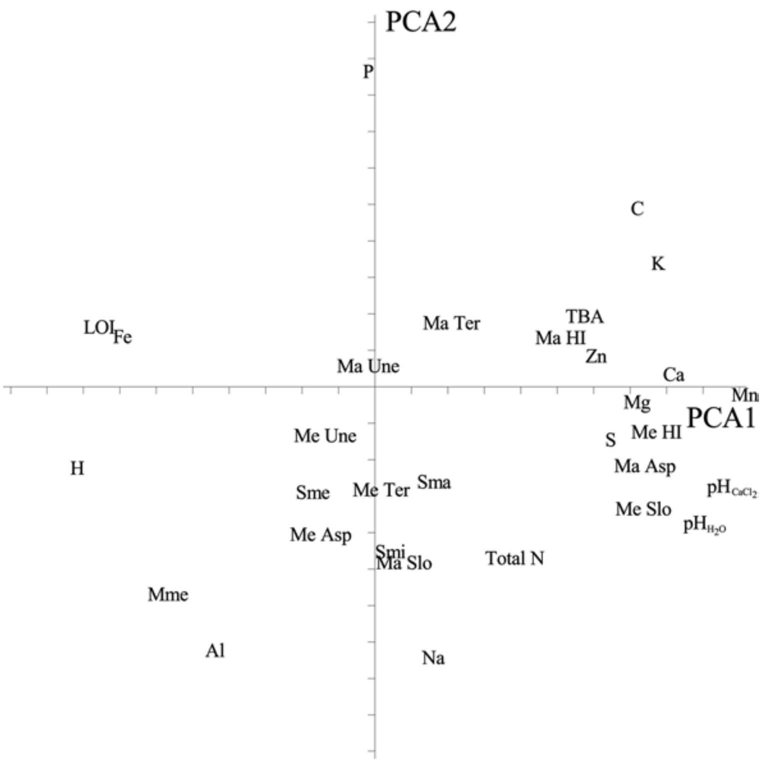

Fig. 197. Åmotsdalen: PCA ordination of 31 environmental variables. Abbreviations in accordance with Table 2), axes 1 (horizontal) and 2 (vertical). Positions of variables in the ordination space give the head of variable vectors. Tickmarks indicate 0.1 units along both axes.

Table 12. Åmotsdalen: Kendall's rank correlation coefficients τ between 31 environmental variables in the 50 meso plots (lower triangle), with significance probabilities (upper triangle). Statistically significant correlations ($P<0.05$) in bold face. Names of explanatory variables abbreviated in accordance with Table 2.

	1	2	3	4	5	6	7	8	9	10	11	12	13	14	15	16
01 Ma Slo	*	**0.009**	**0.022**	**0.020**	0.488	0.298	0.124	**0.003**	0.806	0.655	0.767	0.536	0.604	0.531	**0.010**	0.660
02 Ma Asp	**0.278**	*	**0.000**	0.744	0.322	0.141	**0.000**	0.264	**0.000**	0.442	0.316	0.717	0.353	0.556	0.080	**0.011**
03 Ma HI	**–0.236**	**0.539**	*	0.051	0.137	0.164	**0.001**	0.164	**0.000**	0.885	0.546	0.592	0.096	0.867	**0.004**	**0.015**
04 Ma Ter	**–0.273**	0.038	0.218	*	0.472	0.971	0.771	0.346	0.821	0.660	0.545	0.759	0.737	0.167	0.312	0.377
05 Ma Une	0.079	–0.110	–0.162	–0.089	*	0.473	**0.016**	0.206	**0.003**	**0.005**	**0.044**	0.287	0.432	**0.002**	0.586	0.351
05 TBA	–0.111	0.154	0.142	0.004	–0.081	*	0.185	**0.012**	0.100	0.650	**0.000**	0.686	0.565	0.886	**0.000**	**0.008**
07 Me Slo	0.165	**0.633**	**0.353**	–0.034	**–0.272**	0.140	*	0.719	**0.000**	0.979	0.257	0.606	0.767	0.642	0.137	**0.008**
08 Me Asp	**0.319**	0.119	–0.144	0.111	0.144	**–0.269**	0.039	*	**0.011**	0.966	0.470	0.052	**0.009**	0.185	**0.025**	0.252
09 Me HI	0.025	**0.480**	**0.394**	–0.025	**–0.322**	0.168	**0.747**	**–0.265**	*	0.946	0.294	0.530	0.116	0.162	**0.009**	**0.008**
10 Me Ter	–0.048	–0.081	0.015	0.051	**–0.315**	–0.048	0.003	–0.005	0.007	*	0.523	0.939	0.384	0.122	0.491	0.677
11 Me Une	0.031	–0.102	–0.060	–0.068	**0.220**	**–0.394**	–0.116	0.075	–0.104	–0.066	*	0.185	0.363	**0.020**	0.089	0.188
12 Smi	–0.064	–0.037	–0.053	0.034	0.116	–0.041	0.053	0.201	–0.062	–0.008	0.131	*	**0.000**	**0.000**	0.621	0.575
13 Sme	0.055	–0.096	–0.168	–0.038	0.087	–0.060	–0.031	**0.278**	–0.159	–0.091	–0.092	**0.413**	*	0.074	0.096	0.400
14 Sma	–0.065	–0.060	–0.017	0.155	**0.335**	–0.015	–0.048	0.137	–0.138	–0.158	**0.230**	**0.461**	0.180	*	0.927	0.172
15 Mme	**0.266**	–0.176	**–0.282**	–0.113	–0.059	**–0.353**	–0.151	**0.231**	**–0.256**	0.070	0.168	0.049	0.167	–0.009	*	**0.000**
16 LOI	0.045	**–0.257**	**–0.240**	–0.099	–0.101	**–0.268**	**–0.270**	0.118	**–0.262**	0.042	0.130	–0.055	0.084	–0.134	**0.344**	*
17 Total N	–0.066	–0.032	0.059	0.111	–0.190	0.089	–0.003	0.001	0.006	0.151	**–0.244**	0.011	–0.069	0.034	–0.032	**–0.218**
18 pH_{H_2O}	0.046	**0.352**	**0.312**	–0.002	–0.018	**0.232**	**0.364**	–0.146	**0.368**	0.023	–0.127	–0.032	–0.179	0.059	**–0.270**	**–0.634**
19 pH_{CaCl_2}	0.015	**0.355**	**0.324**	0.019	–0.029	**0.268**	**0.376**	–0.177	**0.397**	0.008	–0.147	–0.013	**–0.204**	0.066	**–0.329**	**–0.654**
20 H	0.085	**–0.322**	**–0.333**	–0.038	0.036	**–0.234**	**–0.354**	**0.212**	**–0.407**	0.106	0.131	–0.014	0.182	–0.057	**0.486**	**0.522**
21 Al	0.080	–0.112	–0.085	–0.022	–0.059	–0.172	–0.093	0.102	–0.162	**0.258**	0.107	0.040	0.067	0.016	**0.438**	0.118
22 Ca	**–0.238**	0.168	**0.202**	0.167	–0.048	**0.309**	**0.252**	–0.160	**0.308**	–0.125	–0.164	–0.032	–0.091	–0.014	**–0.551**	**–0.326**
23 Fe	0.038	**0.296**	**0.205**	0.048	–0.061	**0.208**	**0.287**	–0.022	**0.292**	–0.087	**–0.220**	–0.039	–0.169	0.012	**–0.383**	**–0.396**
24 C	–0.195	**–0.435**	**–0.297**	0.048	0.108	–0.056	**–0.446**	0.048	**–0.419**	0.061	–0.029	0.098	0.150	0.022	**0.200**	**0.370**
25 K	–0.104	0.191	0.167	0.096	0.032	**0.333**	**0.240**	**–0.210**	**0.272**	–0.163	–0.136	0.022	–0.040	0.101	**–0.473**	**–0.368**
26 Mg	0.047	0.122	0.066	0.090	0.082	0.186	0.125	–0.039	0.123	–0.068	–0.168	0.086	–0.042	0.159	**–0.278**	**–0.461**
27 Mn	0.033	**0.470**	**0.397**	0.099	–0.074	**0.345**	**0.451**	–0.174	**0.473**	–0.061	–0.141	–0.045	–0.185	0.006	**–0.406**	**–0.592**
28 Na	0.163	0.068	–0.041	0.123	–0.078	–0.005	0.180	0.191	0.016	0.089	0.027	**0.290**	**0.214**	**0.249**	**0.210**	**–0.192**
29 P	–0.165	–0.135	–0.092	–0.022	0.019	0.050	–0.055	–0.137	0.025	–0.177	–0.032	–0.172	–0.074	–0.104	**–0.264**	**0.203**
30 S	–0.087	**0.232**	0.171	0.199	**–0.215**	**0.297**	**0.355**	–0.086	**0.318**	0.037	–0.192	0.106	0.019	0.114	**–0.218**	**–0.375**
31 Zn	0.096	**0.266**	0.143	–0.016	0.122	**0.220**	**0.276**	–0.006	**0.238**	**–0.218**	–0.178	–0.022	0.093	0.037	**–0.269**	**–0.197**

Table 12 (continued). Åmotsdalen: Kendall's rank correlation coefficients τ between 31 environmental variables in the 50 meso plots (lower triangle), with significance probabilities (upper triangle). Statistically significant correlations (P<0.05) in bold face. Names of explanatory variables abbreviated in accordance with Table 2.

	17	18	19	20	21	22	23	24	25	26	27	28	29	30	31
01 Ma Slo	0.520	0.653	0.886	0.407	0.436	**0.020**	0.709	0.058	0.310	0.648	0.748	0.111	0.108	0.397	0.352
02 Ma Asp	0.749	**0.000**	**0.000**	**0.001**	0.267	0.096	**0.003**	**0.000**	0.103	0.226	**0.000**	0.501	0.178	**0.021**	**0.008**
03 Ma HI	0.547	**0.002**	**0.001**	**0.001**	0.384	**0.040**	**0.036**	**0.002**	0.088	0.503	**0.000**	0.676	0.349	0.082	0.145
04 Ma Ter	0.321	0.986	0.864	0.732	0.843	0.134	0.665	0.665	0.386	0.417	0.377	0.271	0.843	0.074	0.885
05 Ma Une	0.079	0.867	0.792	0.738	0.586	0.660	0.574	0.316	0.765	0.449	0.493	0.471	0.860	**0.047**	0.260
05 TBA	0.381	**0.022**	**0.008**	**0.021**	0.089	**0.002**	**0.040**	0.578	**0.001**	0.066	**0.001**	0.960	0.625	**0.003**	**0.030**
07 Me Slo	0.973	**0.000**	**0.000**	**0.001**	0.362	**0.013**	**0.005**	**0.000**	**0.018**	0.218	**0.000**	0.076	0.589	**0.000**	**0.007**
08 Me Asp	0.993	0.159	0.086	**0.039**	0.321	0.120	0.832	0.641	**0.041**	0.703	0.091	0.063	0.183	0.401	0.953
09 Me HI	0.953	**0.000**	**0.000**	**0.000**	0.099	**0.002**	**0.003**	**0.000**	**0.006**	0.212	**0.000**	0.874	0.795	**0.001**	**0.016**
10 Me Ter	0.137	0.825	0.939	0.296	**0.011**	0.218	0.391	0.546	0.108	0.502	0.546	0.381	0.082	0.715	**0.032**
11 Me Une	**0.013**	0.200	0.138	0.183	0.280	0.095	**0.025**	0.769	0.167	0.089	0.152	0.782	0.744	0.051	0.072
12 Smi	0.913	0.744	0.893	0.887	0.682	0.744	0.694	0.319	0.821	0.379	0.645	**0.003**	0.080	0.280	0.821
13 Sme	0.491	0.075	**0.043**	0.069	0.501	0.364	0.093	0.135	0.687	0.674	0.064	**0.033**	0.459	0.853	0.355
14 Sma	0.731	0.547	0.503	0.564	0.874	0.887	0.900	0.821	0.303	0.106	0.953	**0.011**	0.288	0.245	0.706
15 Mme	0.744	**0.006**	**0.001**	**0.000**	**0.000**	**0.000**	**0.000**	**0.040**	**0.000**	**0.004**	**0.000**	**0.032**	**0.007**	**0.026**	**0.006**
16 LOI	**0.026**	**0.000**	**0.000**	**0.000**	0.225	**0.001**	**0.000**	**0.000**	**0.000**	**0.000**	**0.000**	**0.049**	**0.037**	**0.000**	**0.044**
17 Total N	*	**0.004**	**0.007**	0.541	**0.012**	0.808	0.143	0.770	0.457	0.408	0.195	**0.009**	**0.003**	**0.004**	0.757
18 pH_{H_2O}	**0.280**	*	**0.000**	**0.000**	0.847	**0.010**	**0.000**	**0.000**	**0.001**	**0.000**	**0.000**	0.130	**0.004**	**0.000**	**0.020**
19 pH_{CaCl_2}	**0.264**	**0.907**	*	**0.000**	0.340	**0.001**	**0.000**	**0.000**	**0.000**	**0.000**	**0.000**	0.216	**0.025**	**0.000**	**0.009**
20H	–0.060	**–0.520**	**–0.585**	*	**0.000**	**0.000**	**0.000**	**0.000**	**0.000**	**0.000**	**0.000**	0.967	0.213	**0.006**	**0.000**
21 Al	**0.246**	–0.019	–0.093	**0.437**	*	**0.000**	**0.000**	**0.005**	**0.000**	**0.000**	**0.002**	**0.005**	**0.000**	0.874	**0.000**
22 Ca	0.024	**0.252**	**0.329**	**–0.468**	**–0.440**	*	**0.000**	**0.015**	**0.000**	**0.001**	**0.000**	0.389	**0.002**	**0.000**	**0.000**
23 Fe	0.143	**0.476**	**0.536**	**–0.626**	**–0.386**	**0.394**	*	**0.000**	**0.000**	**0.000**	**0.000**	0.328	0.353	**0.028**	**0.001**
24 C	–0.029	**–0.439**	**–0.456**	**0.535**	**0.275**	**–0.238**	**–0.458**	*	**0.001**	**0.001**	**0.000**	0.245	0.847	0.103	**0.017**
25 K	0.073	**0.324**	**0.385**	**–0.491**	**–0.411**	**0.667**	**0.391**	**–0.313**	*	**0.000**	**0.000**	0.757	**0.005**	**0.000**	**0.000**
26 Mg	0.081	**0.368**	**0.418**	**–0.544**	**–0.360**	**0.313**	**0.553**	**–0.327**	**0.427**	*	**0.000**	0.162	0.645	**0.026**	**0.000**
27 Mn	0.127	**0.617**	**0.678**	**–0.639**	**–0.298**	**0.476**	**0.536**	**–0.530**	**0.535**	**0.425**	*	0.622	0.913	**0.000**	**0.000**
28 Na	**0.256**	0.148	0.121	–0.004	**0.275**	–0.084	–0.096	–0.113	0.030	0.136	0.048	*	**0.000**	**0.000**	0.719
29 P	**–0.293**	**–0.283**	**–0.220**	–0.122	**–0.577**	**0.308**	0.091	–0.019	**0.272**	0.045	–0.011	**–0.365**	*	0.488	**0.039**
30 S	**0.282**	**0.365**	**0.393**	**–0.269**	–0.016	**0.455**	**0.215**	–0.159	**0.494**	**0.218**	**0.443**	**0.353**	0.068	*	**0.026**
31 Zn	–0.030	**0.227**	**0.254**	**–0.352**	**–0.396**	**0.358**	**0.331**	**–0.233**	**0.407**	**0.340**	**0.353**	0.035	**0.202**	**0.218**	*

correlated, but not strongly correlated with other variables. Soil moisture and LOI were negatively correlated with pH and most other extractable elements, and positively correlated with each other. pH was positively correlated with total N, C, Ca, K, Mg, Mn and Zn and negatively correlated with H and Fe. Extractable P was negatively correlated with soil moisture, total N, pH, Na and Zn, and positively correlated with LOI and C.

PCA ordination of environmental variables

The first two PCA axes accounted for 34.6% and 12.4% of the variance in standardised transformed environmental variables, respectively (eigenvalues of 0.346 and 0.124).

pH_{H_2O}, pH_{CaCl_2}, Ca, K and Mn obtained high loadings along PCA axis 1 together with extractable C, macro plot aspect unfavourability, macro and meso plot slope and meso plot heat index, while low loadings were obtained by H, Fe, meso plot heat index and soil moisture (Fig. 197). These two groups of variables were negatively correlated with each other.

Extractable P obtained high loading on PCA axis 2, while Na, Al and soil moisture obtained low loadings.

The PCA results were consistent with the correlation matrix of the environmental variables, showing that variables related to soil richness and soil moisture made up the strongest environmental complex gradients in the Åmotsdalen reference area.

DCA ordination

The gradient length of the two first DCA axes was 3.54 and 1.79 S.D. units, and the eigenvalues were 0.519 and 0.106, respectively. Accordingly, the only strong gradient in species composition was DCA 1. The plots partly segregated into two groups; one group with 40 samples occurred to the left in the DCA diagram (DCA 1 scores between 0 and 1.9 S.D. units on axis 1), while the remaining 10 plots occurred to the right (2.5–3.5 S.D. units) (Fig. 198).

GNMDS ordination

The GNMDS ordination diagram (Fig. 199) was visually similar to the DCA diagram (Fig 198). The correlation between GNMDS axis 1 and DCA axis 1 was $\tau = 0.931$ and the correlation between GNMDS axis 2 and DCA axis 2 was $\tau = 0.620$.

Split-plot GLM analysis of relationships between ordination axes and environmental variables

Variation (in plot scores) along DCA axis 1 was partitioned with 96.03 % at the macro plot scale (i.e. between macro plots) and 3.97 % at the (between) meso plot scale within macro plots (Table 13). For the second ordination axis, 56.03 % of the variation was explained at the macro plot scale and 43.97 % at the plot scale (Table 14).

At the macro plot scale, eight environmental variables were significantly (at the $\alpha = 0.05$ level) related to DCA 1 while three variables (also at the $\alpha = 0.05$ level) were related to DCA 2. At the meso plot scale level, five environmental variables were significantly related to DCA 1 and two variables to DCA 2 (Tables 13 and 14).

At the macro plot scale, tree basal area, pH and soil concentrations of Total N, Ca, Mn, and

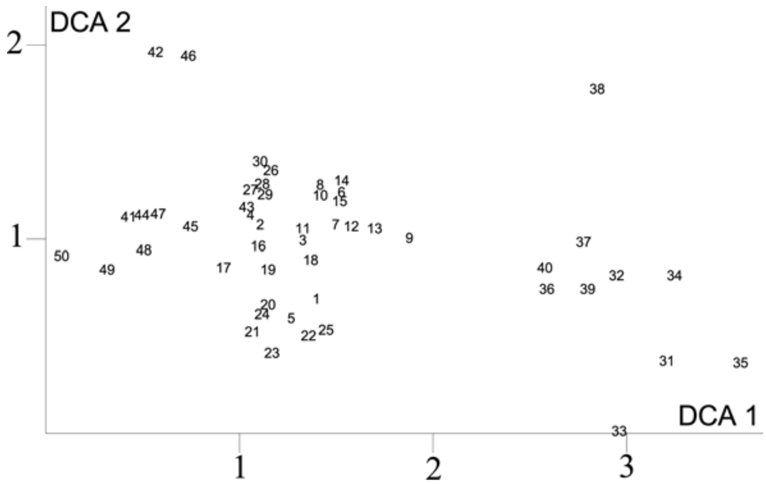

Fig. 198. Åmotsdalen: DCA ordination diagram of 50 meso plots, axes 1 (horizontal) and 2 (vertical). Meso plot number are plotted just right of the sample plot positions. Scaling of axes in S.D. units.

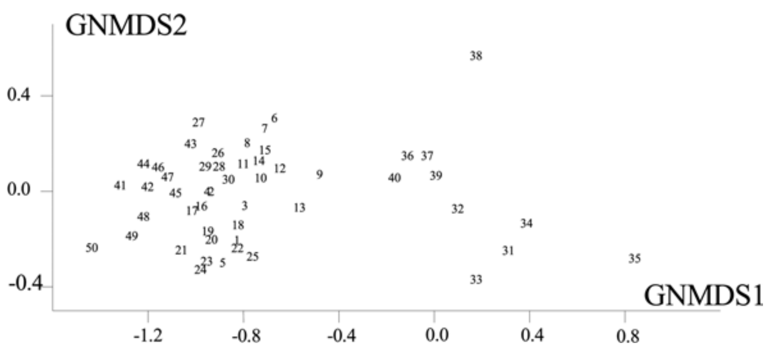

Fig.199. Åmotsdalen: GNMDS ordination biplot diagram of 50 meso plots (indicated by their number).

S increased significantly along DCA 1 while loss-on-ignition decreased. Predictors with significant relationship (positive) to this axis on the meso plot scale were maximum soil depth, soil moisture, pH measures and soil concentrations of Al.

At the macro plot scale, DCA 2 was positively related to minimum soil depth and negatively related to macro plot terrain form and the concentration of Mn in soil. At the meso plot scale, DCA axis 2 was significantly negatively related to macro plot slope and positively correlated to soil concentration of Na (Table 14).

Table 13. Åmotsdalen: Split-plot GLM analysis and Kendall's nonparametric correlation coefficient τ between DCA 1 and 31 environmental variables (predictor) in the 50 meso plots. df_{resid}: degrees of freedom for the residuals; *SS*: total variation; *FVE*: fraction of total variation attributable to a given scale (macro plot or meso plot); SS_{expl}/SS: fraction of the variation attributable to the scale in question, explained by a variable; *r*: model coefficient (only given when significant at the α = 0.05 level, otherwise blank); *F*: *F* statistic for test of the hypothesis that *r* = 0 against the two-tailed alternative. Split-plot GLM relationships significant at level α = 0.05, *P*, *F*, *r* and SS_{expl}/SS, and Kendall's nonparametric correlation coefficient $|\tau| \geq 0.30$ are given in bold face. Numbers and abbreviations for names of environmental variables are in accordance with Tab. 2.

Predictor	Dependent variable = DCA 1 (*SS* = 34.3416)								Correlation between predictor and DCA 1
	Error level								
	Macro plot df_{resid} = 8 $SS_{macro\ plot}$ = 32.9770 *FVE* = 0.9603 of *SS*				Meso plot within macro plot df_{resid} = 39 $SS_{meso\ plot}$ = 1.36464 *FVE* = 0.0397 of *SS*				Total
	$SS_{expl}/SS_{macro\ plot}$	*r*	*F*	*P*	$SS_{expl}/SS_{meso\ plot}$	*r*	*F*	*P*	τ
Ma Slo	0.2773		3.0701	0.1178	0.0812		3.4454	0.0710	–0.041
Ma Asp	0.0285		0.2351	0.6408	0.0192		0.7627	0.3878	0.166
Ma HI	0.1310		1.2061	0.3041	0.0017		3.6437	0.0927	0.148
Ma Ter	0.3714		4.7258	0.0614	0.0184		0.7295	0.3983	0.147
Ma Une	0.0371		0.3082	0.5939	0.0264		1.0563	0.3104	–0.09
TBA	**0.4875**	**2.7191**	**7.6086**	**0.0247**	0.0000		0.0001	0.9935	0.257
Me Slo	0.3861		5.0319	0.0552	0.0002		0.0096	0.9226	0.208
Me Asp	0.0045		0.0365	0.8533	0.0043		0.1686	0.6836	–0.135
Me HI	0.3129		3.6437	0.0927	0.0000		0.0009	0.9930	–0.248
Me Ter	0.0517		0.4364	0.5274	0.0041		0.1618	0.6897	0.045
Me Une	0.2576		2.7753	0.1343	0.0026		0.1010	0.7523	–0.22
Smi	0.0191		0.1557	0.7034	0.0209		0.8327	0.3671	0.088
Sme	0.0776		0.6734	0.4356	0.0121		0.4778	0.4935	–0.065
Sma	0.0951		0.8407	0.3860	**0.1008**	**0.3049**	**4.3729**	**0.0431**	0.123
Mme	0.1495		1.4064	0.2697	**0.1043**	**0.3367**	**4.5427**	**0.0394**	–0.235
LOI	**0.6934**	**–2.4254**	**18.0930**	**0.0028**	0.0019		0.0757	0.7847	**–0.536**
Total N	**0.5493**	**3.7831**	**9.7483**	**0.0142**	0.0630		2.6229	0.1134	**0.361**
pH_{H_2O}	**0.7879**	**2.8417**	**29.7260**	**0.0006**	**0.1581**	**0.5362**	**7.3260**	**0.0100**	**0.572**
pH_{CaCl_2}	**0.7507**	**2.5896**	**24.0870**	**0.0012**	**0.1604**	**0.6187**	**7.4522**	**0.0095**	**0.590**
H	0.2968		3.3771	0.1034	0.0015		0.0583	0.8104	**–0.387**
Al	0.0000		0.0000	0.9965	**0.1050**	**0.4716**	**4.5746**	**0.0388**	–0.047
C	0.1925		1.9072	0.2046	0.0367		1.4857	0.2302	0.297
Ca	**0.4048**	**2.6665**	**5.4417**	**0.0480**	0.0055		0.2173	0.6437	**0.407**
Fe	0.2194		2.2483	0.1721	0.0705		2.9584	0.0934	0.240
K	0.3225		3.8073	0.0868	0.0082		0.3240	0.5725	**0.409**
Mg	0.3895		5.1030	0.0538	0.0290		1.1634	0.2874	**0.423**
Mn	**0.6383**	**2.2069**	**14.1160**	**0.0056**	0.0451		1.8438	0.1823	**0.594**
Na	0.2159		2.2022	0.1761	0.0361		1.4605	0.2341	0.206
P	0.3249		3.8497	0.0854	0.0807		3.4217	0.0719	–0.227
S	**0.5611**	**3.1651**	**10.2280**	**0.0127**	0.0412		1.6741	0.2033	**0.477**
Zn	0.1902		1.8793	0.2076	0.0266		1.0677	0.3078	0.214

Table 14. Åmotsdalen: Split-plot GLM analysis and Kendall's nonparametric correlation coefficient τ between DCA 2 and 31 environmental variables (predictor) in the 50 meso plots. df_{resid}: degrees of freedom for the residuals; *SS*: total variation; *FVE*: fraction of total variation attributable to a given scale (macro plot or meso plot); SS_{expl}/SS: fraction of the variation attributable to the scale in question, explained by a variable; *r*: model coefficient (only given when significant at the α = 0.05 level, otherwise blank); *F*: *F* statistic for test of the hypothesis that *r* = 0 against the two-tailed alternative. Split-plot GLM relationships significant at level α = 0.05, *P*, *F*, *r* and SS_{expl}/SS, and Kendall's nonparametric correlation coefficient $|\tau| \geq 0.30$ are given in bold face. Numbers and abbreviations for names of environmental variables are in accordance with Tab. 2.

Predictor	Dependent variable = DCA 2 (*SS* = 6.8792)								Correlation between predictor and DCA 2
	Error level								
	Macro plot df_{resid} = 8 $SS_{macro\ plot}$ = 3.8547 *FVE* = 0.5603 of *SS*				Meso plot within macro plot df_{resid} = 39 $SS_{meso\ plot}$ = 3.02452 *FVE* = 0.4397 of *SS*				Total
	$SS_{expl}/SS_{macro\ plot}$	*r*	*F*	*P*	$SS_{expl}/SS_{meso\ plot}$	*r*	*F*	*P*	τ
Ma Slo	0.3067		3.5387	0.0967	**0.1704**	**–1.258**	**8.0085**	**0.0073**	–0.073
Ma Asp	0.0106		0.0856	0.7772	0.0364		1.4717	0.2324	–0.247
Ma HI	0.6403		14.244	0.0054	0.0129		0.5098	0.4795	–0.260
Ma Ter	**0.6765**	**–2.1084**	**16.7320**	**0.0035**	0.0275		1.1025	0.3002	–0.112
Ma Une	0.2552		2.7419	0.1363	0.0000		0.0011	0.9740	0.145
TBA	0.1339		1.2370	0.2983	0.0638		2.6599	0.1110	–0.182
Me slo	0.3133		3.6499	0.0925	0.0004		0.0153	0.9023	–0.259
Me Asp	0.0106		0.0856	0.7773	0.0415		1.6880	0.2015	–0.063
Me HI	0.3842		4.9904	0.0559	0.0245		0.9801	0.3283	–0.258
Me Ter	0.0209		0.1710	0.6901	0.0038		0.1473	0.7032	–0.057
Me Une	0.1369		1.2687	0.2927	0.0039		0.1531	0.6977	0.176
Smi	**0.4365**	**1.1815**	**6.1975**	**0.0376**	0.0382		1.5504	0.2205	0.22
Sme	0.2872		3.2238	0.1103	0.0479		1.9638	0.1690	0.213
Sma	0.3009		3.4433	0.1006	0.0293		1.1752	0.2850	0.217
Mme	0.3035		3.4854	0.0989	0.0871		3.7220	0.0610	**0.304**
LOI	0.1425		1.3298	0.2821	0.0000		0.0016	0.9680	0.205
Total N	0.2089		2.1126	0.1842	0.0862		3.6790	0.0625	–0.002
pH_{H_2O}	0.2511		2.6822	0.1401	0.0019		0.0755	0.7849	–0.241
pH_{CaCl_2}	0.2819		3.1400	0.1143	0.0028		0.1086	0.7435	–0.269
H	0.2490		2.6520	0.1421	0.0183		0.7268	0.3991	0.289
Al	0.1730		1.6735	0.2319	0.0272		1.0908	0.3027	0.254
C	0.2866		3.2141	0.1108	0.0000		0.0013	0.9715	–0.245
Ca	0.2705		2.9670	0.1233	0.0428		1.7432	0.1944	**–0.407**
Fe	0.3879		5.0707	0.0544	0.0230		0.9193	0.3436	**0.433**
K	0.1437		1.3431	0.2799	0.0061		0.2401	0.6269	–0.161
Mg	0.0471		0.3952	0.5471	0.0192		0.7622	0.3880	–0.184
Mn	**0.4339**	**–0.6221**	**6.1308**	**0.0384**	0.0610		2.5347	0.1194	–0.387
Na	0.0754		0.6527	0.4425	**0.2264**	**0.9904**	**11.4150**	**0.0017**	0.231
P	0.0042		0.0339	0.8584	0.0000		0.0007	0.9785	–0.059
S	0.0567		0.4810	0.5076	0.0618		2.5672	0.1172	–0.008
Zn	0.0267		0.2198	0.6517	0.0165		0.6553	0.4231	–0.097

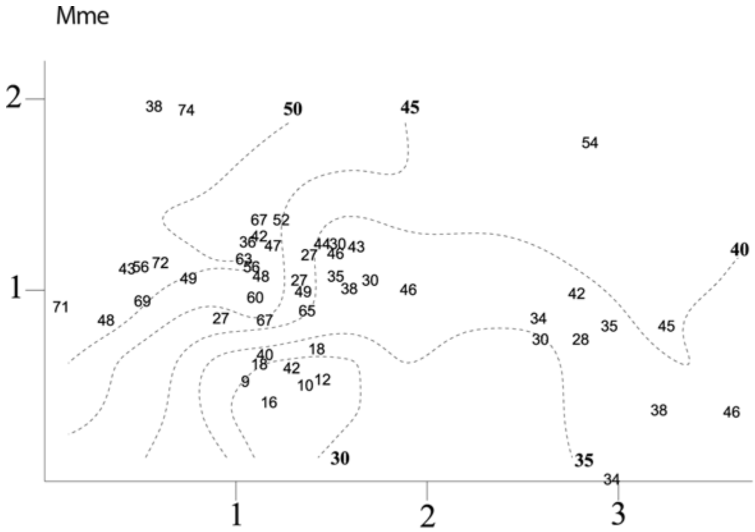

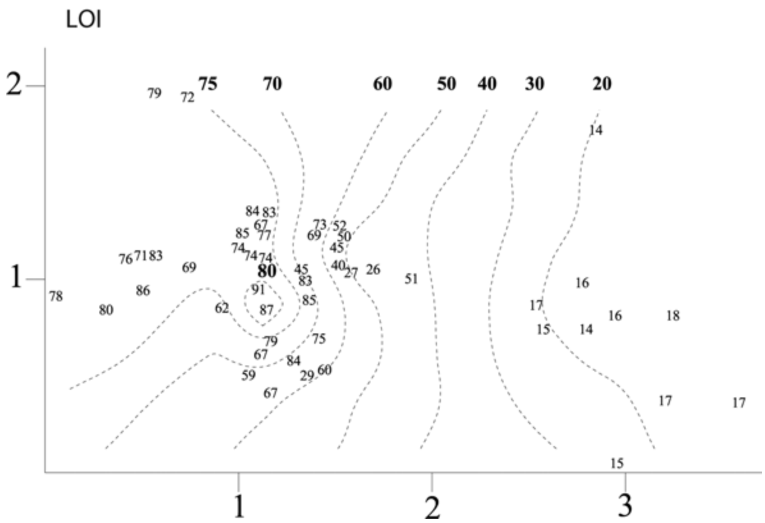

Figs 200-201. Åmotsdalen: isolines for environmental variables in the DCA ordinations of 50 meso plots, axes 1 (horizontal) and 2 (vertical). Values for the environmental variables are plotted onto the meso plots' positions. Scaling in S.D. units. Fig. 200. Mme (Soil moisture) ($R^2 = 0.503$). Fig. 201. LOI ($R^2 = 0.771$). Names of environmental variables in accordance with Table 2.

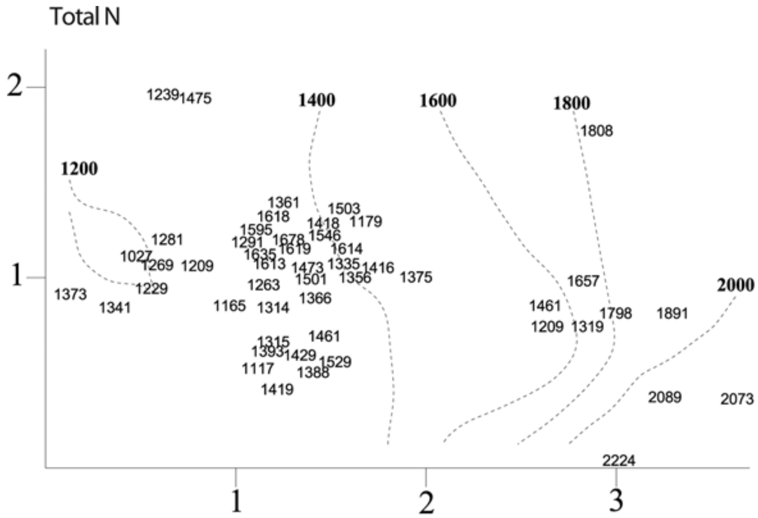

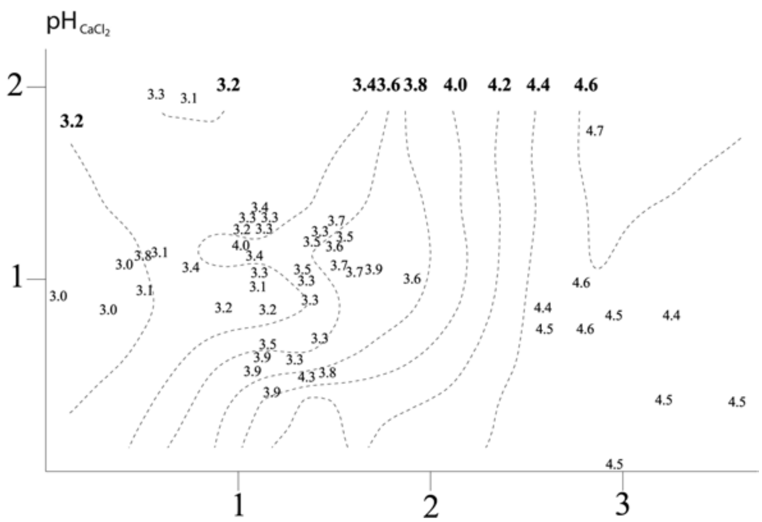

Figs 202-203. Åmotsdalen: isolines for environmental variables in the DCA ordinations of 50 meso plots, axes 1 (horizontal) and 2 (vertical). Values for the environmental variables are plotted onto the meso plots' positions. Scaling in S.D. units. Fig. 202. Total N (R^2 = 0.694). Fig. 203. pH_{CaCl_2} (R^2 = 0.787). R^2 refers to the coefficient of determination between original and smoothened values as interpolated from the isolines. Names of environmental variables in accordance with Table 2.

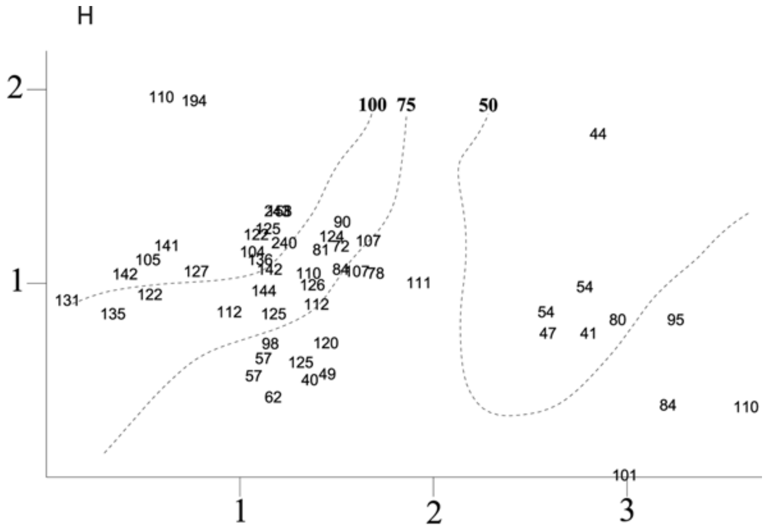

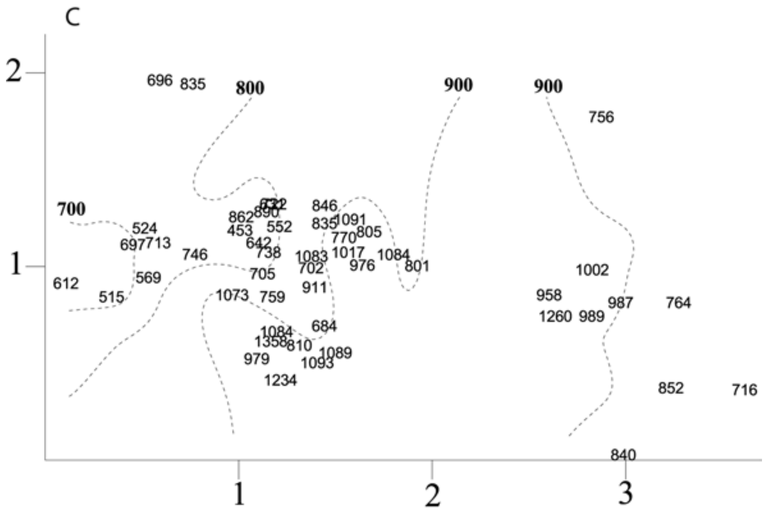

Figs 204-205. Åmotsdalen: isolines for environmental variables in the DCA ordinations of 50 meso plots, axes 1 (horizontal) and 2 (vertical). Values for the environmental variables are plotted onto the meso plots' positions. Scaling in S.D. units. Fig. 204. H (R^2 = 0.693). Fig. 205. C (R^2 = 0.675). R^2 refers to the coefficient of determination between original and smoothened values as interpolated from the isolines. Names of environmental variables in accordance with Table 2.

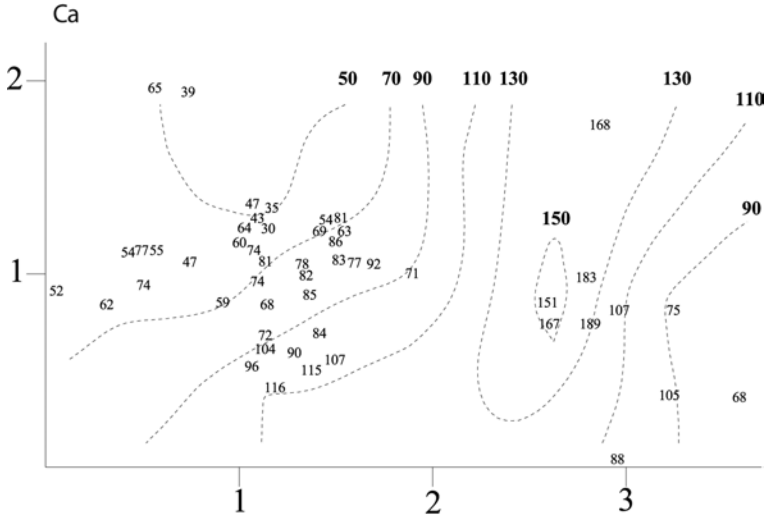

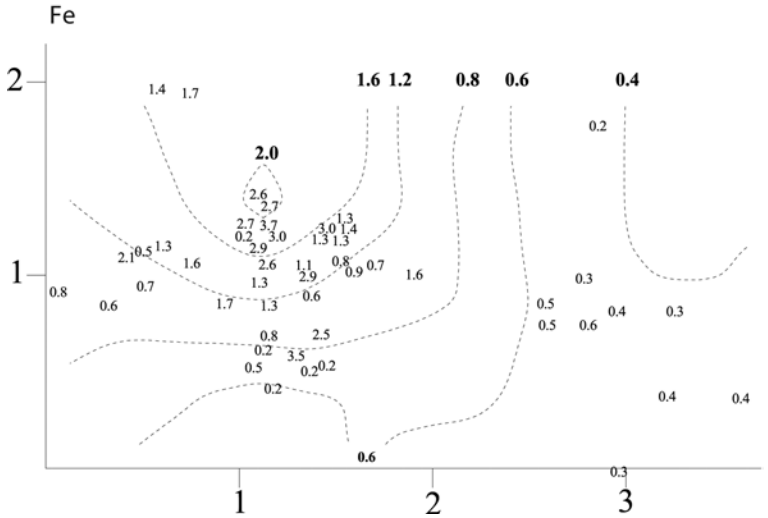

Figs 206-207. Åmotsdalen: isolines for environmental variables in the DCA ordinations of 50 meso plots, axes 1 (horizontal) and 2 (vertical). Values for the environmental variables are plotted onto the meso plots' positions. Scaling in S.D. units. 206. Ca ($R^2 = 0.824$). Fig. 207. Fe ($R^2 = 0.557$). Fig. R^2 refers to the coefficient of determination between original and smoothened values as interpolated from the isolines. Names of environmental variables in accordance with Table 2.

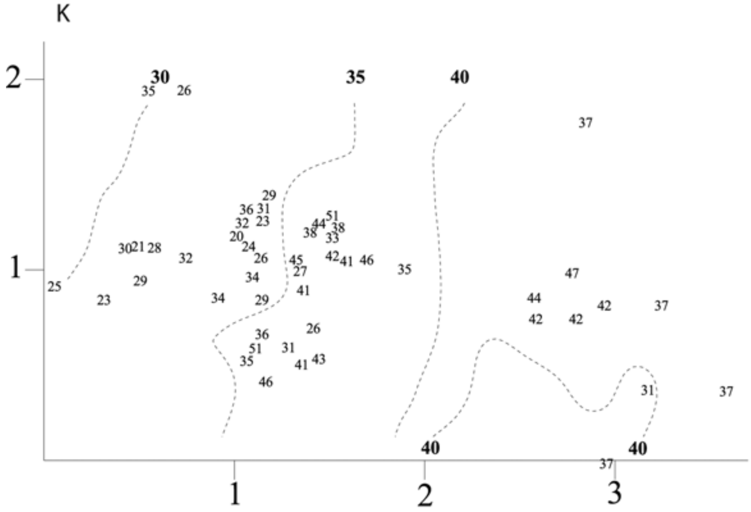

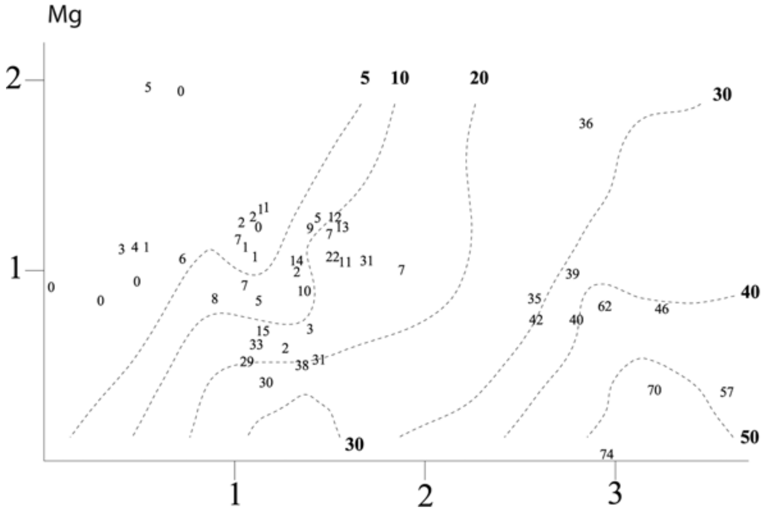

Figs 208-209. Åmotsdalen: isolines for environmental variables in the DCA ordinations of 50 meso plots, axes 1 (horizontal) and 2 (vertical). Values for the environmental variables are plotted onto the meso plots' positions. Scaling in S.D. units. Fig. 196. K (R^2 = 0.366). Fig. 197. Mg (R^2 = 0.778). R^2 refers to the coefficient of determination between original and smoothened values as interpolated from the isolines. Names of environmental variables in accordance with Table 2.

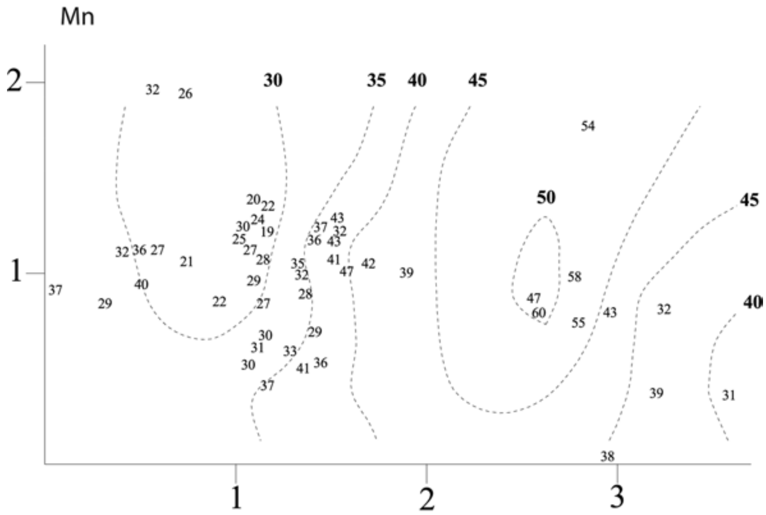

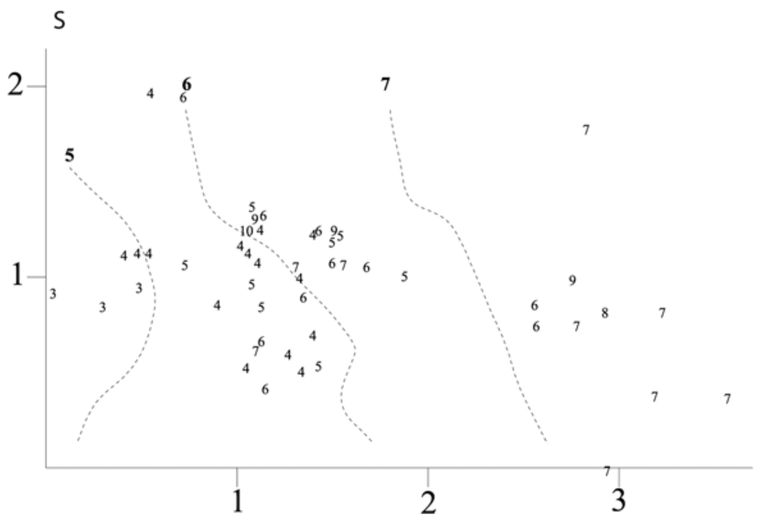

Figs 210-211. Åmotsdalen: isolines for environmental variables in the DCA ordinations of 50 meso plots, axes 1 (horizontal) and 2 (vertical). Values for the environmental variables are plotted onto the meso plots' positions. Scaling in S.D. units. Fig. 210. Mn ($R^2 = 0.821$). Fig. 211. S ($R^2 = 0.821$). R^2 refers to the coefficient of determination between original and smoothened values as interpolated from the isolines. Names of environmental variables in accordance with Table 2.

Correlations between DCA ordination axes and environmental variables

The variables most strongly positively correlated with DCA axis 1 (Table 13) were soil extractable Mn (τ = 0.594, Fig. 210) and pH_{CaCl_2} (τ = 0.590, Fig. 203), while loss-on-ignition (τ = –0.536, Fig. 201) and exchangeable hydrogen (Fig. 204) were negatively correlated with this axis. Other variables that were positively correlated (τ > 0.300) with DCA axis 1 were Total N (Fig. 202), Ca (Fig. 206), K (Fig. 208), Mg (Fig. 209), and S (Fig. 211). No variables, except LOI and H (Fig. 201 and 204), had equally strong negative correlations.

Fe (τ = 0.433, Fig. 207) and soil moisture (τ = 0.304, Fig. 200) had the strongest positive correlations with DCA axis 2. Extractable Ca (Fig. 206) and Mn (Fig. 210) were the only variables that were negatively correlated with DCA axis 2 at the $|\tau| > 0.300$ level. None of the topographical variables were significantly correlated with the first two DCA axes.

Frequent species

A total of 90 species were recorded within the 50 meso plots: 53 vascular plants, 14 mosses, 9 liverworts and 14 lichens. The most frequent species were (the sum of subplot frequencies in brackets): *Vaccinium myrtillus* (761 out of 800), *Avenella flexuosa* (743), *Vaccinium vitis-idaea* (724), *Empetrum nigrum* spp. *hermaphroditum* (607), *Polytrichum commune* (520), *Calluna vulgaris* (439), *Pleurozium schreberi* (363), *Barbilophozia lycopodoides* (367), *Trientalis europaea* (331) and *Chamaepericlymenum suecicum* (315).

The distribution of species abundance in the DCA ordination

Forty-seven of the total 90 species occurred in 5 or more of the sample plots (Figs 212–258).

Vaccinium myrtillus (Fig. 217), *Vaccinium vitis-idaea* (Fig. 219), *Avenella flexuosa* (Fig. 241) and *Polytrichum commune* (Fig. 250) had wide ecological amplitudes and were highly abundant in most of the sample plots.

Many species were mainly restricted to the right part of the DCA ordination diagram (high DCA axis 1 scores), showing preferences for soils with high values of pH, extractable elements (e.g. Ca, K, Mg, Mn) and total N and low values of loss-on-ignition. Examples of such species were *Deschampsia cespitosa* (Fig. 240) and *Rhytidiadelphus squarrosus* (Fig. 253), mainly restricted to the driest sites (lower right part of the DCA ordination diagram), while *Alchemilla alpina* (Fig. 220), *Bistorta vivipara* (Fig. 221) *Geranium sylvaticum* (Fig. 223), *Gymnocarpium dryopteris* (Fig. 224), *Maianthemum bifolium* (Fig. 227), *Orthilia secunda* (Fig. 229), *Oxalis acetosella* (Fig. 230), *Pyrola minor* (Fig. 232), *Ranunculus acris* (Fig. 221), *Veronica officinalis* (Fig. 236) and *Agrostis capillaris* (Fig. 237) were more or less present in both the lower and upper right part of the DCA ordination diagram. *Rhodobryum roseum* (Fig. 252) had its optimum for intermediate to high DCA axis 1 and axis 2 scores.

Examples of species mainly restricted to sample plots with low values of pH, extractable elements and higher loss on ignition (the left part of the DCA ordination diagram) were *Betula nana* (Fig. 212), *Vaccinium uliginosum* (Fig. 218), *Dicranum fuscescens* (Fig. 245), *Ptilidium ciliare* (Fig. 256), *Cladonia chlorophaea* (Fig. 257) and *Cladonia rangiferina* (Fig. 258). Of these *Betula nana* occupied the most moist plots at high DCA axis 2 scores. Species such as *Calluna vulgaris* (Fig. 214), *Empetrum nigrum* (Fig. 215), *Dicranum scoparium* (Fig. 247), *Hylocomium splendens* (Fig. 248), *Pleurozium schreberi* (Fig. 249) and *Barbilophozia lycopodioides* (Fig. 254) also preferred less nutrient-rich soils in the left part of DCA axis 1.

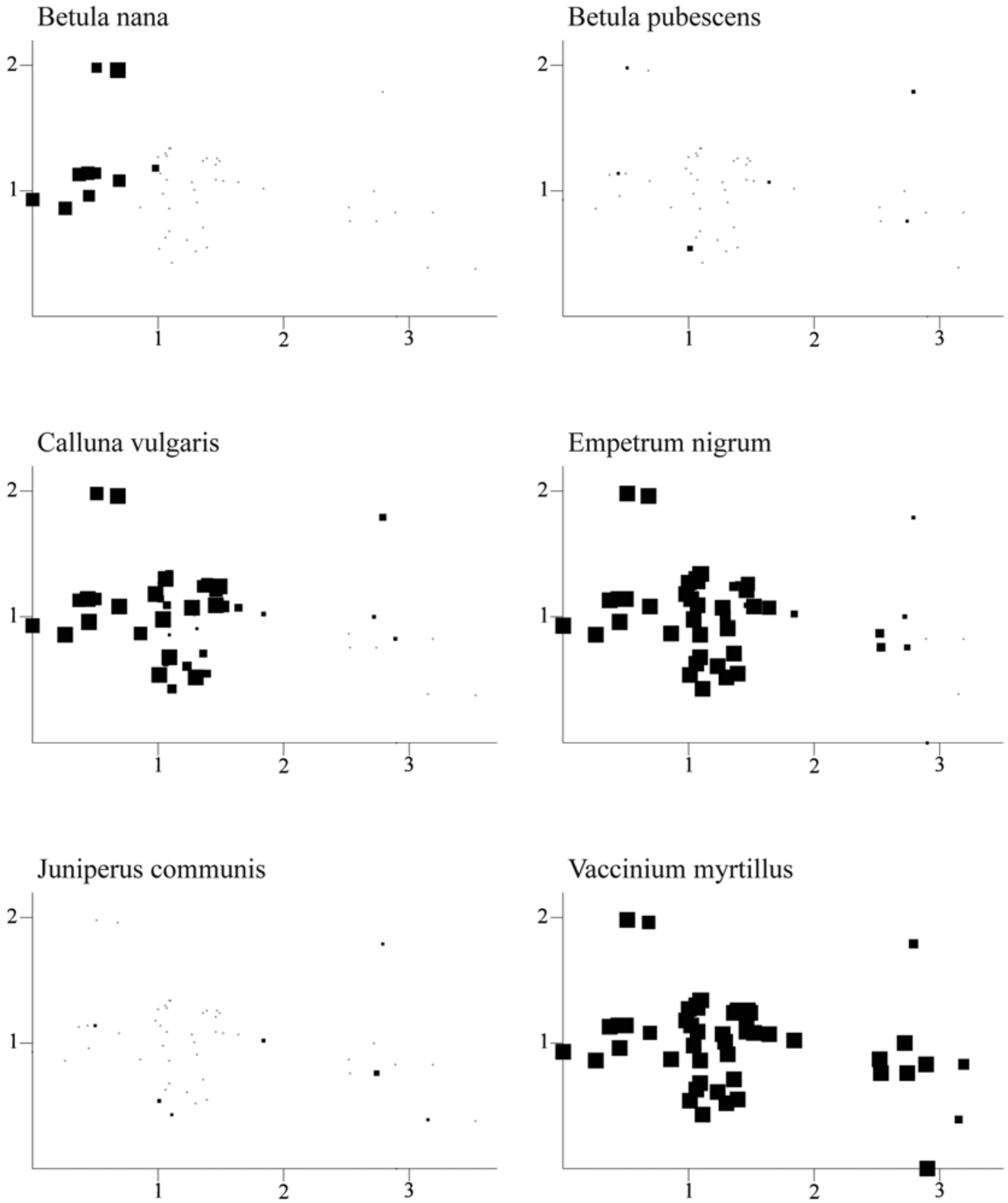

Figs 212-217. Åmotsdalen: distributions of species abundances in the DCA ordination of 50 meso plots, axes 1 (horizontal) and 2 (vertical). Frequency in subplots for each species in each meso plot proportional to quadrate size. Scaling in S.D. units. Fig. 212. *Betula nana*. Fig. 213. *Betula pubescens*. Fig. 214. *Calluna vulgaris*. Fig. 215. *Empetrum nigrum*. Fig. 216. *Juniperus communis*. Fig. 217. *Vaccinium myrtillus*.

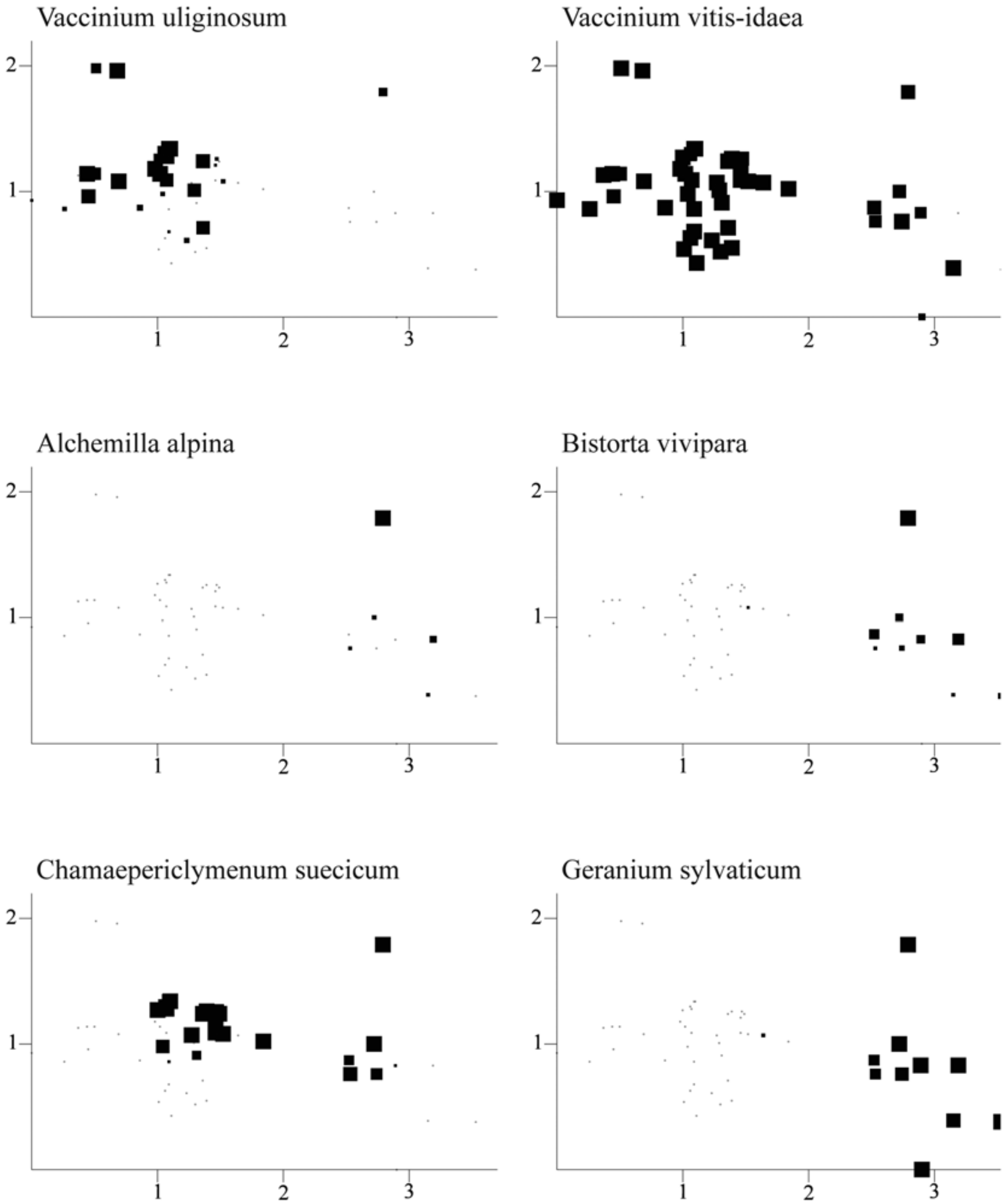

Figs 218-223. Åmotsdalen: distributions of species abundances in the DCA ordination of 50 meso plots, axes 1 (horizontal) and 2 (vertical). Frequency in subplots for each species in each meso plot proportional to quadrate size. Scaling in S.D. units. Fig. 218. *Vaccinium uliginosum*. Fig. 219. *Vaccinium vitis-idaea*. Fig. 220. *Alchemilla alpina*. Fig. 221. *Bistorta vivipara*. Fig. 222. *Chamaepericlymenum suecicum*. Fig. 223. *Geranium sylvaticum*.

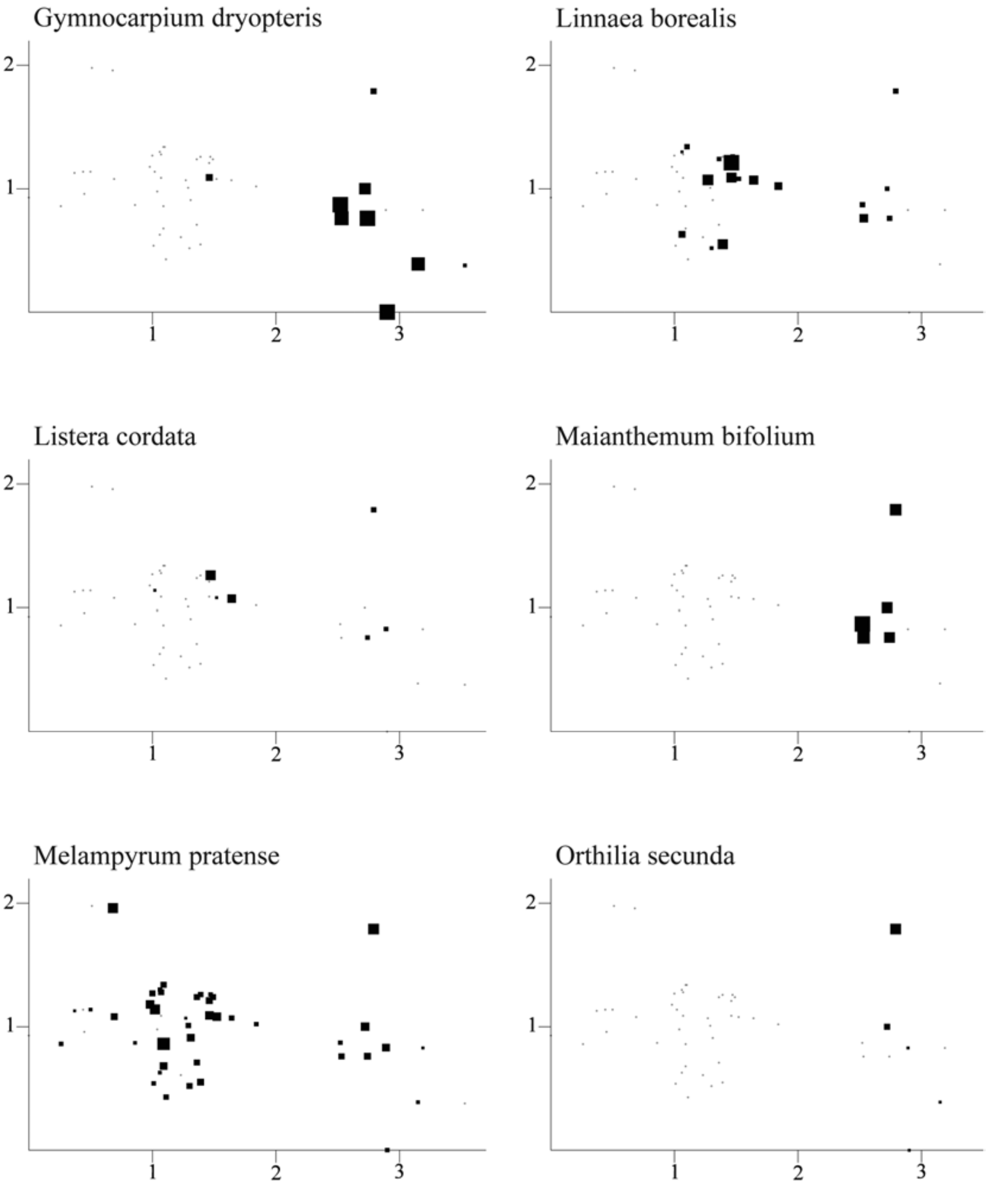

Figs 224-229. Åmotsdalen: distributions of species abundances in the DCA ordination of 50 meso plots, axes 1 (horizontal) and 2 (vertical). Frequency in subplots for each species in each meso plot proportional to quadrate size. Scaling in S.D. units. Fig. 224. *Gymnocarpium dryopteris*. Fig. 225. *Linnaea borealis*. Fig. 226. *Listera cordata*. Fig. 227. *Maianthemum bifolium*. Fig. 228. *Melampyrum pratense*. Fig. 229. *Orthilia secunda*.

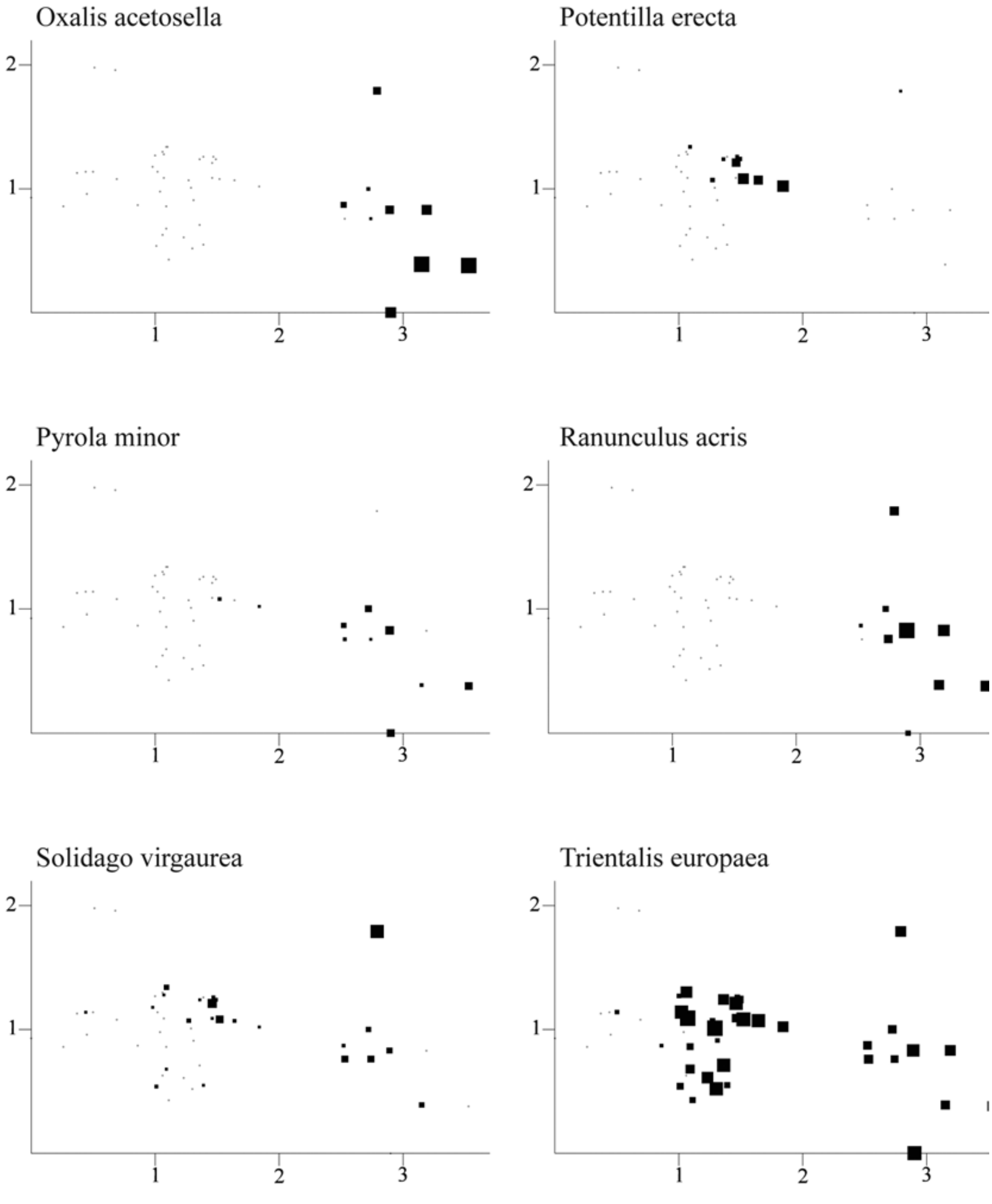

Figs 230-235. Åmotsdalen: distributions of species abundances in the DCA ordination of 50 meso plots, axes 1 (horizontal) and 2 (vertical). Frequency in subplots for each species in each meso plot proportional to quadrate size. Scaling in S.D. units. Fig. 230. *Oxalis acetosella*. Fig. 231. *Potentilla erecta*. Fig. 232. *Pyrola minor*. Fig. 233. *Ranunculus acris*. Fig. 234. *Solidago virgaurea*. Fig. 235. *Trientalis europaea*.

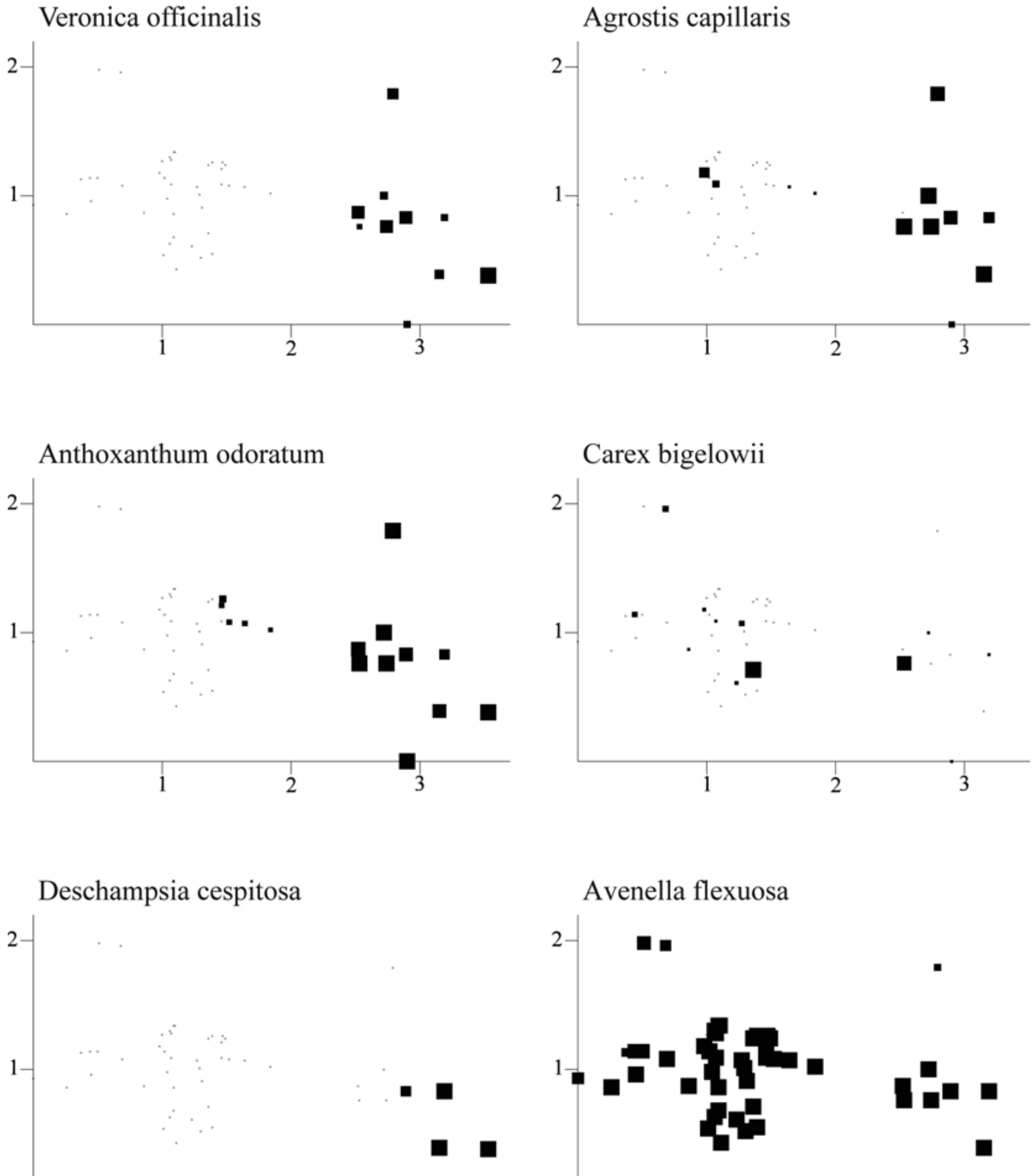

Figs 236-241. Åmotsdalen: distributions of species abundances in the DCA ordination of 50 meso plots, axes 1 (horizontal) and 2 (vertical). Frequency in subplots for each species in each meso plot proportional to quadrate size. Scaling in S.D. units. Fig. 236. *Veronica officinalis*. Fig. 237. *Agrostis capillaris*. Fig. 238. *Anthoxanthum odoratum*. Fig. 239. *Carex bigelowii*. Fig. 240. *Deschampsia cespitosa*. Fig. 241. *Avenella flexuosa*.

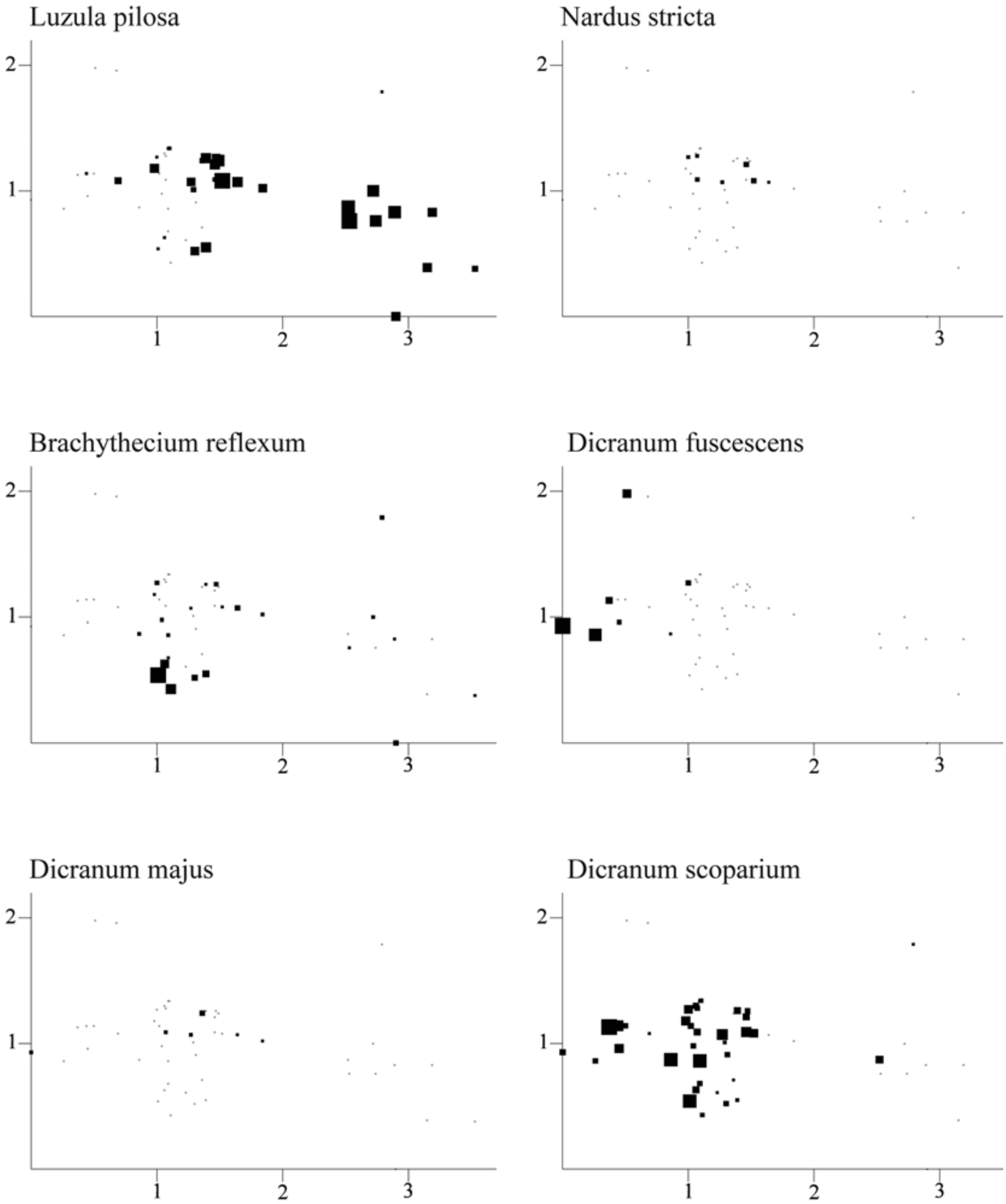

Figs 242-247. Åmotsdalen: distributions of species abundances in the DCA ordination of 50 meso plots, axes 1 (horizontal) and 2 (vertical). Frequency in subplots for each species in each meso plot proportional to quadrate size. Scaling in S.D. units. Fig. 242. *Luzula pilosa*. Fig. 243. *Nardus stricta*. Fig. 244. *Brachythecium reflexum*. Fig. 245. *Dicranum fuscescens*. Fig. 246. *Dicranum majus*. Fig. 247. *Dicranum scoparium*.

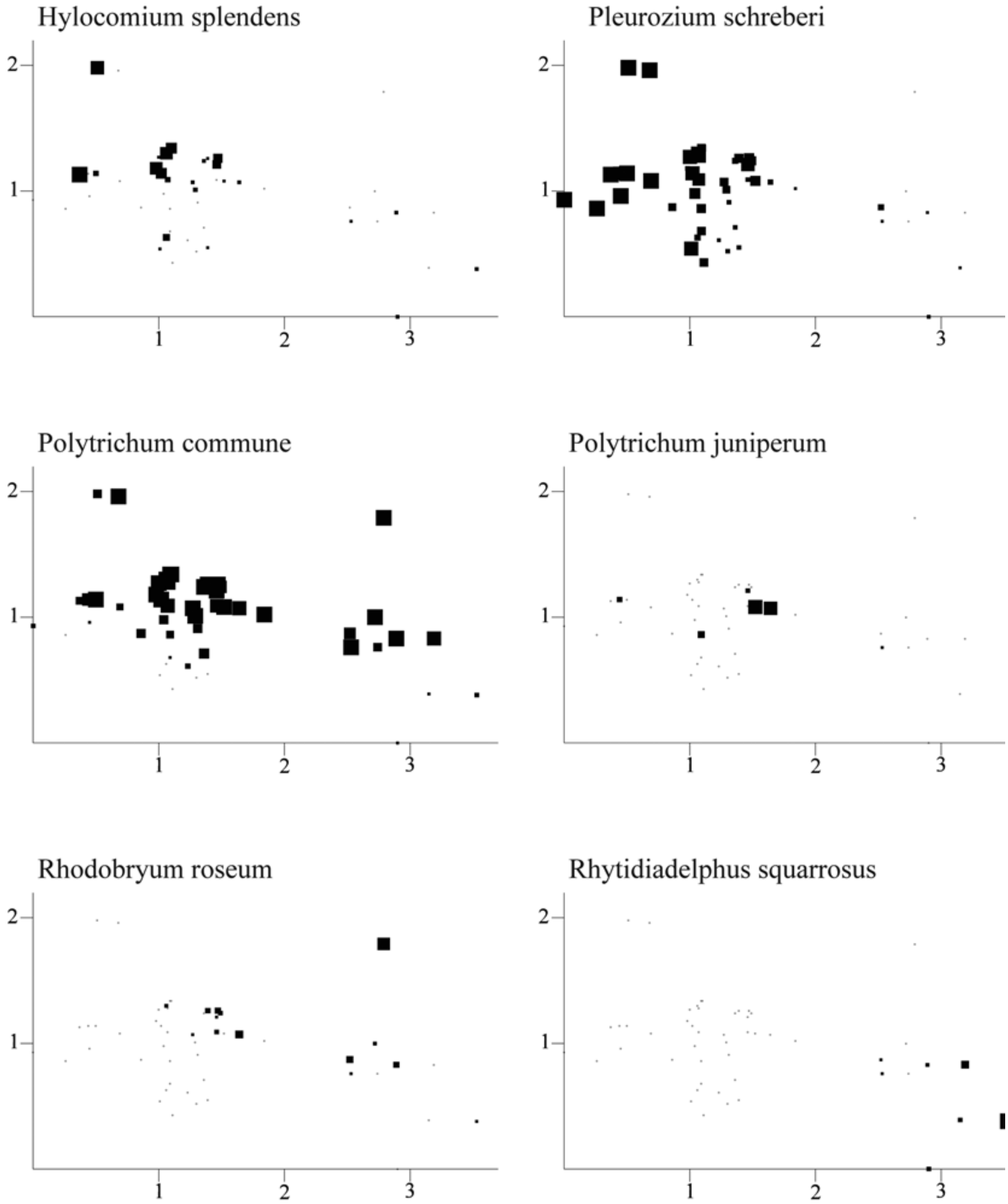

Figs 248-253. Åmotsdalen: distributions of species abundances in the DCA ordination of 50 meso plots, axes 1 (horizontal) and 2 (vertical). Frequency in subplots for each species in each meso plot proportional to quadrate size. Scaling in S.D. units. Fig. 248. *Hylocomium splendens*. Fig. 249. *Pleurozium schreberi*. Fig. 250. *Polytrichum commune*. Fig. 251. *Polytrichum juniperinum*. Fig. 252. *Rhodobryum roseum*. Fig. 253. *Rhytidiadelphus squarrosus*.

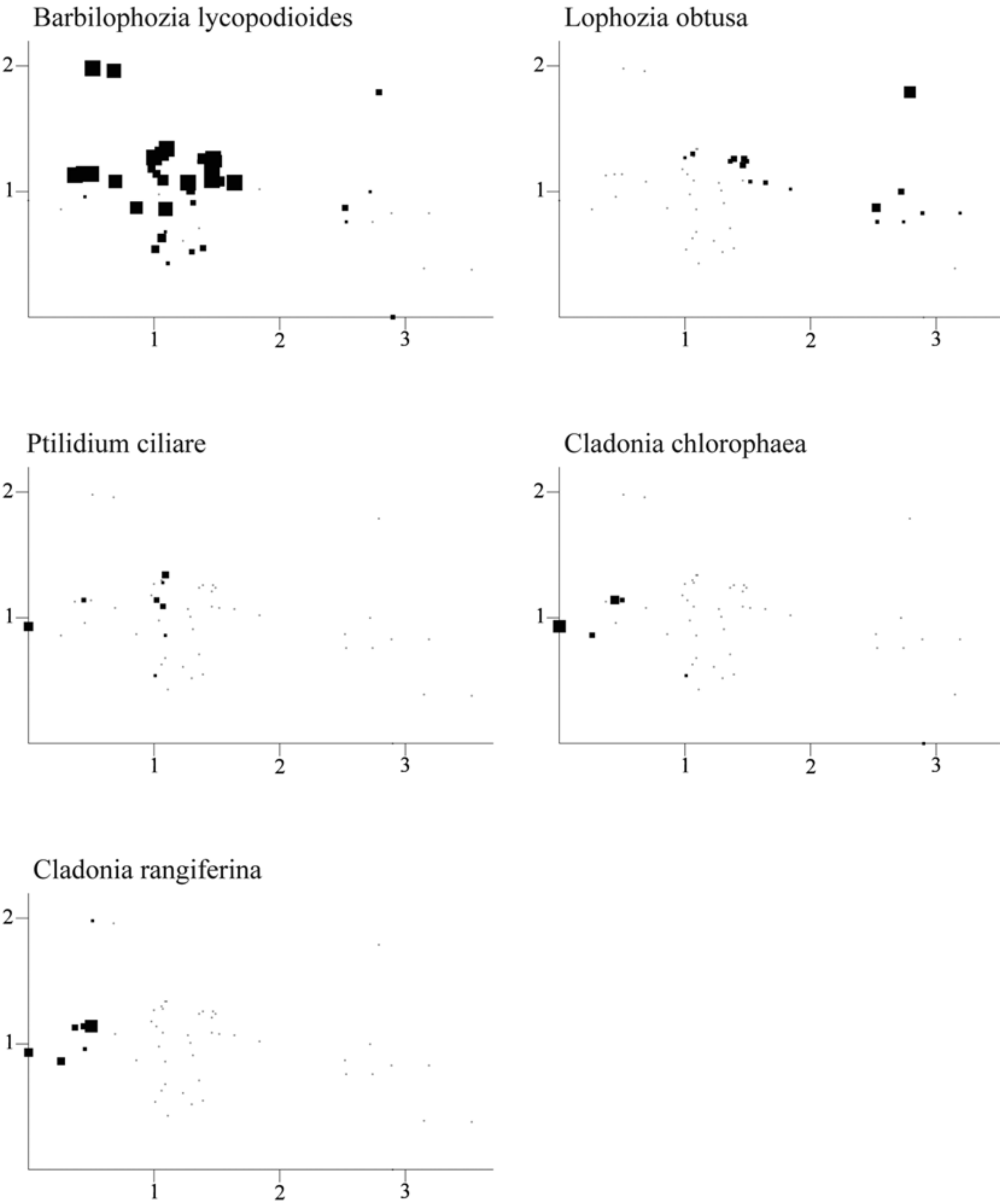

Figs 254-258. Åmotsdalen: distributions of species abundances in the DCA ordination of 50 meso plots, axes 1 (horizontal) and 2 (vertical). Frequency in subplots for each species in each meso plot proportional to quadrate size. Scaling in S.D. units. 254. *Barbilophozia lycopodioides*. Fig. 255. *Lophozia obtusa*. Fig. 256. *Ptilidium ciliare*. Fig. 257. *Cladonia chlorophaea*. Fig. 258. *Cladonia rangiferina*.

BØRGEFJELL REFERENCE AREA

Correlations between environmental variables

Many variables had strong pairwise correlations (Table 15). Macro and meso plot slope were negatively correlated with soil moisture, loss-on-ignition, exchangeable H and extractable Al, and positively correlated with variables reflecting soil nutrient richness, such as pH, P, Ca, Mg and K. Macro plot slope was also positively correlated with tree basal area which also was positively correlated with pH and extractable cations. Soil depth (Sme and Sma) was, in general, negatively correlated with extractable elements that reflected soil richness and positively correlated with LOI and soil acidity (H and low pH values). Soil moisture was positively correlated with LOI, and both were negatively correlated with soil nutrient richness variables. Variables reflecting soil nutrient richness (pH, P, N, Ca, Mg, Na, K, Mn) were positively correlated with each other and negatively correlated with soil acidity (exchangeable H and extractable Al).

Thus the Børgefjell reference area shows variation from soils poor in nutrients, high acidity and high loss-on-ignition on rather flat sites to plots richer in soil nutrients with denser forests on steeper slopes.

PCA ordination of environmental variables

The first two PCA axes accounted for 37.3% and 14.3% of the variance in the matrix of standardised transformed environmental variables, respectively (eigenvalues of 0.373 and 0.143).

pH_{H_2O}, pH_{CaCl_2}, extractable C, K, Mn, S and Zn obtained the highest loadings on PCA axis 1 while loss-on-ignition, extractable Al, exchangeable H and soil moisture (Mme) obtained low values on the same axis (Fig. 259). Macro and meso plot slope, tree aspect, total N and extractable Ca, Mg and P also had relatively high loadings on PCA axis 1.

Macro and meso plot heat indices obtained the highest loadings on PCA axis 2 while macro and meso plot aspect unfavourability indices obtained the lowest loadings

The strong correlations between variables related to soil nutrient richness and slope steepness, and between soil acidity, LOI and soil moisture, are consistent with the correlation matrix of the environmental variables in Table 15.

DCA ordination

The gradient length of the first two DCA axes was 2.54 and 1.79 S.D. units with eigenvalues of 0.316 and 0.168, respectively. The sample plots segregated into four relatively distinct clusters along the two first axes (Fig. 260). The first cluster, consisting of five sample plots (from macro plot 7) had low DCA axis 1 values (> 0.8 S.D. units) and medium high DCA axis 2 values. The next cluster, which also had the highest number of sample plots, occupied the middle of the diagram. The last two clusters were located at the right-hand side of the diagram and only these two clusters segregated along the second axis.

Table 15. Børgefjell: Kendall's rank correlation coefficients τ between 31 environmental variables in the 50 meso plots (lower triangle), with significance probabilities (upper triangle). Statistically significant correlations (P<0.05) in bold face. Names of explanatory variables abbreviated in accordance with Table 2.

	1	2	3	4	5	6	7	8	9	10	11	12	13	14	15	16
01 Ma Slo	*	0.364	**0.022**	0.178	0.083	**0.015**	**0.000**	0.702	0.171	0.212	**0.003**	**0.046**	0.086	**0.014**	**0.001**	**0.000**
02 Ma Asp	0.100	*	**0.000**	**0.035**	0.388	0.979	0.421	**0.001**	**0.000**	0.421	0.511	**0.031**	0.290	0.212	0.785	0.658
03 Ma HI	**0.245**	**–0.697**	*	0.264	0.539	0.292	**0.040**	**0.000**	**0.000**	0.891	**0.012**	0.577	0.680	0.960	0.124	0.198
04 Ma Ter	0.154	**0.241**	–0.125	*	0.435	0.344	0.232	**0.021**	0.184	**0.006**	0.552	0.087	0.618	0.772	0.100	**0.046**
05 Ma Une	–0.204	–0.102	–0.071	0.096	*	0.536	0.097	0.540	0.848	0.956	**0.000**	0.802	0.742	0.230	**0.002**	**0.027**
05 TBA	**0.263**	–0.003	0.111	–0.107	–0.072	*	0.158	0.605	0.635	0.725	0.392	0.704	1.000	0.325	**0.032**	**0.007**
07 Me Slo	**0.636**	0.086	**0.213**	0.133	–0.190	0.148	*	0.308	**0.007**	0.207	**0.007**	**0.012**	0.076	**0.037**	**0.004**	**0.000**
08 Me Asp	–0.040	**0.361**	**–0.372**	**0.253**	0.069	–0.054	–0.104	*	**0.000**	0.404	0.174	0.726	0.762	0.846	0.476	0.873
09 Me HI	0.142	**–0.459**	**0.583**	–0.144	–0.021	0.048	**0.271**	**–0.626**	*	0.946	0.091	0.511	0.847	0.591	0.222	0.307
10 Me Ter	0.136	0.088	0.015	**0.315**	0.007	–0.038	0.134	0.088	–0.007	*	0.333	0.315	0.284	0.885	0.845	0.188
11 Me Une	**–0.306**	0.068	**–0.257**	–0.065	**0.470**	–0.088	**–0.271**	0.136	–0.167	–0.100	*	0.281	0.244	0.056	**0.001**	**0.008**
12 Smi	**–0.219**	**–0.237**	0.060	–0.196	0.030	0.041	**–0.269**	0.037	–0.068	–0.110	–0.112	*	**0.000**	0.308	0.151	0.260
13 Sme	–0.180	–0.111	0.042	–0.054	–0.037	0.000	–0.180	0.030	0.019	–0.111	–0.116	**0.400**	*	**0.000**	0.180	0.076
14 Sma	**–0.258**	–0.132	0.005	0.032	0.136	–0.102	**–0.214**	–0.020	0.054	–0.015	0.191	0.108	**0.351**	*	**0.004**	**0.015**
15 Mme	**–0.337**	–0.028	–0.155	–0.177	**0.346**	**–0.219**	**–0.290**	0.071	–0.119	–0.020	**0.325**	0.149	0.132	**0.285**	*	**0.000**
16 LOI	**–0.474**	–0.046	–0.130	**–0.215**	**0.245**	**–0.272**	**–0.361**	0.016	–0.100	–0.135	**0.261**	0.117	0.175	**0.243**	**0.598**	*
17 Total N	0.169	0.085	–0.115	0.074	0.043	**0.355**	0.108	0.028	–0.072	0.062	–0.021	–0.039	–0.175	–0.115	–0.091	**–0.202**
18 pH$_{H_2O}$	**0.407**	0.066	0.060	0.070	–0.216	**0.451**	**0.233**	–0.049	0.030	0.119	–0.157	–0.156	**–0.202**	**–0.202**	**–0.474**	**–0.627**
19 pH$_{CaCl_2}$	**0.344**	0.056	–0.009	0.036	–0.161	**0.341**	0.193	–0.043	0.041	0.054	–0.160	–0.142	**–0.195**	**–0.210**	**–0.424**	**–0.592**
20H	**–0.251**	–0.069	0.060	0.017	0.168	**–0.395**	–0.154	0.016	0.044	0.013	0.109	0.118	**0.238**	**0.200**	**0.360**	**0.478**
21 Al	**–0.372**	–0.053	–0.040	0.034	**0.300**	**–0.288**	**–0.294**	0.011	–0.020	–0.038	**0.312**	0.073	**0.215**	**0.365**	**0.280**	**0.437**
22 C	**0.536**	0.090	0.086	0.145	**–0.261**	**0.350**	**0.375**	0.056	0.003	0.113	**–0.244**	–0.138	**–0.246**	**–0.310**	**–0.551**	**–0.740**
23 Ca	**0.286**	–0.028	0.154	0.079	–0.065	**0.252**	**0.228**	–0.064	0.124	0.064	**–0.231**	–0.050	**–0.198**	**–0.307**	**–0.388**	**–0.453**
24 Fe	–0.091	0.106	–0.057	0.083	0.176	0.003	–0.049	0.011	–0.041	0.055	**0.213**	0.092	0.190	**0.273**	0.043	0.102
25 K	**0.450**	0.118	0.009	**0.232**	**–0.223**	**0.255**	**0.356**	0.133	–0.046	0.109	**–0.238**	–0.094	**–0.251**	**–0.314**	**–0.468**	**–0.654**
26 Mg	0.009	0.139	–0.155	0.087	–0.055	0.041	0.047	0.039	–0.069	0.027	–0.009	–0.007	**–0.276**	**–0.250**	–0.133	**–0.195**
27 Mn	**0.511**	0.063	0.084	0.121	**–0.326**	**0.266**	**0.365**	–0.046	0.057	0.139	**–0.261**	–0.172	**–0.264**	**–0.309**	**–0.546**	**–0.752**
28 Na	–0.007	**0.279**	**–0.267**	0.140	0.132	**0.248**	–0.035	0.078	–0.177	0.095	0.131	–0.134	–0.002	–0.063	0.064	0.097
29 P	**0.350**	**0.203**	–0.135	**0.249**	–0.128	0.147	**0.258**	0.168	–0.106	0.137	–0.105	–0.122	**–0.327**	**–0.284**	**–0.296**	**–0.453**
30 S	**0.473**	0.109	0.021	0.192	–0.192	**0.357**	**0.297**	0.104	–0.046	0.109	–0.182	–0.096	**–0.203**	**–0.265**	**–0.500**	**–0.680**
31 Zn	**0.501**	0.138	0.038	0.175	–0.186	**0.245**	**0.408**	0.041	0.026	0.181	**–0.215**	**–0.228**	**–0.306**	**–0.322**	**–0.424**	**–0.551**

Table 15 (continued). Børgefjell: Kendall's rank correlation coefficients τ between 31 environmental variables in the 50 meso plots (lower triangle), with significance probabilities (upper triangle). Statistically significant correlations (P<0.05) in bold face. Names of explanatory variables abbreviated in accordance with Table 2.

	17	18	19	20	21	22	23	24	25	26	27	28	29	30	31
01 Ma Slo	0.103	**0.000**	**0.001**	**0.015**	**0.000**	**0.000**	**0.006**	0.377	**0.000**	0.932	**0.000**	0.946	**0.001**	**0.000**	**0.000**
02 Ma Asp	0.413	0.523	0.591	0.506	0.609	0.385	0.785	0.306	**0.000**	0.178	0.539	**0.007**	**0.050**	0.291	0.184
03 Ma HI	0.256	0.556	0.933	0.550	0.693	0.396	0.128	0.573	0.926	0.124	0.405	**0.008**	0.181	0.833	0.705
04 Ma Ter	0.495	0.517	0.740	0.875	0.753	0.178	0.463	0.442	**0.031**	0.421	0.263	0.196	**0.021**	0.074	0.104
05 Ma Une	0.701	0.053	0.149	0.130	**0.007**	**0.019**	0.559	0.112	**0.045**	0.622	**0.003**	0.235	0.250	0.083	0.093
05 TBA	**0.000**	**0.000**	**0.001**	**0.000**	**0.005**	**0.001**	**0.013**	0.973	**0.012**	0.685	**0.009**	**0.015**	0.150	**0.000**	**0.016**
07 Me Slo	**0.282**	0.021	0.056	0.126	**0.003**	**0.000**	**0.023**	0.626	**0.000**	0.638	**0.000**	0.724	**0.010**	**0.003**	**0.000**
08 Me Asp	0.782	0.626	0.669	0.873	0.913	0.574	0.518	0.913	0.182	0.693	0.645	0.435	0.092	0.294	0.681
09 Me HI	0.462	0.757	0.676	0.651	0.841	0.973	0.203	0.676	0.639	0.482	0.558	0.071	0.277	0.639	0.789
10 Me Ter	0.547	0.248	0.598	0.899	0.715	0.273	0.535	0.593	0.288	0.792	0.177	0.355	0.182	0.288	0.079
11 Me Une	0.834	0.112	0.106	0.265	**0.002**	**0.013**	**0.019**	**0.030**	**0.016**	0.927	**0.008**	0.183	0.288	0.064	**0.029**
12 Smi	0.707	0.135	0.172	0.252	0.484	0.183	0.632	0.374	0.365	0.946	0.098	0.194	0.239	0.356	**0.028**
13 Sme	0.076	**0.042**	**0.049**	**0.016**	**0.029**	**0.013**	**0.044**	0.054	**0.011**	**0.005**	**0.007**	0.987	**0.001**	**0.039**	**0.002**
14 Sma	**0.250**	**0.044**	**0.036**	**0.045**	**0.000**	**0.002**	**0.002**	**0.006**	**0.002**	**0.012**	**0.002**	0.529	**0.004**	**0.008**	**0.001**
15 Mme	0.353	**0.000**	**0.000**	**0.000**	**0.004**	**0.000**	**0.000**	0.658	**0.000**	0.173	**0.000**	0.509	**0.002**	**0.000**	**0.000**
16 LOI	**0.039**	**0.000**	**0.000**	**0.000**	**0.000**	**0.000**	**0.000**	0.296	**0.000**	**0.046**	**0.000**	0.320	**0.000**	**0.000**	**0.000**
17 Total N	*	**0.000**	**0.000**	**0.000**	**0.010**	**0.000**	**0.004**	0.770	**0.000**	**0.000**	**0.003**	**0.001**	**0.000**	**0.000**	**0.009**
18 pH_{H_2O}	**0.428**	*	**0.000**	**0.000**	**0.000**	**0.000**	**0.000**	0.713	**0.000**	**0.015**	**0.000**	**0.041**	**0.000**	**0.000**	**0.000**
19 pH_{CaCl_2}	**0.426**	**0.822**	*	**0.000**	**0.000**	**0.000**	**0.000**	0.238	**0.000**	**0.002**	**0.000**	0.259	**0.000**	**0.000**	**0.000**
20H	**–0.482**	**–0.712**	**–0.709**	*	**0.000**	**0.000**	**0.000**	0.093	**0.000**	**0.000**	**0.000**	0.075	**0.000**	**0.000**	**0.000**
21 Al	**–0.252**	**–0.397**	**–0.408**	**0.476**	*	**0.000**	**0.000**	**0.000**	**0.000**	**0.004**	**0.000**	0.610	**0.000**	**0.000**	**0.000**
22 C	**0.376**	**0.694**	**0.682**	**–0.538**	**–0.517**	*	**0.000**	0.103	**0.000**	**0.001**	**0.000**	0.874	**0.000**	**0.000**	**0.000**
23 Ca	**0.278**	**0.455**	**0.490**	**–0.479**	**–0.412**	**0.435**	*	**0.023**	**0.000**	**0.002**	**0.000**	0.553	**0.008**	**0.000**	**0.000**
24 Fe	–0.029	–0.036	–0.116	0.164	**0.509**	–0.159	**–0.221**	*	**0.010**	0.072	**0.034**	**0.015**	**0.018**	0.311	**0.001**
25 K	**0.342**	**0.540**	**0.574**	**–0.464**	**–0.603**	**0.740**	**0.404**	**–0.252**	*	**0.000**	**0.000**	0.927	**0.000**	**0.000**	**0.000**
26 Mg	**0.442**	**0.238**	**0.303**	**–0.388**	**–0.282**	**0.314**	**0.308**	–0.176	**0.394**	*	**0.006**	0.173	**0.000**	**0.000**	**0.007**
27 Mn	**0.293**	**0.699**	**0.676**	**–0.549**	**–0.515**	**0.802**	**0.424**	**–0.207**	**0.690**	**0.270**	*	0.670	**0.000**	**0.000**	**0.000**
28 Na	**0.336**	**0.200**	0.111	–0.174	0.050	0.016	0.058	**0.238**	–0.009	0.133	–0.042	*	0.980	0.380	0.564
29 P	**0.360**	**0.397**	**0.433**	**–0.358**	**–0.455**	**0.556**	**0.259**	**–0.231**	**0.701**	**0.422**	**0.535**	0.002	*	**0.000**	**0.000**
30 S	**0.424**	**0.729**	**0.738**	**–0.569**	**–0.433**	**0.835**	**0.443**	–0.099	**0.762**	**0.342**	**0.739**	0.086	**0.584**	*	**0.000**
31 Zn	**0.256**	**0.461**	**0.457**	**–0.381**	**–0.572**	**0.641**	**0.350**	**–0.313**	**0.714**	**0.265**	**0.646**	–0.056	**0.638**	**0.603**	*

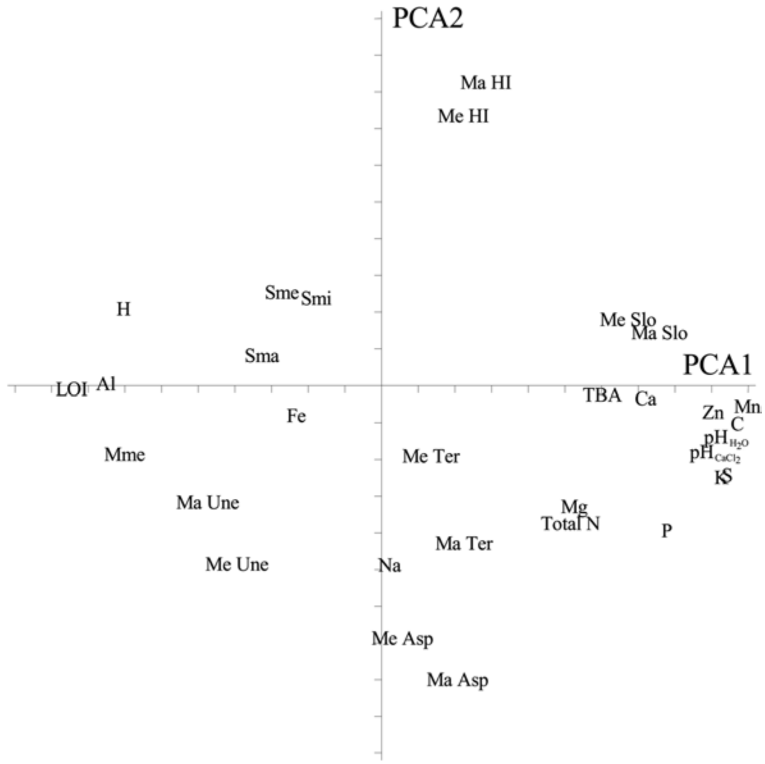

Fig. 259. Børgefjell: PCA ordination of 31 environmental variables. Abbreviations in accordance with Table 2, axes 1 (horizontal) and 2 (vertical). Positions of variables in the ordination space give the head of variable vectors. Tickmarks indicate 0.1 units along both axes.

GNMDS ordination

The GNMDS ordination diagram (Fig. 261) showed good visual similarity with the DCA diagram (Fig. 260).The correlation between GNMDS axis 1 and DCA axis 1 was $\tau = 0.855$ and the correlation between GNMDS axis 2 and DCA axis 2 was $\tau = 0.631$.

Split-plot GLM analysis of relationships between ordination axes and environmental variables

The variation (in plot scores) along DCA axis 1 was partitioned with 94.38 % at the macro plot scale (i.e. between macro plots) and 5.62 % at the (between) meso plot scale within macro plots (Table 16). For the second ordination axis, 83.37 % of the variation was explained at the macro plot scale and 16.63 % at the meso plot scale (Table 17).

At the macro plot scale, seven environmental variables were significantly (at the $\alpha = 0.05$ level) related to DCA 1 while five variables (also at the $\alpha = 0.05$ level) were related to DCA 2. At the meso plot scale, nine environmental variables were significantly related to DCA 1 and two variables to DCA 2 (Tables 16 and 17).

At the macro plot scale, soil concentrations of Total N, C and S, pH and tree basal area increased

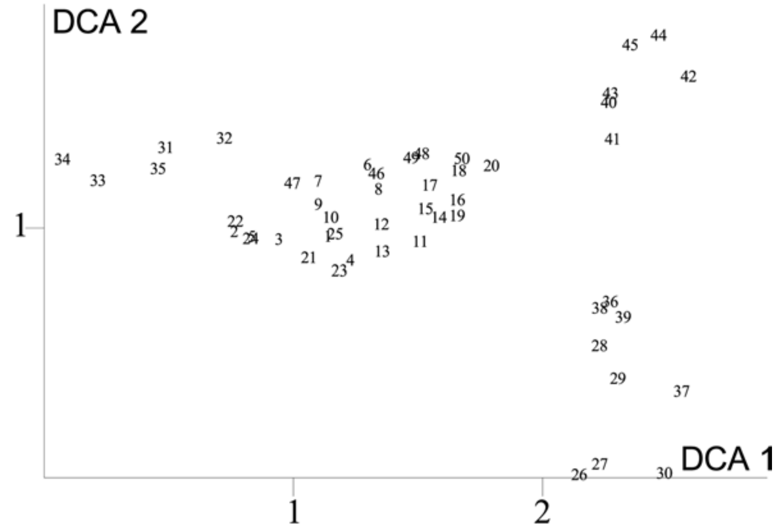

Fig. 260. Børgefjell: DCA ordination diagram of 50 meso plots, axes 1 (horizontal) and 2 (vertical). Meso plot number are plotted just right of the sample plot positions. Scaling of axes in S.D. units.

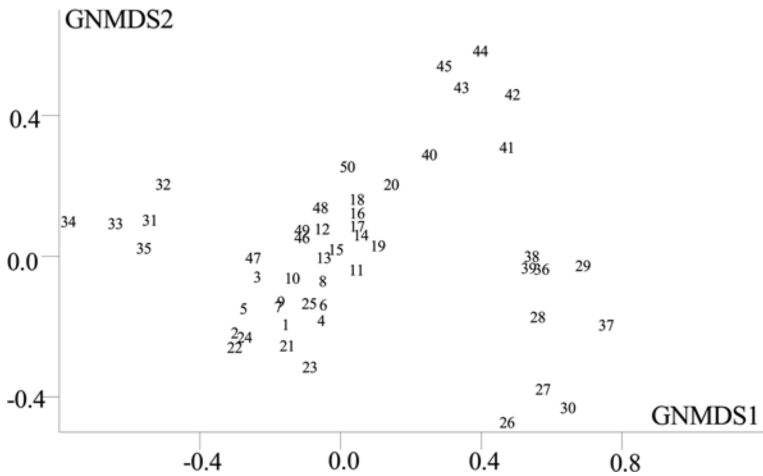

Fig. 261. Børgefjell: GNMDS ordination biplot diagram of 50 meso plots (indicated by their number).

Table 16. Børgefjell: Split-plot GLM analysis and Kendall's nonparametric correlation coefficient τ between DCA 1 and 31 environmental variables (predictor) in the 50 meso plots. df_{resid}: degrees of freedom for the residuals; *SS*: total variation; *FVE*: fraction of total variation attributable to a given scale (macro plot or meso plot); SS_{expl}/SS: fraction of the variation attributable to the scale in question, explained by a variable; *r*: model coefficient (only given when significant at the α = 0.05 level, otherwise blank); *F*: *F* statistic for test of the hypothesis that *r* = 0 against the two-tailed alternative. Split-plot GLM relationships significant at level α = 0.05, *P*, *F*, *r* and SS_{expl}/SS, and Kendall's nonparametric correlation coefficient $|τ| \geq 0.30$ are given in bold face. Numbers and abbreviations for names of environmental variables are in accordance with Tab. 2.

Predictor	Dependent variable = DCA 1 (*SS* = 20.9353)								Correlation between predictor and DCA 1
	Error level								
	Macro plot df_{resid} = 8 $SS_{macro\ plot}$ = 19.7589 *FVE* = 0.9438 of *SS*				Meso plot within macro plot df_{resid} = 39 $SS_{meso\ plot}$ = 1.17638 *FVE* = 0.0562 of *SS*				Total
	$SS_{expl}/SS_{macro\ plot}$	*r*	*F*	*P*	$SS_{expl}/SS_{meso\ plot}$	*r*	*F*	*P*	τ
Ma Slo	0.1245		1.1379	0.3172	**0.1934**	**0.4761**	**9.3517**	**0.0040**	0.248
Ma Asp	0.0189		0.1539	0.7051	*	*	*	*	0.060
Ma HI	0.0107		0.0862	0.7765	**0.1878**	**2.8563**	**9.0161**	**0.0046**	–0.045
Ma Ter	0.0009		0.0074	0.9335	0.0229		0.9149	0.3447	0.055
Ma Une	0.0153		0.1240	0.7338	0.0003		0.0131	0.9096	–0.030
TBA	**0.4038**	**1.4490**	**5.4194**	**0.0483**	0.0199		0.7935	0.3785	**0.448**
Me Slo	0.1159		1.0492	0.3357	**0.0979**	**0.2335**	**4.2309**	**0.0464**	0.201
Me Asp	0.2404		0.0800	0.0985	0.0122		2.6560	0.1112	0.096
Me HI	0.0186		0.1517	0.7071	0.0074		0.2898	0.5934	–0.049
Me Ter	0.0853		0.7465	0.4127	0.0135		0.5350	0.4689	0.027
Me Une	0.0316		0.2614	0.6230	0.0548		2.2609	0.1407	–0.081
Smi	0.0010		0.0082	0.9302	0.0013		0.0525	0.8200	0.012
Sme	0.0843		0.7364	0.4158	0.0044		0.1731	0.6796	–0.109
Sma	0.0483		0.4061	0.5418	0.0052		0.2020	0.6556	–0.136
Mme	0.0643		0.5501	0.4795	0.0022		0.0867	0.7700	–0.190
LOI	0.2273		2.3533	0.1636	0.0365		1.4792	0.2312	**–0.360**
Total N	**0.8972**	**2.8637**	**69.8410**	**0.0000**	0.0088		0.3453	0.5602	**0.639**
pH_{H_2O}	**0.6472**	**2.6795**	**14.6780**	**0.0050**	0.0227		0.9071	0.3467	**0.560**
pH_{CaCl_2}	**0.7237**	**3.1055**	**20.9500**	**0.0018**	0.0318		1.2810	0.2646	**0.562**
H	**0.7863**	**–3.1976**	**29.4330**	**0.0006**	0.0111		0.4395	0.5113	**–0.546**
Al	0.2055		2.0688	0.1883	**0.1172**	**–0.5758**	**5.1772**	**0.0285**	–0.265
C	**0.4007**	**1.7924**	**5.3498**	**0.0495**	**0.1928**	**0.6805**	**9.3154**	**0.0041**	**0.509**
Ca	0.3404		4.1294	0.0766	**0.1067**	**0.3177**	**4.6599**	**0.0371**	0.298
Fe	0.0073		0.0592	0.8140	0.0000		0.0001	0.9910	–0.063
K	0.2928		3.3120	0.1063	**0.3075**	**1.0645**	**17.3140**	**0.0002**	**0.520**
Mg	0.3097		3.5887	0.0948	0.0565		2.3363	0.1345	0.288
Mn	0.2837		3.1692	0.1129	0.0015		0.0571	0.8123	**0.412**
Na	0.1702		1.6405	0.2361	0.0142		0.5599	0.4588	0.210
P	0.3580		4.4607	0.0677	**0.1432**	**0.8311**	**6.5174**	**0.0147**	**0.447**
S	**0.5827**	**2.2077**	**11.1710**	**0.0102**	**0.1079**	**0.5103**	**4.7160**	**0.0360**	**0.582**
Zn	0.1823		1.7835	0.2185	0.0899		3.8512	0.0569	**0.404**

Table 17. Børgefjell: Split-plot GLM analysis and Kendall's nonparametric correlation coefficient τ between DCA 2 and 31 environmental variables (predictor) in the 50 meso plots. df_{resid}: degrees of freedom for the residuals; *SS*: total variation; *FVE*: fraction of total variation attributable to a given scale (macro plot or meso plot); SS_{expl}/SS: fraction of the variation attributable to the scale in question, explained by a variable; *r*: model coefficient (only given when significant at the α = 0.05 level, otherwise blank); *F*: *F* statistic for test of the hypothesis that *r* = 0 against the two-tailed alternative. Split-plot GLM relationships significant at level α = 0.05, *P*, *F*, *r* and SS_{expl}/SS, and Kendall's nonparametric correlation coefficient $|\tau| \geq 0.30$ are given in bold face. Numbers and abbreviations for names of environmental variables are in accordance with Tab. 2.

Predictor	Dependent variable = DCA 2 (*SS* = 7.5495)								Correlation between predictor and DCA 2
	Error level								
	Macro plot, $df_{resid} = 8$, $SS_{macro\ plot} = 6.2941$, *FVE* = 0.8337 of *SS*				Meso plot within macro plot, $df_{resid} = 39$, $SS_{meso\ plot} = 1.25535$, *FVE* = 0.1663 of *SS*				Total
	$SS_{expl}/SS_{macro\ plot}$	*r*	*F*	*P*	$SS_{expl}/SS_{meso\ plot}$	*r*	*F*	*P*	τ
Ma Slo	0.3104		3.6006	0.0943	0.0089		0.3491	0.5580	0.229
Ma Asp	0.0006		0.0051	0.9446	*	*	*	*	–0.005
Ma HI	0.1631		1.5587	0.2472	0.0096		0.3793	0.5416	0.271
Ma Ter	0.0038		0.0306	0.8656	0.0018		0.0687	0.7946	0.053
Ma Une	**0.4209**	**–0.6629**	**5.8159**	**0.0424**	0.0477		1.9543	0.1700	–0.271
TBA	0.0330		0.2729	0.6155	**0.1474**	**0.7126**	**6.7451**	**0.0132**	0.224
Me slo	0.3182		3.7328	0.0894	0.0034		0.1343	0.7160	0.277
Me Asp	0.0663		0.5679	0.4727	0.0712		0.0476	0.8285	–0.136
Me HI	0.1266		1.1595	0.3130	0.0012		0.0717	0.7903	0.185
Me Ter	0.0483		0.4061	0.5417	0.0016		2.3695	0.1318	0.066
Me Une	0.3249		3.8495	0.0854	0.0741		3.1197	0.0852	–0.218
Smi	0.0611		0.5206	0.4911	**0.1217**	**–0.2805**	**5.4028**	**0.0254**	–0.195
Sme	0.1170		1.0600	0.3333	0.0896		3.8400	0.0572	–0.091
Sma	**0.4261**	**–2.3678**	**5.9403**	**0.0407**	0.0002		0.0080	0.9292	–0.165
Mme	**0.6029**	**–4.5734**	**12.1440**	**0.0083**	0.0134		0.5310	0.4705	**–0.411**
LOI	**0.4099**	**–0.8743**	**5.5572**	**0.0462**	0.0411		1.6700	0.2039	**–0.427**
Total N	0.1320		1.2167	0.3021	0.0046		0.1819	0.6721	–0.140
pH_{H_2O}	0.0763		0.6612	0.4397	0.0294		1.1814	0.2837	0.286
pH_{CaCl_2}	0.0535		0.4523	0.5202	0.0877		3.7489	0.0601	0.186
H	0.0214		0.1745	0.6871	0.0683		2.8601	0.0988	–0.149
Al	0.3909		5.1344	0.0532	0.0004		0.0176	0.8953	–0.262
C	0.2515		2.6875	0.1398	0.0778		3.2891	0.0774	**0.337**
Ca	0.2633		2.8596	0.1293	0.0529		2.1775	0.1481	0.252
Fe	0.1586		1.5076	0.2544	0.0018		0.0692	0.7939	–0.019
K	0.3201		3.7662	0.0883	0.0447		1.8245	0.1846	0.280
Mg	0.0334		0.2765	0.6133	0.0218		0.8700	0.3567	–0.016
Mn	0.3438		4.1910	0.0748	0.0117		0.4614	0.5010	**0.411**
Na	0.2244		2.3153	0.1666	0.0002		0.0059	0.9392	–0.066
P	0.1159		1.0491	0.3357	0.0042		0.1634	0.6882	0.115
S	0.1125		1.0143	0.3434	0.0561		2.3197	0.1358	0.244
Zn	**0.4495**	**1.1885**	**6.5323**	**0.0339**	0.0023		0.0915	0.7640	0.278

significantly (at the $\alpha = 0.05$ level) along DCA 1 while the concentration of H decreased. At the meso plot scale, macro and meso plot slope, macro plot heat index and soil concentrations of C, Ca, K, P and S increased while the concentration of Al decreased.

At the macro plot scale, DCA 2 was positively related to the concentration of Zn and negatively related to meso plot unevenness, maximum soil depth, soil moisture and loss on ignition. At the meso plot scale, DCA axis 2 was significantly positively related to tree basal area and negatively related to minimum soil depth (at the $\alpha = 0.05$ level) (Table 17).

Correlations between DCA ordination axes and environmental variables

Thirteen out of the 31 environmental variables were correlated with DCA axis 1 or/and DCA axis 2 at the $|\tau| > 0.300$ level (Tables 16 and 17). Total N ($\tau = 0.639$, Fig. 265), extractable S ($\tau = 0.582$, Fig. 272), pH [pH_{H_2O} ($\tau = 0.562$, Fig. 266)] and exchangeable H ($\tau = -0.546$, Fig. 267) were most strongly correlated with DCA axis 1. The only two variables that were correlated with DCA axis 2 at the $|\tau| > 0.300$ level were soil moisture ($\tau = -0.411$, Fig. 263) loss-on-ignition ($\tau = -0.427$, Fig. 264), extractable Mn ($\tau = 0.411$, Fig. 270) and extractable C ($\tau = 0.337$, Fig. 268).

Frequent species

A total of 80 species were recorded within the fifty 1×1 m meso plots: 40 vascular plants, 17 mosses, 13 liverworts and 24 lichens. The most frequent species (the sum of subplot frequencies in brackets) were: *Vaccinium myrtillus* (783 out of 800), *Avenella flexuosa* (755), *Barbilophozia lycopodioides* (724), *Chamaepericlymenum suecicum* (695), *Empetrum nigrum* (583), *Dicranum scoparium* (547), *Pleurozium schreberi* (542), *Brachythecium reflexum* (481), *Vaccinium vitis-idaea* (378) and *Gymnocarpium dryopteris* (343).

The distribution of species abundance in the DCA ordination

Forty-seven of the totally 80 species occurred in 5 or more of the sample plots (Figs 274–320).

Examples of species with wide ecological amplitude were *Vaccinium myrtillus* (Fig. 279), *Chamaepericlymenum suecicum* (Fig. 283), *Avenella flexuosa* (Fig. 294) and partly *Barbilophozia lycopodioides* (Fig. 307), which all were abundant in most of the sample plots.

Species restricted to plots in the left part of the DCA ordination diagram, reflecting soils with low pH values and low amounts of total N, S, K, C, P and Mn, were *Calluna vulgaris* (Fig. 277), *Cladonia arbuscula* (Fig. 312), *Cladonia rangiferina* (Fig. 319) and *Cladonia uncialis* (Fig. 320), and partly *Empetrum nigrum* (Fig. 278) and *Pleurozium schreberi* (Fig. 302). The lichen species *Cladonia arbuscula*, *C. rangiferina* and *C. uncialis* were also mainly restricted to high DCA axis 2 scores, typically having dry soil (cf. Fig. 263).

In contrast *Cicerbita alpina* (Fig. 282) and *Brachythecium salebrosum* (Fig. 297) and to some extent *Gymnicarpium dryopteris* (Fig. 285) were mostly restricted to sample plots with high pH values and high concentrations of total N, S, K, C, P and Mn. Species with optimum at high DCA axis 1 values differed with respect to distribution along DCA axis 2. *Dryopteris expansa* (Fig. 284) and to some extent *Plagiothecium* sp. (Fig. 301) showed preference for the lower right-hand corner of the diagram, reflecting affinities to slightly moister soils. *Hieracium* sect. *Hieracium* (Fig. 286), *Polygonatum verticillatum* (Fig. 290) and *Anthoxanthum odoratum* (Fig. 293) are examples of species that occurred mostly in the upper right-hand corner of the diagram, reflecting affinities to slightly

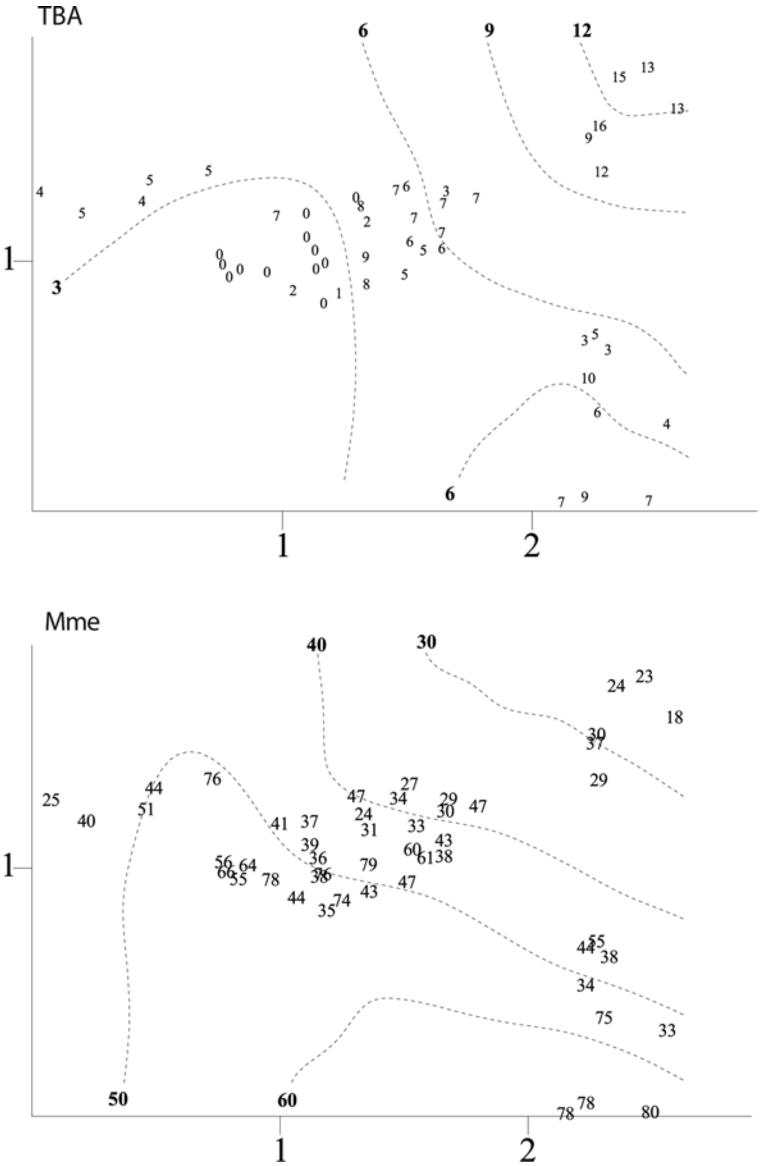

Figs 262-263. Børgefjell: isolines for environmental variables in the DCA ordinations of 50 meso plots, axes 1 (horizontal) and 2 (vertical). Values for the environmental variables are plotted onto the meso plots' positions. Scaling in S.D. units. Fig. 262. TBA (R^2 = 0.719). Fig. 263. Mme (Soil moisture) (R^2 = 0.603). Names of environmental variables in accordance with Table 2.

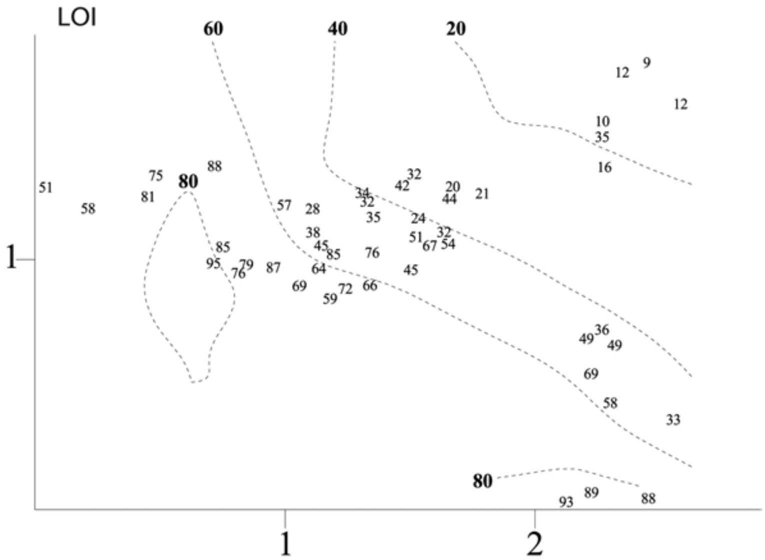

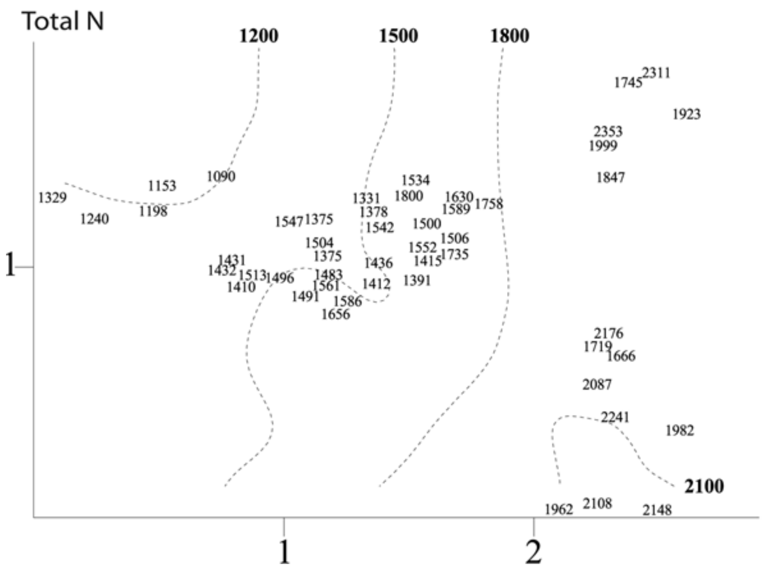

Figs 264-265. Børgefjell: isolines for environmental variables in the DCA ordinations of 50 meso plots, axes 1 (horizontal) and 2 (vertical). Values for the environmental variables are plotted onto the meso plots' positions. Scaling in S.D. units. Fig. 264. LOI ($R^2 = 0.794$). Fig. 265. Total N. C ($R^2 = 0.839$). R^2 refers to the coefficient of determination between original and smoothened values as interpolated from the isolines. Names of environmental variables in accordance with Table 2.

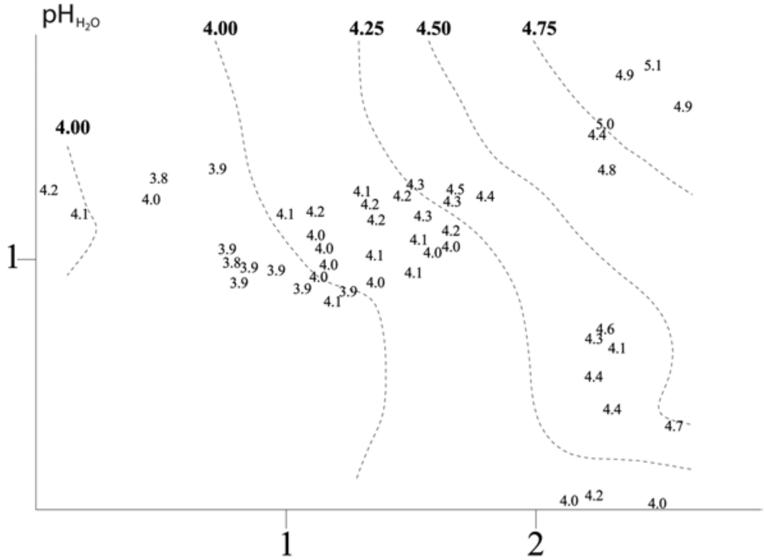

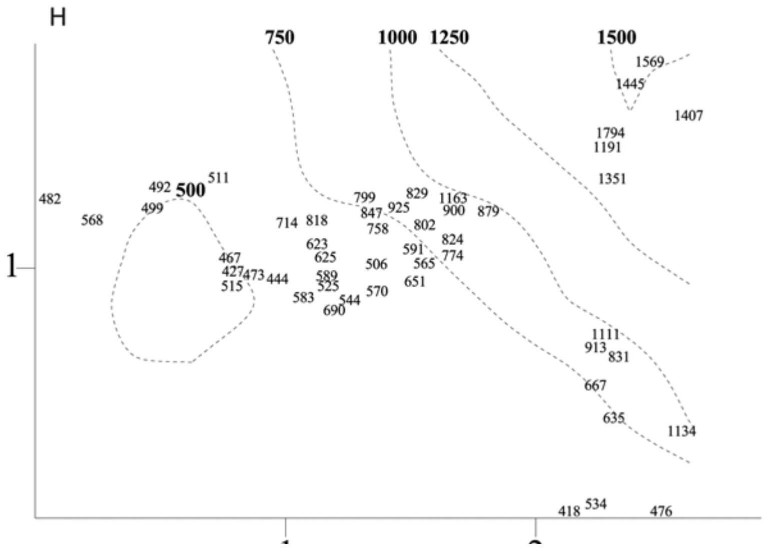

Figs 266-267. Børgefjell: isolines for environmental variables in the DCA ordinations of 50 meso plots, axes 1 (horizontal) and 2 (vertical). Values for the environmental variables are plotted onto the meso plots' positions. Scaling in S.D. units. Fig. 266. pH$_{H_2O}$ ($R^2 = 0.792$). Fig. 267. H ($R^2 = 0.760$). R^2 refers to the coefficient of determination between original and smoothened values as interpolated from the isolines. Names of environmental variables in accordance with Table 2.

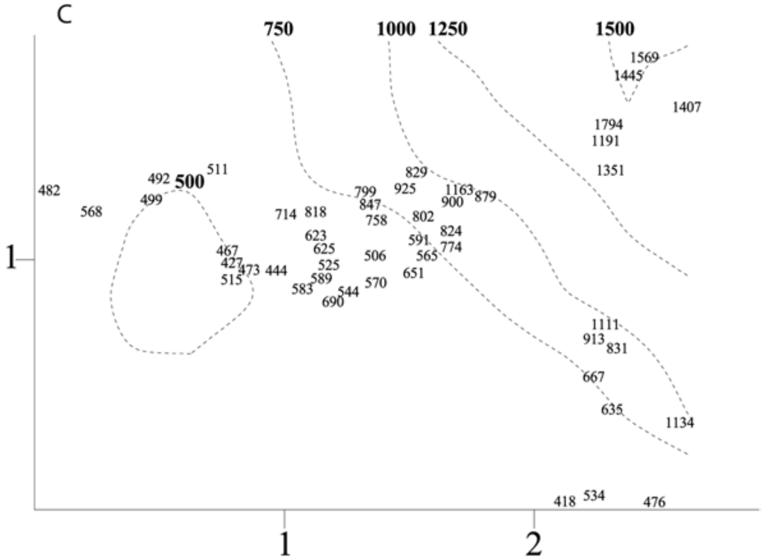

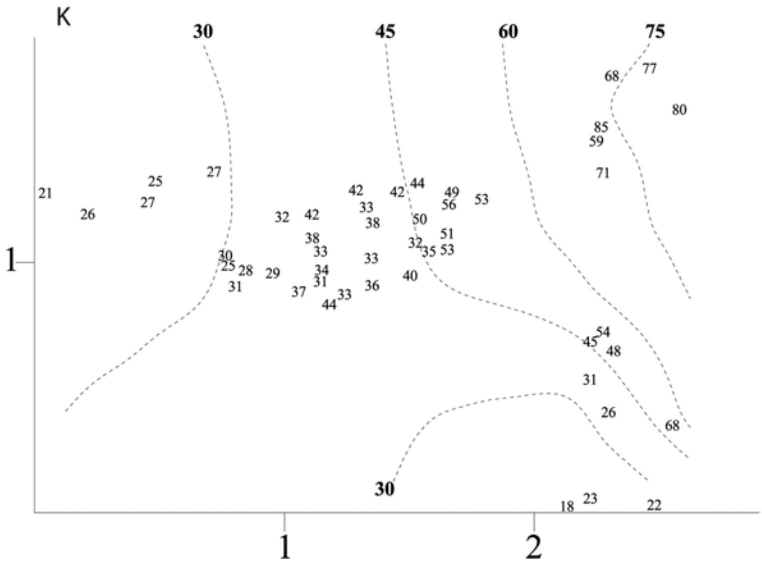

Figs 268-269. Børgefjell: isolines for environmental variables in the DCA ordinations of 50 meso plots, axes 1 (horizontal) and 2 (vertical). Values for the environmental variables are plotted onto the meso plots' positions. Scaling in S.D. units. Fig. 268. C ($R^2 = 0.799$). Fig. 269. K ($R^2 = 0.830$). R^2 refers to the coefficient of determination between original and smoothened values as interpolated from the isolines. Names of environmental variables in accordance with Table 2.

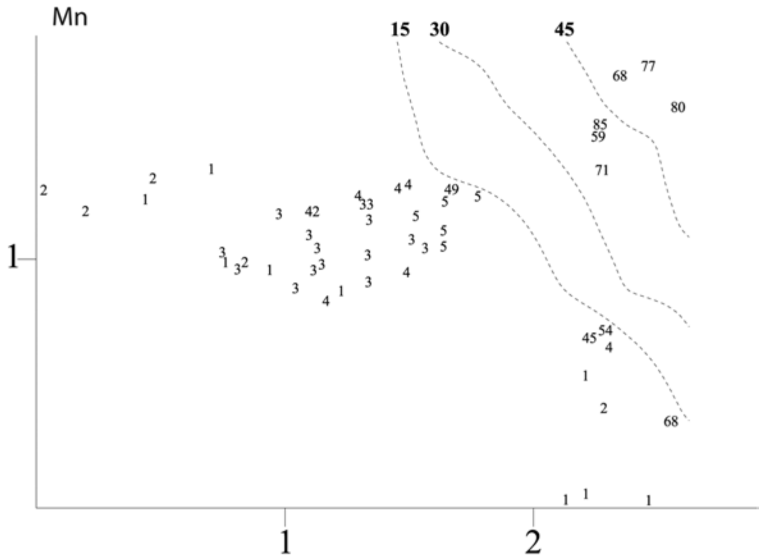

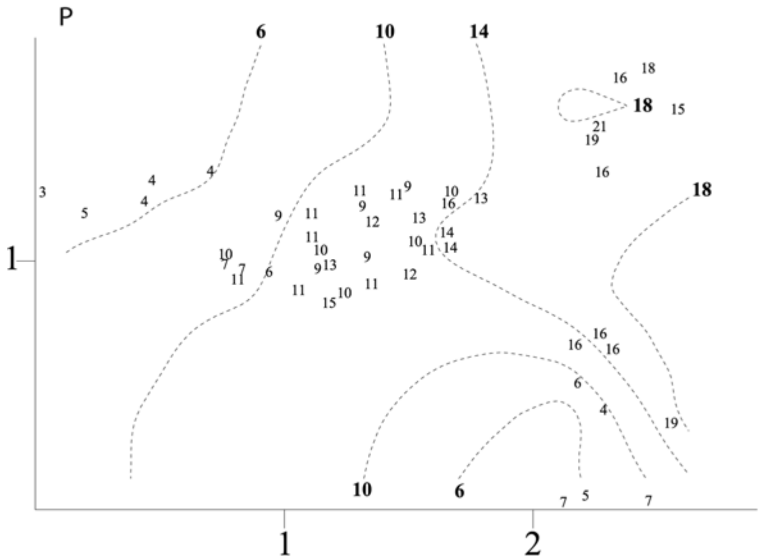

Figs 270-271. Børgefjell: isolines for environmental variables in the DCA ordinations of 50 meso plots, axes 1 (horizontal) and 2 (vertical). Values for the environmental variables are plotted onto the meso plots' positions. Scaling in S.D. units. Fig. 270. Mn ($R^2 = 0.761$). Fig. 271. P ($R^2 = 0.729$). R^2 refers to the coefficient of determination between original and smoothened values as interpolated from the isolines. Names of environmental variables in accordance with Table 2.

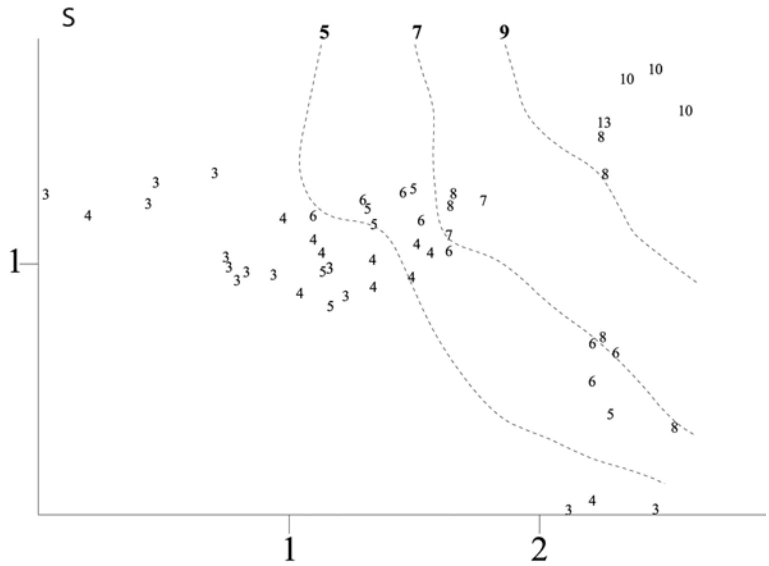

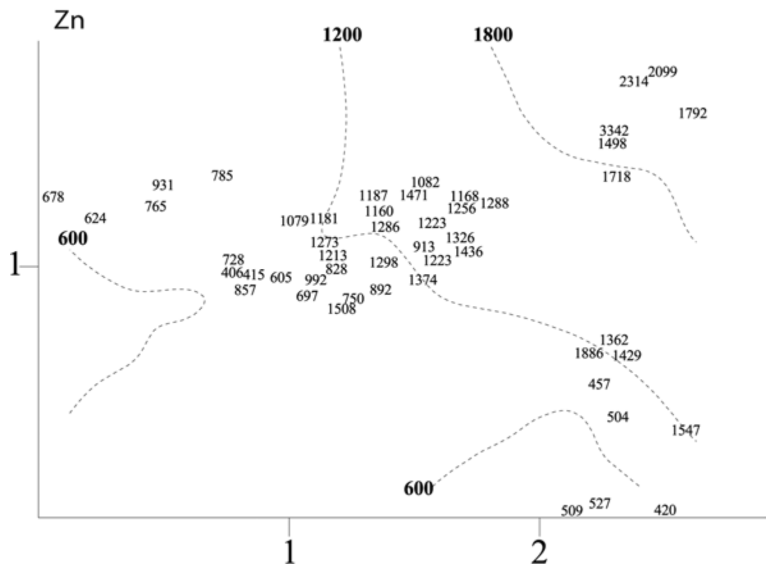

Figs 272-273. Børgefjell: isolines for environmental variables in the DCA ordinations of 50 meso plots, axes 1 (horizontal) and 2 (vertical). Values for the environmental variables are plotted onto the meso plots' positions. Scaling in S.D. units. Fig. 272. S ($R^2 = 0.803$). Fig. 273. Zn ($R^2 = 0.710$). R^2 refers to the coefficient of determination between original and smoothened values as interpolated from the isolines. Names of environmental variables in accordance with Table 2.

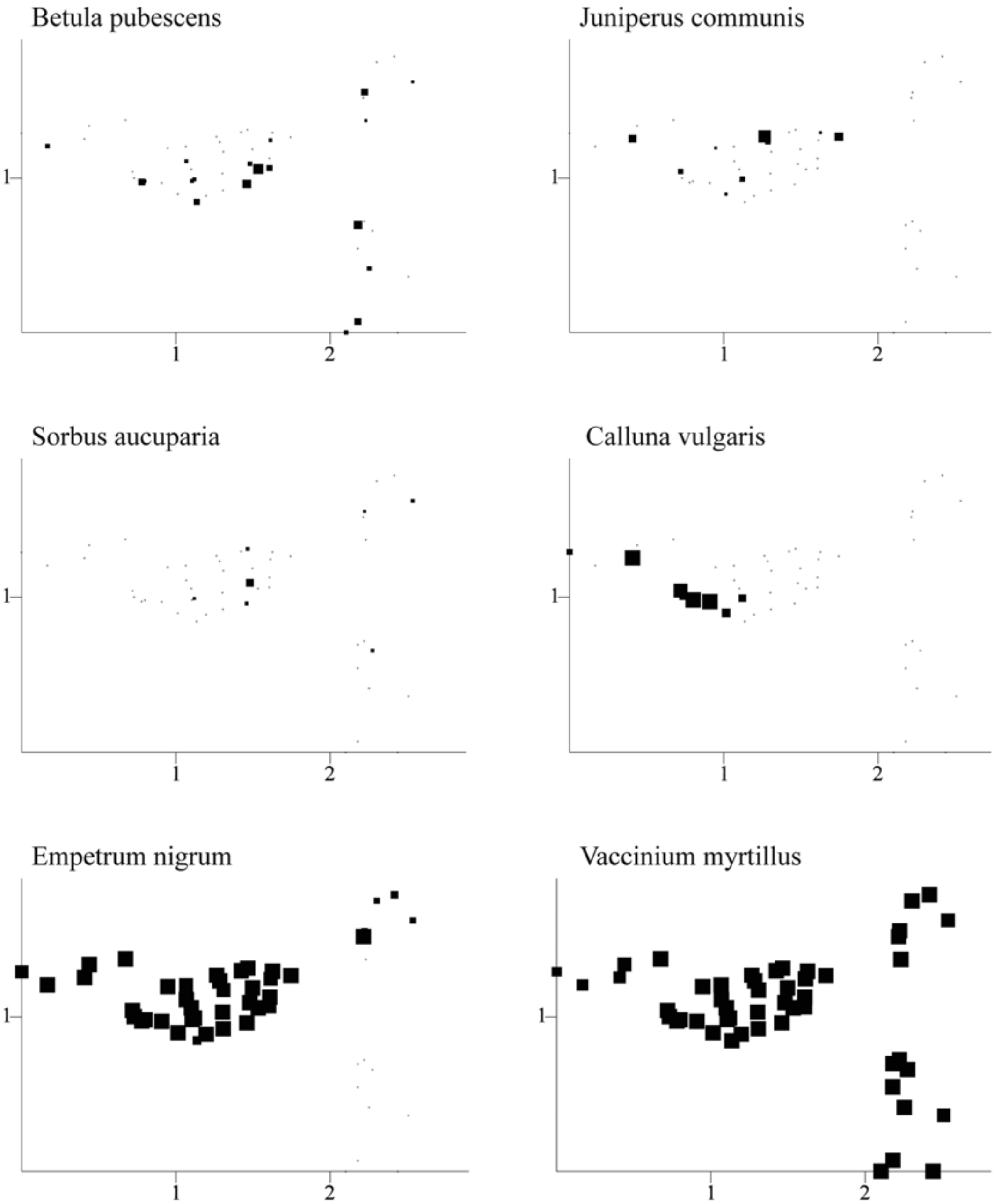

Fig. 274-279. Børgefjell: distributions of species abundances in the DCA ordination of 50 meso plots, axes 1 (horizontal) and 2 (vertical). Frequency in subplots for each species in each meso plot proportional to quadrate size. Scaling in S.D. units. Fig. 274. *Betula pubescens*. Fig. 275. *Juniperus communis*. Fig. 276. *Sorbus aucuparia*. Fig. 277. *Calluna vulgaris*. Fig. 278. *Empetrum nigrum*. Fig. 279. *Vaccinium myrtillus*.

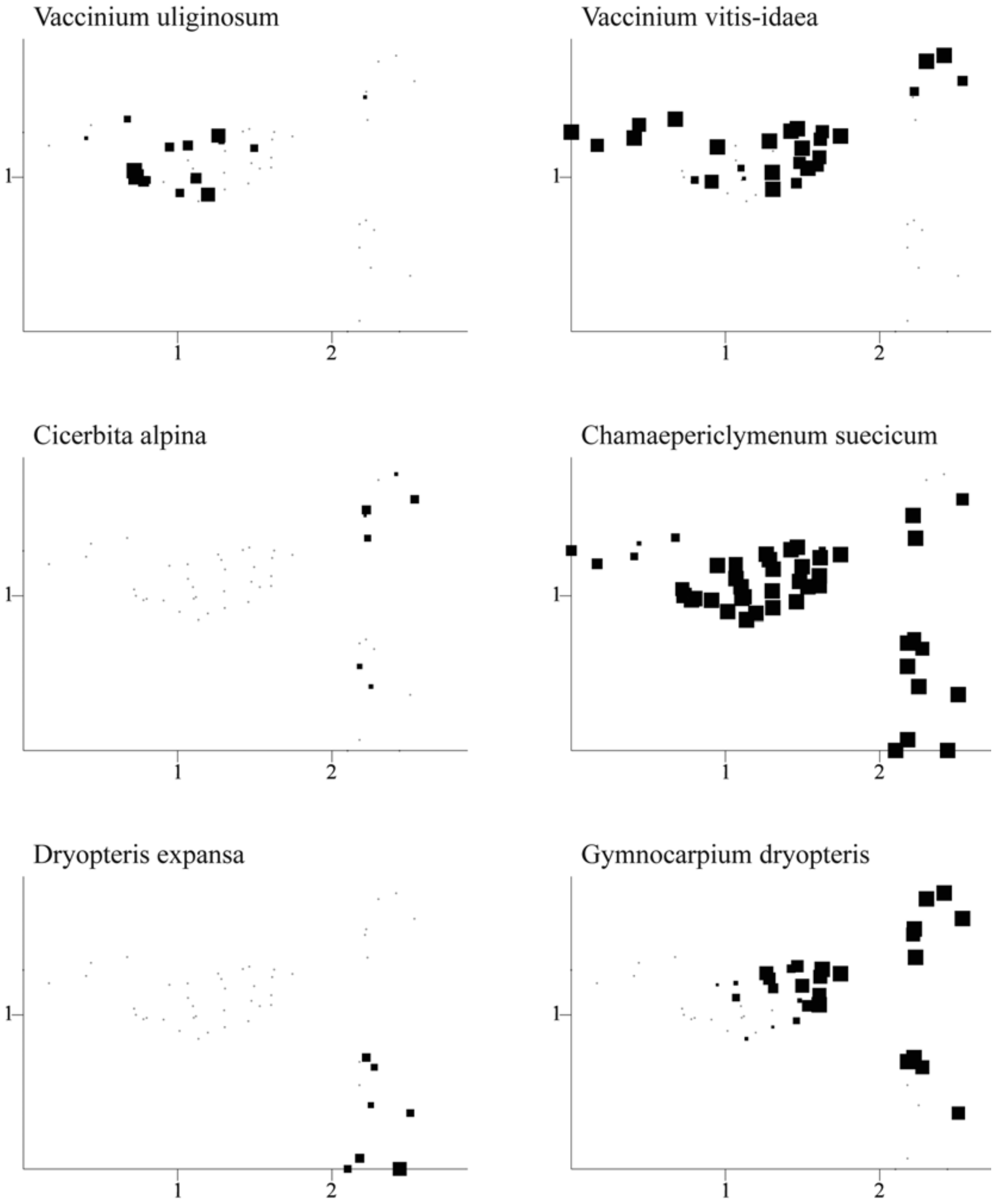

Figs 280-285. Børgefjell: distributions of species abundances in the DCA ordination of 50 meso plots, axes 1 (horizontal) and 2 (vertical). Frequency in subplots for each species in each meso plot proportional to quadrate size. Scaling in S.D. units. Fig. 280. *Vaccinium uliginosum*. Fig. 281. *Vaccinium vitis-idaea*. Fig. 282. *Cicerbita alpina*. Fig. 283. *Chamaepericlymenum suecicum*). Fig. 284. *Dryopteris expansa*. Fig. 285. *Gymnocarpium dryopteris*.

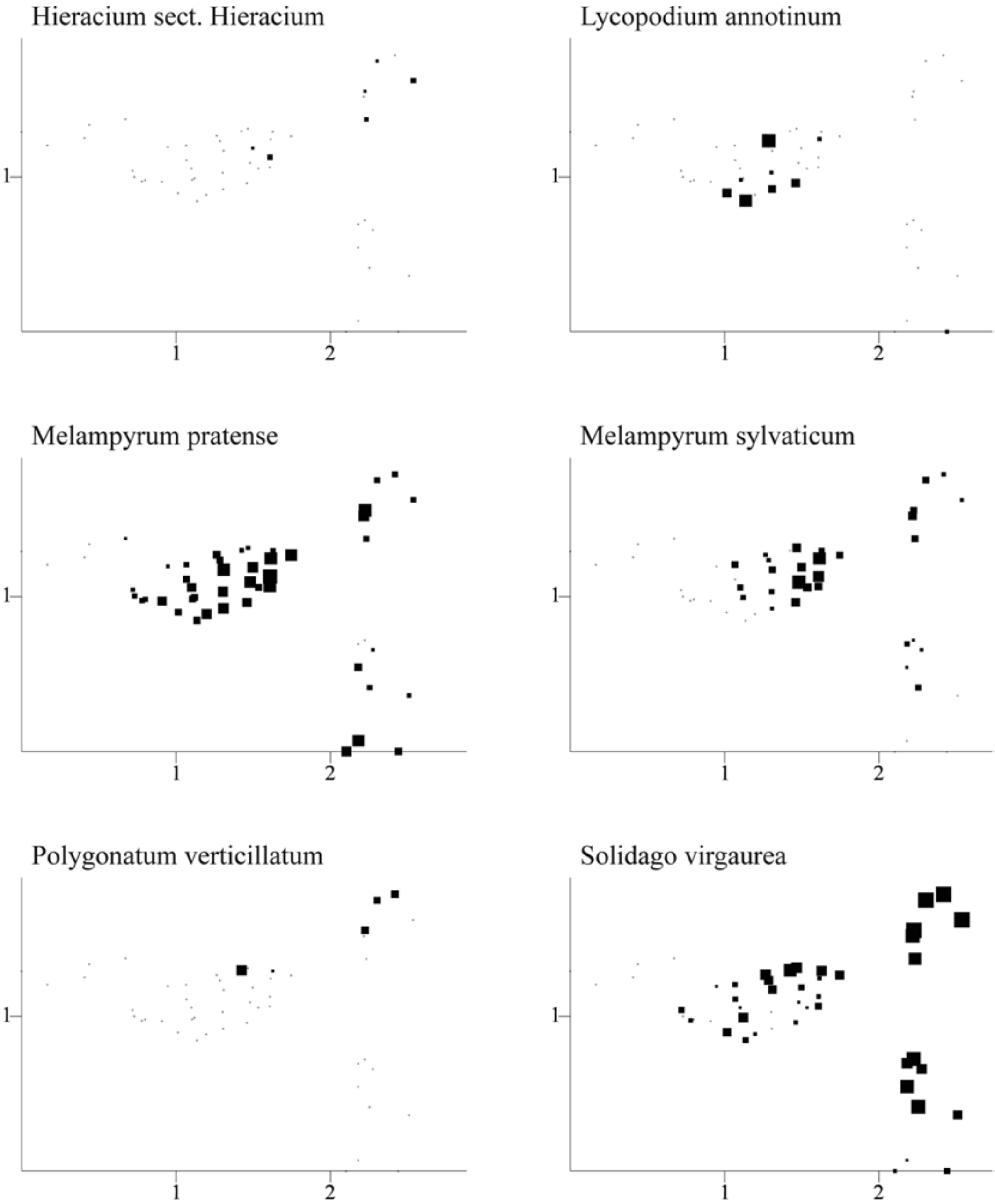

Figs 286-291. Børgefjell: distributions of species abundances in the DCA ordination of 50 meso plots, axes 1 (horizontal) and 2 (vertical). Frequency in subplots for each species in each meso plot proportional to quadrate size. Scaling in S.D. units. Fig. 286. *Hieracium* sect. *Hieracium*. Fig. 287. *Lycopodium annotinum*. Fig. 288. *Melampyrum pratense*. Fig. 289. *Melampyrum sylvaticum*. Fig. 290. *Polygonatum verticillatum*. Fig. 291. *Solidago virgaurea*.

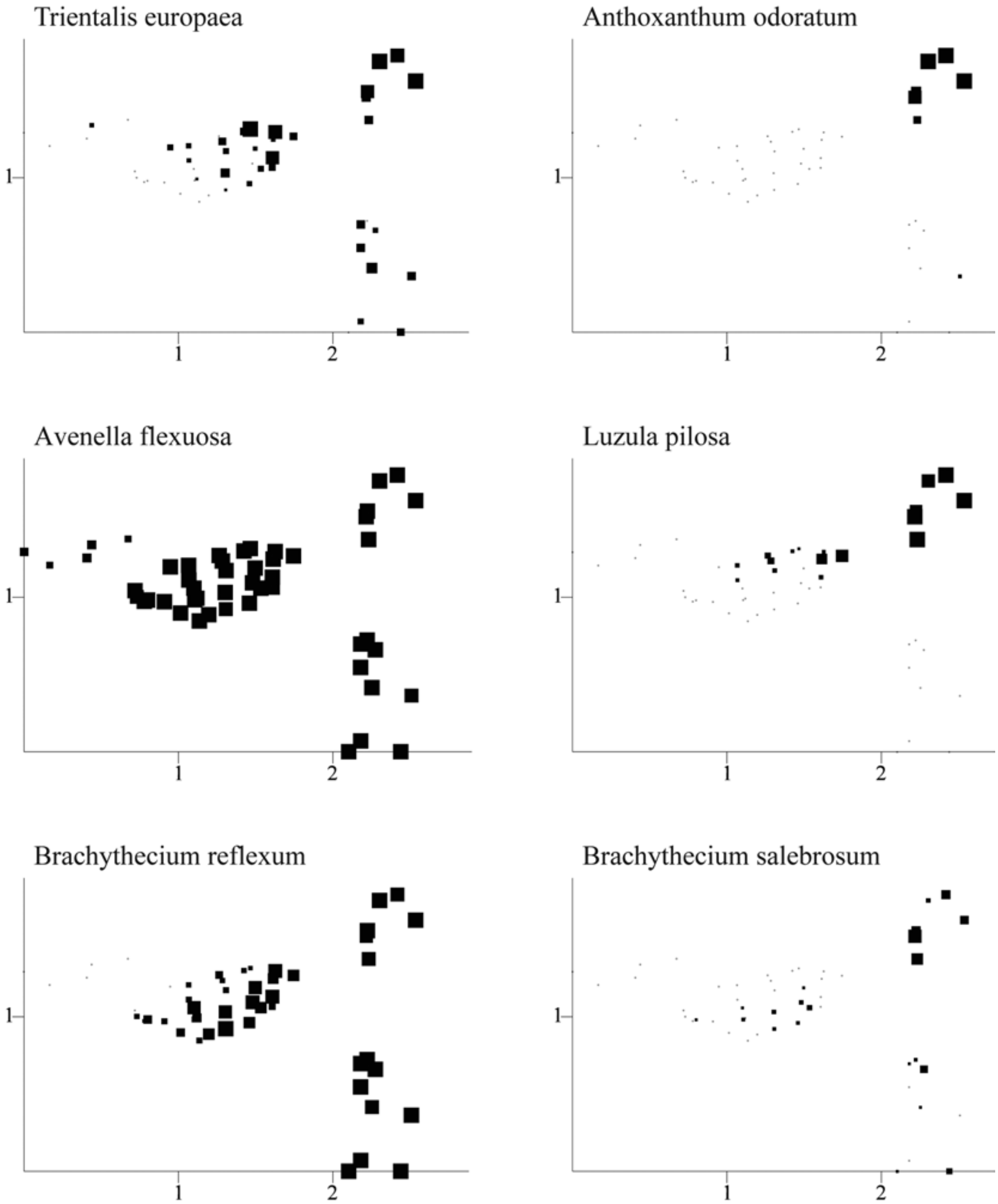

Figs 292-297. Børgefjell: distributions of species abundances in the DCA ordination of 50 meso plots, axes 1 (horizontal) and 2 (vertical). Frequency in subplots for each species in each meso plot proportional to quadrate size. Scaling in S.D. units. Fig. 292. *Trientalis europaea*. 293. *Anthoxanthum odoratum*. Fig. 294. *Avenella flexuosa*. Fig. 295. *Luzula pilosa*. Fig. 296. *Brachythecium reflexum*. Fig. 297. *Brachythecium salebrosum*.

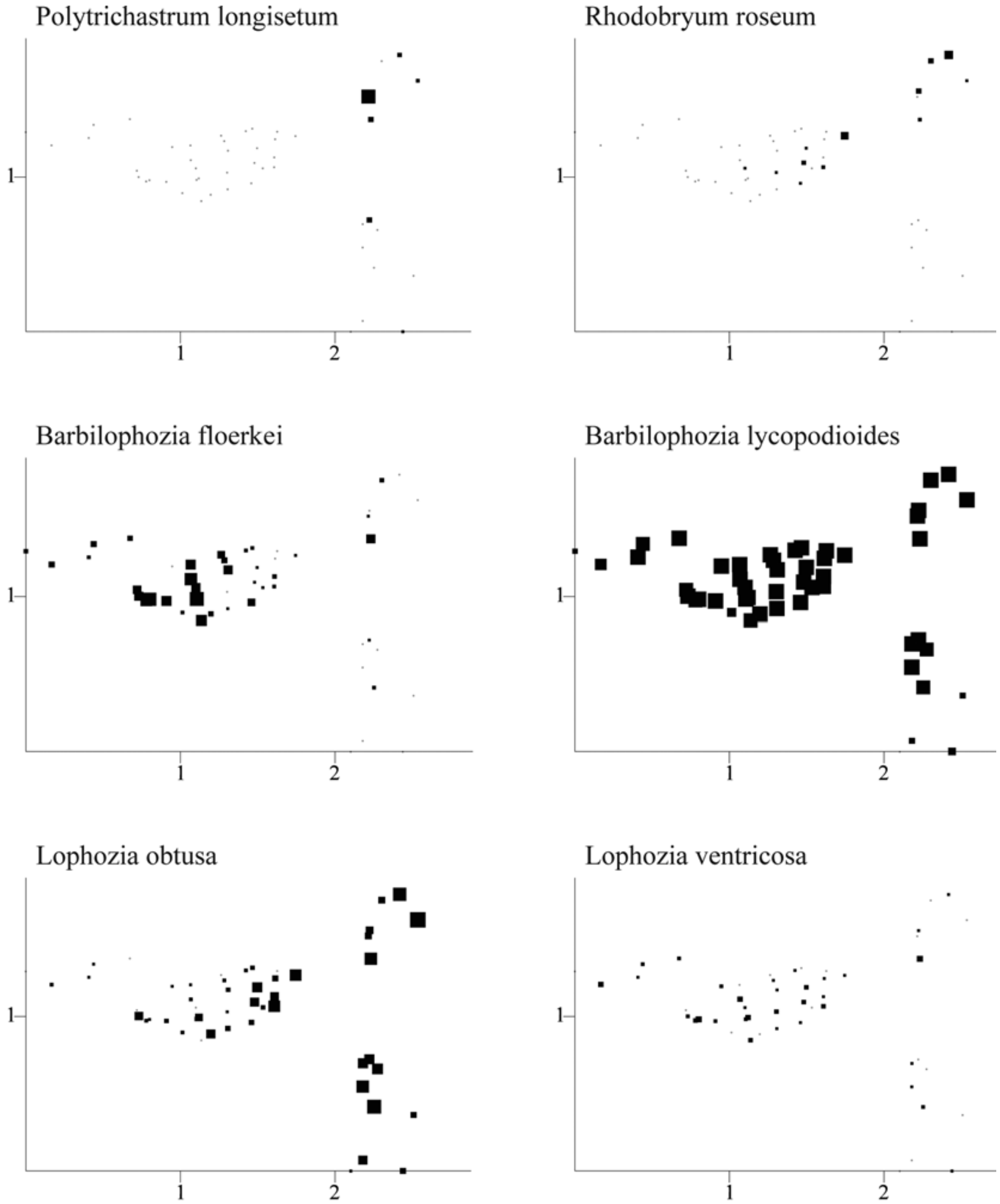

Figs 304-309. Børgefjell: distributions of species abundances in the DCA ordination of 50 meso plots, axes 1 (horizontal) and 2 (vertical). Frequency in subplots for each species in each meso plot proportional to quadrate size. Scaling in S.D. units. Fig. 304. *Polytrichastrum longisetum*. Fig. 305. *Rhodobryum roseum*. Fig. 306. *Barbilophozia floerkei*. Fig. 307. *Barbilophozia lycopodioides*. Fig. 308. *Lophozia obtusa*. Fig. 309. *Lophozia ventricosa*.

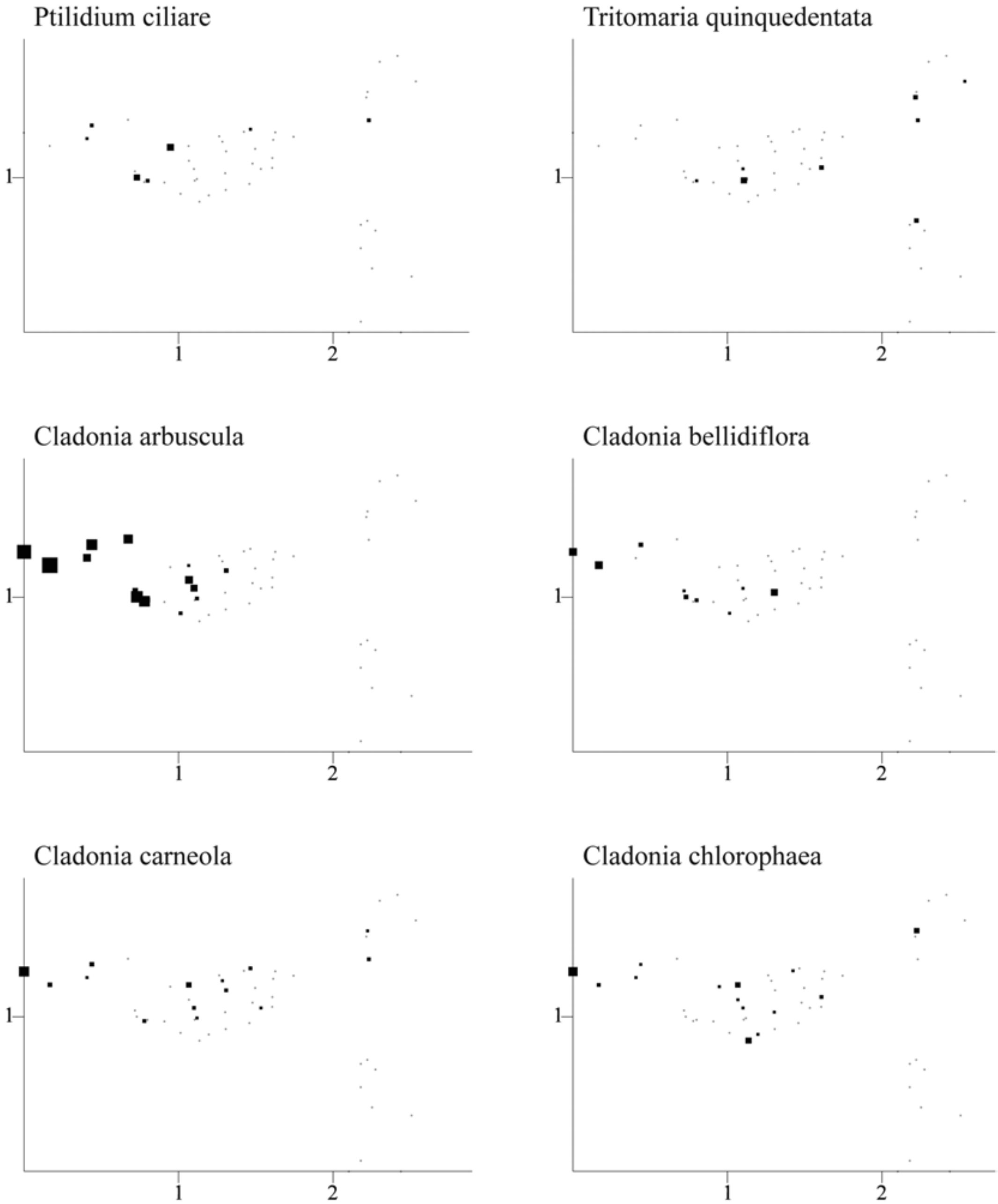

Figs 310-315. Børgefjell: distributions of species abundances in the DCA ordination of 50 meso plots, axes 1 (horizontal) and 2 (vertical). Frequency in subplots for each species in each meso plot proportional to quadrate size. Scaling in S.D. units. Fig. 310 *Ptilidium ciliare*. Fig. 311. *Tritomaria quinquedentata*. Fig. 312. *Cladonia arbuscula*. Fig. 313. *Cladonia bellidiflora*. Fig. 314. *Cladonia carneola*. Fig. 315. *Cladonia chlorophaea*.

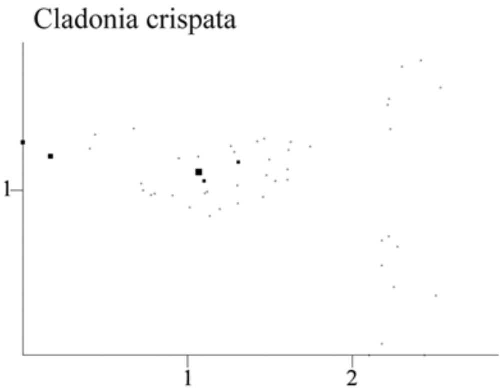

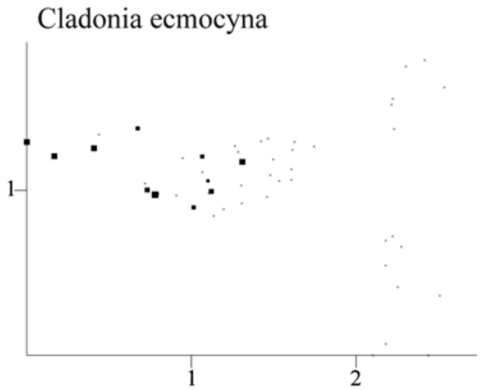

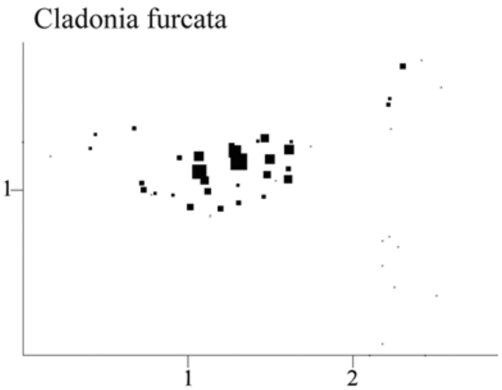

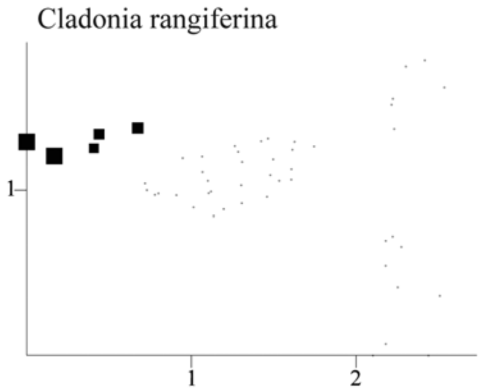

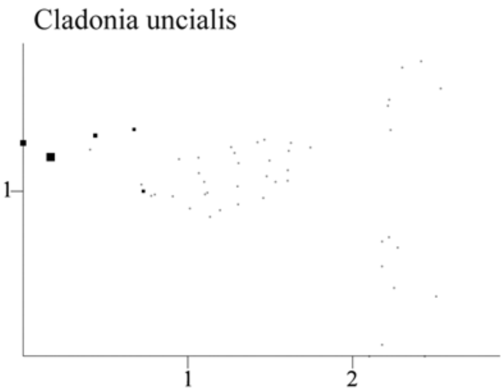

Figs 316-320. Børgefjell: distributions of species abundances in the DCA ordination of 50 meso plots, axes 1 (horizontal) and 2 (vertical). Frequency in subplots for each species in each meso plot proportional to quadrate size. Scaling in S.D. units. Fig. 316. *Cladonia crispata*. Fig. 317. *Cladonia ecmocyna*. Fig. 318. *Cladonia furcata*. Fig. 319. *Cladonia rangiferina*. Fig. 320. *Cladonia uncialis*.

drier soils.

Lycopodium annotinum (Fig. 287) was with one exception restricted to the central cluster in the DCA ordination diagram.

DIVIDALEN REFERENCE AREA

Correlations between environmental variables

There were strong pairwise correlations between several of the topographical variables, between topographical variables and soil variables and between soil variables (Table 18).

Macro plot slope was negatively correlated with aspect unfavourabilites and positively correlated with heat indices. Both macro plot and meso plot terrain form and terrain unevenness were positively correlated with soil moisture. Tree basal area was positively correlated with macro plot aspect unfavourability and the heat index. Loss-on-ignition was negatively correlated with aspect, soil pH, total N, extractable C and Ca, and positively correlated with soil moisture and exchangeable H. Soil pH was positively correlated with total N, extractable C, Ca, Mn, S and Zn and negatively correlated with extractable Al, K, Mg, P and exchangeable H.

PCA ordination of environmental variables

The first two PCA axes accounted for 30.3% and 17.5% of the variance in the matrix of standardised transformed environmental variables, respectively (eigenvalues of 0.303 and 0.175).

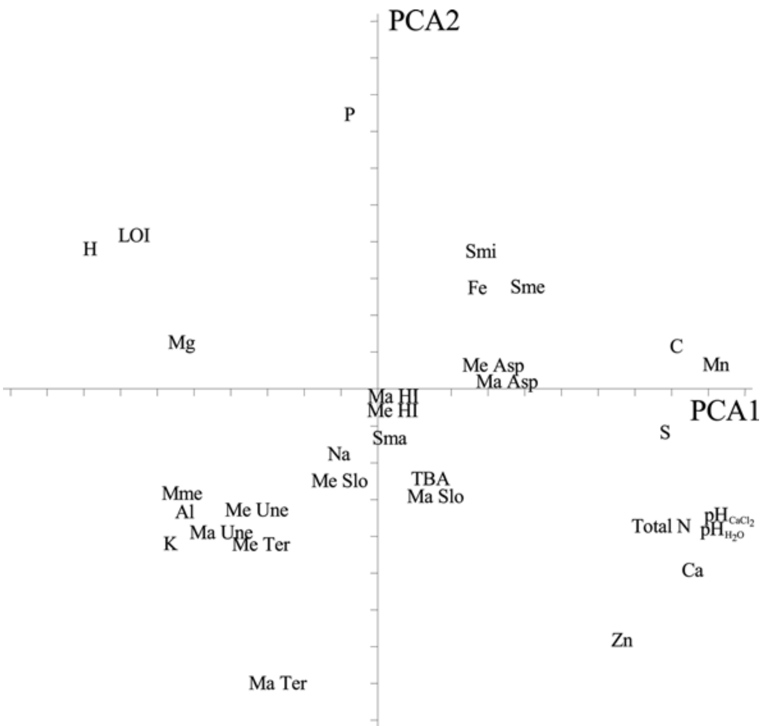

Fig. 321. Dividalen: PCA ordination of 31 environmental variables. Abbreviations in accordance with Table 2, axes 1 (horizontal) and 2 (vertical). Positions of variables in the ordination space give the head of variable vectors. Tickmarks indicate 0.1 units along both axes.

Table 18. Dividalen: Kendall's rank correlation coefficients τ between 31 environmental variables in the 50 meso plots (lower triangle), with significance probabilities (upper triangle). Statistically significant correlations (P<0.05) in bold face. Names of explanatory variables abbreviated in accordance with Table 2.

	1	2	3	4	5	6	7	8	9	10	11	12	13	14	15	16
01 Ma Slo	*	**0.000**	**0.000**	0.327	0.595	**0.000**	0.536	**0.003**	**0.000**	0.227	0.321	**0.022**	0.345	0.726	**0.001**	0.347
02 Ma Asp	**–0.418**	*	**0.000**	0.380	**0.000**	0.020	**0.023**	**0.000**	**0.000**	0.065	**0.001**	0.971	0.816	0.197	0.402	**0.025**
03 Ma HI	**0.595**	**–0.880**	*	0.661	**0.008**	**0.002**	**0.031**	**0.000**	**0.000**	0.215	**0.008**	0.612	0.427	0.223	0.743	0.155
04 Ma Ter	0.122	–0.114	0.054	*	**0.002**	0.262	0.077	0.648	0.719	**0.000**	**0.007**	0.051	0.262	0.317	**0.025**	0.273
05 Ma Une	–0.062	**–0.455**	**0.305**	**0.424**	*	0.879	1.000	**0.002**	0.336	**0.002**	**0.000**	0.330	0.376	1.000	**0.000**	**0.001**
05 TBA	**0.460**	**–0.258**	**0.329**	0.136	–0.017	*	0.774	0.095	**0.000**	0.261	0.567	**0.032**	0.722	0.186	0.304	0.329
07 Me Slo	–0.077	**0.294**	**–0.261**	0.251	0.000	0.035	*	0.205	0.236	0.206	0.865	**0.008**	0.790	0.801	0.886	0.475
08 Me Asp	**–0.330**	**0.759**	**–0.644**	–0.058	**–0.367**	–0.181	0.160	*	**0.000**	0.244	**0.031**	0.363	0.471	0.251	0.462	0.051
09 Me HI	**0.419**	**–0.543**	**0.568**	–0.043	0.108	**0.503**	–0.140	**–0.699**	*	0.877	0.806	0.068	0.382	0.315	0.388	0.694
10 Me Ter	0.148	–0.235	0.149	**0.497**	**0.414**	0.134	0.176	–0.146	–0.018	*	**0.000**	0.329	0.908	0.233	**0.025**	0.418
11 Me Une	0.113	**–0.380**	**0.299**	**0.352**	**0.510**	–0.064	–0.022	**–0.252**	0.027	**0.487**	*	0.692	0.154	0.219	**0.044**	0.310
12 Smi	**–0.242**	0.004	–0.053	–0.236	0.112	**–0.222**	**–0.318**	0.098	–0.184	–0.116	0.044	*	**0.002**	1.000	0.973	0.297
13 Sme	0.099	–0.025	0.082	–0.135	–0.101	–0.036	–0.032	0.077	–0.088	0.014	–0.157	**0.315**	*	0.486	0.110	0.650
14 Sma	–0.044	0.167	–0.149	0.143	0.000	–0.161	–0.036	0.146	–0.119	–0.167	–0.161	0.000	–0.084	*	0.972	0.808
15 Mme	**–0.344**	–0.090	–0.033	**0.264**	**0.549**	–0.103	0.017	–0.077	–0.085	**0.259**	**0.218**	–0.003	–0.159	–0.004	*	**0.001**
16 LOI	–0.097	**–0.241**	0.144	–0.129	**0.372**	–0.098	–0.084	–0.206	0.039	0.094	0.110	0.105	–0.045	–0.029	**0.322**	*
17 Total N	**0.217**	0.099	0.011	–0.061	**–0.323**	0.195	0.103	0.011	0.154	–0.223	**–0.322**	–0.180	0.027	0.118	**–0.277**	**–0.523**
18 pH_{H_2O}	0.009	0.049	–0.014	–0.058	–0.058	0.073	–0.070	0.060	0.026	–0.158	–0.105	0.124	0.142	–0.004	–0.140	**–0.476**
19 pH_{CaCl_2}	0.004	0.045	–0.011	–0.078	–0.056	0.058	–0.077	0.054	0.026	–0.171	–0.113	0.137	0.165	–0.004	–0.147	**–0.462**
20 H	–0.022	–0.034	0.003	0.040	0.030	–0.047	0.103	–0.057	–0.035	0.125	0.072	–0.115	–0.115	–0.020	0.113	**0.425**
21 Al	–0.107	0.191	**–0.242**	0.225	0.061	–0.012	**0.251**	0.051	–0.058	0.132	0.081	**–0.314**	**–0.360**	0.094	**0.195**	0.050
22 C	**0.285**	0.013	0.103	**–0.271**	**–0.452**	0.170	–0.165	–0.049	0.190	**–0.241**	**–0.246**	–0.019	0.186	–0.045	**–0.407**	**–0.412**
23 Ca	0.046	0.050	–0.004	0.013	–0.057	0.086	–0.031	0.026	0.070	–0.105	–0.134	0.025	0.115	0.037	–0.159	**–0.481**
24 Fe	0.158	**–0.371**	**0.346**	–0.086	0.113	0.059	**–0.256**	**–0.245**	0.187	0.029	0.061	**0.256**	**0.264**	–0.135	–0.120	0.133
25 K	–0.062	**0.222**	**–0.261**	**0.321**	0.143	0.024	**0.303**	0.128	–0.106	0.156	0.079	**–0.334**	**–0.370**	0.118	**0.247**	0.122
26 Mg	**0.213**	0.084	–0.038	0.143	–0.168	0.088	**0.265**	0.053	–0.026	0.134	0.023	**–0.283**	–0.079	0.135	–0.051	0.185
27 Mn	**0.309**	–0.149	**0.241**	–0.198	**–0.234**	0.163	**–0.284**	–0.057	0.169	–0.199	–0.132	0.184	**0.308**	–0.078	**–0.365**	**–0.393**
28 Na	**–0.395**	–0.088	–0.021	–0.033	**0.448**	**–0.229**	**–0.260**	–0.066	–0.068	–0.042	0.121	**0.278**	–0.105	–0.012	**0.474**	**0.218**
29 P	–0.034	–0.065	0.086	**–0.266**	–0.099	–0.097	–0.184	0.030	–0.065	–0.143	–0.076	0.184	0.177	–0.069	–0.100	**0.234**
30 S	0.142	–0.065	0.125	**–0.232**	–0.182	0.024	–0.217	–0.143	0.184	–0.219	–0.132	0.034	0.169	–0.045	–0.171	**–0.345**
31 Zn	–0.043	**0.229**	–0.181	0.193	–0.208	0.036	0.055	0.111	–0.024	–0.065	–0.110	–0.105	–0.077	0.086	–0.073	**–0.580**

Table 18 (continued). Dividalen: Kendall's rank correlation coefficients τ between 31 environmental variables in the 50 meso plots (lower triangle), with significance probabilities (upper triangle). Statistically significant correlations (P<0.05) in bold face. Names of explanatory variables abbreviated in accordance with Table 2.

	17	18	19	20	21	22	23	24	25	26	27	28	29	30	31
01 Ma Slo	**0.035**	0.932	0.966	0.832	0.298	**0.006**	0.654	0.125	0.548	**0.038**	**0.003**	**0.000**	0.741	0.167	0.678
02 Ma Asp	0.354	0.649	0.675	0.748	0.074	0.901	0.643	**0.001**	0.301	0.433	0.164	0.412	0.544	0.544	**0.032**
03 Ma HI	0.913	0.893	0.913	0.980	**0.017**	0.309	0.966	**0.001**	**0.010**	0.705	**0.017**	0.833	0.396	0.216	0.073
04 Ma Ter	0.607	0.621	0.509	0.734	0.056	**0.021**	0.915	0.467	**0.006**	0.225	0.093	0.778	**0.024**	**0.049**	0.101
05 Ma Une	**0.004**	0.605	0.618	0.789	0.581	**0.000**	0.605	0.310	0.200	0.130	**0.036**	**0.000**	0.373	0.101	0.061
05 TBA	0.053	0.469	0.567	0.637	0.906	0.092	0.391	0.556	0.814	0.381	0.106	**0.023**	0.337	0.814	0.724
07 Me Slo	0.380	0.554	0.513	0.380	**0.032**	0.159	0.791	**0.029**	**0.010**	**0.023**	**0.015**	**0.026**	0.116	0.063	0.639
08 Me Asp	0.914	0.572	0.609	0.591	0.628	0.641	0.802	**0.020**	0.223	0.616	0.591	0.530	0.774	0.173	0.290
09 Me HI	0.117	0.795	0.795	0.719	0.552	0.053	0.477	0.057	0.280	0.795	0.086	0.487	0.508	0.062	0.808
10 Me Ter	0.054	0.174	0.140	0.281	0.256	**0.037**	0.365	0.802	0.178	0.248	0.086	0.714	0.218	0.059	0.576
11 Me Une	**0.003**	0.331	0.297	0.506	0.451	**0.023**	0.214	0.575	0.462	0.834	0.220	0.262	0.484	0.220	0.310
12 Smi	0.072	0.220	0.173	0.253	**0.002**	0.853	0.801	**0.011**	**0.001**	**0.005**	0.067	**0.006**	0.067	0.737	0.297
13 Sme	0.788	0.155	0.098	0.246	**0.000**	0.062	0.246	**0.008**	**0.000**	0.429	**0.002**	0.290	0.075	0.089	0.439
14 Sma	0.315	0.972	0.972	0.862	0.426	0.703	0.755	0.253	0.315	0.253	0.510	0.917	0.556	0.703	0.467
15 Mme	**0.005**	0.152	0.132	0.245	**0.046**	**0.000**	0.103	0.219	**0.011**	0.598	**0.000**	**0.000**	0.304	0.080	0.457
16 LOI	**0.000**	**0.000**	**0.000**	**0.000**	0.610	**0.000**	**0.000**	0.173	0.213	0.058	**0.000**	**0.026**	**0.016**	**0.000**	**0.000**
17 Total N	*	**0.000**	**0.000**	**0.000**	0.296	**0.000**	**0.000**	0.509	0.281	0.096	**0.000**	**0.042**	**0.012**	**0.000**	**0.000**
18 pH_{H_2O}	**0.481**	*	**0.000**	**0.000**	**0.001**	**0.000**	**0.000**	0.114	**0.016**	**0.000**	**0.000**	0.245	**0.008**	**0.000**	**0.000**
19 pH_{CaCl_2}	**0.464**	**0.957**	*	**0.000**	**0.001**	**0.000**	**0.000**	0.136	**0.010**	**0.000**	**0.000**	0.228	**0.012**	**0.000**	**0.000**
20H	**–0.445**	**–0.854**	**–0.846**	*	**0.001**	**0.004**	**0.000**	0.157	0.106	**0.000**	**0.000**	0.148	**0.001**	**0.000**	**0.000**
21 Al	–0.102	**–0.332**	**–0.333**	**0.311**	*	0.051	**0.040**	**0.000**	**0.000**	**0.000**	**0.000**	0.757	**0.004**	0.134	0.587
22 C	**0.487**	**0.345**	**0.365**	**–0.285**	–0.190	*	**0.000**	0.993	**0.000**	0.184	**0.000**	**0.005**	0.266	**0.000**	**0.002**
23 Ca	**0.553**	**0.777**	**0.765**	**–0.752**	**–0.200**	**0.363**	*	0.587	0.114	**0.000**	**0.000**	0.587	**0.001**	**0.000**	**0.000**
24 Fe	–0.064	0.155	0.146	–0.138	**–0.696**	0.001	0.053	*	**0.001**	**0.001**	**0.005**	0.328	**0.005**	0.808	0.069
25 K	–0.105	**–0.237**	**–0.251**	0.158	**0.442**	**–0.484**	–0.154	**–0.334**	*	**0.001**	**0.000**	0.980	**0.000**	**0.000**	0.682
26 Mg	–0.162	**–0.548**	**–0.551**	**0.515**	**0.391**	–0.130	**–0.499**	**–0.322**	**0.339**	*	**0.001**	**0.000**	0.437	**0.006**	**0.017**
27 Mn	**0.373**	**0.525**	**0.537**	**–0.471**	**–0.481**	**0.621**	**0.435**	**0.275**	**–0.523**	**–0.336**	*	0.207	0.328	**0.000**	**0.018**
28 Na	**–0.198**	0.114	0.118	–0.141	–0.030	**–0.277**	0.053	0.096	0.002	**–0.388**	–0.123	*	0.353	0.887	0.874
29 P	**–0.244**	**–0.258**	**–0.246**	**0.316**	**–0.278**	0.109	**–0.329**	**0.272**	**–0.412**	0.076	0.096	–0.091	*	0.380	**0.000**
30 S	**0.453**	**0.458**	**0.495**	**–0.414**	–0.146	**0.636**	**0.496**	–0.024	**–0.375**	**–0.269**	**0.509**	–0.014	–0.086	*	**0.000**
31 Zn	**0.525**	**0.522**	**0.511**	**–0.528**	0.053	**0.296**	**0.623**	–0.177	0.040	**–0.233**	**0.231**	0.016	**–0.478**	**0.383**	*

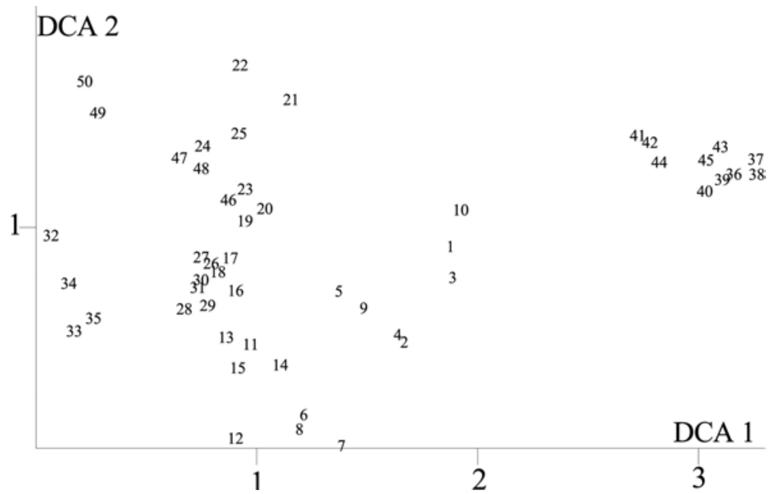

Fig. 322. Dividalen: DCA ordination diagram of 50 meso plots, axes 1 (horizontal) and 2 (vertical). Meso plot number are plotted just right of the sample plot positions. Scaling of axes in S.D. units.

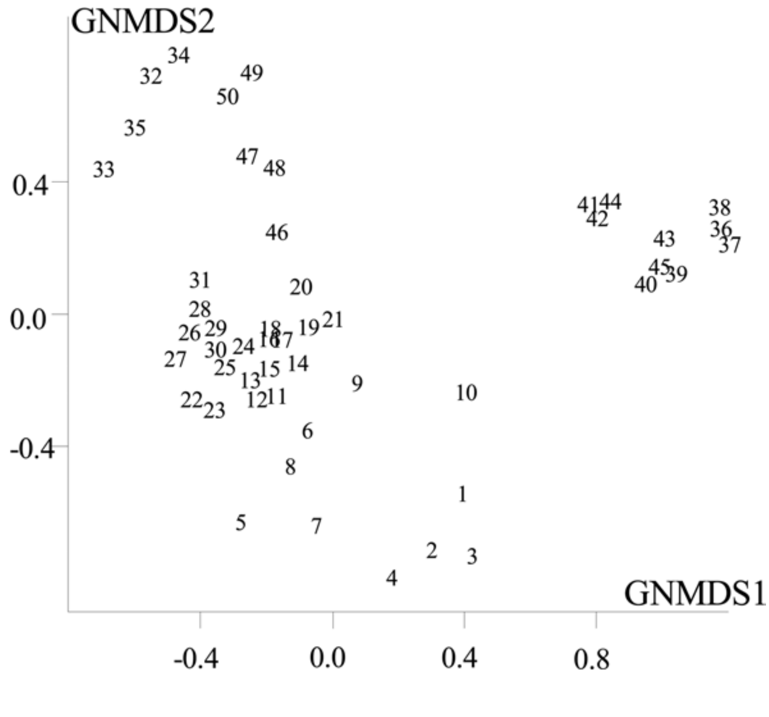

Fig. 323. Dividalen: GNMDS ordination biplot diagram of 50 meso plots (indicated by their number).

pH_{H_2O} and pH_{CaCl_2} obtained the highest loadings on PCA axis 1, together with extractable C, Ca, Mn, S and Zn and total N (Fig. 321). Low loadings were among others obtained by exchangeable H, extractable Mg and loss-on-ignition.

Extractable P obtained highest loadings on PCA axis 2 while extractable Zn and macro plot terrain form obtained low loadings.

The PCA results were thus consistent with the correlation matrix of the environmental variables (Table 18), showing that soil pH and exchangeable H had a central position in the correlation structure of the variables.

DCA ordination

The gradient length of the first two DCA axes was 3.0 and 1.8 S.D. units with eigenvalues of 0.517 and 0.119, respectively, showing that the first axis by far was the strongest gradient in species composition. The sample plots segregated into two main clusters along the first DCA axis. One cluster, consisted of 40 sample plots with DCA 1 scores < 2 S.D. units, while the other (consisting of plots in macro plots 8 and 9) formed a tight group of sample plots with DCA axis 1 scores > 2.6 S.D. units (Fig. 322). The latter cluster showed almost no variation along DCA axis 2.

GNMDS ordination

The GNMDS ordination diagram (Fig. 323) had acceptable visual similarity with the DCA diagram (Fig. 322), although some differences along the second axes were visible. The correlation between GNMDS axis 1 and DCA axis 1 was $\tau = 0.786$ and the correlation between GNMDS axis 2 and DCA axis 2 was $\tau = 0.393$.

Split-plot GLM analysis of relationships between ordination axes and environmental variables

Variation (in plot scores) along DCA axis 1 was partitioned with 96.72 % at the macro plot scale (i.e. between macro plots) and 3.28 % at the (between) meso plot scale within macro plots (Table 19). For the second ordination axis, 80.94 % of the variation was explained at the macro plot scale and 19.06 % at the meso plot scale (Table 20).

At the macro plot scale, ten environmental variables were significantly (at the $\alpha = 0.05$ level) related to DCA 1 while two variables (also at the $\alpha = 0.05$ level) were related to DCA 2. At the meso plot scale level, eleven environmental variables were significantly related to DCA 1 and seven variables were significantly related to DCA 2 (Tables 19 and 20).

At the macro plot scale, pH and soil concentrations of Total N, C, Ca, Mn, S and Zn increased significantly along DCA 1 while concentrations of H and loss-on-ignition decreased. At the meso plot scale, many of these variables showed the same tendencies. Soil concentrations of K and Mg were the only additional significant predictors (both negatively related to the axis) while loss-on-ignition, however, was not significantly related to DCA 1 on the meso plot scale.

At the macro plot scale, DCA 2 was positively related to the concentration of Zn and negatively related to P. At the meso plot scale, DCA axis 2 was significantly negatively related to loss-on-ignition and soil concentrations of H, Mg and P. Variables significantly positively related to DCA 2 at the meso plot scale were pH and soil concentrations of Ca and Zn (Table 20).

Table 19. Dividalen: Split-plot GLM analysis and Kendall's nonparametric correlation coefficient τ between DCA 1 and 31 environmental variables (predictor) in the 50 meso plots. df_{resid}: degrees of freedom for the residuals; *SS*: total variation; *FVE*: fraction of total variation attributable to a given scale (macro plot or meso plot); SS_{expl}/SS: fraction of the variation attributable to the scale in question, explained by a variable; *r*: model coefficient (only given when significant at the α = 0.05 level, otherwise blank); *F*: *F* statistic for test of the hypothesis that *r* = 0 against the two-tailed alternative. Split-plot GLM relationships significant at level α = 0.05, *P*, *F*, *r* and SS_{expl}/SS, and Kendall's non-parametric correlation coefficient $|\tau| \geq 0.30$ are given in bold face. Numbers and abbreviations for names of environmental variables are in accordance with Tab. 2.

Predictor	Dependent variable = DCA 1 (*SS* = 44.0948)								Correlation between predictor and DCA 1
	Error level								
	Macro plot df_{resid} = 8 $SS_{macro\ plot}$ = 42.6490 *FVE* = 0.9672 of *SS*				Meso plot within macro plot df_{resid} = 39 $SS_{meso\ plot}$ = 1.44584 *FVE* = 0.0328 of *SS*				Total
	$SS_{expl}/SS_{macro\ plot}$	*r*	*F*	*P*	$SS_{expl}/SS_{meso\ plot}$	*r*	*F*	*P*	τ
Ma Slo	0.1295		1.1895	0.3072	*	*	*	*	0.069
Ma Asp	0.0001		0.0008	0.9786	0.0018		0.0690	0.7942	–0.090
Ma HI	0.0469		0.3939	0.5477	0.0018		0.0690	0.7942	0.135
Ma Ter	0.0089		0.0721	0.7951	*	*	*	*	–0.150
Ma Une	0.0754		0.6527	0.4425	0.0000		0.0003	0.9863	–0.010
TBA	0.0849		0.7426	0.4139	0.0054		0.2134	0.6467	–0.251
Me Slo	0.1423		1.3274	0.2825	0.0007		0.0281	0.8677	0.024
Me Asp	0.0010		0.0079	0.9313	0.0244		0.9760	0.3293	–0.036
Me HI	0.0376		0.3128	0.5913	0.0003		0.0102	0.9200	0.088
Me Ter	0.0426		0.3561	0.5672	0.0048		0.1876	0.6673	–0.134
Me Une	0.0453		0.3791	0.5552	0.0084		0.3323	0.5676	–0.034
Smi	0.0009		0.0071	0.9349	0.0468		1.9147	0.1743	0.186
Sme	0.1517		1.4303	0.2660	0.0157		0.6203	0.4357	0.194
Sma	0.0849		0.7426	0.4139	0.0871		3.7209	0.0610	–0.061
Mme	0.2193		2.2471	0.1722	0.0255		1.0199	0.3188	–0.120
LOI	**0.5221**	**–2.3527**	**8.7413**	**0.0182**	0.0348		1.4043	0.2432	**–0.334**
Total N	**0.6667**	**3.5942**	**16.005**	**0.0039**	**0.1473**	**0.6576**	**6.7371**	**0.0132**	**0.363**
pH_{H_2O}	**0.6429**	**2.7107**	**14.406**	**0.0053**	**0.2272**	**0.8335**	**11.469**	**0.0016**	**0.618**
pH_{CaCl_2}	**0.6549**	**2.6664**	**15.183**	**0.0045**	**0.2447**	**0.8509**	**12.638**	**0.0010**	**0.637**
H	**0.6298**	**–2.9630**	**13.608**	**0.0061**	**0.1854**	**–0.7888**	**8.8745**	**0.0049**	**–0.621**
Al	0.0863		0.7556	0.4100	0.0196		0.7803	0.3825	–0.252
C	**0.6245**	**3.3661**	**13.305**	**0.0065**	**0.1354**	**0.5572**	**6.1087**	**0.0179**	**0.429**
Ca	**0.7473**	**3.0154**	**23.6600**	**0.0012**	**0.3507**	**1.1397**	**21.0680**	**0.0000**	**0.680**
Fe	0.0006		0.0048	0.9465	0.0137		0.5416	0.4662	0.076
K	0.2229		2.2947	0.1683	**0.1044**	**–0.4686**	**4.5447**	**0.0394**	–0.298
Mg	0.2640		2.8692	0.1287	**0.2134**	**–0.9498**	**10.5780**	**0.0024**	**–0.535**
Mn	**0.6089**	**2.4474**	**12.4550**	**0.0077**	**0.1777**	**0.5649**	**8.4292**	**0.0060**	**0.533**
Na	0.0075		0.0604	0.8120	0.0001		0.0045	0.9468	0.102
P	0.1350		1.2481	0.2963	0.0678		2.8382	0.1000	–0.159
S	**0.8128**	**5.0199**	**34.7330**	**0.0004**	**0.2289**	**0.6457**	**11.5760**	**0.0016**	**0.554**
Zn	**0.5117**	**2.2557**	**8.3818**	**0.0200**	**0.2877**	**0.9038**	**15.7530**	**0.0003**	**0.424**

Table 20. Dividalen: Split-plot GLM analysis and Kendall's nonparametric correlation coefficient τ between DCA 2 and 31 environmental variables (predictor) in the 50 meso plots. df_{resid}: degrees of freedom for the residuals; *SS*: total variation; *FVE*: fraction of total variation attributable to a given scale (macro plot or meso plot); SS_{expl}/SS: fraction of the variation attributable to the scale in question, explained by a variable; *r*: model coefficient (only given when significant at the $\alpha = 0.05$ level, otherwise blank); *F*: *F* statistic for test of the hypothesis that $r = 0$ against the two-tailed alternative. Split-plot GLM relationships significant at level $\alpha = 0.05$, *P*, *F*, *r* and SS_{expl}/SS, and Kendall's nonparametric correlation coefficient $|\tau| \geq 0.30$ are given in bold face. Numbers and abbreviations for names of environmental variables are in accordance with Tab. 2.

Predictor	Dependent variable = DCA 2 (SS = 9.3501)								Correlation between predictor and DCA 2
	Error level								
	Macro plot df_{resid} = 8 $SS_{macro\ plot}$ = 7.5677 FVE =0.8094 of SS				Meso plot within macro plot df_{resid} = 39 $SS_{meso\ plot}$ = 1.78235 FVE = 0.1906 of SS				Total
	SS_{expl}/ $SS_{macro\ plot}$	*r*	*F*	*P*	SS_{expl}/ $SS_{meso\ plot}$	*r*	*F*	*P*	τ
Ma Slo	0.0106		0.0857	0.7771	*	*	*	*	–0.010
Ma Asp	0.1484		1.3944	0.2716	0.0055		0.2169	0.6440	0.254
Ma HI	0.2026		2.0330	0.1917	0.0055		0.2169	0.6440	–0.275
Ma Ter	0.0812		0.7073	0.4248	*	*	*	*	0.200
Ma Une	0.0402		0.3353	0.5785	0.0171		0.6796	0.4147	–0.121
TBA	0.1528		1.4430	0.2640	0.0000		0.0001	0.9908	0.241
Me slo	0.0002		0.0015	0.9704	0.0189		0.7528	0.3909	0.031
Me Asp	0.0468		0.3925	0.5484	0.0115		0.4546	0.5041	0.104
Me HI	0.0516		0.4357	0.5278	0.0053		0.2059	0.6525	–0.081
Me Ter	0.0102		0.0825	0.7813	0.0217		0.8650	0.3581	0.112
Me Une	0.0524		0.4425	0.5246	0.0818		3.4758	0.0698	–0.057
Smi	0.2173		2.2209	0.1745	0.0006		0.0249	0.8753	–0.229
Sme	0.1090		0.9790	0.3514	0.0073		0.2864	0.5956	–0.127
Sma	0.1528		1.4430	0.2640	0.0447		1.8270	0.1843	0.045
Mme	0.0011		0.0085	0.9287	0.0397		1.6127	0.2116	–0.048
LOI	0.2681		2.9302	0.1253	**0.2251**	**–0.6875**	**11.3300**	**0.0017**	**–0.314**
Total N	0.3507		4.3204	0.0713	0.0035		0.1355	0.7148	0.301
pH_{H_2O}	0.1560		1.4786	0.2587	**0.1222**	**0.6787**	**5.4304**	**0.0251**	**0.260**
pH_{CaCl_2}	0.1263		1.1564	0.3136	0.0904		3.8740	0.0562	0.247
H	0.1944		1.9300	0.2022	**0.1210**	**–0.7075**	**5.3666**	**0.0259**	**–0.304**
Al	0.1634		1.5631	0.2465	0.0252		1.0093	0.3213	0.224
C	0.0012		0.0095	0.9247	0.0336		1.3571	0.2511	0.027
Ca	0.2636		2.8641	0.1290	**0.1637**	**0.8646**	**7.6354**	**0.0087**	**0.331**
Fe	0.3111		3.6119	0.0939	0.0047		0.1843	0.6700	–0.296
K	0.3092		3.5802	0.0951	0.0547		2.2555	0.1412	0.297
Mg	0.0019		0.0155	0.9040	**0.2114**	**–1.0498**	**10.4550**	**0.0025**	**–0.032**
Mn	0.0088		0.0711	0.7965	0.0048		0.1868	0.6680	–0.048
Na	0.0002		0.0014	0.9712	0.0224		0.8919	0.3508	–0.051
P	**0.7898**	**–1.6488**	**30.0590**	**0.0006**	**0.3768**	**–0.9903**	**23.5800**	**0.0000**	**–0.607**
S	0.0856		0.7485	0.4121	0.0005		0.0181	0.8937	0.153
Zn	**0.6320**	**1.0560**	**13.7390**	**0.0060**	**0.1190**	**0.6455**	**5.2697**	**0.0272**	**0.509**

Correlations between DCA ordination axes and environmental variables

Eleven out of the 31 measured environmental variables were correlated with either DCA axis 1, DCA axis 2 or both at the $|\tau| > 0.300$ level (Table 19 and 20). Exctractable Ca ($\tau = 0.680$, Fig. 329), pH [pH ($CaCl_2$) ($\tau = 0.637$, Fig. 326)] and exchangeable H ($\tau = -0.621$, Fig. 327), S ($\tau = 0.554$, Fig. 333), Mg ($\tau = -0.535$, Fig. 330) and Mn ($\tau = 0.533$, Fig. 331) were the variables best correlated with DCA axis 1. The variables that were best correlated with DCA axis 2 were extractable P ($\tau = -0.607$, Fig. 332) and Zn ($\tau = -0.509$, Fig. 334).

Dividalen was the only reference area in which the macro plots were distributed along an altitudinal gradient. Thus correlation coefficients were also calculated between DCA scores and the altitude of each sample plot. Altitude was highly significantly correlated with DCA axis 2 ($\tau = 0.563$).

Frequent species

A total of 141 species was found within the fifty 1×1 m meso plots in the Dividalen reference area: 74 vascular plants, 24 mosses, 18 liverworts and 25 lichens. The most frequent species (the sum of subplot frequencies in brackets) were: *Avenella flexuosa* (755 out of 800), *Vaccinium myrtillus* (602), *Vaccinium vitis-idaea* (519), *Barbilophozia lycopodioides* (496), *Chamaepericlymenum suecicum* (474), *Linnaea borealis* (398), *Anthoxanthum odoratum* (356) and *Pleurozium schreberi* (320).

The distribution of species abundance in the DCA ordination

Out of total 141 recorded species, 71 occurred in five or more of the fifty sample plots. *Vaccinium myrtillus* (Fig. 341), *Vaccinium vitis-idaea* (Fig. 343), *Avenella flexuosa* (Fig. 374) and *Barbilophozia lycopodioides* (Fig. 391) had wide ecological amplitudes along both DCA axes, and they were also highly abundant in most of the sample plots.

Species that occurred mostly on the right side of the diagram and thus had preferences for sites with relatively high values of soil pH, Ca, Mg and S were *Salix phylicifolia* (Fig. 338), *Alchemilla glabra* (Fig. 344), *Cerastium fontanum* (Fig. 345), *Myosotis decumbens* (Fig. 356), *Omalotheca norvegica* (Fig. 357), *Rumex acetosa* (Fig. 363), *Saussurea alpina* (Fig. 364), *Trollius europaeus* (Fig. 368), *Poa alpina* (Fig. 377) and *Mnium spinosum* (Fig. 383).

Species that were restricted to plots with low DCA axis 1 scores, i.e. sites poorer in soil nutrients, e.g. lower pH and lower concentrations of Ca, Mg, Mg and S, were *Betula nana* (Fig. 335), *Pedicularis lapponica* (Fig. 359), *Dicranum scoparium* (Fig. 381), *Cladonia arbuscula* (Fig. 394), *Cladonia bellidiflora* (Fig. 395), *Cladonia chlorophaea* (Fig. 396), *Cladonia ecmocyna* (Fig. 398), *Cladonia furcata* (Fig 399), *Cladonia rangiferina* (Fig. 401), *Cladonia sulphurina* (Fig. 402) and *Peltigera aphthosa* (Fig. 405).

Some species also showed distinct patterns along the second DCA axis, related to differences in altitude ($\tau = 0.563$) and soil extractable P (Table 20). Species with preference for higher altitudes and lower amounts of P (plots with high DCA axis 2 scores) were *Phyllodoce caerulea* (Fig. 340), partly also *Equisetum sylvaticum* (Fig. 347), *Pedicularis lapponica* (Fig. 359), *Calamagrostis lapponica* (Fig. 371) and *Nephroma arcticum* (Fig. 404). Examples of species that preferred sites at lower altitudes with higher soil contents of extractable P and Zn were *Gymnocarpium dryopteris* (Fig. 350), *Melampyrum sylvaticum* (Fig. 354), *Orthilia secunda* (Fig. 358), *Luzula pilosa* (Fig. 376) and *Brachythecium salebrosum* (Fig. 379).

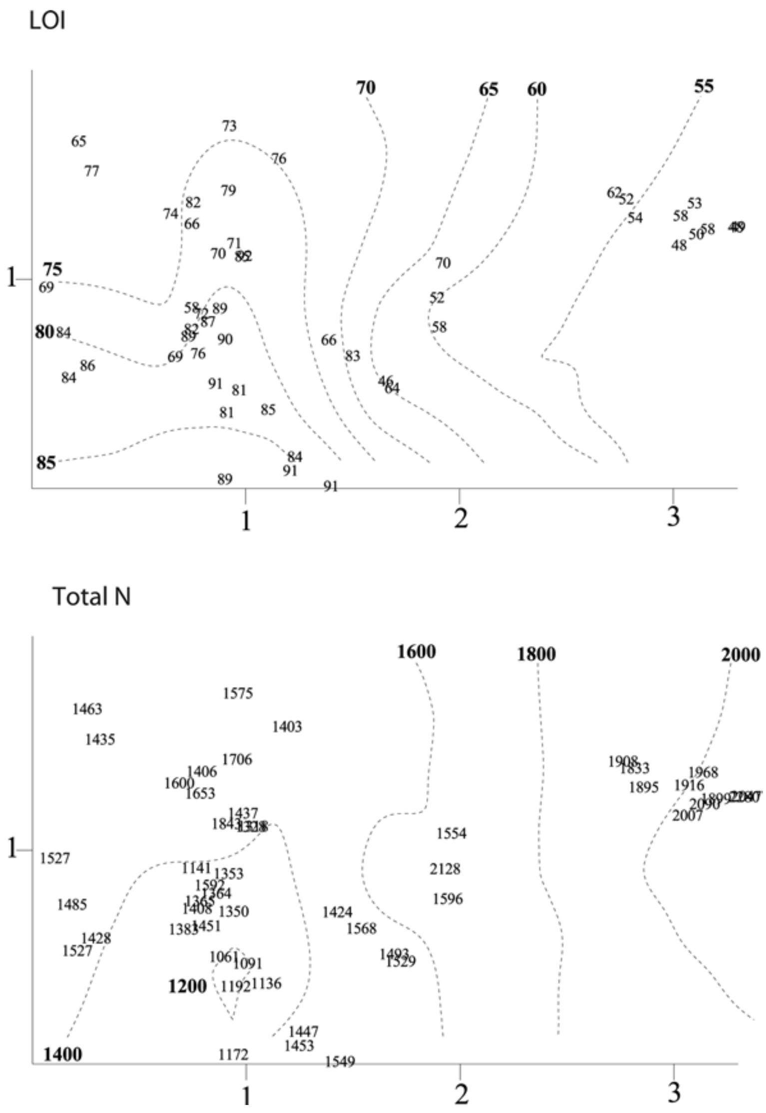

Figs 324-325. Dividalen: isolines for environmental variables in the DCA ordinations of 50 meso plots, axes 1 (horizontal) and 2 (vertical). Values for the environmental variables are plotted onto the meso plots' positions. Scaling in S.D. units. Fig. 324. LOI ($R^2 = 0.629$). Fig. 325. Total N ($R^2 = 0.630$). R^2 refers to the coefficient of determination between original and smoothened values as interpolated from the isolines. Names of environmental variables in accordance with Table 2.

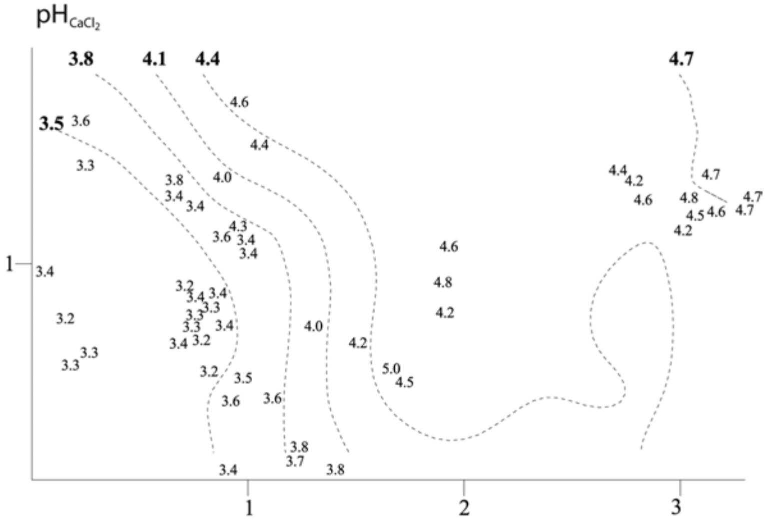

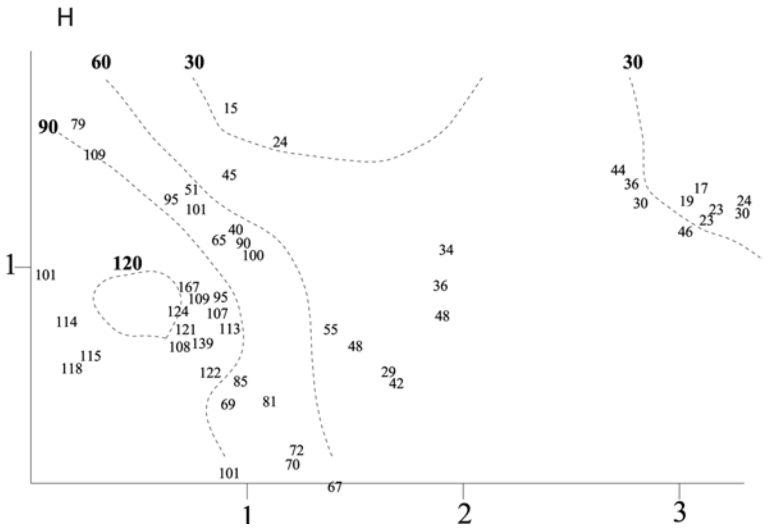

Figs 326-327. Dividalen: isolines for environmental variables in the DCA ordinations of 50 meso plots, axes 1 (horizontal) and 2 (vertical). Values for the environmental variables are plotted onto the meso plots' positions. Scaling in S.D. units. Fig. 326. pH_{CaCl_2} ($R^2 = 0.889$). Fig. 327. H ($R^2 = 0.899$). R^2 refers to the coefficient of determination between original and smoothened values as interpolated from the isolines. Names of environmental variables in accordance with Table 2.

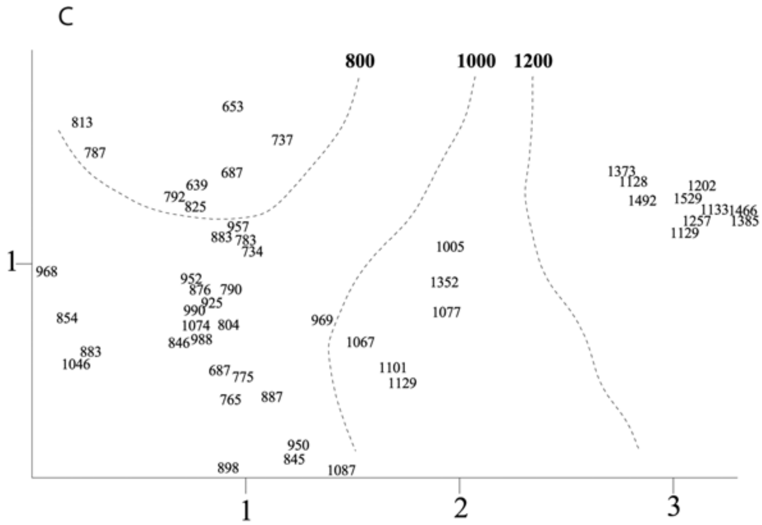

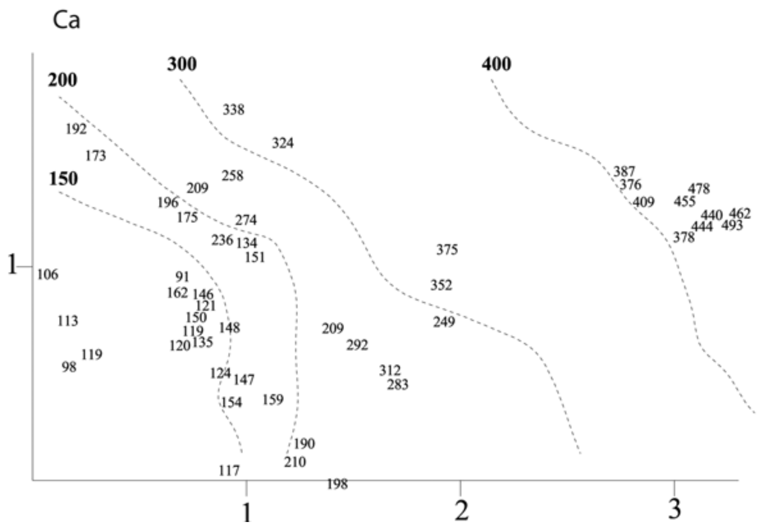

Figs 328-329. Dividalen: isolines for environmental variables in the DCA ordinations of 50 meso plots, axes 1 (horizontal) and 2 (vertical). Values for the environmental variables are plotted onto the meso plots' positions. Scaling in S.D. units. Fig. 328. C ($R2 = 0.832$). Fig. 329. Ca ($R2 = 0.895$). R2 refers to the coefficient of determination between original and smoothened values as interpolated from the isolines. Names of environmental variables in accordance with Table 2.

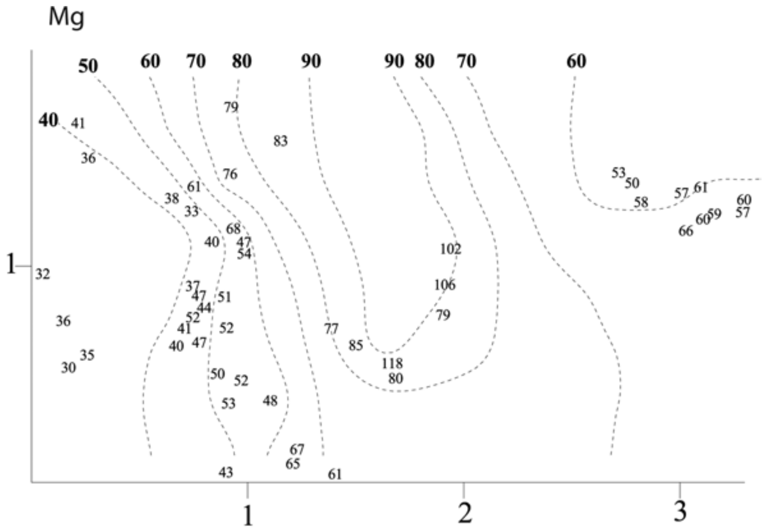

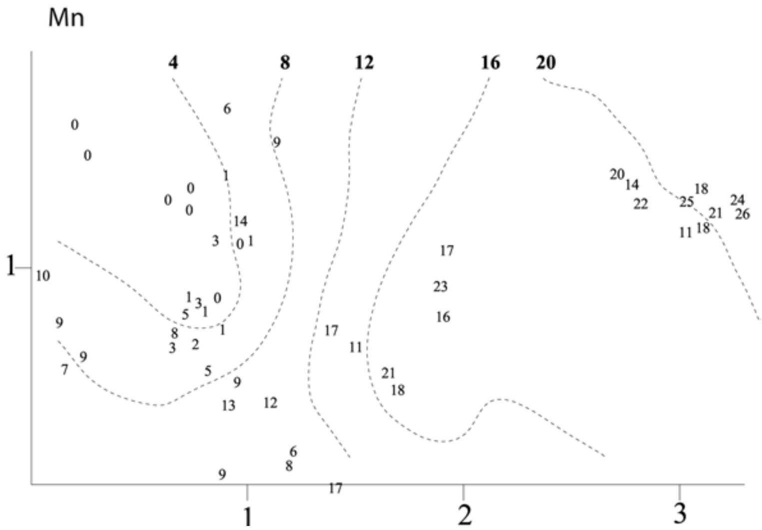

Figs 330-331. Dividalen: isolines for environmental variables in the DCA ordinations of 50 meso plots, axes 1 (horizontal) and 2 (vertical). Values for the environmental variables are plotted onto the meso plots' positions. Scaling in S.D. units. Fig. 330. Mg ($R^2 = 0.821$). Fig. 331. Mn ($R^2 = 0.859$). R^2 refers to the coefficient of determination between original and smoothened values as interpolated from the isolines. Names of environmental variables in accordance with Table 2.

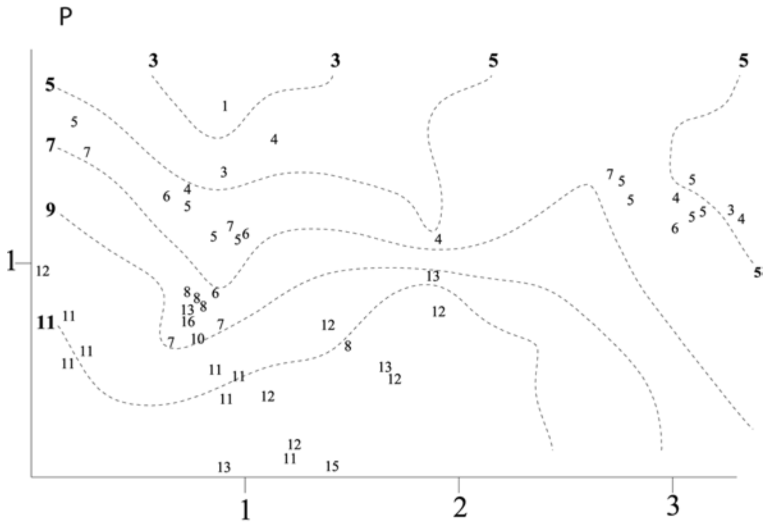

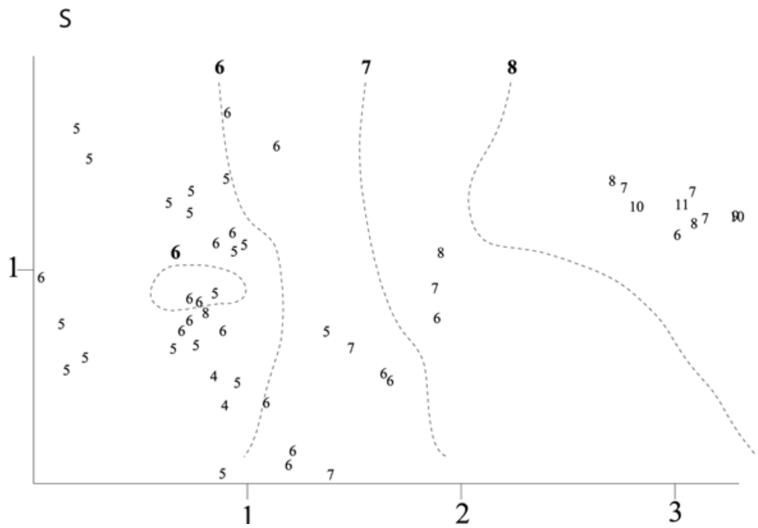

Figs 332-333. Dividalen: isolines for environmental variables in the DCA ordinations of 50 meso plots, axes 1 (horizontal) and 2 (vertical). Values for the environmental variables are plotted onto the meso plots' positions. Scaling in S.D. units. Fig. 332. P (R^2 = 0.830). Fig. 333. S (R^2 = 0.726). R^2 refers to the coefficient of determination between original and smoothened values as interpolated from the isolines. Names of environmental variables in accordance with Table 2.

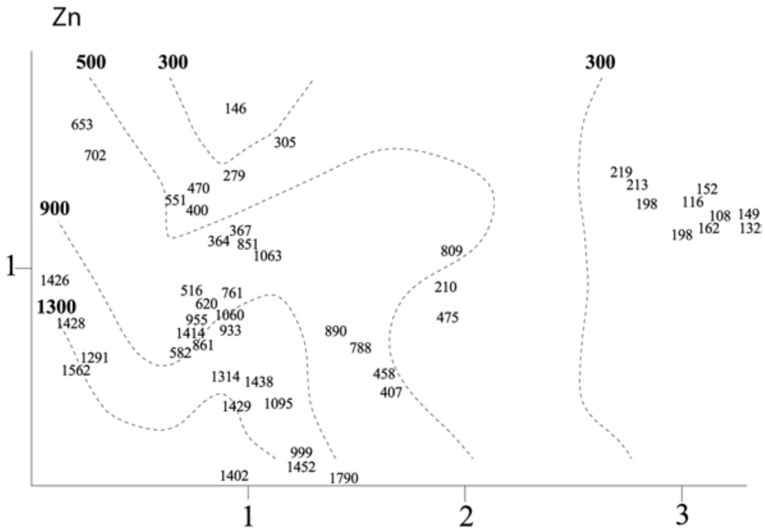

Fig. 334. Dividalen: isolines for environmental variables in the DCA ordinations of 50 meso plots, axes 1 (horizontal) and 2 (vertical). Values for the environmental variables are plotted onto the meso plots' positions. Scaling in S.D. units. Fig. 334. Zn (R^2 = 0.872). R^2 refers to the coefficient of determination between original and smoothened values as interpolated from the isolines. Names of environmental variables in accordance with Table 2.

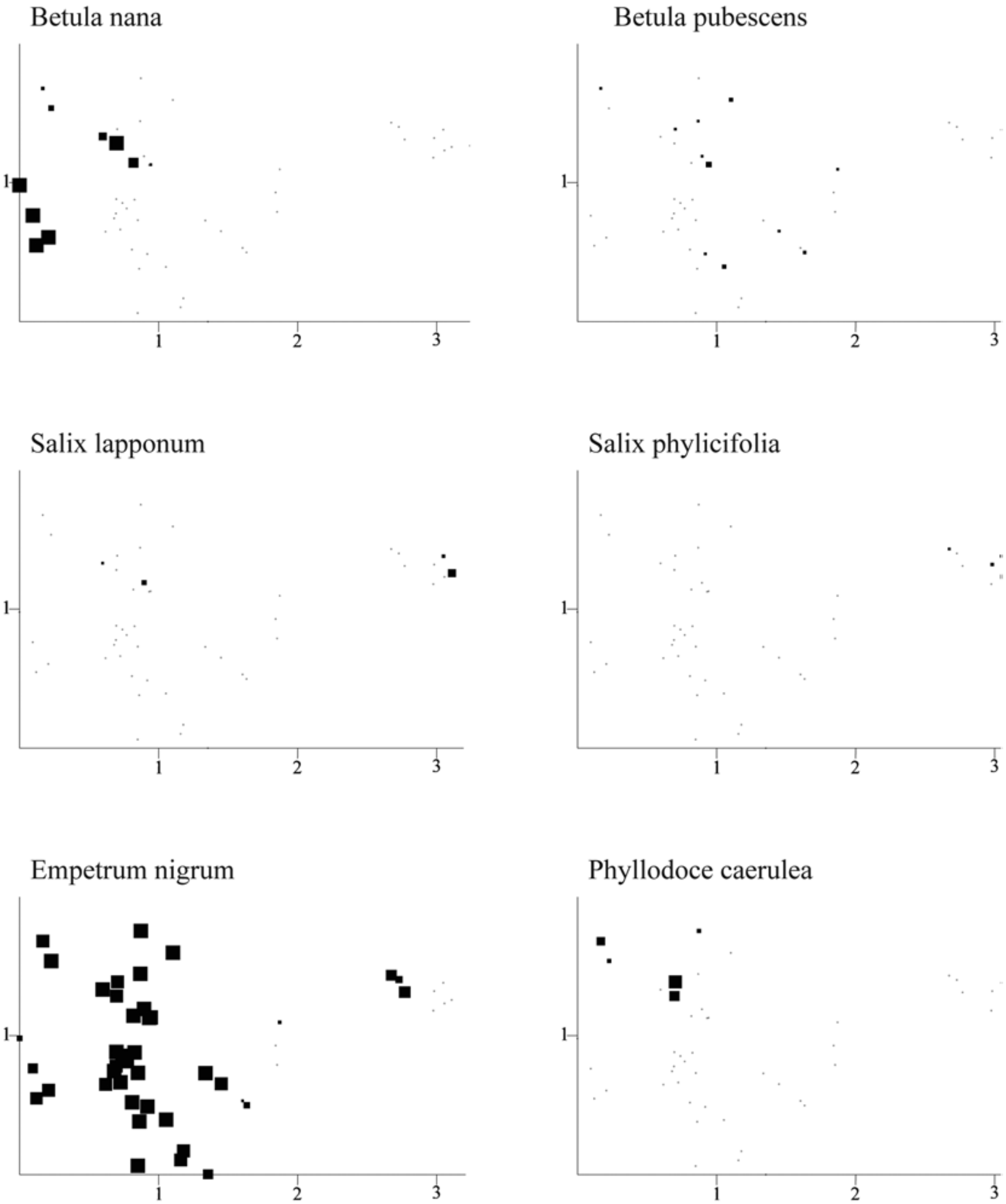

Fig. 335-340. Dividalen: distributions of species abundances in the DCA ordination of 50 meso plots, axes 1 (horizontal) and 2 (vertical). Frequency in subplots for each species in each meso plot proportional to quadrate size. Scaling in S.D. units. Fig. 335. *Betula nana*. Fig. 336. *Betula pubescens*. Fig. 337. *Salix lapponum*. Fig. 338. *Salix phylicifolia*. Fig. 339. *Empetrum nigrum*. Fig. 340. *Phyllodoce caerulea*.

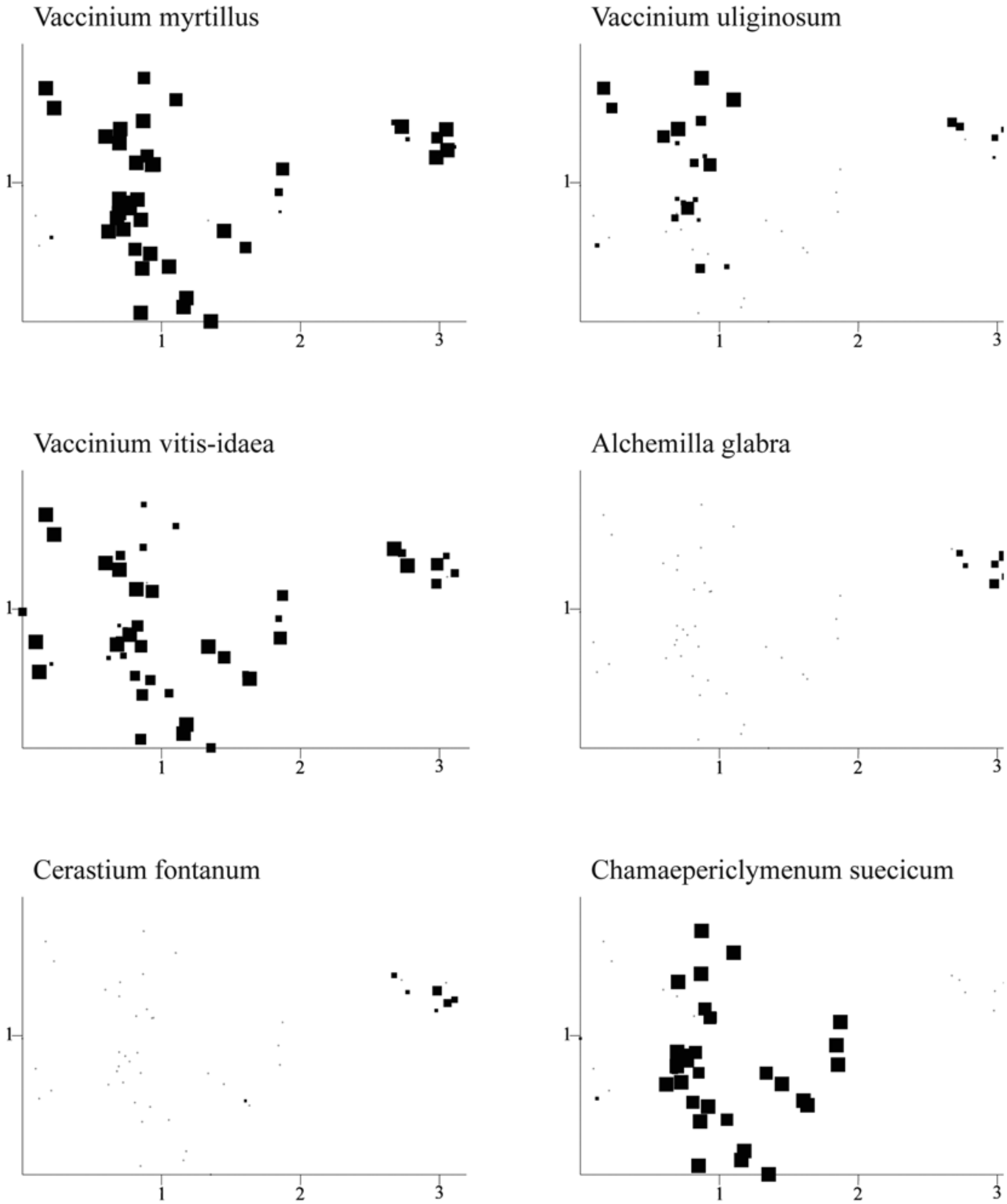

Figs 341-346. Dividalen: distributions of species abundances in the DCA ordination of 50 meso plots, axes 1 (horizontal) and 2 (vertical). Frequency in subplots for each species in each meso plot proportional to quadrate size. Scaling in S.D. units. Fig. 341. *Vaccinium myrtillus*. Fig. 342. *Vaccinium uliginosum*. Fig. 343. *Vaccinium vitis-idaea*. Fig. 344. *Alchemilla glabra*. Fig. 345. *Cerastium fontanum*. Fig. 346. *Chamaepericlymenum suecicum*.

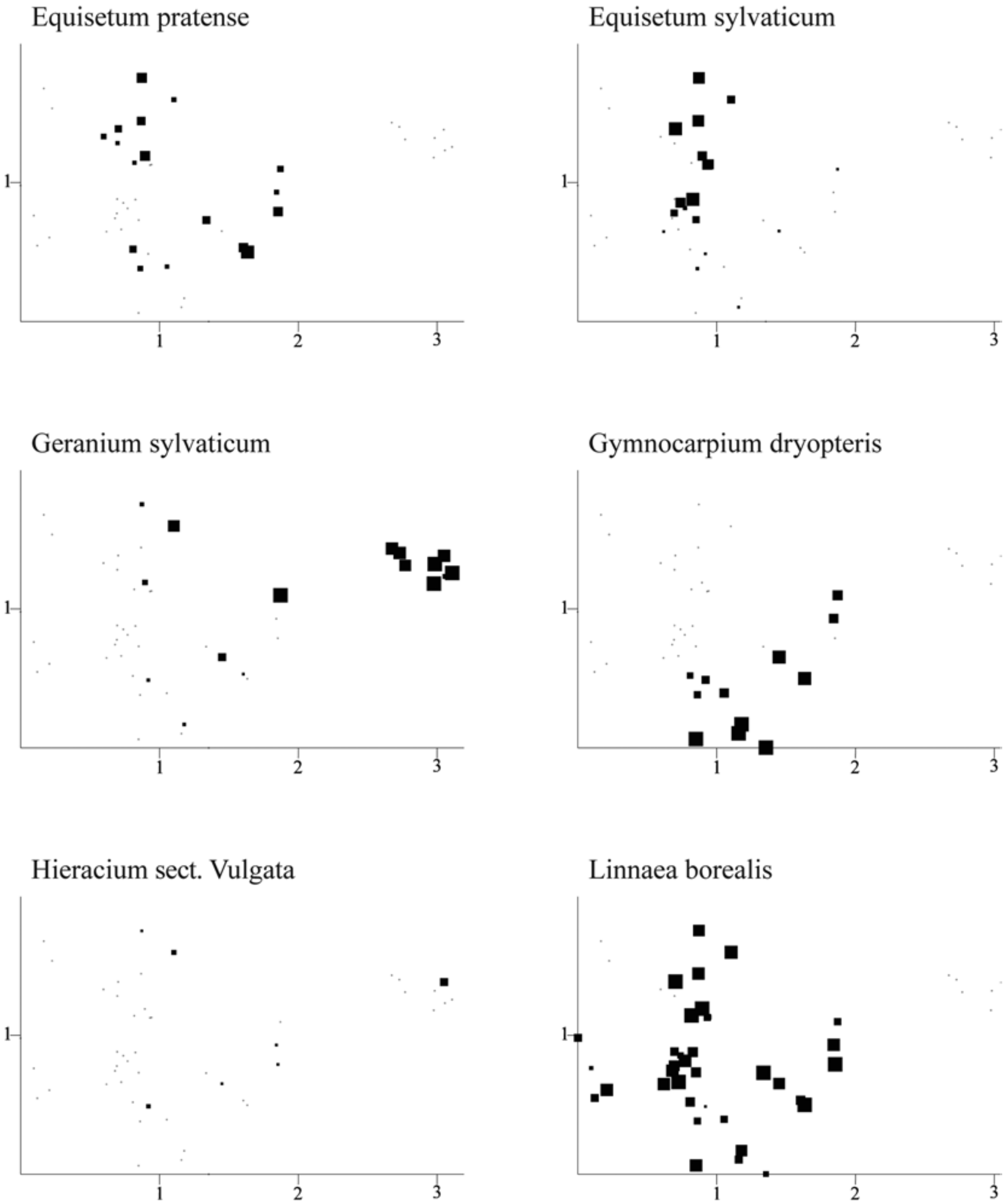

Figs 347-352. Dividalen: distributions of species abundances in the DCA ordination of 50 meso plots, axes 1 (horizontal) and 2 (vertical). Frequency in subplots for each species in each meso plot proportional to quadrate size. Scaling in S.D. units. Fig. 347. *Equisetum pratense*. Fig. 348. *Equisetum sylvaticum*. Fig. 349. *Geranium sylvaticum*. Fig. 350. *Gymnocarpium dryopteris*. Fig. 351. *Hieracium* sect. *Vulgata*. Fig. 352. *Linnaea borealis*.

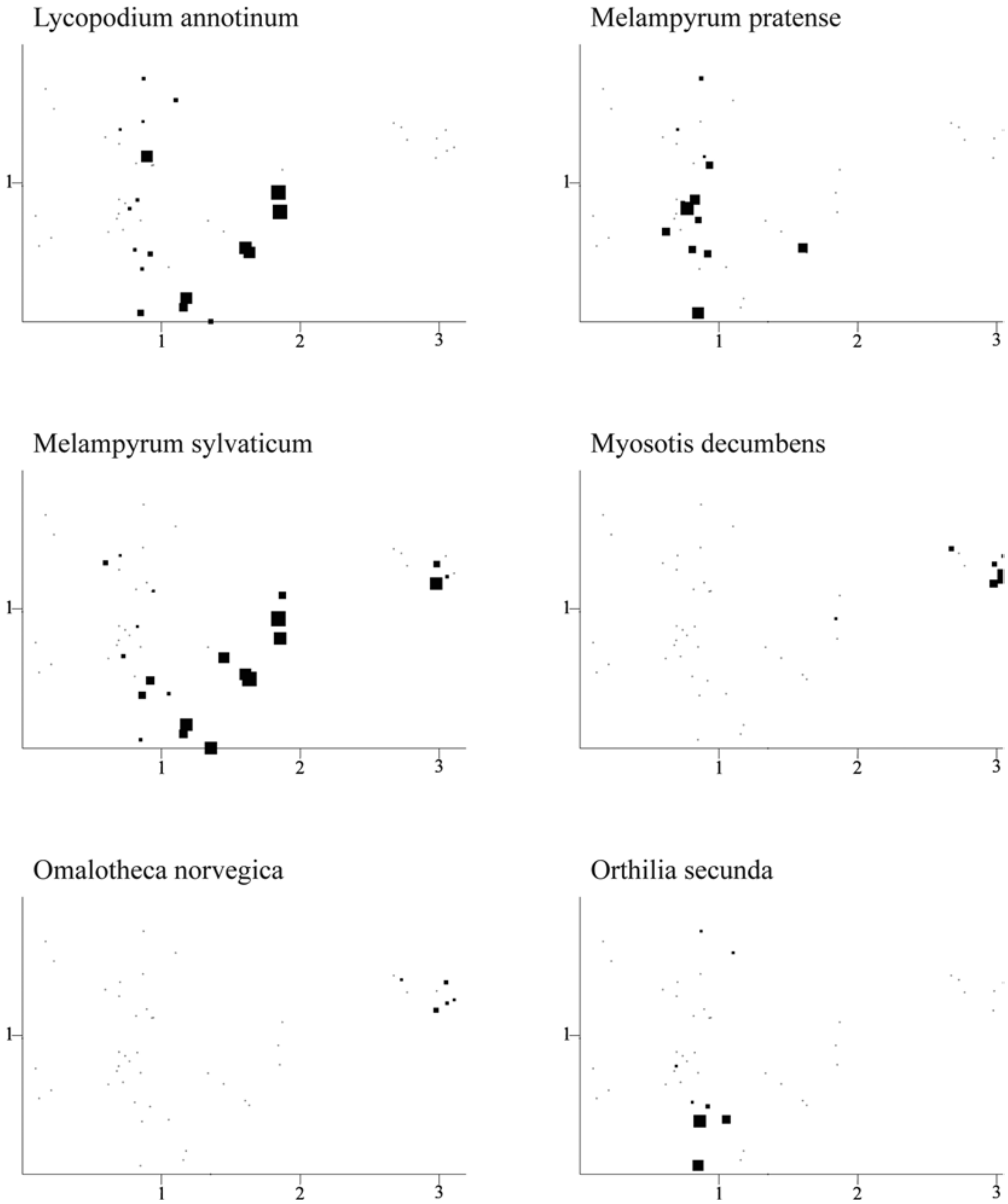

Figs 353-358. Dividalen: distributions of species abundances in the DCA ordination of 50 meso plots, axes 1 (horizontal) and 2 (vertical). Frequency in subplots for each species in each meso plot proportional to quadrate size. Scaling in S.D. units. Fig. 353. *Lycopodium annotinum*. Fig. 354. *Melampyrum pratense*. Fig. 355. *Melampyrum sylvaticum*. Fig. 356. *Myosotis decumbens*. Fig. 357. *Omalotheca norvegica*. Fig. 358. *Orthilia secunda*.

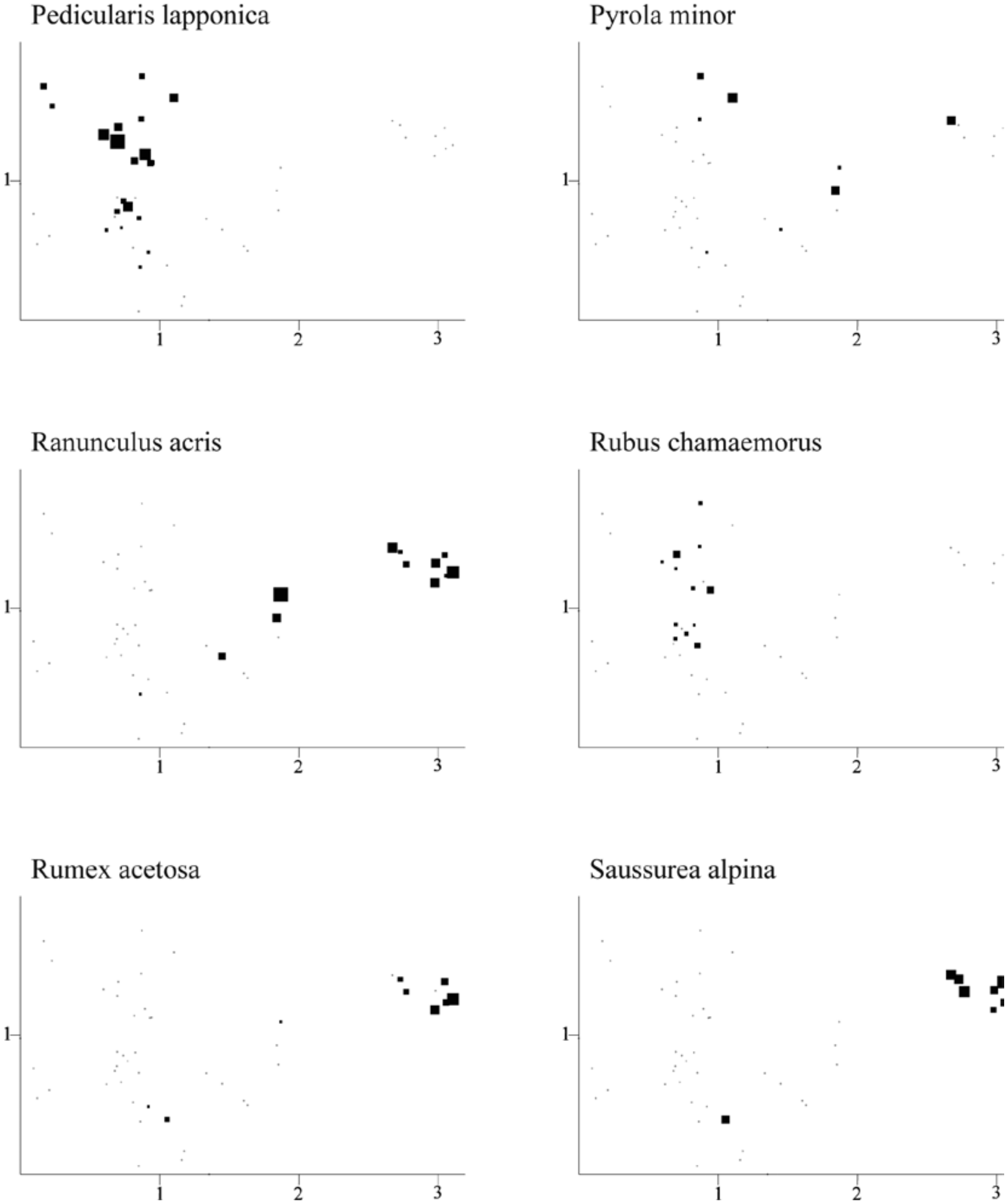

Figs 359-364. Dividalen: distributions of species abundances in the DCA ordination of 50 meso plots, axes 1 (horizontal) and 2 (vertical). Frequency in subplots for each species in each meso plot proportional to quadrate size. Scaling in S.D. units. Fig. 359. *Pedicularis lapponica.* Fig. 360. *Pyrola minor*. Fig. 361. *Ranunculus acris*. Fig. 362. *Rubus chamaemorus*. Fig. 363. *Rumex acetosa*. Fig. 364. *Saussurea alpina*.

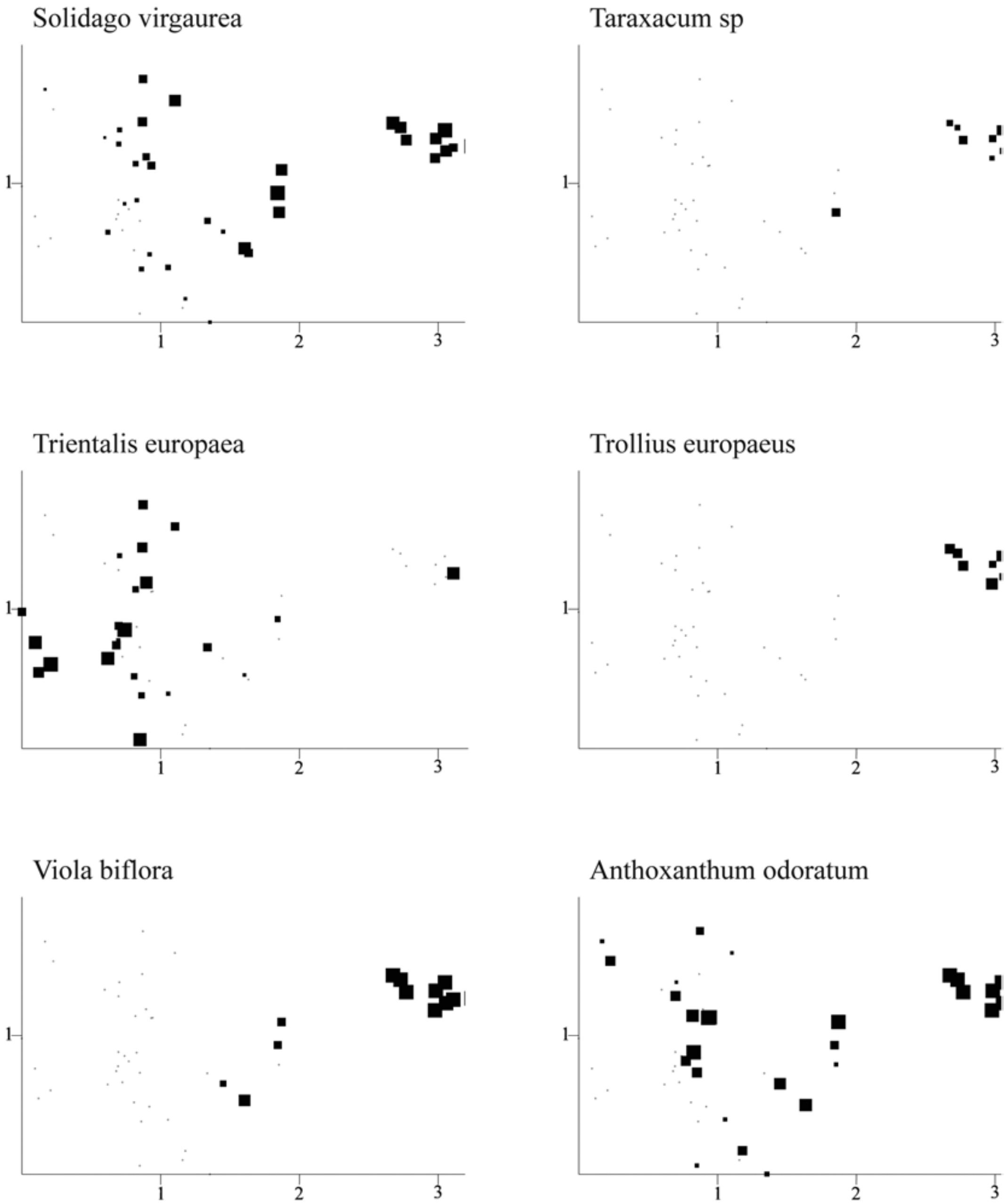

Figs 365-370. Dividalen: distributions of species abundances in the DCA ordination of 50 meso plots, axes 1 (horizontal) and 2 (vertical). Frequency in subplots for each species in each meso plot proportional to quadrate size. Scaling in S.D. units. Fig. 365. *Solidago virgaurea*. Fig. 366. *Taraxacum* sp. Fig. 367. *Trientalis europaea*. Fig. 368. *Trollius europaeus*. Fig. 369. *Viola biflora*. 370. *Anthoxanthum odoratum*.

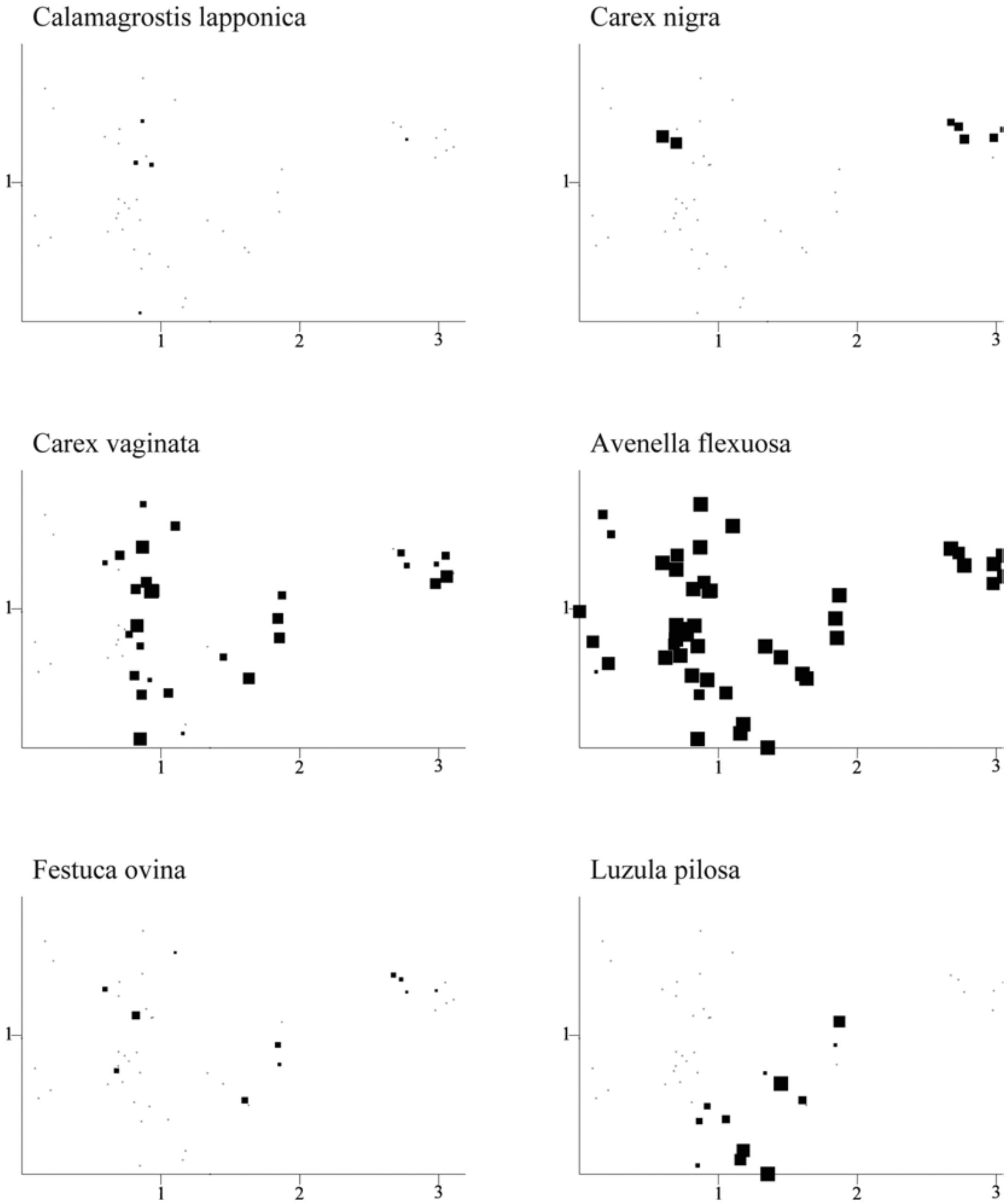

Figs 371-376. Dividalen: distributions of species abundances in the DCA ordination of 50 meso plots, axes 1 (horizontal) and 2 (vertical). Frequency in subplots for each species in each meso plot proportional to quadrate size. Scaling in S.D. units. Fig. 371. *Calamagrostis lapponica*. Fig. 372. *Carex nigra*. Fig. 373. *Carex vaginata*. Fig. 374. *Avenella flexuosa*. Fig. 375. *Festuca ovina*. Fig. 376. *Luzula pilosa*.

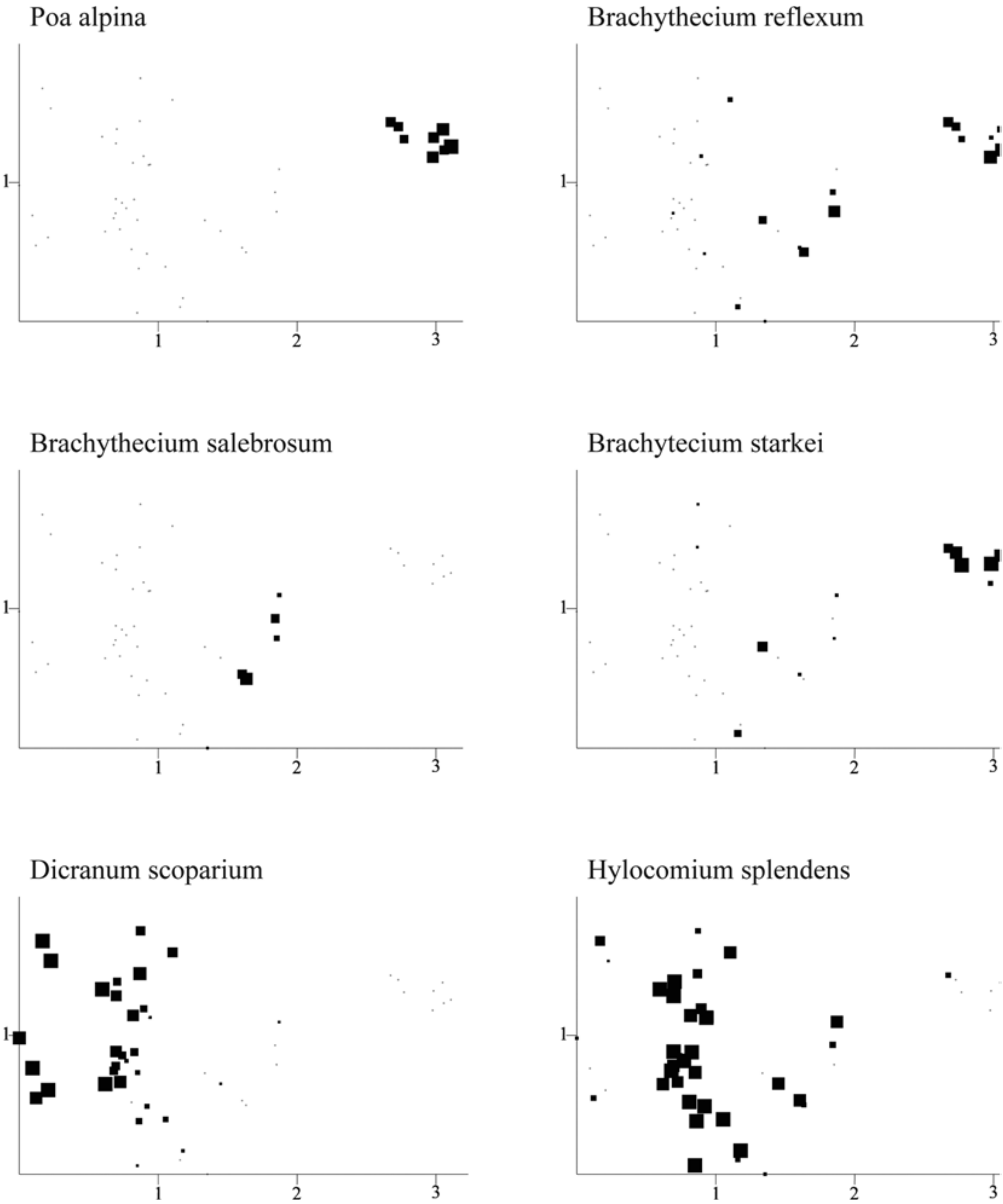

Figs 377-382. Dividalen: distributions of species abundances in the DCA ordination of 50 meso plots, axes 1 (horizontal) and 2 (vertical). Frequency in subplots for each species in each meso plot proportional to quadrate size. Scaling in S.D. units. Fig. 377. *Poa alpina*. Fig. 378. *Brachythecium reflexum*. Fig. 379. *Brachythecium salebrosum*. Fig. 380. *Brachythecium starkei*. Fig. 381. *Dicranum scoparium*. Fig. 382. *Hylocomium splendens*.

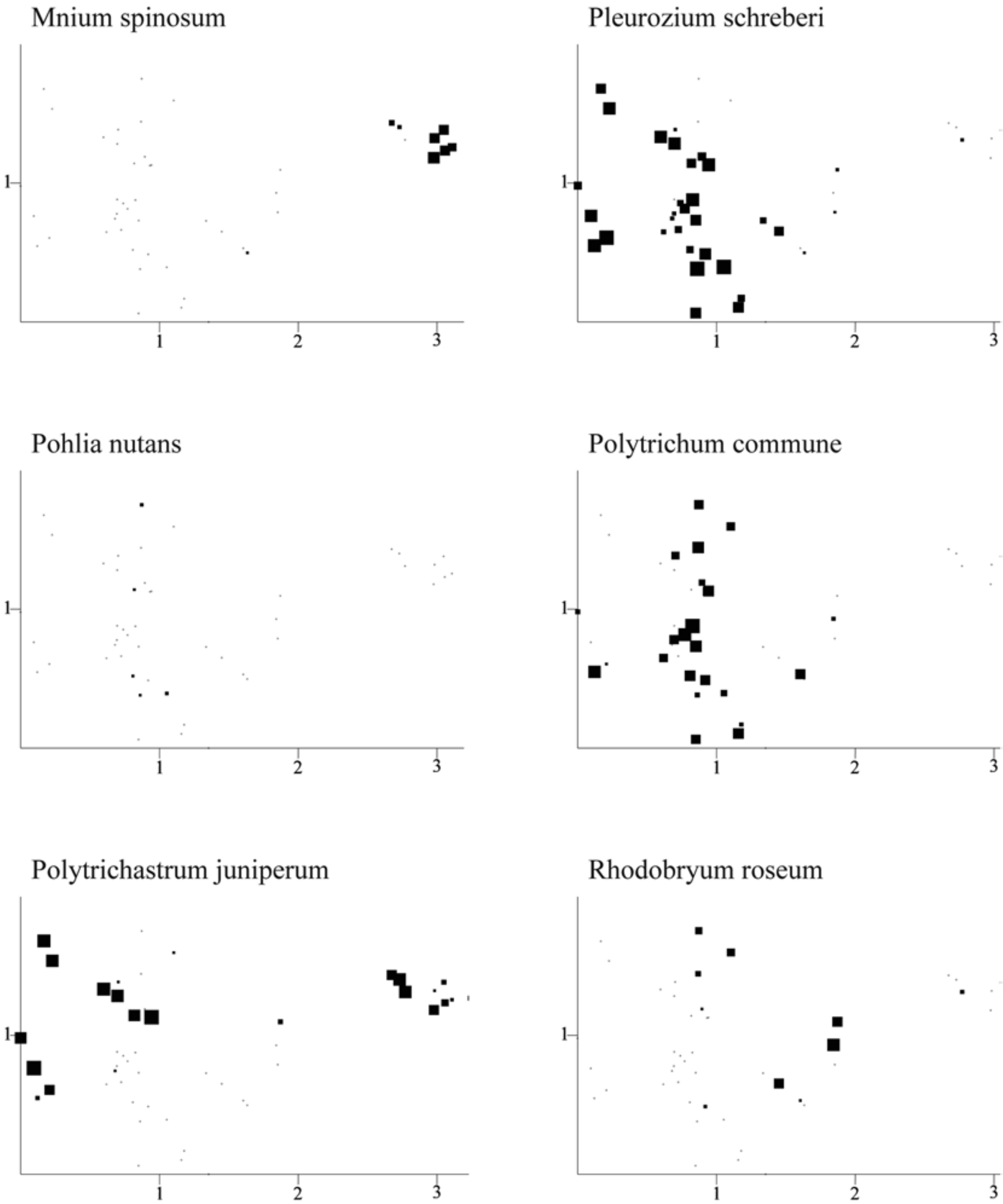

Figs 383-388. Dividalen: distributions of species abundances in the DCA ordination of 50 meso plots, axes 1 (horizontal) and 2 (vertical). Frequency in subplots for each species in each meso plot proportional to quadrate size. Scaling in S.D. units. Fig. 383. *Mnium spinosum*. Fig. 384. *Pleurozium schreberi*. Fig. 385. *Pohlia nutans*. Fig. 386. *Polytrichum commune*. Fig. 387. *Polytrichastrum juniperum*. Fig. 388. *Rhodobryum roseum*.

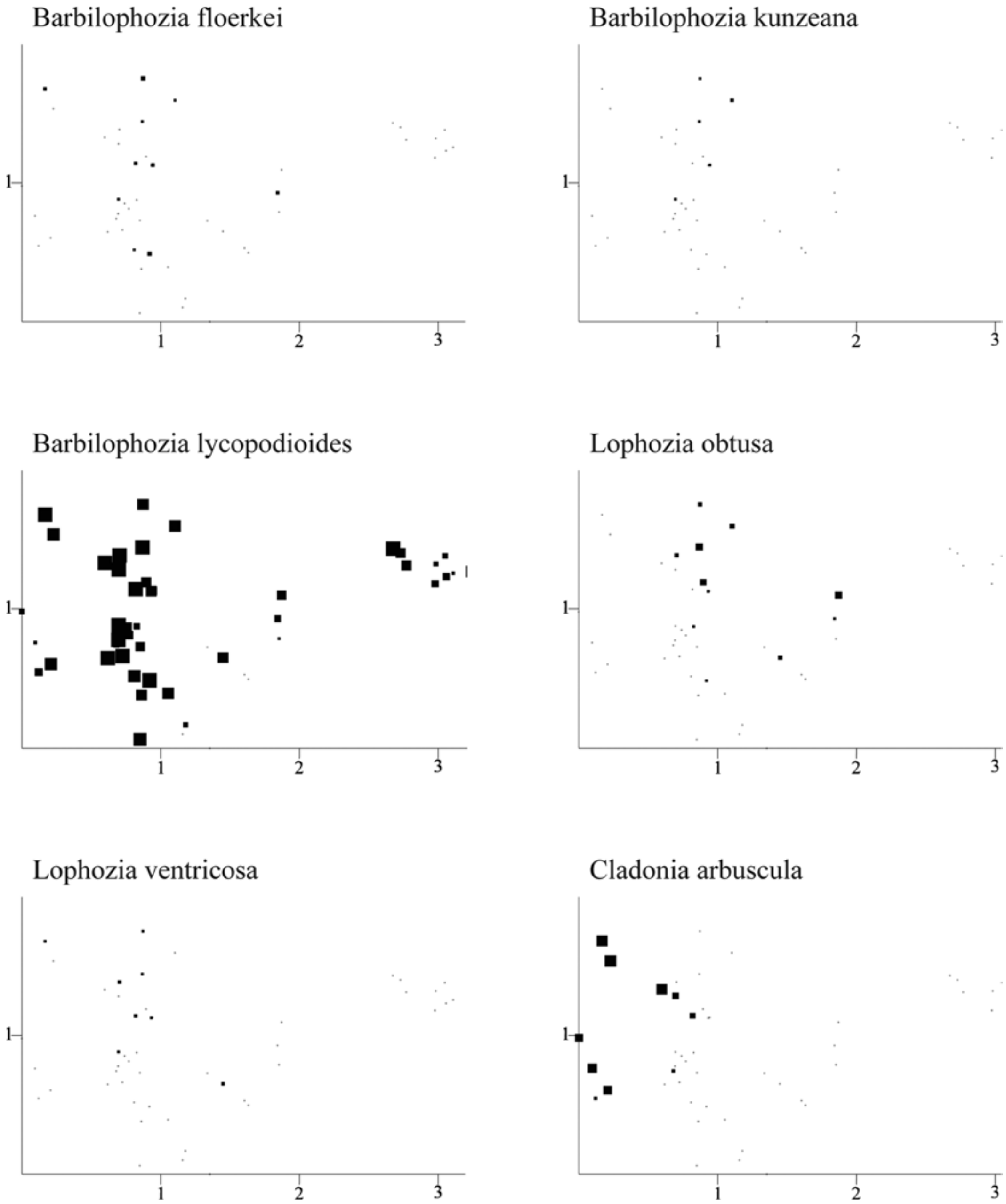

Figs 389-394. Dividalen: distributions of species abundances in the DCA ordination of 50 meso plots, axes 1 (horizontal) and 2 (vertical). Frequency in subplots for each species in each meso plot proportional to quadrate size. Scaling in S.D. units. Fig. 389. *Barbilophozia floerkei*. Fig. 390. *Barbilophozia kunzeana*. Fig. 391. *Barbilophozia lycopodioides*. Fig. 392. *Lophozia obtusa*. Fig. 393. *Lophozia ventricosa*. Fig. 394. *Cladonia arbuscula*.

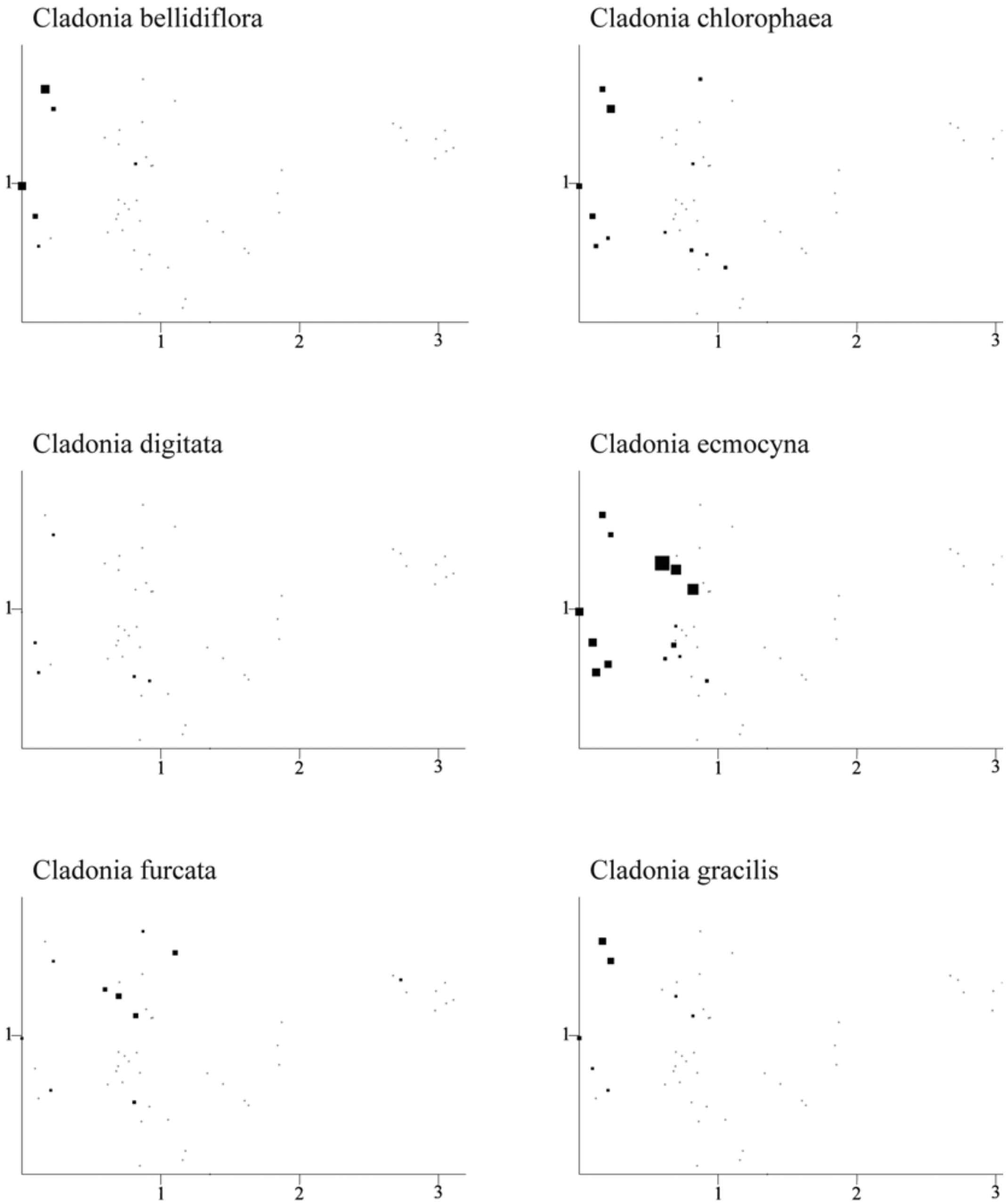

Figs 395-400. Dividalen: distributions of species abundances in the DCA ordination of 50 meso plots, axes 1 (horizontal) and 2 (vertical). Frequency in subplots for each species in each meso plot proportional to quadrate size. Scaling in S.D. units. Fig. 395. *Cladonia bellidiflora*. Fig. 396. *Cladonia chlorophaea*. Fig. 397. *Cladonia digitata*. Fig. 398. *Cladonia ecmocyna*. Fig. 399. *Cladonia furcata*. Fig. 400. *Cladonia gracilis*.

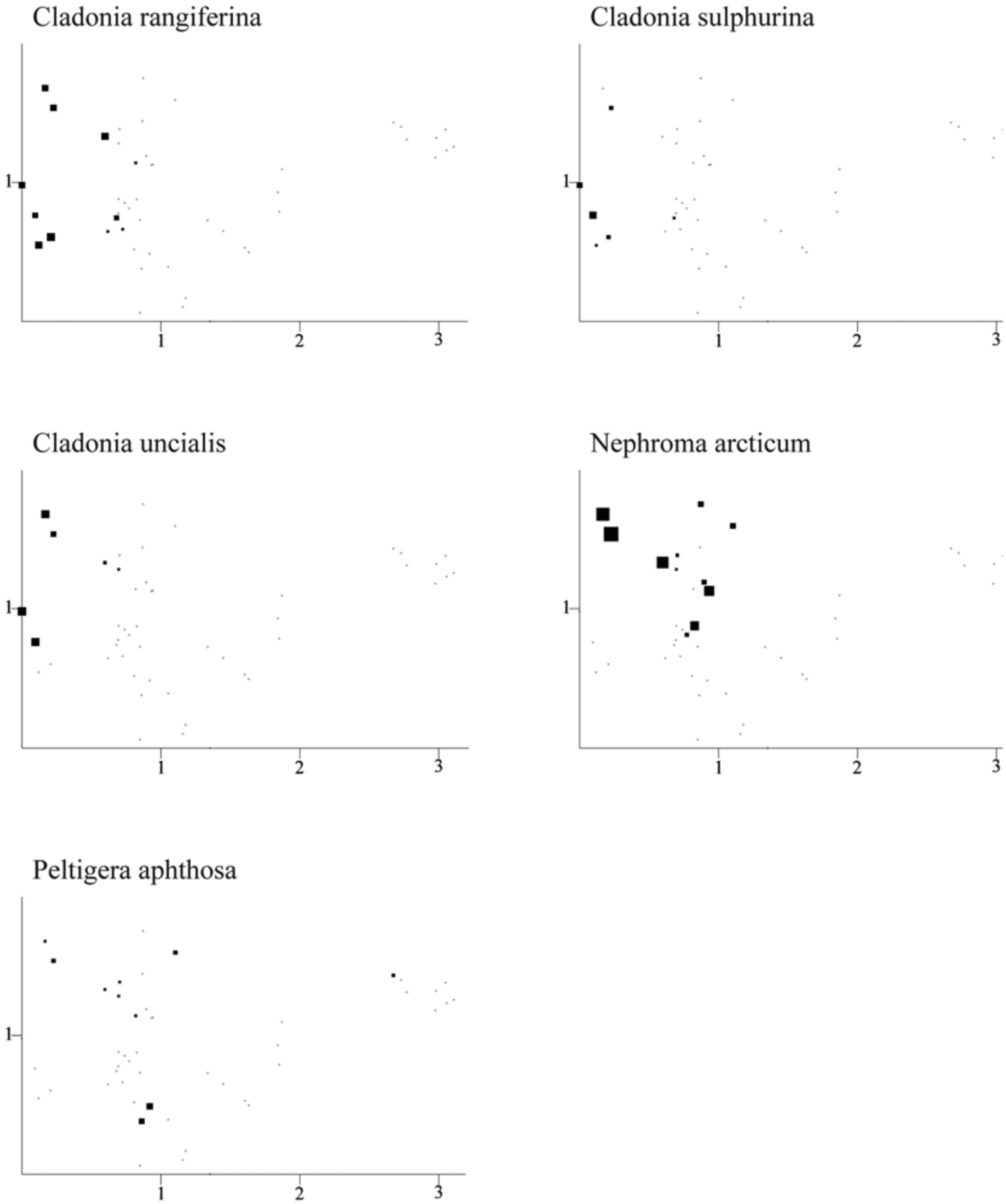

Figs 401-405. Dividalen: distributions of species abundances in the DCA ordination of 50 meso plots, axes 1 (horizontal) and 2 (vertical). Frequency in subplots for each species in each meso plot proportional to quadrate size. Scaling in S.D. units. Fig. 401. *Cladonia rangiferina*. Fig. 402. *Cladonia sulphurina*. Fig. 403. *Cladonia uncialis*. Fig. 404. *Nephroma arcticum*. Fig. 405. *Peltigera aphthosa*.

THE TOTAL DATA SET

Variation in species composition between reference areas

Twenty-one species were restricted to the southermost reference area Lund, located in the middle boreal vegetation zone in the western (O2) vegetation section (Moen 1999). These were *Anemone nemorosa, Blechnum spicant, Carex pilulifera, Danthonia decumbens, Huperzia selago* spp. *selago, Luzula sylvatica, Oreopteris limbosperma, Populus tremula, Pteridium aquilinum, Chiloscyphus coadunatus, Dicranum polysetum, Diplophyllum taxifolium, Hylocomiastrum umbratum, Hypnum cupressiforme, Lepidozia reptans, Leucobryum glaucum, Plagiothecium undulatum, Polytrichastrum formosum, Sphagnum capillifolium* and *Sphagnum quinquefarium.*

Several species that were common in most of the other reference areas were very rare or totally absent in Lund, such as *Anthoxanthum odoratum, Barbilophozia lycopodioides, Betula nana, Brachythecium reflexum, B. salebrosum, Deschampsia cespitosa, Empetrum nigrum, Geranium sylvaticum, Lophozia obtusa, Polytrichum commune, P. juniperinum, Ranunculus acris, Rhodobryum roseum, Solidago virgaurea* and all lichen species.

The other reference areas, all located in the northern boreal zone, shared a majority of species. However, the Dividalen reference area located in the continental vegetation section, partly on calcaerous bedrock, differed considerable from the others in species composition, as exemplified by the occurrence of species such as *Carex lapponica, Cerastium fontanum, Equisetum pratense, Myosotis decumbens, Poa alpina, Saussurea alpina* and *Trollius europaeus.*

Variation in environmental variables between reference areas

Differences among reference areas with respect to range and median values of environmental variables were also found (Table 21). These differences should be interpreted as between area (those included in this study) variation rather than regional biogeographical trends of these variables in Norway. Median soil depth was higher, while the meso plot aspect unfavourability was lower in more northerly situated areas. The median value of loss-on-ignition was highest in Gutulia and lowest in Møsvatn and Børgefjell. The southernmost reference area, Lund, had the lowest median pH value, while the northernmost area, Dividalen, had the highest value. Lund and Åmotsdalen had the lowest median value of extractable Ca concentrations while the highest value of both of Ca and Mg were found for Dividalen. The median value of extractable Mn was lowest in Lund and highest in Gutulia, while extractable P was highest in Børgefjell and Møsvatn. Lund had the highest soil moisture content and Lund and Gutulia had the highest median value of total N.

DCA ordination of the total data set, all reference areas included

All fifty sample plots from the Lund reference area were clearly separated from sample plots of the other reference areas in the DCA ordination, all restricted to low DCA axis 1 scores (Fig. 406). The other reference areas formed a cluster at medium to high axis 1 scores. Sample plots from Dividalen obtained the highest median score. The sample plots from Lund occupied a narrow interval along DCA axis 2 while sample plots from Møsvatn almost spanned the entire second ordination axis.

DCA ordination of five reference areas, sample plots from Lund excluded

In a DCA ordination without sample plots from Lund, sample plots from the other reference areas mixed almost completely along DCA axis 1, but less so along DCA axis 2 (Fig. 407). Sample plots from Dividalen obtained the lowest values along the second ordination axis, followed by sample plots from Åmotsdalen, Gutulia, Møsvatn and Børgefjell. Sample plots from Møsvatn showed increasing DCA axis 2 scores with increasing DCA axis 1 scores (Fig. 407).

Correlations between DCA axes (sample plots from Lund excluded) and local and regional climatic/ geographical variables

Soil pH and extractable C, Ca, Mn and S concentrations and total N were the variables most strongly positively correlated with DCA axis 1, while exchangeable H and loss on ignition were most strongly negatively correlated, all with $|\tau| > 0.3$ (Table 22). Extractable Mn and S were also strongly correlated with DCA axis 2, as was also effective temperature sum. Latitude was the only variable strongly negatively correlated with DCA axis 2 (Table 23).

Split-plot GLM analysis of relationships between ordination axes and environmental variables

Variation (in plot scores) along DCA axis 1 was partitioned with 4.30 % at the area scale (i.e. between areas), 89.15 % at the macro plot scale (i.e. between macro plots) and 6.55 % at the (between) meso plot scale within macro plots (Table 22). Along the second ordination axis, 55.21 % of the variation was explained at the between area scale, 36.35 % at the macro plot scale and 8.44 % at the meso plot scale (Table 23).

At the area scale, four variables were significantly (at the $\alpha = 0.05$ level) related to DCA 1, while two variables (also at the $\alpha = 0.05$ level) were related to DCA 2. At the macro plot scale level, sixteen environmental variables were significantly related to DCA 1 and twelve variables to DCA 2 (Tables 22 and 23). At the meso plot scale level, ten environmental variables were significantly related to DCA 1 and four variables to DCA 2 (Tables 22 and 23).

At the area scale, DCA 1 was positively related to the concentration of Al, Na and P and negatively related to meso plot terrain form (at the $\alpha = 0.05$ level). At the macro plot scale, altitude, macro and meso plot slope, tree basal area, pH and soil concentrations of C, Ca, K, Mn, Na, S and Zn increased significantly along DCA 1 while loss-on-ignition and exchangeable H decreased. At the meso plot scale, many of these variables showed the same tendencies. Predictors which were significantly related to DCA 1 at the macro plot but not at the meso plot scale were macro and meso plot slope, tree basal area and concentrations of K and Na.

The only variables significantly related (at the $\alpha = 0.05$ level) to DCA axis 2 at the area scale (both positively) were the concentrations of Na and P. At the macro plot scale, DCA 2 was positively related to macro and meso plot aspect unfavourability, meso plot uneveness and soil concentrations of C, K Mn, Na, S and Zn and negatively related to meso plot heat index, minimum soil depth and altitude. At the meso plot level, DCA 2 was positively significant related to soil concentrations of Mn, S and Zn and negatively related to maximum soil depth (Table 23).

Partial DCA ordination (sample plots from Lund excluded) with variation due to regional climatic/ geographical variables partialled out

The partial DCA with the seven climatic/geographical variables as covariables (compare Figs 407 and 408) had a shorter first DCA axis (gradient length in S.D. units) while DCA axis 2 had approximately the same gradient length in both ordinations. Plots were largely similarly distributed in the ordination diagrams, but some differences existed. In the partial DCA ordination the Møsvatn plots did not span the entire DCA 1 axis, but were not represented among plots with the highest DCA 1 scores. Sample plots from Gutulia obtained generally higher scores along DCA axis 2 in the partial ordination, mixing with sample plots from Børgefjell. Correlations between corresponding axes in the two DCA ordinations were high; $\tau = 0.743$ for the first and $\tau = 0.605$ for the second axes.

Correlations between partial DCA ordination axes (sample plots from Lund excluded) with variation due to regional climatic/geographical variables partialled out, and local environmental variables

The relationships between partial DCA axes and explanatory variables (Tables 24 and 25) closely resembled those of the ordinary DCA ordination (without covariables; Tables 22 and 23).

Split-plot GLM analysis of relationships between partial ordination axes and environmental variables

Variation (in plot scores) along partial DCA axis 1 was partitioned with 6.16 % at the area scale (i.e. between areas), 83.93 % at the macro plot scale (i.e. between macro plots) and 9.91 % at the (between) meso plot scale within macro plots (Table 24). Along the second partial ordination axis, 49.62 % of the variation was explained at the between-area scale, 39.63 % at the macro plot scale and 10.74 % at the meso plot scale (Table 25).

At the area scale, three variables were significantly (at the $\alpha = 0.05$ level) related to partial DCA axis 1, while no variables (also at the $\alpha = 0.05$ level) were related to partial DCA axis 2. At the macro plot scale level, seventeen environmental variables were significantly related to partial DCA axis 1 and nine variables to partial DCA axis 2 (Tables 24 and 25). At the meso plot scale level, ten environmental variables were significantly related to partial DCA axis 1 and seven variables to partial DCA axis 2 (Tables 24 and 25).

At the area scale, partial DCA axis 1 was positively related to the concentration of P and negatively related to meso plot slope and terrain form (at the $\alpha = 0.05$ level). At the macro plot scale, macro and meso plot slope, macro plot aspect unfavourability, tree basal area, pH, Total N and soil concentrations of, C, Ca, K, Mn, Na, S and Zn increased significantly along partial DCA axis 1 while soil moisture, loss-on-ignition and exchangeable H decreased. At the meso plot scale, meso plot uneveness, maximum soil depth, pH, Total N and soil concentrations of, C, Ca, K, Mn, and S increased significantly along partial DCA axis 1 while loss-on-ignition and exchangeable H decreased.

At the area scale, partial DCA axis 2 was not significant related at the $\alpha = 0.05$ level to any of the measured variables. At the macro plot scale, partial DCA axis 2 was positively related to tree basal area, meso plot slope and soil concentrations of C, K, Mg, Mn and S and negatively related to median soil depth and loss-on-ignition. At the meso plot scale, partial DCA axis 2 was positively significant related to tree basal area and soil concentrations of Ca, K and Mg and negatively related to maximum soil depth and exchangeable H and extractable Al (Table 25).

Distribution of species abundances in the partial DCA ordination (sample plots from Lund excluded) with variation due to regional climatic/geographical variables partialled out

Species more or less restricted to plots with high scores along partial DCA axis 1 (the right side of the ordination diagram), hence showing preference for nutrient-rich sites with high soil pH, were *Bistorta vivipara* (Fig. 415), *Geranium sylvaticum* (Fig. 419), *Ranunculus acris* (Fig. 424), *Rumex acetosa* (Fig. 410), *Solidago virgaurea* (Fig. 427), *Anthoxanthum odoratum* (Fig. 431) and *Brachythecium salebrosum* (Fig. 434). The opposite pattern of distribution in the partial DCA ordination was shown by species more or less restricted to the left-hand side of the ordination (more nutrient-poor sites) e.g. *Arctostaphylos alpina* (Fig. 410), *Betula nana* (Fig. 409*), Calluna vulgaris* (Fig. 411), *Empetrum nigrum* (Fig. 412), *Cetraria islandica* (Fig. 444), *Cladonia furcata* (Fig. 445) and *Cladonia rangiferina* (Fig. 446).

A few species such as *Vaccinium uliginosum* (Fig. 413) and *Polytrichum juniperum* (Fig. 438) spanned the entire first axis (i.e. the entire gradient related to soil nutrient and base richness represented by variables such as pH, concentrations of Mn, Ca, etc.), but showed a clear preference for plots with low partial DCA axis 2 scores. *Barbilophozia floerkei* (Fig. 443) occurred along the entire first partial DCA axis but were concentrated to high partial DCA axis 2 scores.

The second partial DCA axis separated sample plots with high partial DCA axis 1 scores better than sample plots with low partial DCA axis 1 scores. The sample plots thus occupied a triangle-like area in the space spanned by the two first partial ordination axes (Fig. 407). Species more or less strongly restricted to plots with high partial DCA axis 1 scores (richer in nutrients) and low partial DCA axis 2 scores (characterised by low concentrations of K and total N and low tree densities), were *Bartsia alpina* (Fig. 414), *Cerastium fontanum* (Fig. 416), *Poa alpina* (Fig. 433), *Saussurea alpina* (Fig. 426) *Trollius europaeus* (Fig. 428), *Viola biflora* (Fig. 430) and *Mnium spinosum* (Fig. 436).

Species with high partial DCA scores on both axes were *Cicerbita alpina* (Fig. 417), *Oxalis acetocella* (Fig. 421), *Phegopteris connectilis* (Fig. 422), *Polygonatum verticillatum* (Fig. 423), *Polytrichastrum longisetum* (Fig. 437), *Rhytidiadelphus squarrosus* (Fig. 442) and *Veronica officinalis* (Fig. 429).

Chamaepericlymenum suecicum (Fig. 418) and *Dicranum scoparium* (Fig. 435) had a wide distributions along both partial DCA axes and were only missing in the lower, right part of the diagram.

Table 21. Statistics for the 31 environmental variables in all six reference areas. Min, Med and Max represent minimum, medium and maximum values, respectively. The units and names of environmental variables are abbreviated in accordance with Table 2.

Evironmental variables	Lund Min	Lund Med	Lund Max	Møsvatn Min	Møsvatn Med	Møsvatn Max	Gutulia Min	Gutulia Med	Gutulia Max	Åmotsdalen Min	Åmotsdalen Med	Åmotsdalen Max	Børgefjell Min	Børgefjell Med	Børgefjell Max	Dividalen Min	Dividalen Med	Dividalen Max
Ma Slo	0	12	60	6	15	30	0	9	60	1	7	19	1	9	20	5	14.5	25
Ma Asp	22.5	162.5	177.5	17.5	157.5	175.5	92.5	150.5	176.5	22.5	42.5	112.5	22.5	52.5	107.5	22.5	67.5	121.5
Ma HI	–1.73	–0.18	0.09	–0.58	–0.17	0.26	–1.65	–0.12	0.00	–0.13	0.07	0.25	–0.07	0.06	0.20	–0.05	0.12	0.25
Ma Ter	–2	0	2	–0.78	0.11	0.78	–1	0	2	–1	0	2	–2	0	2	0	0.5	1
Ma Une	1	3	5	0.19	1.07	2.00	0	2	4	0	2	4	1	1.5	4	1	2	3
TBA	0	3	9	0	7	7	2	14	23	0	4	10	0	5	16	0	5	14
Me Slo	0	19	30	3	12	12	0	10	75	0	9	23	0	9	23	2	15	34
Me Asp	0.5	152.5	178.5	75.0	175.0	175.0	33.5	148.0	177.5	0.5	47.5	103.5	4.5	58.5	175.5	17.5	97.5	384.0
Me HI	–0.54	–0.30	0.25	–0.53	–0.17	0.14	–3.63	–0.11	0.61	–0.01	0.11	0.30	–0.15	0.03	0.41	–0.54	0.10	0.49
Me Ter	–1.06	0.00	0.50	–0.56	0.03	0.03	–2.00	0.00	2.00	–0.40	0.00	0.47	–0.56	0.00	0.44	0.00	1.00	2.00
Me Une	0.00	0.75	2.10	0.00	0.61	0.61	1.00	2.00	4.00	0.00	0.58	2.64	0.00	0.78	1.39	0.00	2.00	5.00
Smi	0.0	2.0	18.0	0.0	2.0	2.0	0.0	3.0	62.0	0.0	6.0	30.0	0.0	2.0	16.0	0.0	6.0	65.0
Sme	1.0	16.5	61.0	3.0	16.5	16.5	1.0	10.0	66.0	4.0	24.0	65.0	3.5	18.8	44.0	5.0	37.5	65.0
Sma	11.0	48.0	78.0	8.0	41.5	41.5	3.0	25.0	85.0	15.0	54.5	103.0	20.0	35.5	83.0	45.0	65.0	65.0
Mme	43.9	74.9	83.9	20.8	41.4	78.3	19.7	67.6	82.4	9.40	42.6	73.9	18.4	41.8	79.8	14.2	63.2	83.3
LOI	32.1	73.6	95.0	16.3	48.1	48.1	41.3	85.5	97.8	14.6	68.4	91.3	9.4	51.4	95.2	46.4	73.5	91.8
Total N	1175	1678	2365	1207	1595	1595	1264	1632	2100	1027	1417	2224	1090	1545	2353	1061	1489	2280
pHH2O	3.61	3.90	4.58	3.68	4.17	4.17	3.57	4.23	5.22	3.81	4.27	5.20	3.77	4.10	5.05	3.86	4.35	5.40
pHCaCl2	2.86	3.09	3.82	2.95	3.52	3.52	2.81	3.53	4.88	3.05	3.52	4.70	2.99	3.35	4.56	3.20	3.74	5.03
H	99	154	309	57	104	104	39	96	188	40	110	243	50	100	155	15	70	168
Al	3.67	15.45	110.13	1.46	6.74	6.74	0.48	4.43	30.72	0.92	12.67	73.46	0.95	2.47	22.66	0.95	2.62	17.22
C	405	574	890	549	866	866	508	874	2794	453	823	1358	418	659	1795	639	952	1530
Ca	5.8	57.5	90.6	38.9	102.9	102.9	51.4	98.3	233.5	30.8	76.4	189.1	74.1	105.5	182.1	91.1	197.3	493.2
Fe	0.3	1.1	7.8	0.2	0.7	0.7	0.1	0.3	13.0	0.2	1.1	3.8	0.1	0.2	0.7	0.1	0.5	3.5
K	11.0	18.5	28.5	17.9	37.4	37.4	12.6	33.3	62.4	20.7	35.8	51.3	18.8	37.2	85.4	21.4	32.4	50.8
Mg	4.4	41.2	64.7	11.0	27.4	27.4	6.6	20.4	55.3	19.6	32.5	60.6	33.5	49.5	85.8	30.9	53.5	118.1
Mn	0.1	0.7	2.4	0.7	10.9	10.9	0.4	18.2	97.2	0.4	8.3	74.5	0.4	4.1	70.1	0.6	9.4	26.8
Na	4.9	7.5	17.3	3.7	6.0	6.0	4.7	9.8	15.8	4.4	12.3	20.1	6.6	9.8	14.6	3.3	7.8	18.2
P	0.1	4.2	8.9	1.1	10.4	10.4	0.1	6.4	20.1	0.1	6.8	19.0	3.8	11.2	21.8	1.7	7.7	16.2
S	3.1	5.2	7.7	4.5	6.8	6.8	3.9	7.2	9.8	3.5	5.8	10.4	3.2	5.1	13.1	4.6	6.4	11.2
Zn	191	1470	2287	286	1274	1274	98	761	2152	279	660	2045	407	1175	3342	108	637	1791

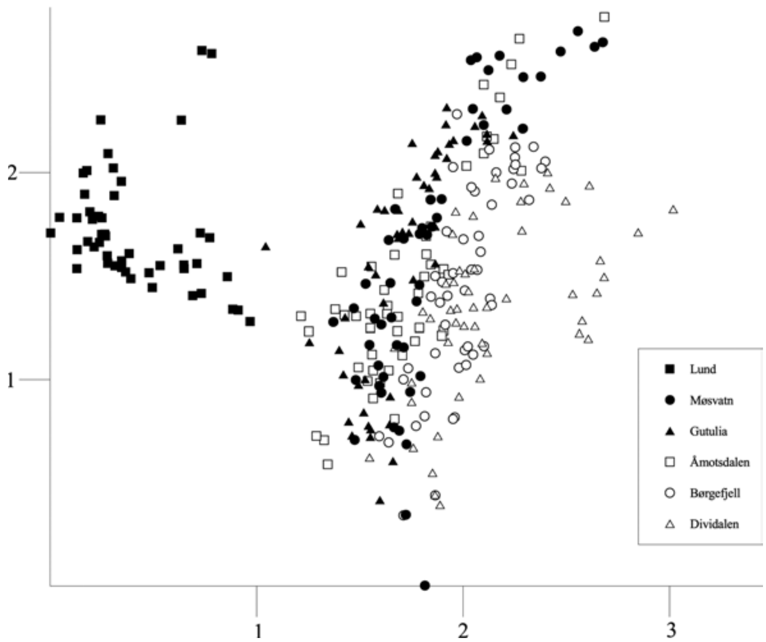

Fig. 406. DCA ordination of the total dataset of 300 meso plots from all reference areas, axes 1 (horizontal) and 2 (vertical). Scaling of axes in S.D. units.

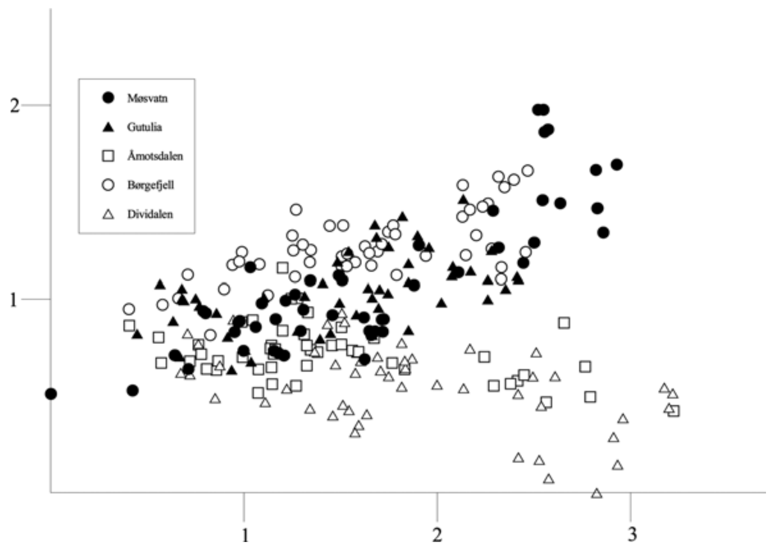

Fig. 407. DCA ordination of 250 meso plots from all reference areas except Lund, axes 1 (horizontal) and 2 (vertical). Scaling of axes in S.D. units.

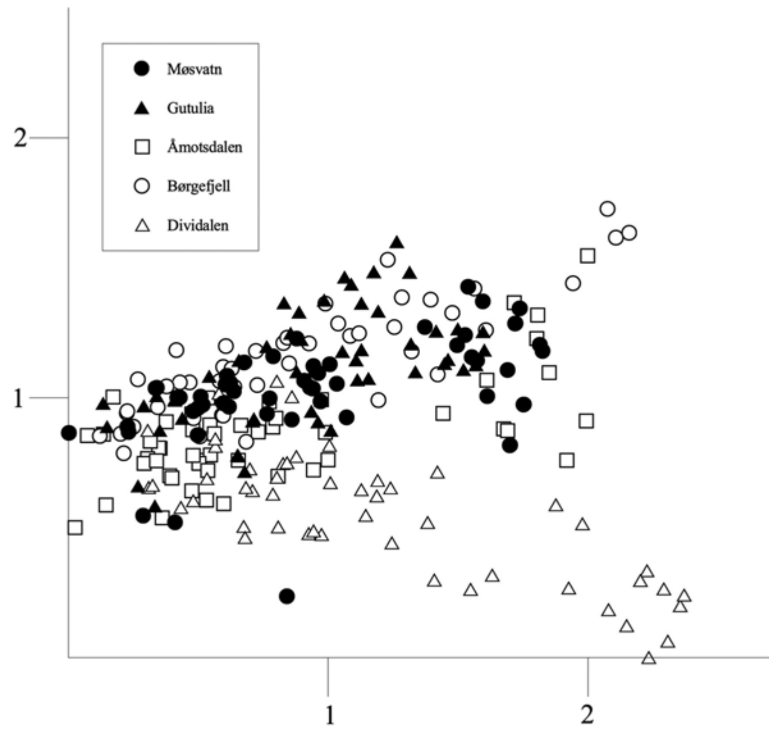

Fig. 408. DCA ordination of 250 meso plots from all reference areas (except Lund), with 7 CCA axes that represent variation exclusively explained by regional climatic/geographical variables as covariables, axes 1 (horizontal) and 2 (vertical). Scaling of axes in S.D. units.

Table 22. The total data set with meso plots from Lund excluded: Split-plot GLM analysis with three levels and Kendall's nonparametric correlation coefficient τ between DCA 1 and 31 environmental variables and 7 regional variables (predictors) in the 50 meso plots. df_{resid}: degrees of freedom for the residuals; *SS*: total variation; *FVE*: fraction of total variation attributable to a given scale (area, macro plot or plot); SS_{expl}/SS: fraction of the variation attributable to the scale in question, explained by a variable; *r*: model coefficient (only given when significant at the α = 0.05 level, otherwise blank); *F*: *F* statistic for test of the hypothesis that $r = 0$ against the two-tailed alternative. * no variation on this scale level. Split-plot GLM relationships significant at level α = 0.05, *P*, *F*, *r* and SS_{expl}/SS, and Kendall's nonparametric correlation coefficient $|\tau| \geq 0.30$ are given in bold face. Numbers and abbreviations for names of environmental variables are in accordance with Table 2.

Predictor	Dependent variable = DCA 1 (*SS* = 105.8581)												Correlation between predictor and DCA 1
	Error level												
	Area $df_{resid} = 3$ $SS_{macro\ plot} = 4.5545$ $FVE = 0.0430$ of *SS*				Macro plot within area $df_{resid} = 44$ $SS_{meso\ plot} = 94.3710$ $FVE = 0.8915$ of *SS*				Meso plot within macro plot $df_{resid} = 199$ $SS_{meso\ plot} = 6.9326$ $FVE = 0.0655$ of *SS*				Total
	$SS_{expl}/SS_{macro\ plot}$	*r*	*F*	*P*	$SS_{expl}/SS_{meso\ plot}$	*r*	*F*	*P*	$SS_{expl}/SS_{meso\ plot}$	*r*	*F*	*P*	τ
Ma Slo	0.2694		1.1061	0.3702	**0.1192**	**1.2737**	**6.0909**	**0.0186**	0.0017		0.3107	0.5780	0.186
Ma Asp	0.0346		0.1074	0.7647	0.0799		4.0130	0.0529	0.0003		0.0530	0.8182	0.140
Ma HI	0.2270		0.8811	0.4172	0.0068		0.3081	0.5824	0.0026		0.4769	0.4908	–0.061
Ma Ter	0.5284		3.3611	0.1641	0.0007		0.0307	0.8619	0.0023		0.4241	0.5159	0.006
Ma Une	0.2774		1.1519	0.3618	0.0126		0.5881	0.4483	0.0023		0.4330	0.5115	–0.032
TBA	0.0001		0.0003	0.9863	**0.3847**	**1.7491**	**27.7050**	**0.0000**	0.0010		0.1858	0.6670	0.292
Me Slo	0.7648		9.7532	0.0524	**0.1103**	**1.5618**	**5.8314**	**0.0211**	0.0031		0.5845	0.4457	0.055
Me Asp	0.0375		0.1169	0.7550	0.0251		1.1606	0.2887	0.0062		1.1655	0.2820	0.066
Me HI	0.2243		0.8674	0.4204	0.0050		0.2230	0.6397	0.0013		0.2391	0.6255	–0.034
Me Ter	**0.8788**	**–1.8439**	**21.7500**	**0.0186**	0.0743		3.6649	0.0638	0.0020		0.3724	0.5426	–0.091
Me Une	0.3404		1.5483	0.3017	0.0060		0.2784	0.6011	0.0108		2.0431	0.1549	–0.016
Smi	0.4208		2.1793	0.2364	0.0431		2.0080	0.1653	0.0022		0.4140	0.5208	–0.087
Sme	0.2838		1.1890	0.3553	0.0120		0.5487	0.4638	0.0051		0.9506	0.3311	–0.046
Sma	0.7477		8.8897	0.0585	0.0001		0.0069	0.9343	0.0177		3.3323	0.0698	–0.072
Mme	0.0836		0.2737	0.6370	0.0394		1.8423	0.1834	0.0160		3.0406	0.0831	–0.038
LOI	0.4422		2.3782	0.2207	**0.5008**	**–1.4731**	**44.0771**	**0.0000**	**0.0331**	**–0.2366**	**6.3761**	**0.0126**	**–0.418**
Total N	0.4030		2.0255	0.2499	**0.5748**	**2.4789**	**67.6840**	**0.0000**	**0.0288**	**0.2658**	**5.5500**	**0.0197**	**0.383**
pH_{H_2O}	0.0496		0.1566	0.7187	**0.7287**	**2.0025**	**114.8530**	**0.0000**	**0.0889**	**0.4606**	**18.0236**	**0.0000**	**0.577**
pH_{CaCl_2}	0.0898		0.2961	0.6242	**0.7383**	**1.9931**	**125.2308**	**0.0000**	**0.0858**	**0.4072**	**17.0468**	**0.0001**	**0.591**

Table 22 (Continued). The total data set with meso plots from Lund excluded: Split-plot GLM analysis with three levels and Kendall's nonparametric correlation coefficient τ between DCA 1 and 31 environmental variables and 7 regional variables (predictors) in the 50 meso plots. df_{resid}: degrees of freedom for the residuals; *SS*: total variation; *FVE*: fraction of total variation attributable to a given scale (area, macro plot or plot); SS_{expl}/SS: fraction of the variation attributable to the scale in question, explained by a variable; *r*: model coefficient (only given when significant at the α = 0.05 level, otherwise blank); *F*: *F* statistic for test of the hypothesis that $r = 0$ against the two-tailed alternative. * no variation on this scale level. Split-plot GLM relationships significant at level α = 0.05, *P*, *F*, *r* and SS_{expl}/SS, and Kendall's nonparametric correlation coefficient $|\tau| \geq 0.30$ are given in bold face. Numbers and abbreviations for names of environmental variables are in accordance with Table 2.

Predictor	Dependent variable = DCA 1 (SS = 105.8581) Error level												Correlation between predictor and DCA 1
	Area $df_{resid} = 3$ $SS_{macro\ plot} = 4.5545$ $FVE = 0.0430$ of SS				Macro plot within area $df_{resid} = 44$ $SS_{meso\ plot} = 94.3710$ $FVE = 0.8915$ of SS				Meso plot within macro plot $df_{resid} = 199$ $SS_{meso\ plot} = 6.9326$ $FVE = 0.0655$ of SS				Total
	$SS_{expl}/SS_{macro\ plot}$	*r*	*F*	*P*	$SS_{expl}/SS_{meso\ plot}$	*r*	*F*	*P*	$SS_{expl}/SS_{meso\ plot}$	*r*	*F*	*P*	τ
H	0.0930		0.3076	0.6178	**0.5646**	**–2.0025**	**57.1259**	**0.0000**	**0.0520**	**–0.2892**	**10.0720**	**0.0018**	**–0.486**
Al	**0.8325**	**3.4700**	**14.9080**	**0.0307**	0.0243		1.1040	0.3006	0.0058		1.0895	0.2982	–0.075
C	0.4148		2.1261	0.2409	**0.4731**	**1.7803**	**38.0929**	**0.0000**	**0.0521**	**0.3462**	**10.3243**	**0.0016**	**0.439**
Ca	0.0204		0.0625	0.8187	**0.5264**	**2.4185**	**47.0737**	**0.0000**	**0.0552**	**0.3513**	**10.8302**	**0.0012**	**0.434**
Fe	0.1319		0.4560	0.5479	0.0152		0.6847	0.4136	0.0000		0.0002	0.9902	–0.055
K	0.2058		0.7774	0.4429	**0.1097**	**0.8832**	**5.5119**	**0.0247**	0.0182		3.5279	0.0622	0.240
Mg	0.0243		0.0746	0.8025	0.0379		1.7451	0.1951	0.0000		0.0060	0.9381	0.110
Mn	0.3495		1.6120	0.2937	**0.5961**	**1.6332**	**68.5629**	**0.0000**	**0.0955**	**0.5316**	**19.5841**	**0.0000**	**0.512**
Na	**0.9046**	**2.7121**	**28.4320**	**0.0129**	**0.2309**	**1.5901**	**14.3091**	**0.0006**	0.0037		0.6906	0.4072	0.296
P	**0.7920**	**3.3161**	**11.4250**	**0.0431**	0.0307		1.4442	0.2375	0.0005		0.0948	0.7586	–0.051
S	0.2726		1.1242	0.3668	**0.6805**	**2.2954**	**91.7113**	**0.0000**	**0.0881**	**0.4394**	**18.0693**	**0.0000**	**0.534**
Zn	0.0173		0.0528	0.8331	**0.1646**	**0.8386**	**8.3288**	**0.0066**	**0.0554**	**0.3276**	**10.8722**	**0.0012**	0.256
Prec.	0.4179		2.1538	0.2385	*	*	*	*	*	*	*	*	–0.083
T	0.2349		0.9210	0.4080	*	*	*	*	*	*	*	*	–0.075
ETS	0.3074		1.3314	0.3321	*	*	*	*	*	*	*	*	–0.053
Tamm's H	0.2351		0.9222	0.4077	*	*	*	*	*	*	*	*	–0.075
Lat.	0.5179		3.2229	0.1705	*	*	*	*	*	*	*	*	0.079
Long.	0.5354		3.4578	0.1599	*	*	*	*	*	*	*	*	0.101
Alt.	0.3303		1.4795	0.3108	**0.0769**	**–0.0078**	**4.2462**	**0.0468**	*	*	*	*	–0.155

Table 23. The total data set with meso plots from Lund excluded: Split-plot GLM analysis with three levels and Kendall's nonparametric correlation coefficient τ between DCA 1 and 31 environmental variables and 7 regional variables (predictors) in the 50 meso plots. df_{resid}: degrees of freedom for the residuals; *SS*: total variation; *FVE*: fraction of total variation attributable to a given scale (area, macro plot or plot); SS_{expl}/SS: fraction of the variation attributable to the scale in question, explained by a variable; *r*: model coefficient (only given when significant at the α = 0.05 level, otherwise blank); *F*: *F* statistic for test of the hypothesis that $r = 0$ against the two-tailed alternative. * no variation on this scale level. Split-plot GLM relationships significant at level α = 0.05, *P*, *F*, *r* and SS_{expl}/SS, and Kendall's nonparametric correlation coefficient $|\tau| \geq 0.30$ are given in bold face. Numbers and abbreviations for names of environmental variables are in accordance with Table 2.

Predictor	Dependent variable = DCA 2 (SS = 30.1342)												Correlation between predictor and DCA 2
	Error level												
	Area $df_{resid} = 3$ $SS_{macro\ plot} = 16.6378$ $FVE = 0.5521$ of SS				Macro plot within area $df_{resid} = 44$ $SS_{meso\ plot} = 10.9532$ $FVE = 0.3635$ of SS				Meso plot within macro plot $df_{resid} = 199$ $SS_{meso\ plot} = 2.5432$ $FVE = 0.0844$ of SS				Total
	$SS_{expl}/SS_{macro\ plot}$	*r*	*F*	*P*	$SS_{expl}/SS_{meso\ plot}$	*r*	*F*	*P*	$SS_{expl}/SS_{meso\ plot}$	*r*	*F*	*P*	τ
Ma Slo	0.0874		0.2873	0.6291	0.0475		2.1484	0.1516	0.0003		0.0539	0.8168	0.080
Ma Asp	0.1518		0.5369	0.5168	**0.0979**	**0.4129**	**4.6759**	**0.0375**	0.0063		1.2234	0.2704	0.093
Ma HI	0.0046		0.0137	0.9141	0.0727		3.1697	0.0837	0.0005		0.0981	0.7545	–0.079
Ma Ter	0.0335		0.1041	0.7681	0.0062		0.2436	0.6247	0.0033		0.6443	0.4234	0.028
Ma Une	0.0274		0.0846	0.7900	0.0303		1.1963	0.2815	0.0001		0.0178	0.8940	0.009
TBA	0.2167		0.8302	0.4294	0.0949		4.0427	0.0521	0.0000		0.0049	0.9441	0.070
Me Slo	0.4751		2.7159	0.1979	0.0504		2.1734	0.1494	0.0001		0.0109	0.9168	0.277
Me Asp	0.0221		0.0677	0.8115	**0.1115**	**0.5441**	**5.1980**	**0.0288**	0.0027		0.5201	0.4719	0.061
Me HI	0.0592		0.1889	0.6932	**0.1261**	**–0.5836**	**5.8388**	**0.0210**	0.0001		0.0136	0.9073	–0.097
Me Ter	0.4435		2.3911	0.2198	0.0766		3.2946	0.0781	0.0181		3.5758	0.0605	0.010
Me Une	0.1282		0.4413	0.5540	**0.0987**	**0.3694**	**4.1317**	**0.0497**	0.0003		0.0527	0.8187	0.090
Smi	0.2200		0.8464	0.4254	**0.1174**	**–0.3621**	**5.2485**	**0.0281**	0.0023		0.4472	0.5046	–0.081
Sme	0.7705		10.0720	0.0503	0.0524		2.2229	0.1449	0.0003		0.0627	0.8025	–0.122
Sma	0.4305		2.2675	0.2292	0.0014		0.0552	0.8156	**0.0334**	**–0.1107**	**6.6331**	**0.0109**	0.211
Mme	0.0037		0.0110	0.9230	0.0101		0.3976	0.5325	0.0078		1.5110	0.2208	–0.053
LOI	0.1861		0.6857	0.4683	0.0358		1.4477	0.2370	0.0003		0.0573	0.8111	–0.055
Total N	0.4125		2.1061	0.2426	0.0551		2.2213	0.1451	0.0031		0.6017	0.4391	0.172
pH_{H_2O}	0.0079		0.0240	0.8867	0.0510		2.0731	0.1588	0.0003		0.0574	0.8110	0.081
pH_{CaCl_2}	0.0383		0.1194	0.7525	0.0635		2.6144	0.1149	0.0050		0.9723	0.3256	0.086

Table 23 (Continued). The total data set with meso plots from Lund excluded: Split-plot GLM analysis with three levels and Kendall's nonparametric correlation coefficient τ between DCA 1 and 31 environmental variables and 7 regional variables (predictors) in the 50 meso plots. df_{resid}: degrees of freedom for the residuals; *SS*: total variation; *FVE*: fraction of total variation attributable to a given scale (area, macro plot or plot); SS_{expl}/SS: fraction of the variation attributable to the scale in question, explained by a variable; *r*: model coefficient (only given when significant at the α = 0.05 level, otherwise blank); *F*: *F* statistic for test of the hypothesis that $r = 0$ against the two-tailed alternative. * no variation on this scale level. Split-plot GLM relationships significant at level α = 0.05, *P*, *F*, *r* and SS_{expl}/SS, and Kendall's nonparametric correlation coefficient $|\tau| \geq 0.30$ are given in bold face. Numbers and abbreviations for names of environmental variables are in accordance with Table 2.

Predictor	Dependent variable = DCA 2 (SS = 30.1342) Error level												Correlation between predictor and DCA 2
	Area $df_{resid} = 3$ $SS_{macro\ plot} = 16.6378$ $FVE = 0.5521$ of SS				Macro plot within area $df_{resid} = 44$ $SS_{meso\ plot} = 10.9532$ $FVE = 0.3635$ of SS				Meso plot within macro plot $df_{resid} = 199$ $SS_{meso\ plot} = 2.5432$ $FVE = 0.0844$ of SS				Total
	$SS_{expl}/SS_{macro\ plot}$	r	F	P	$SS_{expl}/SS_{meso\ plot}$	r	F	P	$SS_{expl}/SS_{meso\ plot}$	r	F	P	τ
H	0.0001		0.0004	0.9855	0.0658		2.7068	0.1089	0.0041		0.7987	0.3728	–0.095
Al	0.2152		0.8225	0.4313	0.0005		0.0207	0.8863	0.0024		0.4646	0.4965	–0.050
C	0.0435		0.1366	0.7363	**0.1192**	**0.3367**	**5.2907**	**0.0275**	0.0001		0.0151	0.9023	0.117
Ca	0.3071		1.3300	0.3324	0.0201		0.7950	0.3787	0.0061		1.2042	0.2741	0.037
Fe	0.4521		2.4752	0.2137	0.0150		0.6006	0.4435	0.0008		0.1649	0.6852	0.077
K	0.2058		0.7774	0.4429	**0.1097**	**0.8832**	**5.5119**	**0.0247**	0.0182		3.5279	0.0622	0.240
Mg	0.0243		0.0746	0.8025	0.0379		1.7451	0.1951	0.0000		0.0060	0.9381	0.110
Mn	0.3495		1.6120	0.2937	**0.5961**	**1.6332**	**68.5629**	**0.0000**	**0.0955**	**0.5316**	**19.5841**	**0.0000**	**0.512**
Na	**0.9046**	**2.7121**	**28.4320**	**0.0129**	**0.2309**	**1.5901**	**14.3091**	**0.0006**	0.0037		0.6906	0.4072	0.296
P	**0.7920**	**3.3161**	**11.4250**	**0.0431**	0.0307		1.4442	0.2375	0.0005		0.0948	0.7586	–0.051
S	0.2726		1.1242	0.3668	**0.6805**	**2.2954**	**91.7113**	**0.0000**	**0.0881**	**0.4394**	**18.0693**	**0.0000**	**0.534**
Zn	0.0173		0.0528	0.8331	**0.1646**	**0.8386**	**8.3288**	**0.0066**	**0.0554**	**0.3276**	**10.8722**	**0.0012**	0.256
Prec.	0.4179		2.1538	0.2385	*	*	*	*	*	*	*	*	0.266
T	0.2349		0.9210	0.4080	*	*	*	*	*	*	*	*	–0.065
ETS	0.3074		1.3314	0.3321	*	*	*	*	*	*	*	*	**0.372**
Tamm's H	0.2351		0.9222	0.4077	*	*	*	*	*	*	*	*	–0.065
Lat.	0.5179		3.2229	0.1705	*	*	*	*	*	*	*	*	**–0.311**
Long.	0.5354		3.4578	0.1599	*	*	*	*	*	*	*	*	–0.198
Alt.	0.3303		1.4795	0.3108	**0.0769**	**–0.0078**	**4.2462**	**0.0468**	*	*	*	*	0.062

Table 24. Partial DCA ordination of the total data set with meso plots from Lund excluded (variation due to 7 regional variables partialled out): Split-plot GLM analysis with three levels and Kendall's nonparametric correlation coefficient τ between DCA 1 and 31 environmental variables and 7 regional variables (predictors) in the 50 plots. df_{resid}: degrees of freedom for the residuals; SS: total variation; FVE: fraction of total variation attributable to a given scale (area, macro plot or plot); SS_{expl}/SS: fraction of the variation attributable to the scale in question, explained by a variable; r: model coefficient (only given when significant at the $\alpha = 0.05$ level, otherwise blank); F: F statistic for test of the hypothesis that $r = 0$ against the two-tailed alternative. * no variation on this scale level. Split-plot GLM relationships significant at level $\alpha = 0.05$, P, F, r and SS_{expl}/SS, and Kendall's nonparametric correlation coefficient $|\tau| \geq 0.30$ are given in bold face. Numbers and abbreviations for names of environmental variables are in accordance with Table 2.

Predictor	Dependent variable = DCA 1 (SS = 76.0027)												Correlation between predictor and DCA 1
	Error level												
	Area $df_{resid} = 3$ $SS_{macro\ plot} = 4.6835$ $FVE = 0.0616$ of SS				Macro plot within area $df_{resid} = 44$ $SS_{meso\ plot} = 63.7860$ $FVE = 0.8393$ of SS				Meso plot within macro plot $df_{resid} = 199$ $SS_{meso\ plot} = 7.5332$ $FVE = 0.0991$ of SS				Total
	$SS_{expl}/SS_{macro\ plot}$	r	F	P	$SS_{expl}/SS_{meso\ plot}$	r	F	P	$SS_{expl}/SS_{meso\ plot}$	r	F	P	τ
Ma Slo	0.1748		0.6357	0.4835	**0.1859**	**0.9411**	**9.3731**	**0.0042**	0.0160		3.3110	0.0707	0.182
Ma Asp	0.0013		0.0038	0.9550	**0.1153**	**0.7066**	**5.8657**	**0.0208**	0.0000		0.0069	0.9339	0.173
Ma HI	0.1028		0.3436	0.5989	0.0145		0.6697	0.4187	0.0025		0.5112	0.4756	–0.082
Ma Ter	0.5343		3.4419	0.1606	0.0017		0.0767	0.7834	0.0022		0.4384	0.5088	0.006
Ma Une	0.1231		0.4210	0.5627	0.0582		2.8668	0.0993	0.0000		0.0091	0.9243	–0.080
TBA	0.1484		0.5225	0.5220	**0.3873**	**1.5238**	**30.7023**	**0.0000**	0.0010		0.1968	0.6579	**0.316**
Me Slo	**0.8910**	**–0.6985**	**24.5110**	**0.0158**	**0.1864**	**1.3242**	**10.0946**	**0.0031**	0.0003		0.0535	0.8174	0.066
Me Asp	0.0069		0.0209	0.8943	0.0334		1.5595	0.2200	0.0032		0.6541	0.4198	0.074
Me HI	0.3008		1.2909	0.3384	0.0043		0.1970	0.6599	0.0069		1.4051	0.2376	–0.029
Me Ter	**0.9300**	**–1.9236**	**39.8370**	**0.0080**	0.0792		3.8936	0.0564	0.0003		0.0534	0.8175	–0.098
Me Une	0.2155		0.8241	0.4309	0.0283		1.3800	0.2480	**0.0194**	**0.1686**	**4.0661**	**0.0454**	–0.012
Smi	0.6894		6.6573	0.0818	0.0543		2.5834	0.1170	0.0000		0.0025	0.9600	–0.120
Sme	0.5735		4.0342	0.1382	0.0122		0.5717	0.4546	0.0008		0.1693	0.6813	–0.060
Sma	0.6578		5.7674	0.0957	0.0000		0.0000	0.9965	**0.0412**	**0.2481**	**8.6869**	**0.0037**	–0.051
Mme	0.0023		0.0069	0.9389	**0.1009**	**–0.6781**	**4.9710**	**0.0323**	0.0069		1.4050	0.2377	–0.127
LOI	0.2463		0.9804	0.3951	**0.6154**	**–1.3247**	**68.4968**	**0.0000**	**0.2475**	**–0.6853**	**68.3389**	**0.0000**	**–0.486**
Total N	0.7285		8.0474	0.0658	**0.5659**	**2.0267**	**67.3720**	**0.0000**	**0.2544**	**0.7621**	**68.7781**	**0.0000**	**0.388**

Table 24 (Cuntinued). Partial DCA ordination of the total data set with meso plots from Lund excluded (variation due to 7 regional variables partialled out): Split-plot GLM analysis with three levels and Kendall's nonparametric correlation coefficient τ between DCA 1 and 31 environmental variables and 7 regional variables (predictors) in the 50 plots. df_{resid}: degrees of freedom for the residuals; *SS*: total variation; *FVE*: fraction of total variation attributable to a given scale (area, macro plot or plot); SS_{expl}/SS: fraction of the variation attributable to the scale in question, explained by a variable; *r*: model coefficient (only given when significant at the $\alpha = 0.05$ level, otherwise blank); *F*: *F* statistic for test of the hypothesis that $r = 0$ against the two-tailed alternative. * no variation on this scale level. Split-plot GLM relationships significant at level $\alpha = 0.05$, *P*, *F*, *r* and SS_{expl}/SS, and Kendall's nonparametric correlation coefficient $|\tau| \geq 0.30$ are given in bold face. Numbers and abbreviations for names of environmental variables are in accordance with Table 2.

Predictor	Dependent variable = DCA 1 ($SS = 76.0027$) Error level												Correlation between predictor and DCA 1
	Area $df_{resid} = 3$ $SS_{macro\ plot} = 4.6835$ $FVE = 0.0616$ of SS				Macro plot within area $df_{resid} = 44$ $SS_{meso\ plot} = 63.7860$ $FVE = 0.8393$ of SS				Meso plot within macro plot $df_{resid} = 199$ $SS_{meso\ plot} = 7.5332$ $FVE = 0.0991$ of SS				Total
	$SS_{expl}/SS_{macro\ plot}$	r	F	P	$SS_{expl}/SS_{meso\ plot}$	r	F	P	$SS_{expl}/SS_{meso\ plot}$	r	F	P	τ
pH_{H_2O}	0.0058		0.0175	0.9032	**0.7937**	**1.7398**	**186.8828**	**0.0000**	0.3664	**0.9744**	**114.2144**	**0.0000**	**0.625**
pH_{CaCl_2}	0.0004		0.0013	0.9738	**0.7727**	**1.7069**	**181.2997**	**0.0000**	0.4665	**1.1005**	**168.2823**	**0.0000**	**0.627**
H	0.0026		0.0077	0.9355	**0.6493**	**–1.8300**	**96.4307**	**0.0000**	**0.2248**	**–0.6874**	**56.6994**	**0.0000**	**–0.531**
Al	0.6065		4.6245	0.1207	0.0422		1.9859	0.1676	0.0026		0.5191	0.4723	–0.088
C	0.1336		0.4628	0.5451	**0.5099**	**1.5517**	**46.5138**	**0.0000**	**0.0767**	**0.4530**	**17.1988**	**0.0001**	**0.434**
Ca	0.0322		0.0997	0.7729	**0.6113**	**2.1373**	**66.2869**	**0.0000**	**0.1602**	**0.5947**	**37.5110**	**0.0000**	**0.467**
Fe	0.2979		1.2732	0.3413	0.0306		1.4067	0.2436	0.0000		0.0027	0.9586	–0.094
K	0.0221		0.0678	0.8114	**0.1544**	**0.9312**	**8.5041**	**0.0061**	**0.0426**	**0.3235**	**9.0543**	**0.0030**	0.279
Mg	0.0519		0.1643	0.7124	0.0726		3.4594	0.0713	0.0098		1.9923	0.1601	0.168
Mn	0.6840		6.4920	0.0841	**0.6196**	**1.3497**	**74.5841**	**0.0000**	**0.1914**	**0.8164**	**49.0223**	**0.0000**	**0.509**
Na	0.6297		5.1019	0.1091	**0.1882**	**1.1826**	**11.0747**	**0.0021**	0.0106		2.1473	0.1448	0.274
P	**0.9456**	**3.6743**	**52.1360**	**0.0055**	0.0319		1.4823	0.2316	0.0112		2.3320	0.1287	–0.052
S	0.0877		0.2884	0.6285	**0.6838**	**1.9605**	**113.9148**	**0.0000**	**0.0909**	**0.5162**	**20.9260**	**0.0000**	**0.513**
Zn	0.1532		0.5426	0.5147	**0.2756**	**0.9933**	**16.3341**	**0.0003**	0.0168		3.4379	0.0656	0.284

Table 25. Partial DCA ordination of the total data set with meso plots from Lund excluded (variation due to 7 regional variables partialled out): Split-plot GLM analysis with three levels and Kendall's nonparametric correlation coefficient τ between DCA 2 and 31 environmental variables and 7 regional variables (predictors) in the 50 plots. df_{resid}: degrees of freedom for the residuals; SS: total variation; FVE: fraction of total variation attributable to a given scale (area, macro plot or plot); SS_{expl}/SS: fraction of the variation attributable to the scale in question, explained by a variable; r: model coefficient (only given when significant at the $\alpha = 0.05$ level, otherwise blank); F: F statistic for test of the hypothesis that $r = 0$ against the two-tailed alternative. * no variation on this scale level. Split-plot GLM relationships significant at level $\alpha = 0.05$, P, F, r and SS_{expl}/SS, and Kendall's nonparametric correlation coefficient $|\tau| \geq 0.30$ are given in bold face. Numbers and abbreviations for names of environmental variables are in accordance with Table 2.

Predictor	Dependent variable = DCA 2 ($SS = 23.5077$) Error level												Correlation between predictor and DCA 2
	Area $df_{resid} = 3$ $SS_{macro\ plot} = 11.6650$ $FVE = 0.4962$ of SS				Macro plot within area $df_{resid} = 44$ $SS_{meso\ plot} = 9.3172$ $FVE = 0.3963$ of SS				Meso plot within macro plot $df_{resid} = 199$ $SS_{meso\ plot} = 2.5255$ $FVE = 0.1074$ of SS				Total
	$SS_{expl}/SS_{macro\ plot}$	r	F	P	$SS_{expl}/SS_{meso\ plot}$	r	F	P	$SS_{expl}/SS_{meso\ plot}$	r	F	P	τ
Ma Slo	0.0057		0.0173	0.9037	0.0521		2.1842	0.1484	0.0006		0.1168	0.7330	0.120
Ma Asp	0.0458		0.1440	0.7296	0.0722		3.1263	0.0858	0.0007		0.1259	0.7232	0.127
Ma HI	0.0172		0.0525	0.8336	0.0007		0.0237	0.8785	0.0016		0.3108	0.5780	–0.005
Ma Ter	0.0023		0.0068	0.9396	0.0093		0.3379	0.5648	0.0023		0.4468	0.5049	0.003
Ma Une	0.1276		0.4388	0.5550	0.0037		0.1345	0.7160	0.0126		2.4372	0.1205	–0.050
TBA	0.0824		0.2693	0.6396	**0.2444**	**0.5453**	**12.5646**	**0.0011**	**0.0256**	**0.0762**	**4.9631**	**0.0273**	0.181
Me Slo	0.6969		6.8973	0.0786	**0.1483**	**0.6719**	**6.9111**	**0.0126**	0.0006		0.1156	0.7343	**0.338**
Me Asp	0.0777		0.2527	0.6498	0.0282		1.0761	0.3067	0.0002		0.0473	0.8281	0.058
Me HI	0.1054		0.3536	0.5939	0.0002		0.0062	0.9376	0.0035		0.6777	0.4116	–0.033
Me Ter	0.7172		7.6095	0.0702	0.0053		0.1933	0.6628	0.0065		1.2493	0.2654	0.022
Me Une	0.0112		0.0341	0.8652	0.0042		0.1519	0.6990	0.0002		0.0302	0.8624	0.006
Smi	0.2906		1.2289	0.3485	0.0855		3.4434	0.0719	0.0093		1.7994	0.1817	–0.102
Sme	0.7224		7.8072	0.0682	**0.1187**	**–0.4301**	**5.1135**	**0.0301**	0.0127		2.4466	0.1198	–0.171
Sma	0.7122		7.4227	0.0723	0.0293		1.1251	0.2961	**0.0271**	**–0.0929**	**5.2595**	**0.0231**	0.176
Mme	0.0624		0.1996	0.6853	0.0246		0.9261	0.3425	0.0101		1.9279	0.1669	–0.161
LOI	0.0171		0.0522	0.8340	**0.1040**	**–0.2816**	**4.4011**	**0.0432**	0.0014		0.2602	0.6107	–0.185
Total N	0.4545		2.5000	0.2120	0.0697		2.7992	0.1032	0.0195		3.7708	0.0539	0.248

Table 25 (Cuntinued). Partial DCA ordination of the total data set with meso plots from Lund excluded (variation due to 7 regional variables partialled out): Split-plot GLM analysis with three levels and Kendall's nonparametric correlation coefficient τ between DCA 2 and 31 environmental variables and 7 regional variables (predictors) in the 50 plots. df_{resid}: degrees of freedom for the residuals; *SS*: total variation; *FVE*: fraction of total variation attributable to a given scale (area, macro plot or plot); SS_{expl}/SS: fraction of the variation attributable to the scale in question, explained by a variable; *r*: model coefficient (only given when significant at the α = 0.05 level, otherwise blank); *F*: *F* statistic for test of the hypothesis that *r* = 0 against the two-tailed alternative. * no variation on this scale level. Split-plot GLM relationships significant at level α = 0.05, *P*, *F*, *r* and SS_{expl}/SS, and Kendall's nonparametric correlation coefficient $|\tau| \geq 0.30$ are given in bold face. Numbers and abbreviations for names of environmental variables are in accordance with Table 2.

Predictor	Dependent variable = DCA 2 (*SS* = 23.5077) Error level												Correlation between predictor and DCA 2
	Area df_{resid} = 3 $SS_{macro\ plot}$ = 11.6650 *FVE* = 0.4962 of *SS*				Macro plot within area df_{resid} = 44 $SS_{meso\ plot}$ = 9.3172 *FVE* = 0.3963 of *SS*				Meso plot within macro plot df_{resid} = 199 $SS_{meso\ plot}$ = 2.5255 *FVE* = 0.1074 of *SS*				Total
	$SS_{expl}/SS_{macro\ plot}$	*r*	*F*	*P*	$SS_{expl}/SS_{meso\ plot}$	*r*	*F*	*P*	$SS_{expl}/SS_{meso\ plot}$	*r*	*F*	*P*	τ
pH_{H_2O}	0.0587		0.1871	0.6946	0.0853		3.5993	0.0661	0.0005		0.0867	0.7688	0.187
pH_{CaCl_2}	0.1338		0.4633	0.5449	0.0829		3.5067	0.0695	0.0006		0.1107	0.7398	0.187
H	0.0389		0.1215	0.7505	0.0767		3.2103	0.0818	**0.0519**	**–0.1797**	**10.2998**	**0.0016**	–0.181
Al	0.5119		3.1469	0.1742	0.0178		0.6751	0.4169	**0.0210**	**–0.1170**	**4.0898**	**0.0448**	–0.114
C	0.2142		0.8179	0.4325	**0.1546**	**0.4277**	**7.0515**	**0.0118**	0.0000		0.0049	0.9444	0.185
Ca	0.2657		1.0854	0.3741	0.0135		0.5177	0.4766	**0.0556**	**0.2298**	**11.2499**	**0.0010**	0.122
Fe	0.4036		2.0299	0.2494	0.0074		0.2702	0.6065	0.0045		0.8725	0.3517	–0.015
K	0.0828		0.2707	0.6388	**0.3211**	**0.5769**	**18.2208**	**0.0001**	**0.0384**	**0.1241**	**7.4801**	**0.0069**	0.218
Mg	0.0402		0.1258	0.7463	**0.2775**	**0.5639**	**14.6870**	**0.0005**	**0.0502**	**0.2029**	**9.9536**	**0.0019**	0.194
Mn	0.6529		5.6431	0.0980	**0.1271**	**0.3336**	**5.7919**	**0.0215**	0.0023		0.4425	0.5069	0.242
Na	0.2778		1.1541	0.3614	0.0503		1.9153	0.1751	0.0151		2.9059	0.0902	0.049
P	0.2989		1.2789	0.3403	0.0260		0.9755	0.3301	0.0059		1.1209	0.2913	0.033
S	0.0783		0.2549	0.6484	**0.1699**	**0.4769**	**8.0191**	**0.0076**	0.0013		0.2486	0.6188	0.181
Zn	0.5816		4.1694	0.1338	0.0049		0.1793	0.6746	0.0045		0.8608	0.3549	0.050

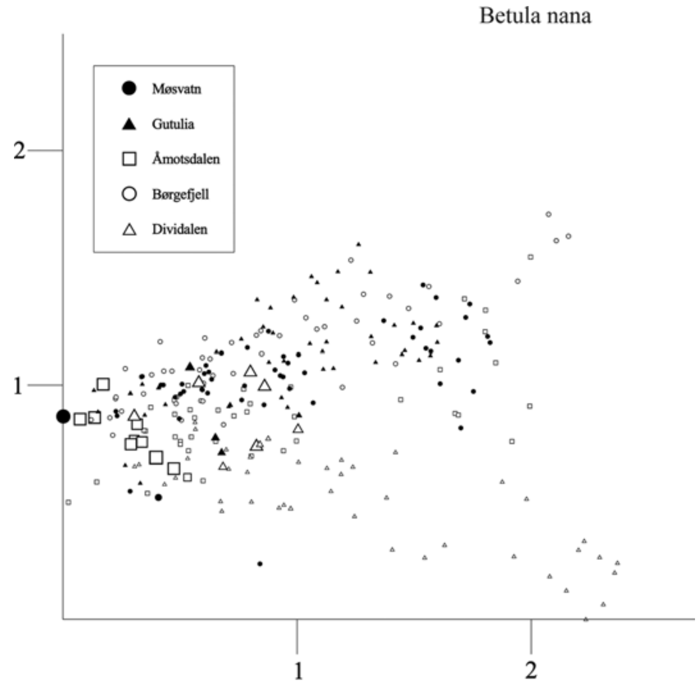

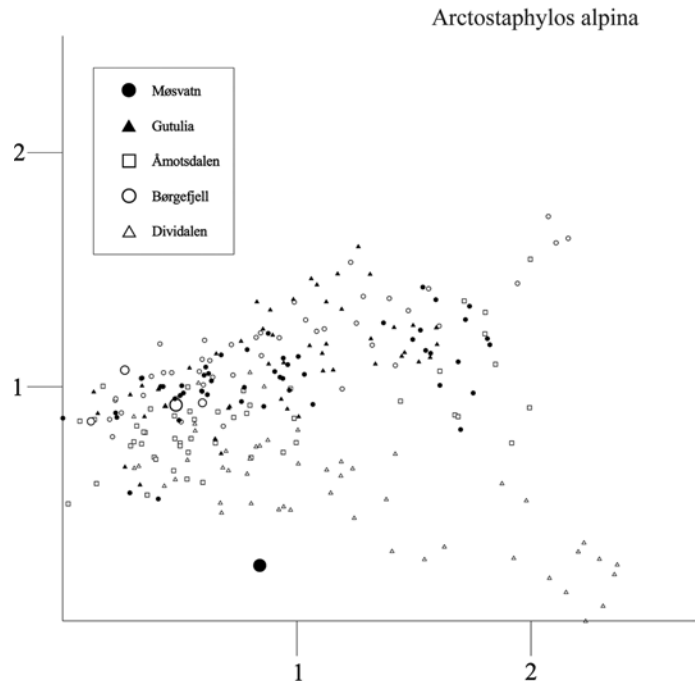

Figs 409-410. The total data set (Lund not included): distributions of species abundances in the DCA ordination of 250 meso plots, axes 1 (horizontal) and 2 (vertical).Frequency in subplots for *Betula nana* (Fig. 409) and *Arctostaphylos alpina* (Fig. 410) in each meso plot proportional to symbol size. Scaling of axes in S.D. units.

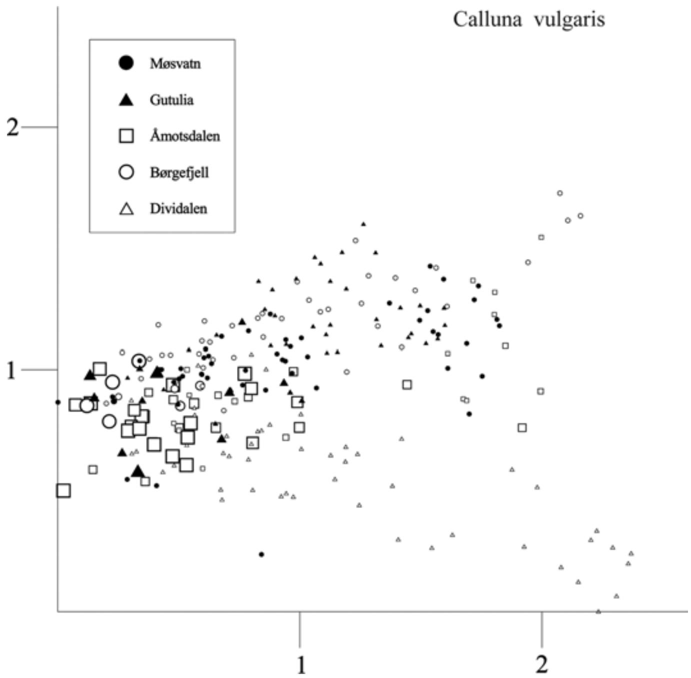

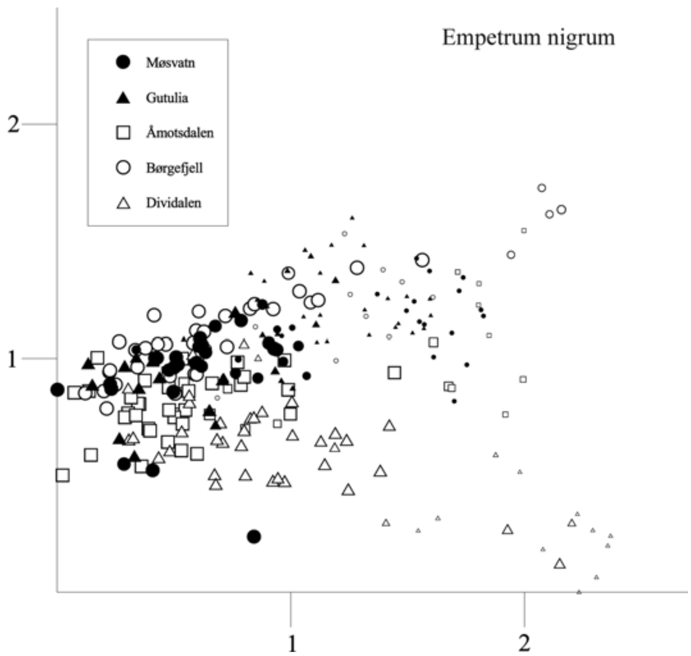

Figs 411-412. The total data set (Lund not included): distributions of species abundances in the DCA ordination of 250 meso plots, axes 1 (horizontal) and 2 (vertical). Frequency in subplots for *Calluna vulgaris* (Fig. 411) and *Empetrum nigrum* (Fig. 412) in each meso plot proportional to symbol size. Scaling in S.D. units.

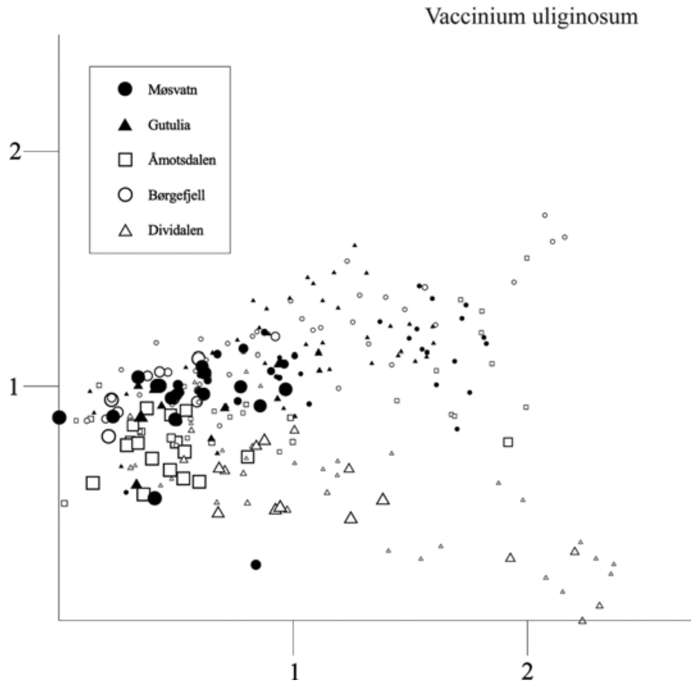

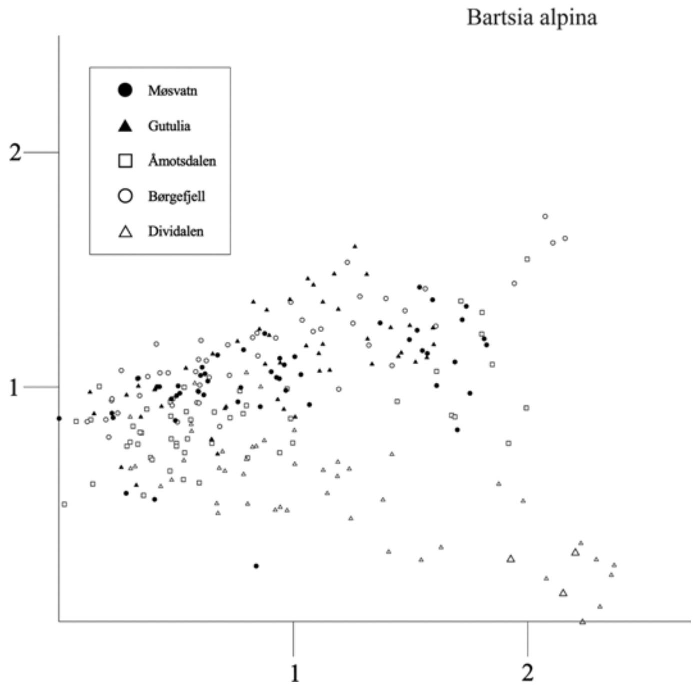

Figs 413-414. The total data set (Lund not included): distributions of species abundances in the DCA ordination of 250 meso plots, axes 1 (horizontal) and 2 (vertical). Frequency in subplots for *Vaccinium uliginosum* (Fig. 413) and *Bartsia alpina* (Fig. 414) in each meso plot proportional to symbol size. Scaling in S.D. units.

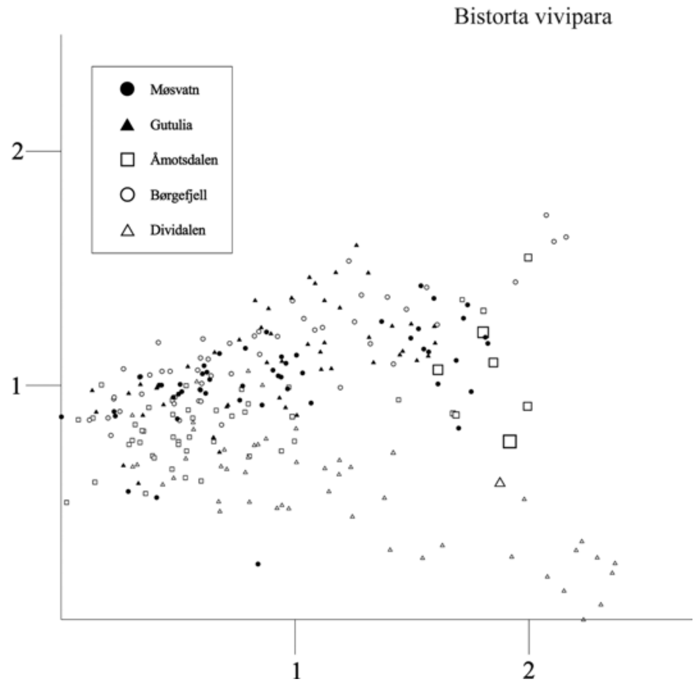

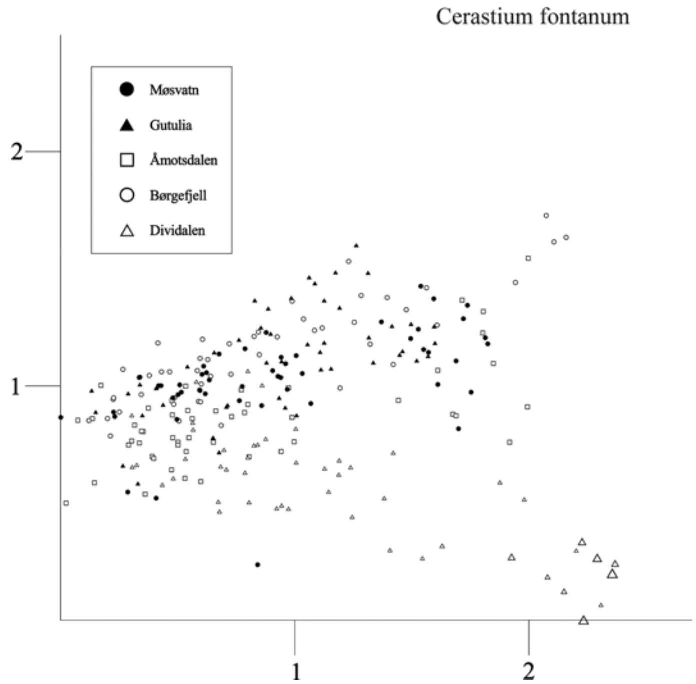

Figs 415-416. The total data set (Lund not included): distributions of species abundances in the DCA ordination of 250 meso plots, axes 1 (horizontal) and 2 (vertical). Frequency in subplots for *Bistorta vivpara* (Fig. 415) and *Cerastium fontanum* (Fig. 416) in each meso plot proportional to symbol size. Scaling in S.D. units.

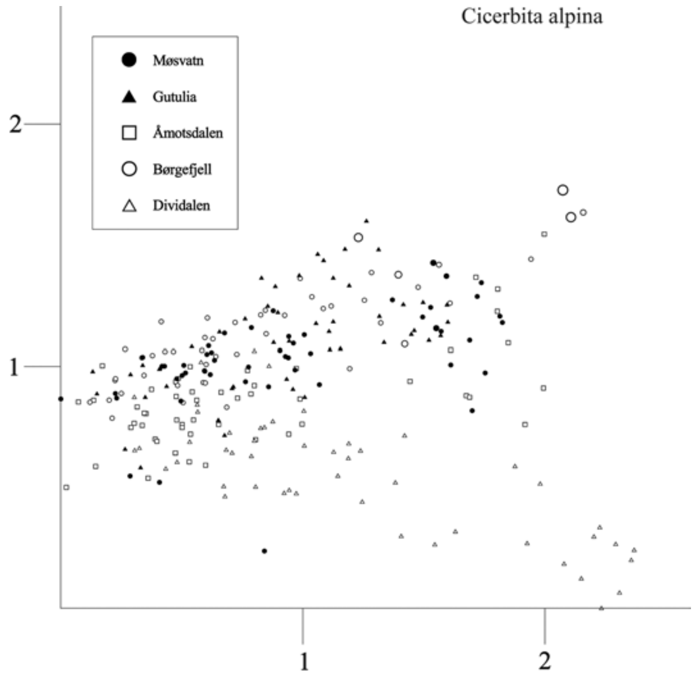

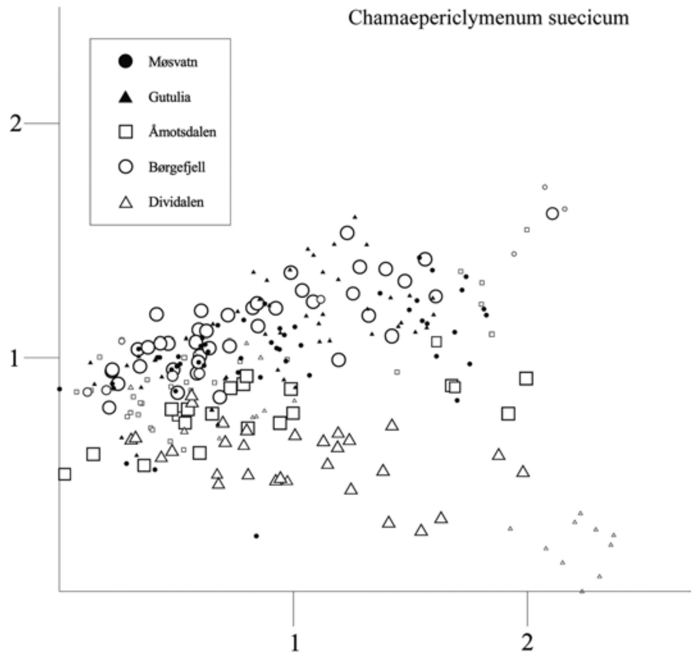

Figs 417-418. The total data set (Lund not included): distributions of species abundances in the DCA ordination of 250 meso plots, axes 1 (horizontal) and 2 (vertical). Frequency in subplots for *Cicerbita alpina* (Fig. 417) and *Chamaepericlymenum suecicum* (Fig. 418) in each meso plot proportional to symbol size. Scaling in S.D. units.

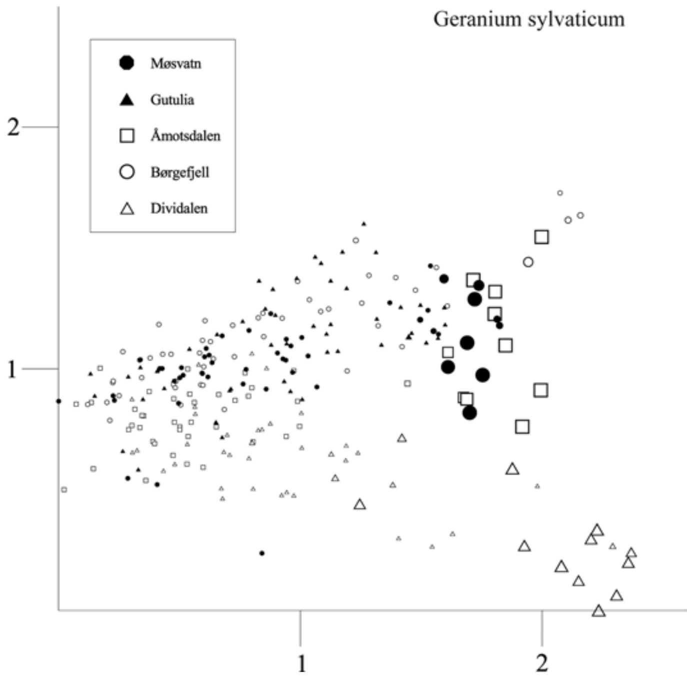

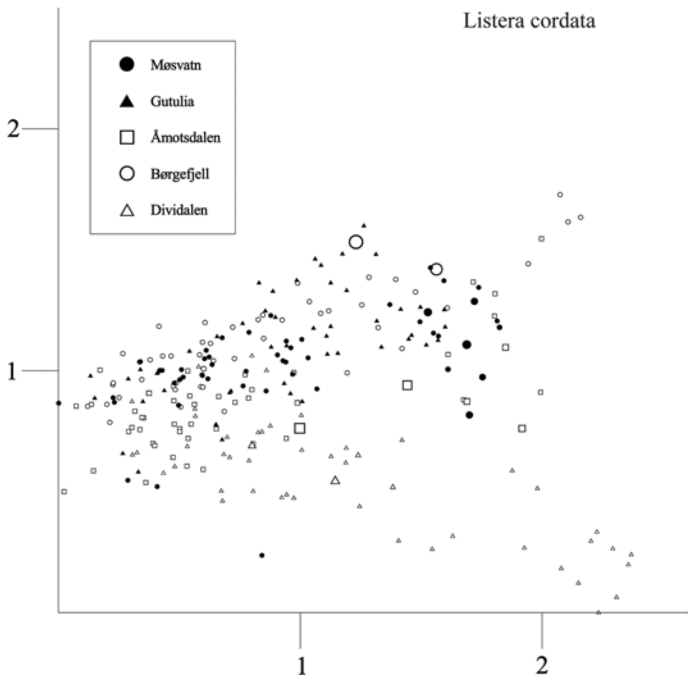

Figs 419-420. The total data set (Lund not included): distributions of species abundances in the DCA ordination of 250 meso plots, axes 1 (horizontal) and 2 (vertical). Frequency in subplots for *Geranium sylvaticum* (Fig. 419) and *Listera cordata* (Fig. 420) in each meso plot proportional to symbol size. Scaling in S.D. units.

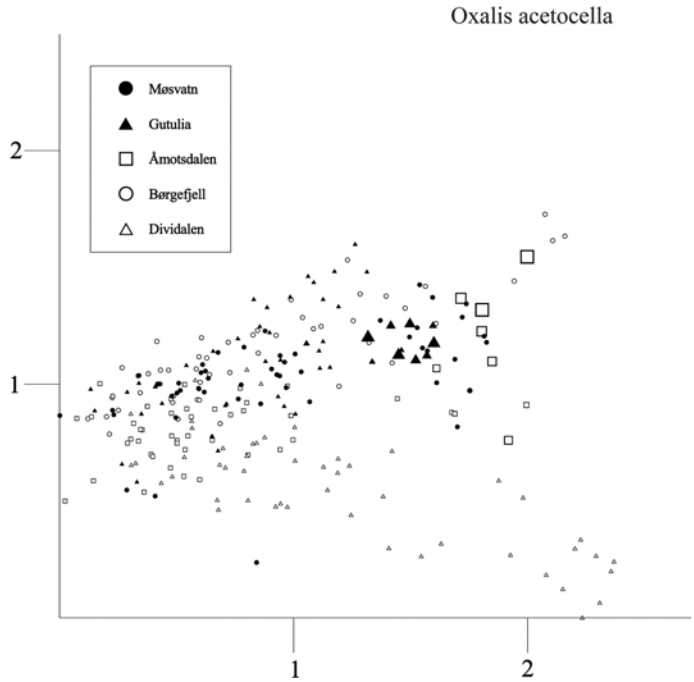

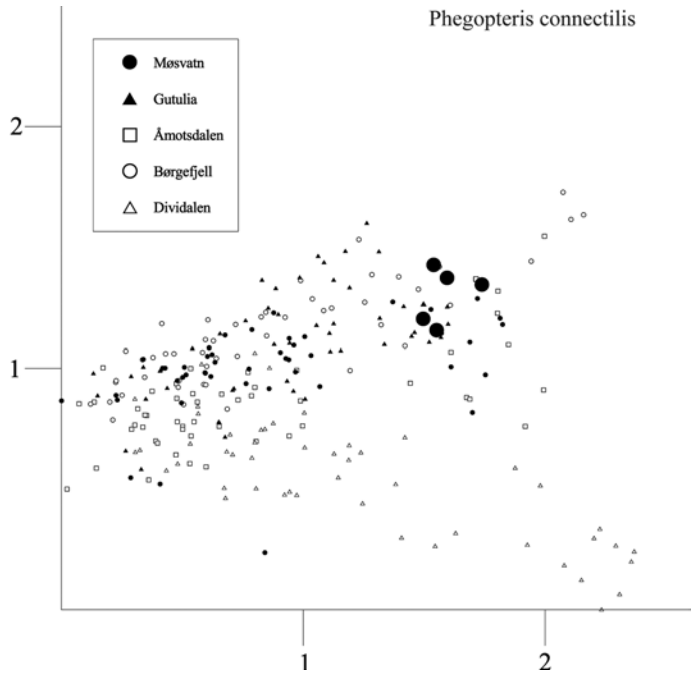

Figs 421-422. The total data set (Lund not included): distributions of species abundances in the DCA ordination of 250 meso plots, axes 1 (horizontal) and 2 (vertical). Frequency in subplots for *Oxalis acetocella* (Fig. 421) and *Phegopteris connectilis* (Fig. 422) in each meso plot proportional to symbol size. Scaling in S.D. units.

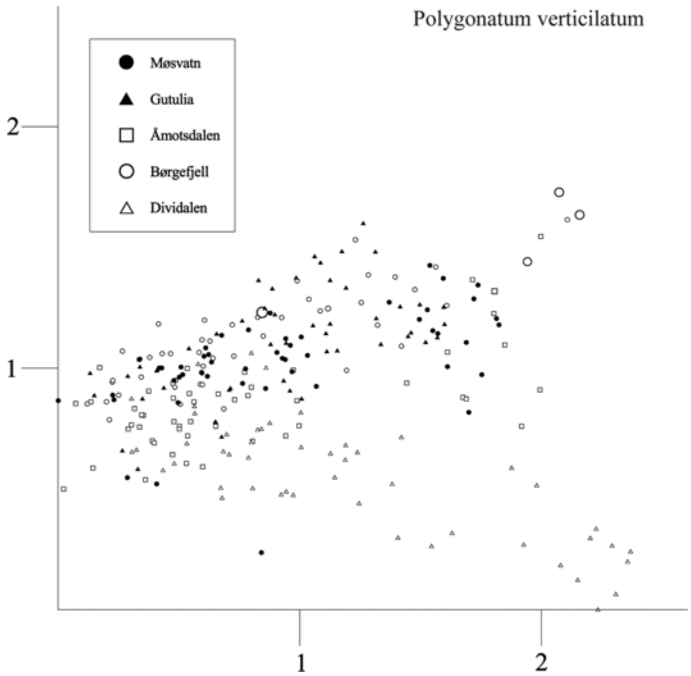

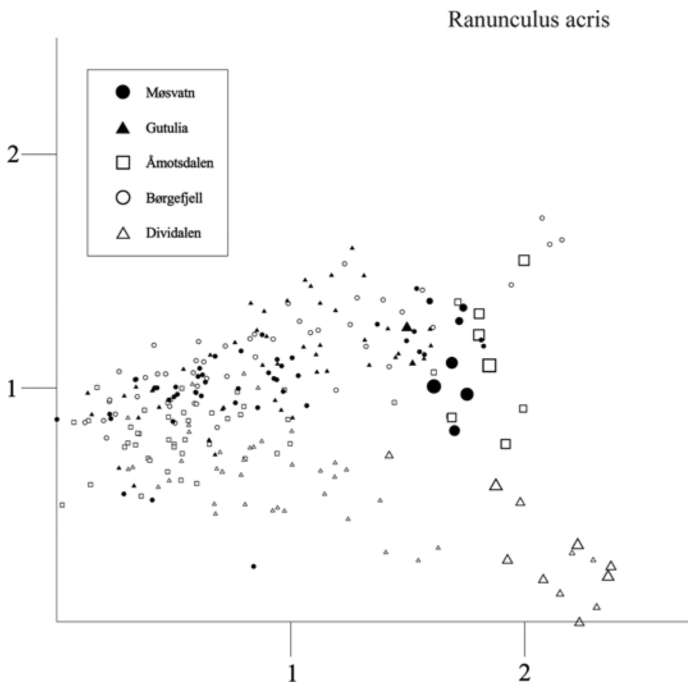

Figs 423-424. The total data set (Lund not included): distributions of species abundances in the DCA ordination of 250 meso plots, axes 1 (horizontal) and 2 (vertical). Frequency in subplots for *Polygonatum verticilatum* (Fig. 423) and *Ranunculus acris* (Fig. 424) in each meso plot proportional to symbol size. Scaling in S.D. units.

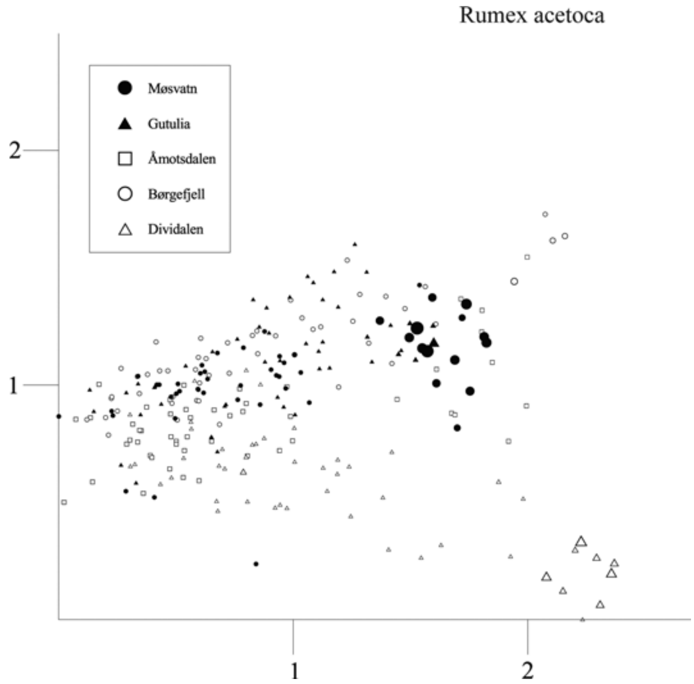

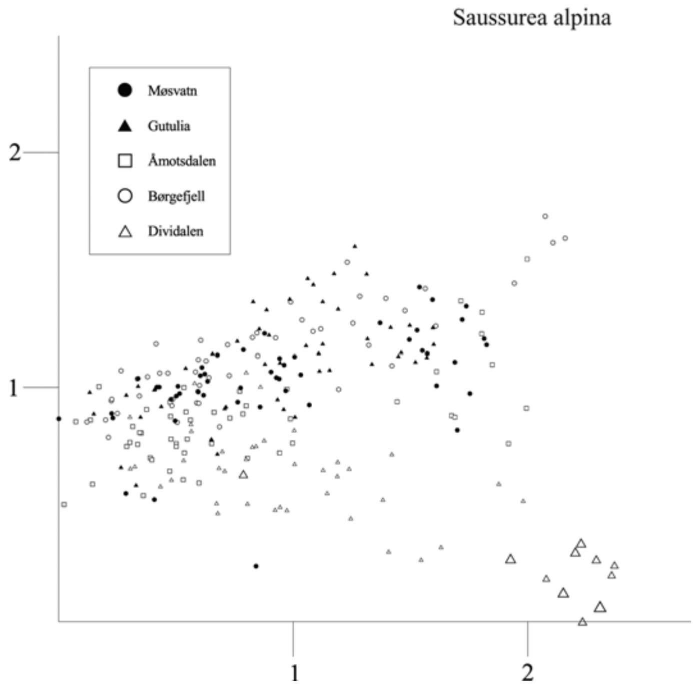

Figs 425-426. The total data set (Lund not included): distributions of species abundances in the DCA ordination of 250 meso plots, axes 1 (horizontal) and 2 (vertical). Frequency in subplots for *Rumex acetosa* (Fig. 425) and *Saussurea alpina* (Fig. 426) in each meso plot proportional to symbol size. Scaling in S.D. units.

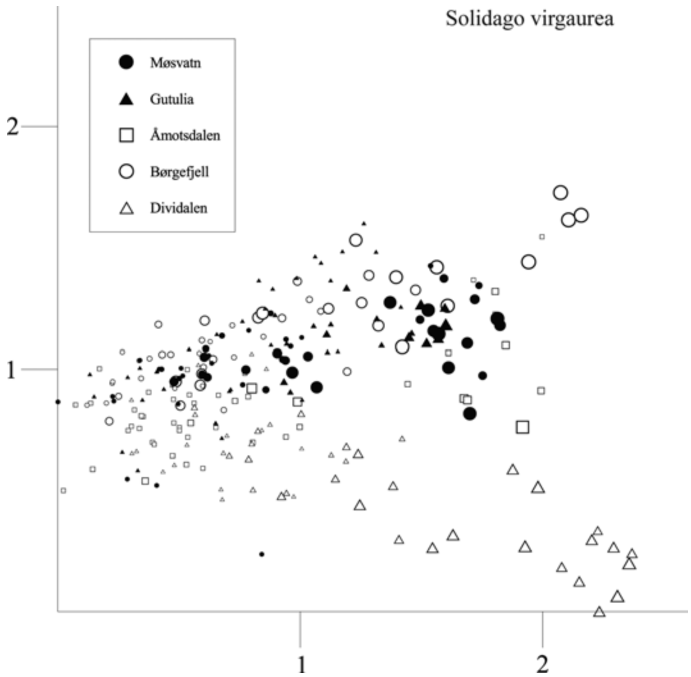

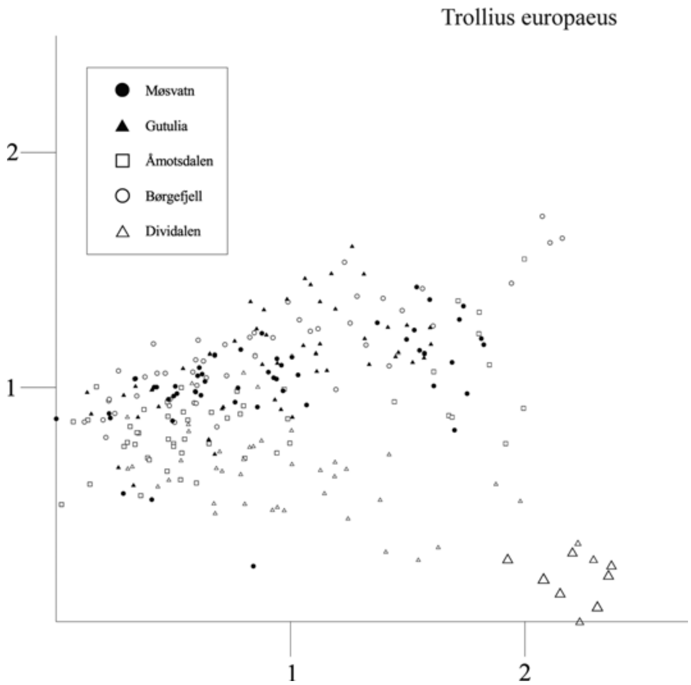

Figs 427-428. The total data set (Lund not included): distributions of species abundances in the DCA ordination of 250 meso plots, axes 1 (horizontal) and 2 (vertical). Frequency in subplots for *Solidago virgaurea* (Fig. 427) and *Trollius europaeus* (Fig. 428) in each meso plot proportional to symbol size. Scaling in S.D. units.

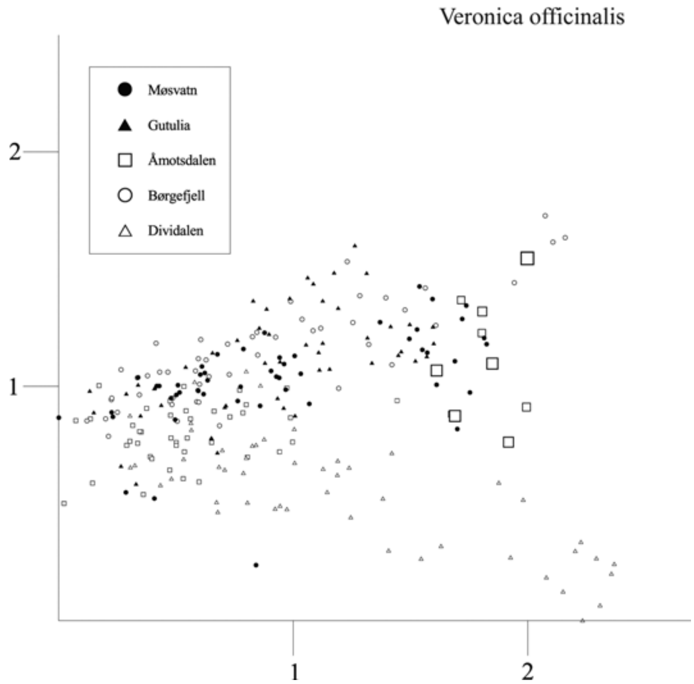

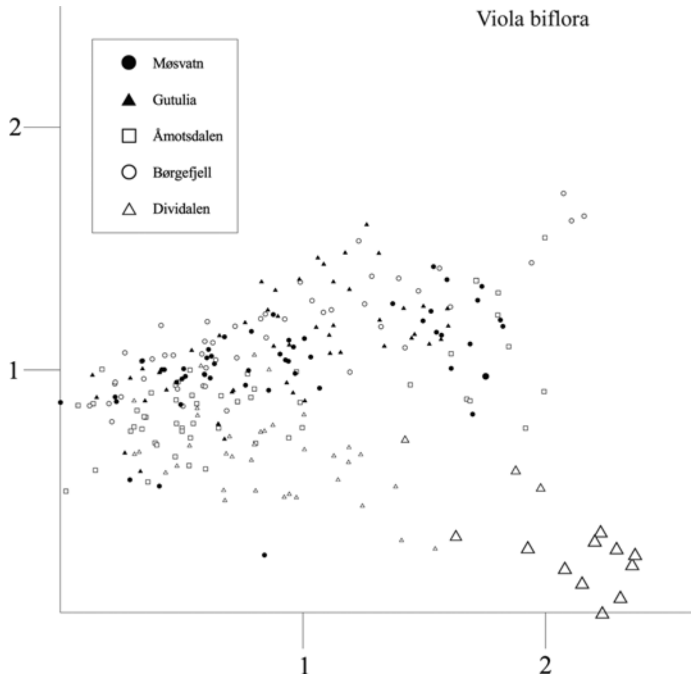

Figs 429-430. The total data set (Lund not included): distributions of species abundances in the DCA ordination of 250 meso plots, axes 1 (horizontal) and 2 (vertical). Frequency in subplots for *Veronica officinalis* (Fig. 429) and *Viola biflora* (Fig. 430) in each meso plot proportional to symbol size. Scaling in S.D. units.

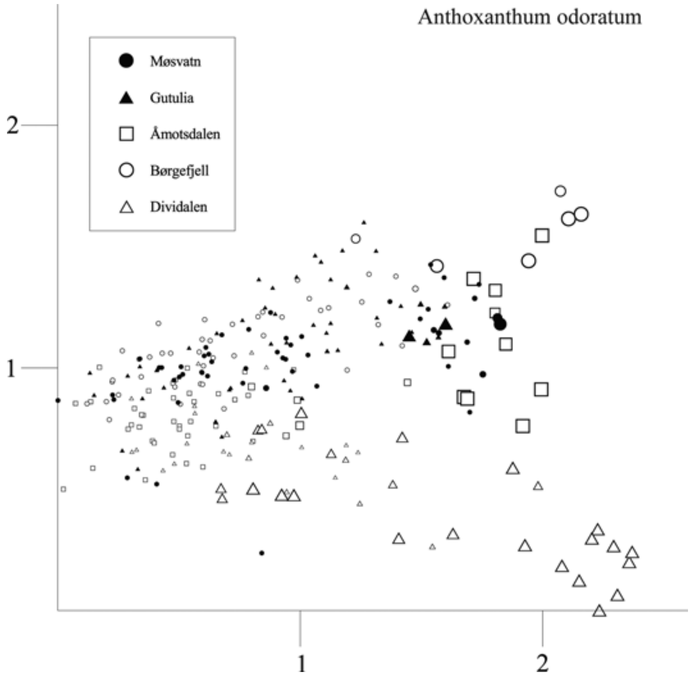

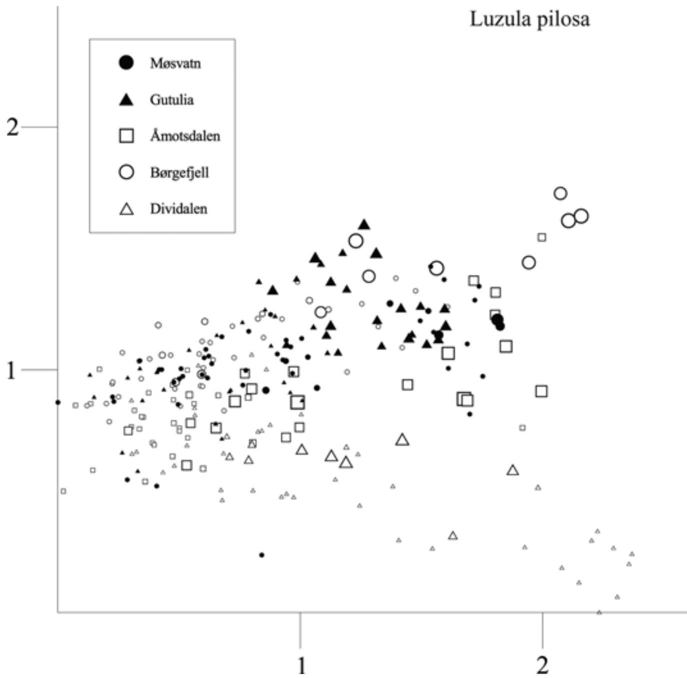

Figs 431-432. The total data set (Lund not included): distributions of species abundances in the DCA ordination of 250 meso plots, axes 1 (horizontal) and 2 (vertical). Frequency in subplots for *Anthoxanthum odoratum* (Fig. 431) and *Luzula pilosa* (Fig. 432) in each meso plot proportional to symbol size. Scaling in S.D. units.

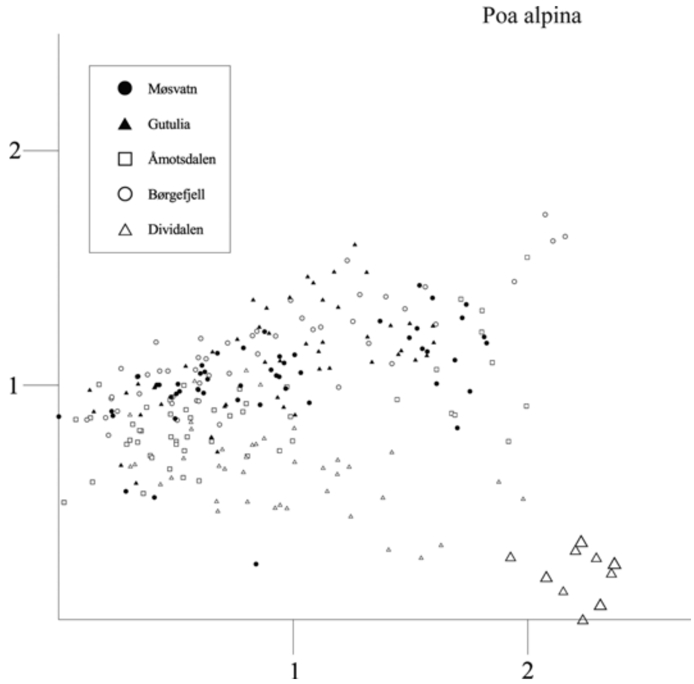

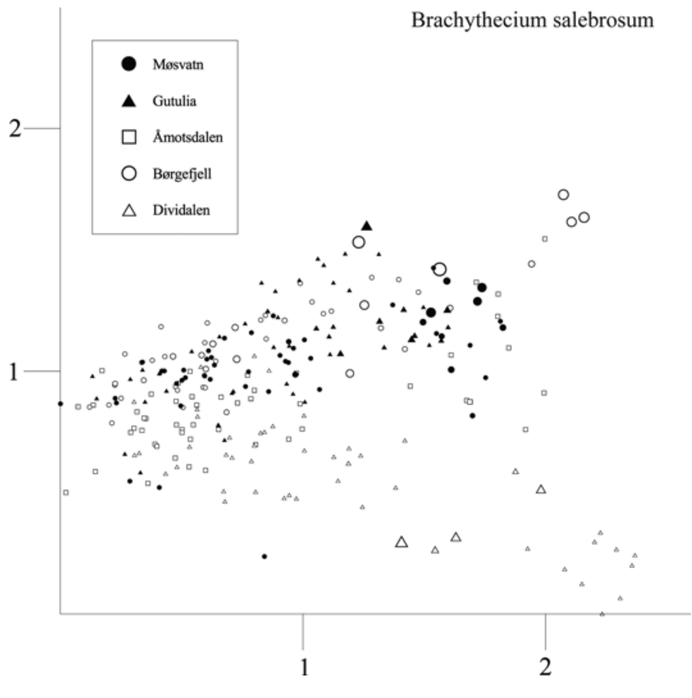

Figs 433-434. The total data set (Lund not included): distributions of species abundances in the DCA ordination of 250 meso plots, axes 1 (horizontal) and 2 (vertical). Frequency in subplots for *Poa alpina* (Fig. 433) and *Brachythecium salebrosum* (Fig. 434) in each meso plot proportional to symbol size. Scaling in S.D. units.

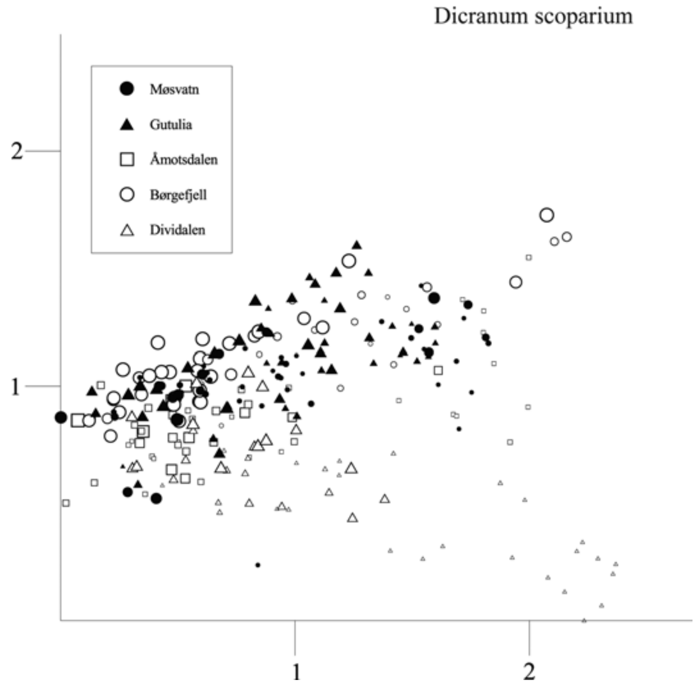

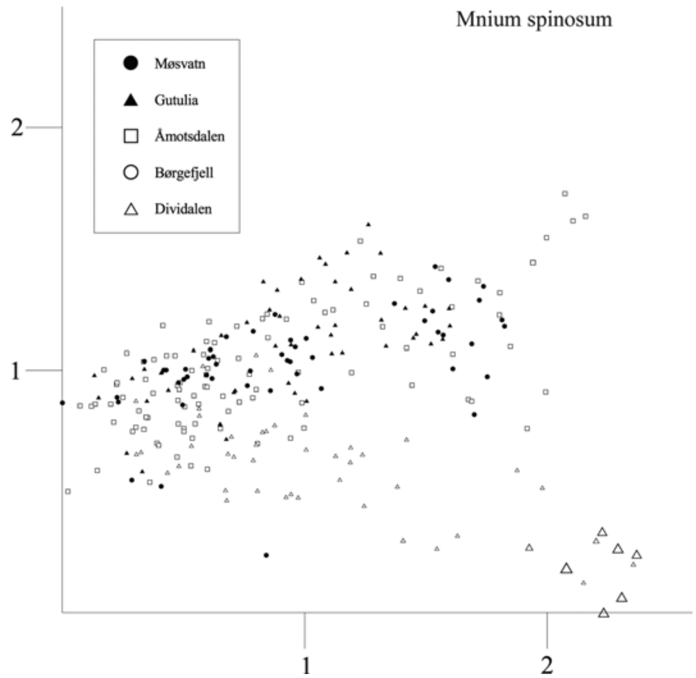

Figs 435-436. The total data set (Lund not included): distributions of species abundances in the DCA ordination of 250 meso plots, axes 1 (horizontal) and 2 (vertical). Frequency in subplots for *Dicranum scoparium* (Fig. 435) and *Mnium spinosum* (Fig. 436) in each meso plot proportional to symbol size. Scaling in S.D. units.

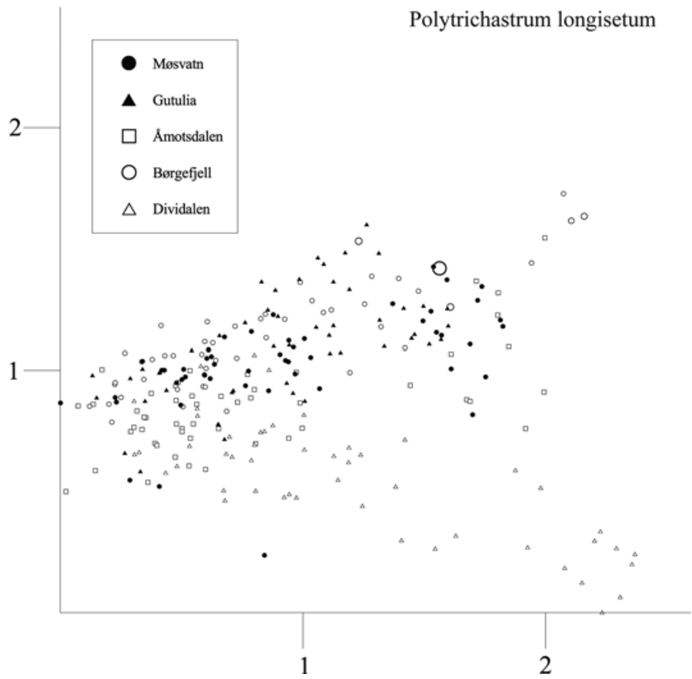

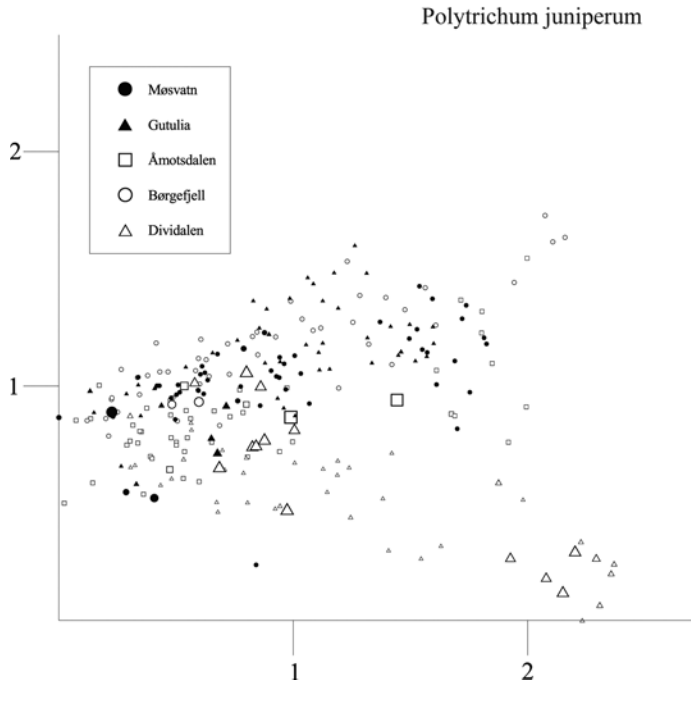

Figs 437-438. The total data set (Lund not included): distributions of species abundances in the DCA ordination of 250 meso plots, axes 1 (horizontal) and 2 (vertical). Frequency in subplots for *Polytrichastrum longisetum* (Fig. 437) *Polytrichum juniperum* (Fig. 438) in each meso plot proportional to symbol size. Scaling in S.D. units.

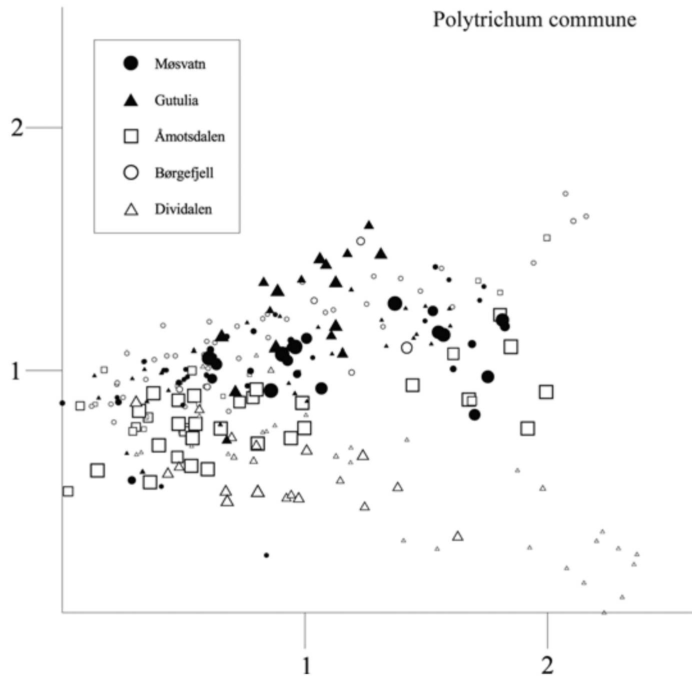

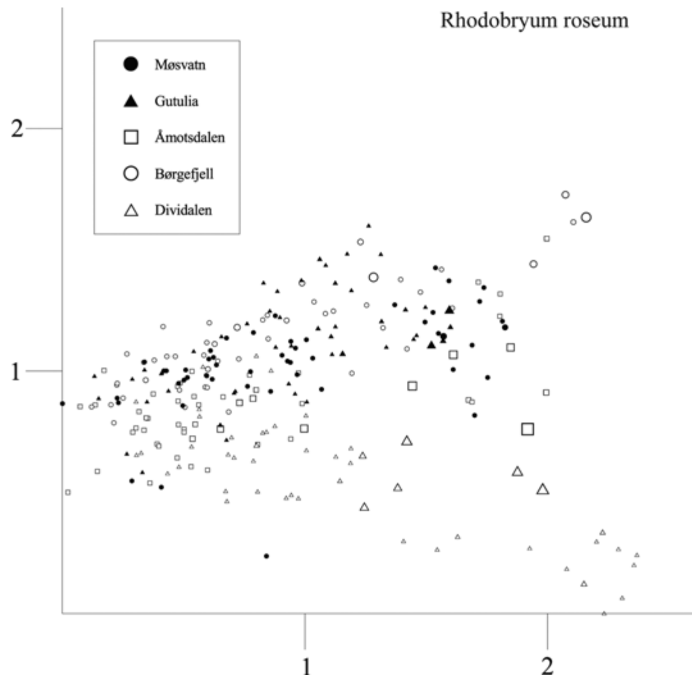

Figs 439-440. The total data set (Lund not included): distributions of species abundances in the DCA ordination of 250 meso plots, axes 1 (horizontal) and 2 (vertical). Frequency in subplots for *Polytrichum commune* (Fig. 439) and *Rhodobryum roseum* (Fig. 440) in each meso plot proportional to symbol size. Scaling in S.D. units.

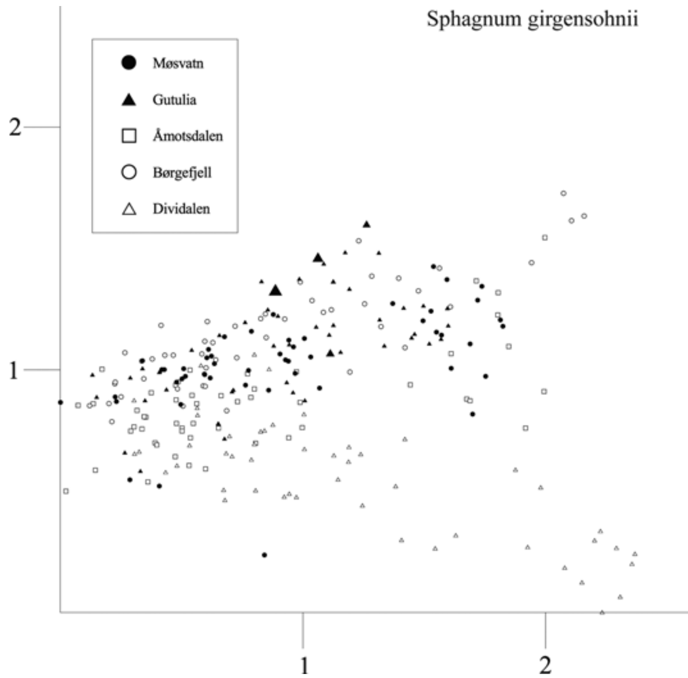

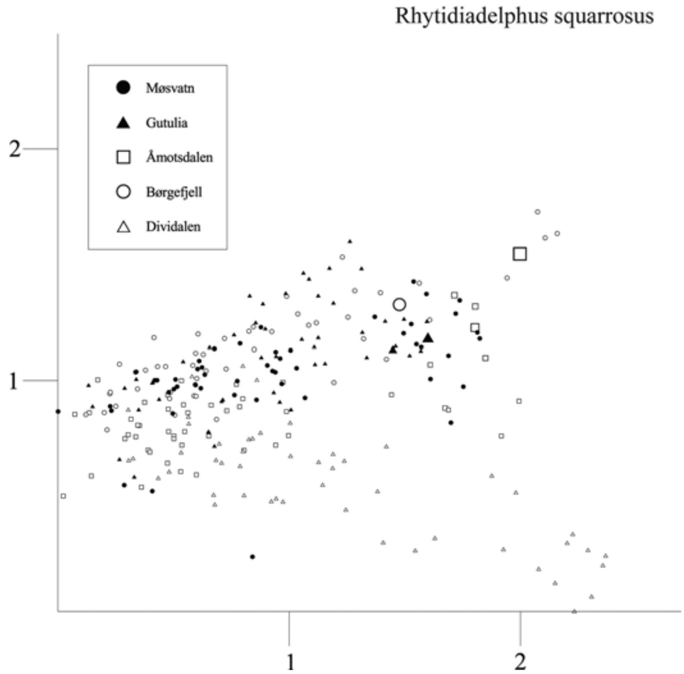

Figs 441-442. The total data set (Lund not included): distributions of species abundances in the DCA ordination of 250 meso plots, axes 1 (horizontal) and 2 (vertical). Frequency in subplots for *Sphagnum girgensohnii* (Fig. 441) and *Rhytidiadelphus squarrosus* (Fig. 442) in each meso plot proportional to symbol size. Scaling in S.D. units.

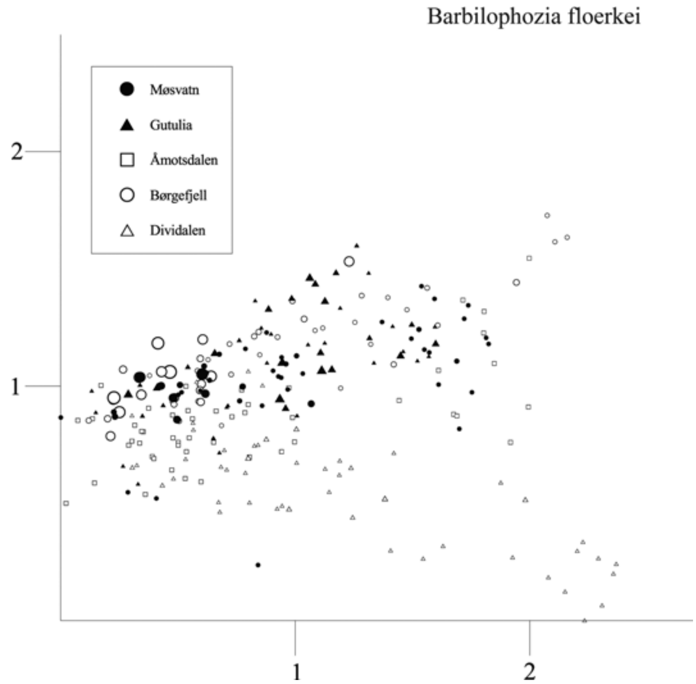

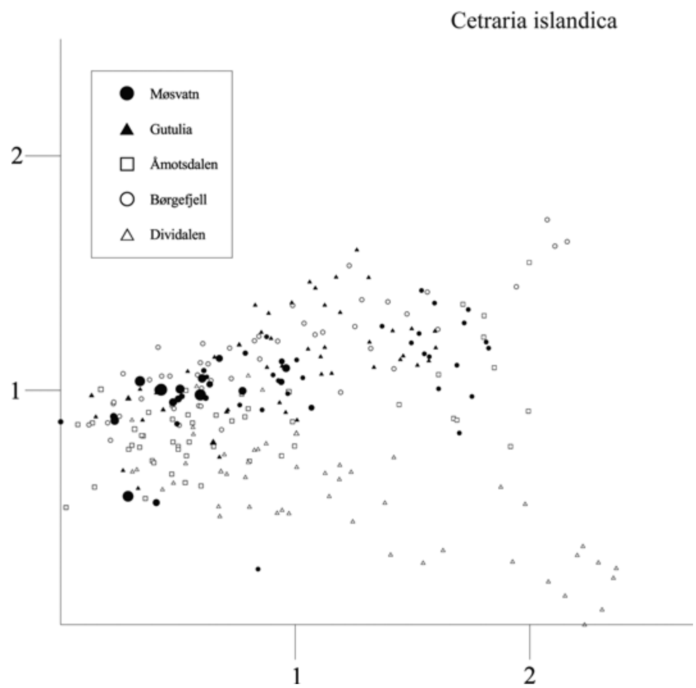

Figs 443-444. The total data set (Lund not included): distributions of species abundances in the DCA ordination of 250 meso plots, axes 1 (horizontal) and 2 (vertical). Frequency in subplots for *Barbilophozia floerkei* (Fig. 443) and *Cetraria islandica* (Fig. 444) in each meso plot proportional to symbol size. Scaling in S.D. units.

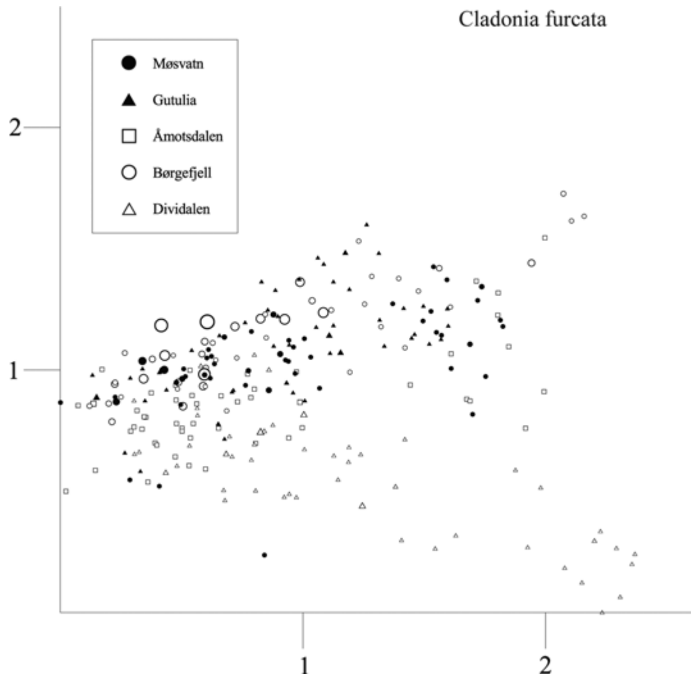

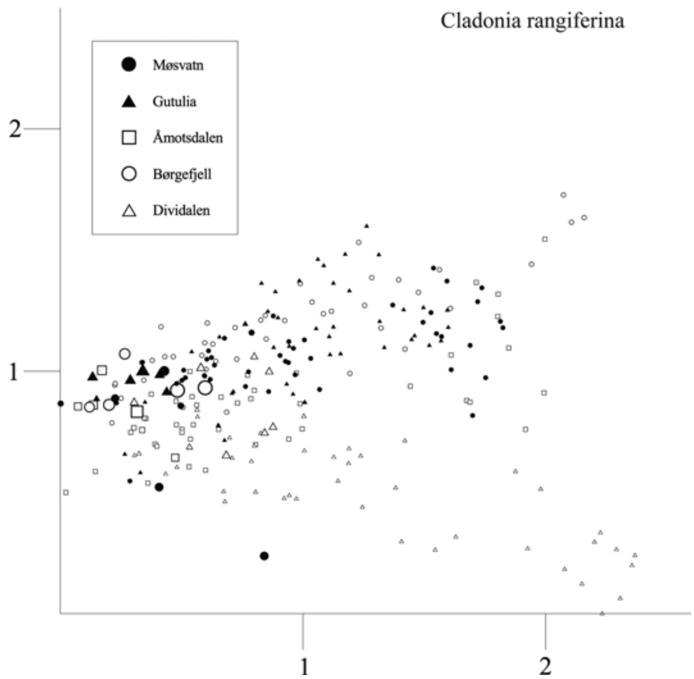

Figs 445-446. The total data set (Lund not included): distributions of species abundances in the DCA ordination of 250 meso plots, axes 1 (horizontal) and 2 (vertical). Frequency in subplots for *Cladonia furcata* (Fig. 445) and *Cladonia rangiferina* (Fig. 446) in each meso plot proportional to symbol size. Scaling in S.D. units.

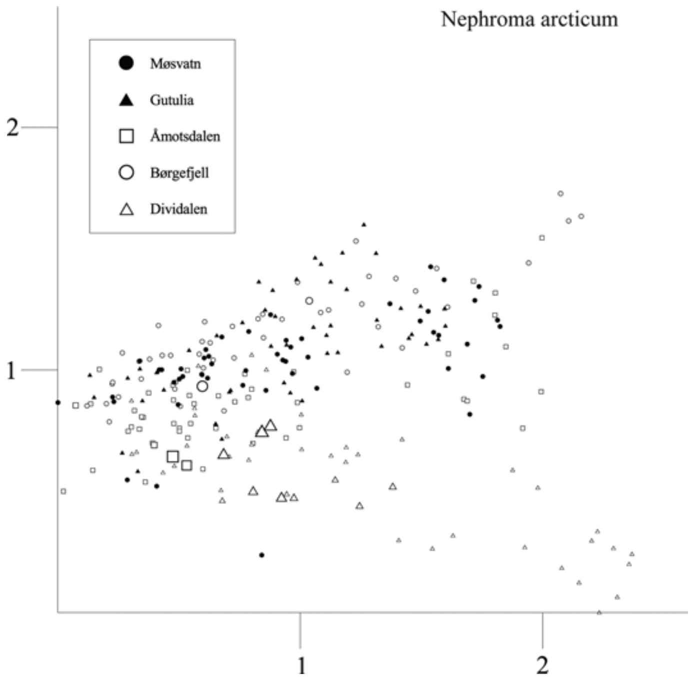

Fig. 447. The total data set (Lund not included): distributions of species abundances in the DCA ordination of 250 meso plots, axes 1 (horizontal) and 2 (vertical). Frequency in subplots for *Nephroma arcticum* in each meso plot proportional to symbol size. Scaling in S.D. units.

DISCUSSION

INTERPRETATION OF MAIN GRADIENTS IN SPECIES COMPOSITION IN EACH REFERENCE AREA

Lund

Sample plots from the Lund reference area span a short gradient in species composition; the gradient length of the first DCA axis is less than 2.5 SD (Fig. 9). The majority of the plots are characterized by species showing low demands for mineral nutrients, such as *Calluna vulgaris* and *Vaccinium* spp. and contain very few herbs (only *Melampyrum pratense*, *Trientalis europaea* and *Maianthemum bifolium* are common). A few plots (to the right in the DCA diagram) are characterized by slightly more nutrient demanding low-fern communities in which *Blechnum spicant*, *Gymnocarpium dryopteris* and *Phegopteris connectilis* occur, and tall fern plant communities with *Dryopteris expansa, Orepoteris limbosperma* and *Pteridium aquilinum* (see Figs 20-56). The relatively species-poor vegetation is probably a result of the acid bedrock (gneiss) of the area, which gives rise to nutrient-poor soils, and the unfavourable north-easterly aspect with low amounts of solar radiation reaching the ground.

Soil pH is by far the environmental variable most strongly related to the main vegetation gradient (DCA axis 1; Table 4). The lowest soil pH values are found in sample plots dominated by *Calluna vulgaris* to the left in the ordination diagram and the highest soil pH values are found in fern communities to the right in the diagram. This confirms our interpretation of the main coenocline (DCA axis 1) as mainly related to the nutrient richness and acid-base status of the soil. Further support from this interpretation comes from the increasing content of total N in soil samples with increasing scores along DCA axis 1.

Fern-dominated plots are found on the steepest slopes, where higher nutrient richness of soils can probably be explained by addition of nutrients by seepage water. However, this coenocline is also positively correlated with aspect unfavourability and negatively correlated with the heat indices, as they face northeast (Fig. 2). The unfavourable local climate of these rather steep northeast-exposed slopes can explain the sparse presence of thermophilous species in these plant communities.

Sample plots dominated by *Vaccinium myrtillus* mostly occur on less steep slopes while plots dominated by *Calluna vulgaris* are situated mainly on flat areas. Thus the variation in species composition in the Lund reference area is mainly caused by complex gradients in soil characteristics and topography-related microclimate. Nevertheless, the variation in species composition (and environmental factors) along these ecoclines is rather restricted.

In most studies of boreal forests soil the concentration of extractable Ca is one of the most important variables explaining variation in species composition, and this element is usually more or less strongly positively correlated with the concentration of extractable Mg and soil pH and negatively correlated with exchangeable H (e.g. Hesselman 1937, Malmstrøm 1949, Kuusipalo 1983b, Taylor et al. 1987, Aarrestad 2002). The Lund sample plots do, however, follow a different pattern with a negative correlation between concentrations of the base cations Ca and Mg on one hand, and soil pH on the other hand, and a positive correlation between pH and exchangeable H. This result strongly conflicts general soil theories on soil acidity (cf. Schroeder 1984). However, a negative correlation between Ca and pH is also found in oceanic spruce forests by T. Økland (1996), who concludes that in humid areas soil Ca is likely not to contribute to a complex-gradient in soil nutrient concentrations, as is typically the case in less humid areas.

On the other hand, the variation in soil characteristics between the 50 sample plots from the Lund reference area is very small. Thus even small errors in soil sampling and/or chemical analyses, or idiosyncracies of single plots or macro plots, may potentially have strong impact on the outcome of statistical analyses.

The second DCA axis for the Lund plots is significantly correlated with soil moisture, loss-on-ignition and topographical indices (Table 5). Thus the second main vegetation gradient is probably related to differences in soil moisture, also affected by variation in topography and buildup of humus and peat layers, as exemplified by the distribution of *Sphagnum quinquefarium* in the ordination diagram (Fig. 51).

Most of the floristic variation, represented by DCA axis 1, occurs on the between macro plot scale (84.49%). The correspondence between the split plot analyses (between macro plot level) and the Kendall nonparametric correlation coefficients is good. However, even if the variation between plots within macro plots is low, 15.51 %, this is in fact the largest amount of explained variation within macro plots found along DCA axis 1 among the six investigated reference areas. On this most detailed scale, meso plot unevenness together with pH (also the most important variable on the between macro plot level and the one most strongly correlated with DCA axis 1 according to Kendall's τ) are found to be the most important contributing variables. Also along DCA axis 2, the major fraction of variation along DCA axis 2 (78.76 %) occurs at the between macro plot level. Along this axis, the best predictor of species composition, revealed by the split-plot tests and by Kendall's τ, is soil moisture.

Møsvatn

In contrast to the Lund area the sample plots from the Møsvatn reference area span a long gradient in species composition. The gradient length of the first DCA axis is 4.5 SD units (Fig. 58). This gradient runs from lichen-dominated plots through bilberry-dominated woodland and small-fern communities to low- and tall herb woodland characterized by species often considered more eutrophic (Fremstad 1997) such as *Cicerbita alpina*, *Geranium sylvaticum, Ranunculus acris, Rumex acetosa* and tall grasses such as *Milium effusum* (Figs 78–125). The main coenocline at Møsvatn represents the longest vegetation gradient in terms of compositional turnover (S.D. units) in any of the six reference areas.

The main vegetation gradient, DCA axis 1, corresponds to a complex soil nutrient richness gradient, along which soil pH and soil nutrient concentrations (C, Ca, K, Mg, Mn, Na, S and total N) increase and loss-on-ignition and soil exchangeable H decrease (Figs 60-78, Table 7). This demonstrates affinity of plant communities with tall herbs to base-rich and nutrient-rich soils. Along the coenocline related to soil richness also slope and maximum soil depth increase while heat indices decrease. Plots richer in soil nutrients are thus typically situated in steeper north-exposed slopes and receive lower lower solar radiation input than other plots. These relatively steep slopes with soil of high nutrient content also have the highest tree density and probably also the highest tree biomass, as shown by the positive correlation of these variables with tree basal area (Table 7 and Fig. 63). The main compositional gradient mainly reflects variation between macro plots (93.62%). The agreement between results of split-plot analysis and Kendall's τ strengthens the interpretation.

The turnover of species along the first DCA axis also reflects variation normally interpreted as variation from drought-resistant to moisture-demanding vegetation. However, no significant or strong relation between soil moisture (Mme) and this axis is found. This may seem counter-intuitive because steep, northerly exposed plots with tall-herb communities are normally assumed to have higher soil water content due to influx of soil seepage water and lower solar radiation than the exposed ridges and less steep slopes with lichen and bilberry woodland (e. g. Schroeder 1984, Brunet 1991, Stoutjesdijk & Barkman 1992, R. Økland & Eilertsen 1993, Aarrestad 2002). The lack of a clear soil relationship of this main vegetation gradient with soil moisture may, however, be an effect of the bulk soil sampling process or of unknown amounts of precipitation immediately before the soil was sampled, levelling out recorded differences in soil moisture between the plots. Other explanations may also apply, like the 'soil moisture deficiency hypothesis' postulated by R. Økland & Eilertsen (1993) (see later in discussion under the 'The gradient in soil moisture' chapter.

The second vegetation gradient (DCA axis 2) is very short in terms of units of compositional turnover (cf. Fig. 58) and none of the measured variables are strongly related to DCA axis 2; the strongest is macro plot aspect ($\tau = 0.298$) and median soil depth; the latter is significant at the within macro-plot variation level in the split-plot analysis. Meso plots with high DCA 2 scores contain vegetation with high abundances of ferns such as *Phegopteris connectilis* while plots with low DCA 2 scores have a vegetation with indicators of soils richer in nutrients, such as *Geranium sylvaticum* and *Ranunculus acris.* Because of the very small amounts of variation in species composition along DCA axis 2, only separating plots in macro plot 9 from the rest, DCA axis 2 is not likely to represent an ecocline of general validity.

Gutulia

Sample plots in the Gutulia reference area span a shorter gradient in species composition than in the Møsvatn reference area; the gradient length of the first DCA axis is 2.8 SD (Fig. 127). The variation along the first DCA axis runs from species-poor dwarf shrub communities with dominance of *Empetrum nigrum* and *Vaccinium* species to slightly more species-rich communities with high abundance of low ferns, grasses and low herbs (Figs 140–196). Gutulia thus lacks tall fern and tall herb communities corresponding to those of the Møsvatn area.

The main vegetation gradient (DCA axis 1) corresponds to a complex soil mineral nutrient and soil base sattus gradient, running from nutrient-poor soils with high organic content in the humus layer and low pH to slightly more nutrient-rich soils with higher pH and lower organic content. This complex soil nutrient gradient is also to some extent related to soil depth, with lower minimum and median soil depths in soils richest in mineral nutrients (Figs 130 and 131). Almost all variation along this axis occurs at the between macro-plot scale level (95.35%). The correspondence between the split plot analysis for this level and Kendall's τ is good.

Only two environmental variables are significantly ($\alpha = 0.05$ level) related to the second DCA ordination axis; both at the macro-plot level at which 77.5% of the variation is explained. This is no more than expected by chance in a multiple-test situation (31 single tests are made at each scale level). In fact, DCA 2 only separates four plots from macro plot 9 and three plots from macro plot 10 from all other plots (these plots obtain high DCA 2 scores). The axis separates lichen-dominated plots with species such as *Cladonia arbuscula, C. bellidiflora, C.cornuta, C. crispata, C. gracilis and C. rangiferina* (Fig. 186, 187, 190, 191, 193,194) with optima at low DCA axis 2 scores from species such as *Rubus chamaemorus* and *Eriophorum vaginatum*. with optima at high DCA axis 2 scores. The high-score plots differ from the rest in having deep soils (Figs 130–131), but no difference in soil moisture was recorded, as suggested by the species compositions of plots occupying contrasting positions along this axis. Like in the Lund area, the lack of a clear soil moisture pattern might be due to errors related to the bulk soil sampling process or precipitation before the soil sampling event, levelling out differences in soil moisture between the plots. There is also a possibility that depth to the ground water table might explain more of this variation in species composition. Because DCA 2 separates small groups of plots only, it may reflect area-specific patterns rather than generally valid ecoclines.

Åmotsdalen

The main vegetation gradient in the Åmotsdalen reference area (DCA axis 1) runs from dwarf-shrub communities dominated by *Betula nana, Calluna vulgaris* and *Empetrum nigrum* with scattered lichens, to communities dominated by low ferns and herbs, with grasses and a few tall herbs such as *Geranium sylvaticum* and *Ranunculus acris*. The gradient length of the first DCA axis is 3.5 SD (Fig. 198 and Figs 212–248). The magnitude of compositional turnover along DCA axis 1 is somewhat larger than in Lund and Gutulia, but smaller than in the Møsvatn reference area.

The main vegetation gradient from dwarf-shrub dominated to herb dominated communities is related to a soil mineral nutrient and base richness gradient, running from low to higher soil pH values and from low to higher concentrations of base cations and total content of nitrogen (Table 13, Figs 200–211). Almost all variation along DCA axis 1 (96.03 %) occurred at the between macro-plot level. Like in the other reference areas, the split plot modelling results accorded well with Kendall's τ correlation coefficients. We conclude that, as in the other reference areas, variaton in soil mineral nutrient availability, is an important structuring factor for the main vegetation gradient.

The variation along the second ordination axis was more evenly split onto the two levels, with 56.03 % between and 43.97 % within macro plots. Only a few variables were significantly related to this axis and the consistency between the results of split-plot analyses and Kendall's τ was low. Soil moisture sorted out by Kendall's τ as relatively strongly related to the axis and indicatively significant ($0.05 < P < 0.10$) at both levels in the split-plot analysis (Table 14). The distributions of species along this axis, e.g. the *Cladonia* species (Figs 257–258) versus species such as *Geranium sylvaticum* and *Ranunculus acris* may suggest that soil moisture, in some way, may be partly responsible for variation along this coenocline. However, the ordination diagram (Fig. 198) also shows that three meso plots obtain particularly high scores along DCA axis 2 (plots 42, 46 and 38) and one plot (No. 33) obtains low score. This opens for the possibility that DCA axis 2 merely reflects peculiarities of the species compositions of single plots (a noise axis; Gauch 1982).

Børgefjell

The main vegetation gradient in the Børgefjell reference area runs from lichen-dominated dwarf shrub communities (dominance by *Cladonia* spp.; Figs 312–320) to low-herb and fern communities with scattered occurrences of tall ferns (*Dryopteris expansa*) and tall herbs (*Cicerbita alpina*). The main vegetation gradient corresponds to a gradient in soil mineral nutrient richness and base status with sites related to differences in soil pH, base cation concentrations, total content of nitrogen and tree densities (Table 16, Figs 262–273).

Of the variation in vegetation composition along the main ecocline (DCA axis 1), 94.38 % was explained at the between macro-plot scale. Like in the other reference areas, large conformity is found between the split-plot results at the between macro-plot level and the nonparametric Kendall's τ correlation coefficients. Thus, like in the other areas, the mineral nutrient status is regarded as the most important structuring factor for vegetation in Børgefjell.

Of the variation along the second ordination axis, 83.37 % is explained on the between macro-plot level. Soil moisture is a strong predictor of plot score at the between macro plot scale level, and this variable is also identified as strongly related to the axis by Kendall's τ. Fig. 263 shows that the six plots (plot 40 and all plots in macro plot 9) which are separated along DCA axis 2 by obtaining high scores (see Fig. 260) have lower soil moisture values than the nine plots with high DCA axis 1 scores and low DCA axis 2 scores (macro plot 6 and the remaining plots in macro plot 8). The variation in vegetation along this axis runs from plots dominated by *Dryopteris expansa* (Fig. 284) on moister soil to plots dominated among others by *Polygonatum verticillatum* (Fig. 290) and *An-*

thoxanthum odoratum (Fig 293) on slightly drier soils. Both *Dryopteris expansa* and *Polygonatum verticillatum* are typical of fern dominated, 'flushed' (cf. Malmström 1949, Dahl 1957) vegetation and the segregation along DCA axis 2 in the Børgefjell area may well only reflect idiosyncrasies of the specific macro plots.

Dividalen

The main vegetation gradient in the Dividalen reference area (DCA axis 1) runs from lichen-dominated dwarf-shrub communities with dominance by *Betula nana* (Fig. 335) and *Cladonia* spp. (Figs 394-403) via low fern and herb dominated communities with grasses to communities dominated by tall-herb species such as *Omalotheca norvegica* (Fig. 357), *Saussurea alpina* (Fig. 364) and *Trollius europaeus* (Fig. 368). Dividalen is the reference area with the highest total number of species.

The main vegetation gradient corresponds to a complex gradient which reflects soil mineral nutrient and base richness, running from soils poor in mineral nutrients (C, Ca, Mn, Na, S, Zn and total N), high organic content in the humus layer and low pH, to *vice versa*. Almost all variation along this compositional gradient is on the between macro plot scale level (96.72%). The agreement between results of split-plot analyses and Kendall's τ is good. No terrain variables explain significant amounts of variation along this main ecocline, perhaps because the macro plots are placed along a line transect up a hillside.

Also along DCA axis 2, most of the variation in plot positions (80.94 %) occurs on the between macro-plot level. Soil concentration of P is the strongest predictor (negatively) of plot position on the between macro-plot scale level. Kendall's τ between DCA axis 2 scores and P is also strong. Species typically occurring in plots with low P (high DCA axis 2 scores) are *Phyllodoce caerulea* (Fig. 340), partly also *Equisetum sylvaticum* (Fig. 347), *Pedicularis lapponica* (Fig 359), *Calamagrostis lapponica* (Fig. 371) and *Nephroma arcticum* (Fig. 404). However, variation along this axis also strongly reflects altitudinal differences ($\tau = 0.563$). Dividalen is the only reference area in which the plots span considerable elevational variation (385–615 m a.s.l., see Table 1). We interpret DCA axis 2 as mainly expressing variation in species composition in the study area that results from placement of macro plots along an altitudinal gradient. Temperature-dependent variation in species composition, due to altitudinal (and south-north) variation is one of the main regional ecoclines (Ahti et al. 1968, Pedersen 1990, Moen 1999, Bakkestuen et al. 2008). The variation in P concentrations along this coenocline may or may not represent a general trend or be due to variation within this particular reference area, for reasons so far not known.

MAIN COMPLEX-GRADIENTS IN (MIDDLE AND NORTH) BOREAL BIRCH FORESTS

The gradient in nutrient conditions

The importance of mineral nutrient availability as a main factor structuring vegetation gradients in boreal forests has been emphasized and documented by many authors (e.g. Dahl et al. 1957, Kuusipalo 1985, R. Økland & Bendiksen 1985, Sepponen 1985, Taylor et al. 1987, R. Økland & Eilertsen 1993, T. Økland 1996, R. Økland & Eilertsen 1996, R. Økland et al. 2001). The mineral nutrient and soil base richness complex gradient is thus considered to be the most important complex gradient for the structuring of vegetation in boreal forests. Birch forest ecosystems are expected to differ slightly, but fundamentally, from coniferous forest ecosystems in properties such as the somewhat more favourable chemical composition and/or rates of decomposition of deciduous versus evergreen coniferous litter (Aarrestad 2002, Fjellberg et al. 2007). This influences the rates of soil biological processes (Saetre 1998), physical soil properties such as texture, humus form and moisture retention capacity (Sirén 1955, Green et al. 1993), and the acidity status and availability of essential elements from soils (e.g. Wittich 1961, Saetre et al. 1997, Ewald 2000, Légaré et al. 2001, Qian et al. 2003, Liu et al. 2008). While in coniferous forests input of needle material occurs at more or less constant rates (Saetre 1998) and this material contributes to natural soil acidification, decomposing birch leaves instead contribute to soil improvement (Dimbleby 1952a, 1952b, Gardiner 1968, Miller 1984, Saetre 1998). Neverthless, a comparison of the reference area minimum, median and maximum pH values (Table 21) with those of T. Økland (1996, see Table 35) for monitoring reference areas in spruce forest, reveals no large differences in pH between birch and spruce forest. It should be noted, however, that the selection of reference areas in birch and spruce forests was not made in ways that make possible a *test* of this particular hypothesis.

Soil pH is highly correlated with main compositional gradient in all six areas and always among the three best predictors. Soil pH is thus the parameter which overall best reflects variation along the main vegetation gradient. This is in correspondence with the results obtained in spruce forest where pH contributes to the main coenocline in nine out of ten reference areas and is the variable most strongly correlated with the gradient in six of these (T. Økland 1996). Other studies also find pH to be the best variable in explaining variation along the main vegetation gradient (Sepponen 1985, Lahti & Väisänen 1987, Taylor et al. 1987, R. Økland & Eilertsen 1993, R. Økland et al. 2001, Aarrestad 2002). However, pH mainly structures the vegetation indirectly by influencing the soil fauna and the plant mineral nutrient availability (cf. Glømme 1932, Larcher 2003).

The relative importance of mineral nutrients concentrations and other variables that make up the nutrient complex-gradient are known to vary between different studies and sites. Soil pH, concentrations of nitrogen and exchangeable Ca are usually reported as important in boreal ecosystems (cf. Malmström 1949, Dahl et al. 1967, Kuusipalo 1983b, 1984, 1985, R. Økland & Eilertsen 1993, T. Økland 1996). The six birch forest reference areas show considerable variation with respect to which variables make up the main complex-gradient, although pH and Ca are almost invariably among the most important. The middle boreal and oceanic birch forest in Lund differs strongly from this main pattern, probably due to the modifying influence of climate, which is very different between Lund and the other reference areas situated in the north boreal zone and in more continental parts of Norway.

Concentrations of S are also correlated with the main vegetation gradient in all areas. Sulphur is, together with P, K, Ca and Mg, defined as one of the macro nutrients which are required in comparatively large amounts (Etherington 1982, Larcher 2003). Plants absorb S in the chemical form of sulphate, although there is some evidence that S-containing amino acids may also be assimilated (Larcher 2003). Sulphur accumulates in leaves and seeds and is an important component of protoplasma and enzymes. In industrial countries significant amounts of sulphur have been added to the soil through the precipitation over the last centuries (Anonymous 2006). H_2S released by waterlogged soils, lake mud and continental shelf sediments also supplies soil with S through natural rainfall, but this is assumed to contribute less than 10 % of the amounts due to industrial pollution (Etherington 1982, Mylona 1993). However, soil concentrations of S are by far not as strong predictors of vegetation gradients in spruce forest (T. Økland 1996) as found in birch forests in our study. The reason for this is still not understood.

Exchangeable concentrations of Ca in soil is highly positively related to the mineral nutrient complex gradient (and thus with pH) in four out of the six areas (Møsvatn, Åmotsdalen, Gutulia and Dividalen). Calcium was also positively related to pH and the main complex-gradient in Børgefjell, but less strongly than in the other four areas. Lund deviated from the other areas by having a negative relationship between Ca and pH and by showing a weak relationship between Ca and all complex-gradients. Most studies of boreal forest vegetation and soils reveal Ca as one of the most important predictors of variation in vegetation along a complex-gradient with soil base status as a central element (cf. Hesselmann 1937, Malmström 1949, Kussipalo 1983b, Taylor et al. 1987, T. Økland 1996). T. Økland (1996) does, however, find that in spruce forests with humid climates Ca and soil moisture co-vary along a different vegetation gradient. Hence T. Økland (1996) suggests that in a humid climate, Ca does not contribute to a 'normal' gradient in soil base status and mineral nutrient concentrations, like is typically the case in less humid areas. The results from birch forests largely agree with these observations. The two areas in which Ca is less strongly related with the main complex-gradient are also the two most humid areas (Lund and Børgefjell). Furthermore, concentrations of Ca are generally lower in Lund than in the other reference areas.

Calcium is an essential part of the plant cell wall structure which provides for normal transport and retention of other elements and general physical strength of the plant. Ca is believed to balance the effect of alkali salts and organic acids within the plant. Calcium is absorbed as Ca^{2+} ions and exists in a fine balance with magnesium and potassium in plants. Too much of any one of these three elements may cause deficiencies of either the other two (Larcher 2003).

Soil content of total nitrogen is highly related to the main mineral nutrient and soil base richness complex-gradient in four of the reference areas (Møsvatn, Åmotsdalen, Børgefjell and Dividalen), to some extent related to this complex-gradient in Gutulia and unrelated to it in Lund. Parallel variation in nitrogen and soil nutrient status and soil base richness along one main complex-gradient is typically found also in other studies in boreal forests (T. Økland 1996). In all reference areas pH and nitrogen are more or less strongly positively correlated. Nitrogen is usually considered as the most limiting resource in boreal forests (cf. Hesselmann 1937, Malmström 1949, Kussipalo 1984, Tamm 1991). Nitrogen is important for building up new material in plants (Kubin 1983), but also for the microbiological activity in the humus (Olsen 1990), as the microbes need nitrogen for their synthesis of organic matter (Kubin 1983). The strong correlation between total amounts of nitrogen and the main compositional gradient in boreal forests accords with other studies (e.g. T. Økland 1996, R. Økland et al. 2001). This study of birch forests thus lends support to the general notion that the total amount of available nitrogen is important for the species composition and hence a good indicator of the main complex-gradient.

Other elements that are highly correlated with the main complex gradient in all areas (except Lund), are potassium and manganese. These elements are also considered as macronutrients by Larcher (2003); both are important among others in regulation of water physiology of plants.

The gradient in soil moisture

Measured volumetric bulk soil moisture is a significant predictor of vegetation composition turnover in Lund (for the secondmost important ecocline represented by DCA axis 2), and partly also in Børgefjell (also DCA axis 2). These two reference areas are the most oceanic ones among the six areas included in this study. In the other four area no relationship between measured soil moisture and vegetation gradients is found in Møsvatn, Gutulia and Dividalen and a possible, weak, relationship is found in Åmotsdalen (but not at the $\alpha = 0.05$ level). The recorded relationship between measured soil moisture and vegetation gradients in birch forest is thus generally weaker than found in spruce-dominated forests where one of the main coenoclines (DCA 1 or DCA 2) are related to soil moisture in most areas (R. Økland & Eilertsen 1993, T. Økland 1996).

The importance of soil moisture as an important structuring factor in boreal forests is emphazised among others by Carleton & Maycock (1980), Bergeron & Borcard (1983), Kuusipalo (1983a), Lahti & Väisänen (1987), R. Økland & Eilertsen (1993) and T. Økland (1996). On a local scale the soil moisture gradient should in principle be assumed to be independent of the complex gradient in soil mineral nutrients and base status (R. Økland & Eilertsen 1993), but these ecoclines may locally or in part be correlated (Lahti & Väisänen 1987, Carleton 1990, T. Økland 1996). In spruce forest nutrient-rich sites are mainly mostly dry while moist sites almost invariably tend to be poor (T. Økland 1996). This is not in accordance with the results found for the studied birch forest reference areas, and may indicate that this result of T. Økland (1996) does not have general validity, not even for spruce forests.

The weak relationship between measured soil moisture and recorded coenoclines in many of the reference areas may be a result of the way soil moisture is measured. Several authors (R. Økland & Eilertsen 1993, T. Økland 1996 and R. Økland et. al 2001) have pointed out that species distributions may be related to moisture in several, principally different ways that are not captured by one type of measurement of soil moisture made at one particular time-point. In the background material for the new division of Norway into nature types, Halvorsen et al. (2008), recognise three ecoclines relevant to soil moisture in boreal forests, of which two are related to 'normal' water availability [spring influence, e.g. the difference between *topogenous* paludification, which occurs in small depressions with poor drainage and stagnant water, and *soligenous* paludification, which is favoured by a cold and humid climate and occurs on slopes where the terrain determines the speed and direction of water movement to flushed slopes with fern dominated vegetation, dependent on more constant supply of water, with springs at the end; and water saturation (paludification), which separates sites according to median ('normal') soil moisture]. The relationship between spring influence and water saturation is explained by Halvorsen (2008), among others by the 'water availability triangle' (Halvorsen 2008: Fig. 6). The third ecocline related to soil moisture and water availability is related to risk of extreme drought (R. Økland & Eilertsen 1993, Halvorsen et al. 2008).

The wettest sites (high water saturation) included in this investigation are paludified slopes with high abundance of *Sphagnum* species, such as *S. girgensohnii* and *S. quinquefarium*, and slopes with ferns such as *Phegopteris connectilis* and *Oreopteris limbosperma*. High abundance of *Sphagnum* only occurs in Lund and Gutulia*; S. girgensohnii* are found in Gutulia sample plots 17 and 26–29 and *S. quinquefarium* is abundant in Lund, macro plots 1 and 3–6. Small hepatics like *Cephalozia* and *Calypogeia* spp. in *Sphagnum* carpets, and *Oreopteris limbosperma*, only occurred in Lund (macro plot 7). Furthermore, variation related to risk of extreme drought is likely to be present in several of the areas. Drought-exposed sites are typically richer in *Cladonia* lichens, *Calluna vulgaris* and *Empetrum nigrum*; species that are tyipcal for one end of the *main* coenocline in several of the birch forest reference areas. The lack of any relationship between this variation in species composition and recorded soil moisture in these cases accords with R. Økland & Eilertsen (1993) who postulated the 'soil moisture deficiency hypothesis' to explain this variation, which was not related to among-plot differences in volumetric soil moisture in their study area. Insufficient sampling of variation in species composition related to soil moisture in the reference areas is a probable partial explanation for the poor relationship between coenoclines and soil moisture in some of the reference areas. Furthermore, volumetric bulk soil moisture, as measured in this study, does not only fail to reflect variation along all three moisture-related coenoclines but is also, in itself, vulnerable to variation in weather conditions at and around the time-point sampling takes place.

T. Økland (1996) finds in many spruce reference areas that soil moisture is related to a gradient from within gaps in the forest to sites below trees. Her study reveals drier soil below trees than in gaps between trees, and restriction of several species to the more moist sites in gaps between trees. This variation in soil moisture from below to between trees is explained as an effect of tree canopies (cf. R. Økland & Eilertsen 1993): (1) a strong gradient in throughfall precipitation (low close to tree stems), caused by canopy interception (C.O Tamm 1953, Beier et al. 1993); (2) stronger water uptake by trees close to stems (cf. Stålfelt 1937b) and large amounts of spruce litter, particularly close to stems, that give rise to a loose and thick humus which dries up rapidly after rainfall, due to a low capacity for retaining moisture (cf. Malmström 1937, Stålfelt 1937b). No such relationships are found in the birch forest reference areas. A likely explanation for this is that the shading effect of the tree layer is less important in birch forests than in spruce forests because the size and density of trees are usually lower in the birch forest. This tendency is likely to be strengthened towards the tree line as the influence of winds increase (R. Økland & Bendiksen 1985).

Disturbance and land use changes

Grazing and trampling by domestic animals (included domestic reindeer) have influenced and are still influencing the vegetation in all reference areas, to stringer or lesser extents. The reference areas Gutulia, Børgefjell and Dividalen are constantly influenced by reindeer grazing while Møsvatn and Åmotsdalen are influenced by cattle and sheep grazing. Lund is also to some extent influenced by sheep grazing. The species composition in these areas reflects the grazing (and trampling) pressure, but the extent to which this is the case is difficult to quantify. The most difficult part is to separate effects of grazing by domestic animals from natural dynamics in the reference areas. An experimental design, with enclosures in which the vegetation was protected from grazing, would have been a valuable reference for such influences. Miles & Kinnairs (1979) have shown that grazing may cause large mortality of birch saplings and that considerable rejuvenation took place in grazer exclosures. One the other hand, Pigott (1983) demonstrates that moderate grazing can promote germination of birch seeds.

Bakkestuen & Erikstad (2002) performed a comparative analysis of aerial photos from 1949 and 1987 in the Møsvatn area, revealing considerably lower summer farm activity in 1989, both in the reference area (birch forest) and in the mountain pasture area close by. Among others, they demonstrate that in 1989 paths were in the process of being overgrown, the forest had grown denser and the openings were smaller and fewer. Such changes in the land use over the last 50–100 years have certainly had, and still have, an impact on the vegetation (cf. Bryn & Daugstad 2001).

MAIN GRADIENTS AND VARIATION IN THE TOTAL DATA SET

Interpretation of main gradients in the total data set

Three different ordinations were performed: one on the total data set, another on the same data set with sample plots from the southernmost reference area Lund excluded, and one partial ordination of the latter data set with variation due to seven climatic/geographical variables partialled out. In the first of these ordinations all sample plots from Lund split off from the rest of plots along the first ordination axis. This ordination is thus not discussed in further detail here as it merely shows that the vegetation in Lund differs strongly from that of the other areas, underpinning the importance of variation along the two main regional (climatic) ecoclines; Lund belongs to another vegetation zone and another vegetation section (see Moen 1998).

The new ordination obtained after removal of sample plots from Lund revealed a first DCA ordination axis along which no segregation of plots from different areas occurred. More than 80 % of the variation in species composition along this axis is explained on the between macro-plot scale level while only approximately 5 % on the between-area scale level. This emphasises that generally applicable local environmental complex-gradients structure variation in vegetation in birch forests (at least within the same vegetation zone).

The corresponding DCA 1 axes in the ordination and in the partial ordination, in which variation due to climatic/geographical variables had been partialled out, are strongly correlated and correspondingly represent the ecoclines. Such similar patterns are exactly what T. Økland (1996) found in her data from spruce forests. This shows that within a relatively narrow range of vegetation zones and sections, boreal forest vegetation is structured by generally important local complex-gradients, the effect of which is considerably stronger than the effect of geographic distance as such.

Our results show that this local complex-gradient runs from sites with low pH and low content of mineral nutrients (low concentrations of macro nutrients like C, Ca, Mn, S and N) and high loss of ignition to *vice versa*.

The second ordination axis, related to soil concentrations of Mn and S, and with about one half of the variation explained at the between-area scale even in the partial ordination from which the effects of geographic/climated variables had been partialled out, is likely mostly to reflect inevitable variation in species composition between areas large distances apart (cf. Nekola & White 1999).

The proportion of unexplained variation was large. The large size of the data set partly contributes to this because the random variation in a vegetational data set increases with increasing size of a data set (cf. Smith & Urban 1988, R. Økland et. al 1990, R. Økland & Eilertsen 1994 & T. Økland 1996). Vegetational responses to environmental gradients and disturbances that occur at spatial scales below the sample plot size of 1 m^2, like fine-scale topography gradients (R. Økland et al. 2001), also contribute to the unexplained variation (see also R. Økland & Eilertsen 1994). The amount of explained vegetational variation in the total data sets from birch forests is of approximately the same magnitude as found by T. Økland (1996) for spruce forests.

Species with regional variation in response to main complex gradients

A few species, such as *Gymnocarpium dryopteris* and *Phegopteris connectilis*, show regional variation in response to the main environmental complex gradient underlying the main coenocline (the first ordination axis of the total data set and of separate ordinations of the different reference areas). Most notably, their amplitudes along the main ecocline differs between areas. These species occur on sites with lower pH and lower mineral nutrient concentrations in the humus in sites with a more humid climate compared to more continental sites, where they reach an optimum on sites with higher pH and higher nutrient concentrations. Correspondence between regional gradients and local environmental gradients has been recognised for a long time. Boyko (1947) refers to this as the geo-ecological law of distribution, which relates to similar concepts such as equivalence of sites (Loucks 1962, Vetaas 1992) and habitat constancy (Walter & Walter 1953, Miehe 1989z), or niche constancy (Ferrer-Castán & Vetaas 2003). A species may thus displace its distribution with respect to a measured environmental variable from one climatic region to another, if the measured variable and the condition of primary physiological importance are affected by climate (T. Økland 1996). In spruce forest even more species, like *Anemone nemorosa, Oxalis acetocella, Rubus saxatilis* and *Rhytidiadelphus squarrosus* agg., have been found to have such a pattern. However, the number of occurrences of these species in birch forest sample plots is too low to allow further discussion of the topic.

Both R. Økland & Bendiksen (1985) and T. Økland (1996) explain this change in optimum by postulating that high soil moisture compensates for lower pH and mineral nutrients contents in the humus layer in a humid climate. This may contradict Boyko's law which says that the amount of nutrients available for these species should be the same on sites where they occur, in the humid reference areas as well as in the more continental. However, in humid climate water flow rates through the humus are higher due to higher precipitation, which is expected to contribute to higher nutrient supplies and probably also higher turnover rates (Varskog 1995, T. Økland 1996). The access to nutrients may then be higher throughout the year despite the lower pH and nutrients measured at one point in time (see T. Økland 1996). Other explanations may also apply, e.g. that other environmental factors are important in different parts of regional gradients. In that case the premises for Boyko's geo-ecological law are not fulfilled.

COMPARISON WITH VEGETATION CLASSIFICATIONS

The driest and most oligotrophic part of the monitored vegetation can be assigned to the A1b type '*Cladonia-Betula pubescens* ssp. *czerepanovii* subtype' of the '*Cladonia* woodland' in Fremstad (1997). Slightly less 'dryish' vegetation accords with the A2c type, 'Va*ccinium vitis-idaea - Empetrum nigrum* coll. subtype' of the '*Vaccinium* woodland'. These types are more or less dominated by lichens and dwarf shrubs, and correspond more or less to the association Cladonio-Betuletum (Nordh.43) K.-Lund 73 and probably to Calamagrostio lapponicae-Pinetum K.-Lund 67 in the northernmost area, Dividalen. Lichen-dominated vegetation is represented in all analysed areas except Lund, and could probably be classified to the drier part of the subxeric topographic moisture series of R. Økland & Bendiksen (1985), due to high abundance of lichens and *Empetrum nigrum* ssp. *hermaphroditum* and the occurrence of *Arctostaphylos alpina*.

A few plots on moist and nutrient-poor soils in Åmotsdalen and Dividalen have a species composition similar to the A3b 'Mountain subtype' of the '*Calluna vulgaris-Vaccinium uliginosum-Pinus sylvestris* woodland' (Fremstad 1997), comparable with Barbilophozio-Pinetum Br.-Bl. et Siss. 39 em. K.-Lund 67 or the equivalent Empetro hermaphroditi-Betuletum tortuosae Nordh. 43 (Betuletum empetro-cladinosum). Characteristic species are *Betula nana, Calluna vulgaris* and *Vaccinium uliginosum*.

The majority of plots recorded from the monitoring areas represent medium dry and slightly mesic vegetation related to the A4c '*Vaccinium myrtillus-Empetrum nigrum* coll. subtype' of the 'Bilberry woodland' (Fremstad 1997), which occurs in all monitoring areas except Lund. This vegetation is comparable with the Myrtillio-Betuletum tortuosae Nordh. 43 (Betuletum myrtillo-hylocomiosum) K.-Lund 71. A few plots in the more termophilous lower parts of Gutulia, in south-eastern Norway, might also be classified to the A4a '*Vaccinium myrtillus* subtype' of the 'Bilberry woodland' comparable to Eu-Piceetum (Caj. 21) K.-Lund 62, sub-association myrtilletosum K.-Lund 81. This major part of the monitored vegetation definitively belongs to the submesic topographic series of R. H. Økland & Bendiksen (1985), due to the dominance of *Vaccinium myrtillus* and species such as *Maianthemum bifolium*, *Trientalis europaea* and *Solidago virgaurea*.

The vegetation of the south-western, humid area Lund is very different from that of the other monitoring areas, comprising both the A4b '*Vaccinium myrtillus-Cornus suecica* subtype' of the 'Bilberry woodland' and the A7c '*Molinia caerulea* subtype' of the 'Poor grassdominated woodlands' (Fremstad 1997). Less grass-dominated vegetation is comparable with Corno-Betuletum pubescentis Aune 73, probably sub-association myrtilletosum Aune 73, however without *Chamaepericlymenum suecicum*. The major part of the monitored vegetation has a species composition reflecting the submesic topographic-moisture series of R. Økland & Bendiksen (1985). However, grass dominated plant communities (*Molinia caerulea*) and tall fern plant communities (*Orepoteris limbosperma, Dryopteris expansa*) probably correspond to their mesic series.

Vegetation of the submesic series, characterized by small ferns (*Gymnocarpium dryopteris, Phegopteris connectilis*) and herbs (e.g. *Potentilla erecta, Rumes acetosa, Silene dioica, Oxalis acetosella*) occurs in monitoring plots mainly in the Møsvatn, Åmotsdalen, Børgefjell and Dividalen areas. Such more nutrient-rich submesic stands are also represented by a few plots in Gutulia. The vegetation can be assigned to the A5c 'Small fern mountain woodland subtype' of the 'Small fern woodland' (Fremstad 1997), comparable to Eu-Piceetum (Caj. 21) K.-Lund 62, sub-association dryopteridetosum K-Lund 81.

Slightly eutrophic submesic to mesic vegetation is only represented in the Møsvatn and Dividalen areas. The sites richest in mineral nutrients occurred on calcareous rocks in Dividalen. The associated, rather species-rich, vegetation can be assigned to the C2c 'Low herb subtype with scattered tall herbs' of the 'Tall herb, downy birch and Norway spruce forest' (Fremstad 1997), with species comparable with Salicetum geraniosum alpicolum Nordh.43 or Betuletum geraniosum subalpinum Nordh. 43. Characteristic species are *Geranium sylvaticum, Ranunculus acris, Saussurea alpine, Pyrola minor, Taraxacum* sp. and bryophytes such as *Mnium spinosum, Plagiomnium* ssp. and *Rhodobryum roseum*.

All reference areas have been more or less grazed by domestic animals. In some areas this has probably contributed to a more grass-dominated vegetation, similar to the A7b '*Deschampsia flexuosa* subtype' of the 'Poor, grass-dominated woodland' (Fremstad 1997). It is also possible that the vegetation on some of the herb and grass-dominated plots is partly a result of former scything, thus being comparable with the wooded grassland vegetation types described in Moen (1990) from scythed areas in boreal uplands in central Norway.

CONCLUSION

The main complex environmental gradient, and the variation in vegetation along this gradient, are more or less the same in birch forest areas all over Norway, and also the same as in coniferous forests. Some variation among areas do, however, occur with respect to which environmental variables that contribute to this main complex-gradient. Furthermore, this main ecocline interacts with regional climatic variation. The main complex gradient governing variation in species composition in all six reference areas was the gradient in mineral nutrient status and soil base richness, best expressed by pH and soil concentrations of Ca, K and S. Other contributing variables, like concentrations of Mn, P and total N in soil, vary to some extent in the strength of their relationship with the gradient between reference areas. The middle boreal birch forest of Lund deviate from this pattern, probably due to the climatic differences between this area and the other areas. Tree influence, topographic unfavourability, heat indices, soil moisture and soil depth may locally be related to the main ecocline.

Most of the variation in the vegetation in the studied birch forests occurs at the between macro-plot scale level, leaving small amounts of variation at the between-area and the between-plot within macro-plot scale level.

ACKNOWLEDGEMENTS

TOV, Terrestrial Monitoring of boreal birch forest ecosystems, is funded by the Directorate for Nature Management (DN). We especially want to thank Signe Nybø, our contact in DN, for many encouraging discussions and for important input to this work during many years. Thanks are also due to Else Løbersli (DN) and Ivar Myklebust (formely DN now Artsdatabanken), for many important contributions to TOV from programme initiation until present.

Substantial contributions to vegetation analyses in the field beside the authors have been given by Egil Bendiksen, Ingvar Brattbakk, Anders Often, Ellen Svalheim and Harald Taagvold. We also thank Bodil Wilmann for extensive work with the TOV data base and Erik Framstad, who through his coordinating position in TOV, has contributed in many ways. Special thanks are also given to Eli Fremstad, who was the coordinator of the vegetation studies in TOV during the first years. We are also grateful to Tonje Økland, who prepared the ground for this study through her work on spruce forests. Great thanks are also given to Rune Halvorsen who introduced us to this approach to vegetation ecology in boreal forests. He has also given us valuable input in the planning and writing process of this manuscript. We are also grateful to several previous and present colleagues at our institutes who in several ways have contributed to, or supported, our work. Thanks are also due to many other persons, too many to mention by names, who have contributed in some way, e.g. with logistic or technical support.

REFERENCES

Anderson, D.J., Cooke, R.C., Elkington, T.T. & Read, D.J. 1966. Studies on structure in plant communities. II. The structure of some dwarf-heath and birch-copse communities in Skjaldfannardalur, North-west Iceland. - J. Ecol. 54: 781-793.

Andreassen, K., Clarke, N., Røsberg, I., Timmermann, V. & Aas, W. 2006 Intensiv skogovervåking i 2005. Resultater fra ICP Forests Level 2 flater i Norge. Intensive forest monitoring in 2005. Results from ICP Forests Level 2 plots in Norway. - Viten fra Skog og landskap 04/2006.

Anonymous. 1998. GS+: geostatistics for the environmental sciences Version 2.1. - Gamma Design Software, Plainwell, Mich.

Anonymous. 1999a. ArcView GIS 3.2. - Environmental Systems Research Institute (ESRI) Inc., Redlands, California.

Anonymous 1999b. SPSS®Base 11.0 User's Guide. - SPSS Inc., Chicago.

Anonymous. 2004a. R Version 2.4.1 for Windows. URL: http://cran.r-project.org [The R foundation for statistical computing].

Anonymous. 2004b. R: a language and environment for statistical computing. URL: http://cran.r-project.org. [The R development core team, The R foundation for statistical computing].

Anonymous. 2006. Overvåking av langtransporterte forurensninger 2005 - Sammendragsrapport. - SFT rapport 957/2006, TA-2183/2006.

Abrahamsen, G., Horntvedt, R. & Tveite, B. 1977. Impacts of acid precipitation on coniferous forest ecosystems. - Wat. Air Soil Pollut. 8: 57-73.

Aune, B. 1993. Temperaturnormaler, normalperiode 1961-1990. - DNMI Rapp. 2: 1-63.

Aune, E.I. 1973. Forest vegetation in Hemne, Sør-Trøndelag, Western Central Norway. - K. Norske Vidensk. Selsk. Mus. Miscellanea 12: 1-87.

Auestad, I., Rydgren, K. & Økland, R.H. 2008. Scale-dependence of vegetation - environment relationships in semi-natural grasslands. - J. Veg. Sci. (in press).

Bakkestuen, V., Erikstad, L. & Økland, R.H. 2008. Step-less models for regional environmental variation in Norway. - J. Biogeogr. (in press).

- , Stabbetorp, O.E. & Eilertsen, O. 1999a. Terrestrisk naturovervåking. Vegetasjonsøkologiske undersøkelser av boreal bjørkeskog i Åmotsdalen, Sør-Trøndelag. - Norsk Inst. Naturforsk. Oppdragsmeld. 610: 1-43.

- , Stabbetorp, O. E. & Eilertsen, O. 1999b. Terrestrisk naturovervåking. Vegetasjonsøkologiske undersøkelser av boreal bjørkeskog i Møsvatn-Austfjell, Telemark. - Norsk Inst. Naturforsk. Oppdragsmeld. 611: 1-47.

- & Erikstad L. 2002. Terrestrisk overvåking. Metodeutvikling med fokus på arealdekkende modeller – analyse av detaljerte vegetasjonsdata og regionale miljøvariable. - Norsk Inst. Naturforsk. Oppdragsmelding 759: 1-35.

Bates, J.W. 1992. Mineral nutrient acquisition and rentention by bryophytes. - J. Bryol. 17. 223-240.

Beier, C., Hansen, K. & Gundersen, P. 1993. Spatial variability of throughfall fluxes in a spruce forest. - Environm. Pollution 81: 257-267.

Benum, P. 1958. The flora of Troms fylke. A floristic and phytogeographical survey of the vascular flora of Troms fylke in northern Norway. - Tromsø Mus. Skr. 6: 1-402.

Bergeron, Y. & Bochard, A. 1983. Use of groups in analysis and classification of plant communities in a section of western Quebec. - Vegetatio 56: 45-63.

Borcard, D., Legendre, P. & Drapeau, P. 1992. Partialling out the spatial component of ecological variation. - Ecology 73: 138-157.
Boyko, H. 1947. On the role of plants as quantitative climate indicators and the geo-ecological law of distribution. - J. Ecol. 35: 138-157.
Braak, C.J.F. ter 1986. Canonical correspondence analysis: a new eigenvector technique for multivariate direct gradient analysis. - Ecology 67: 1167-1179.
- 1987a. The analysis of vegetation-environment relationships by canonical correspondence analysis. - Vegetatio 69: 69-77.
- 1987b. CANOCO - a FORTRAN program for canonical community ordination by (partial) (detrended) (canonical) correspondence analysis, principal components analysis and redundancy analysis (version 2.1). - TNO Inst. Appl. Comp. Sci., Stat. Dept. Wageningen, Wageningen.
- & Prentice, I.C. 1988. A theory of gradient analysis. - Adv. ecol. Res. 18: 271-317.
- 1990. Update notes: CANOCO version 3.10. - Agricult. Math. Group, Wageningen.
- & Smilauer, P. 1998. - CANOCO Reference Manual and User's Guide to Canoco for Windows. Software for Canonical Community Ordination (version 4). - Centre for Biometry Wageningen, 1998.
- & Smilauer, P. 2002. - CANOCO Reference Manual and User's Guide to Canoco for Windows. Software for Canonical Community Ordination (version 4.5). - Centre for Biometry Wageningen, 2002.
Brattbakk, I. 1993. Terrestrisk naturovervåking. Vegetasjonsovervåking i Møsvatn-Austfjell. Norsk Inst. Naturforsk. Oppdragsmelding 209: 1-33.
- , Høyland, K., Halvorsen Økland, R., Wilmann, B. & Engen, S. 1991. Terrestrisk naturovervåking. Vegetasjonsovervåking 1990 i Børgefjell og Solhomfjell. - Norsk Inst. Naturforsk. Oppdragsmelding 91: 1-90.
- , Gaare, E., Fremstad Hansen, K. & Wilmann, B. 1992. Terrestrisk naturovervåking. Vegetasjonsovervåking i Åmotsdalen og Lund 1991. - Norsk Inst. Naturforsk. Oppdragsmelding 131: 1-66.
Braun-Blanquet, J. 1928. Pflanzensoziologie. - Springer Verlag, Berlin.
- 1965. Plant sociology: The study of plant communities. - Hafner, London.
Brown, D.H. & Bates, J.W. 1990. Bryophytes and nutrient cycling. - Bot. J. Linn. Soc. 104: 129-147.
Bryn, A. & Daugstad, K. 2001. Summer farming in the subalpine birch forest. In F.E. Wielgolaski (ed.) Nordic mountain birch ecosystem pp. 307-315. - UNESCO Man and Biosphere Series 27.
Carleton, T.J. 1990. Variation in terricolous bryophyte and macrolichen vegetation along primary gradients in Canadian boreal forests. - J. Veg. Sci. 1: 585-594.
- & Maycock, P.F. 1980. Vegetation of the boreal forest south of James Bay: Non-centered component analysis of the vascular flora. - Ecology 61: 1199-1212.
Conover, W.J. 1980. Practical nonparametric statistics. 2nd. ed. - Wiley, New York.
Crawley, M.J. 2002. Statistical Computing: An Introduction to Data Analysis using S-Plus. - John Wiley & Sons. pp. 761.
Dahl, E. 1957. Rondane. Mountain vegetation in South Norway and its relation to the environment. - Skr. Norske Vidensk. Akad. Mat.- Naturv. Kl. 1956: 1-374.
- 1986. Alpine - subalpine plant communities of South Scandinavia. - Phytocoenologia 15: 455-484.
- , Gjems, O. & Kielland-Lund, J. 1967. On the vegetation types of Norwegian conifer forest in relation to the chemical properties of the humus layer. - Meddr norske SkogforsVesen 25: 505-531.
Dargie, T.C.D. 1984. On the integrated interpretation of indirect site ordination: a case study using

semi-arid vegetation in south-eastern Spain. - Vegetatio 55: 37-55.
Dierschke, H. 1982. Pflanzensoziologie. Grundlagen und Methoden. - E. Ulmberg Verlag, Stuttgart.
Dimbleby, G.W. 1952a. The root sap of birch on a podsol. - Plant and Soil 4: 141-153.
- 1952b. Soil regeneration on the north-east Yorkshire moors. - J. Ecol. 40: 331-341.
Dons, J.A. & Jorde, K. 1978. Geologisk kart over Norge, berggrunnskart Skien 1 : 250000. - Norges geol. unders. (NGU).
- , Helm, M., & Sigmond, E.M.O. 1990. Frøystaul berggrunnskart 1514 I, 1:50000, foreløpig utgave. - Norges geol. unders. (NGU).
Eilertsen, O. & Pedersen, O. 1989. Virkning av nedveiing og artsfjerning ved DCA-ordinasjon av vegetasjonsøkologiske datasett. - Univ. Trondheim, Vitensk. mus. Rapp. bot. Ser. 1988-1: 5-18.
- Økland, R.H., Økland, T. & Pedersen, O. 1990. Data manipulation and gradient length estimation in DCA ordination. - J.Veg. Sci. 1: 261-270.
- & Brattbakk 1994. Terrestrisk naturovervåking. Vegetasjonsøkologiske undersøkelser av boreal bjørkeskog i Øvre Dividal nasjonalpark. - Norsk Inst. Naturforsk. Oppdragsmelding 286: 1-82.
- & Often, A. 1994. Terrestrisk naturovervåking. Vegetasjonsøkologiske undersøkelser av boreal bjørkeskog i Gutulia nasjonalpark. - Norsk Inst. Naturforsk Oppdragsmelding 285: 1-69.
- & Stabbetorp, O. E. 1997. Terrestrisk naturovervåking. Vegetasjonsøkologiske undersøkelser av boreal bjørkeskog i Børgefjell nasjonalpark. - Norsk Inst. Naturforsk Oppdragsmelding 408: 1-84.
- & Stabbetorp, O. 1997. Terrestisk naturovervåking: Vegetasjonsøkologiske undersøkelser av boreal bjørkeskog i Børgefjell nasjonalpark. Norsk Inst. Naturforsk. Oppdragsrapp. 408: 1-81.
Elkington, T.T. & Jones, B.M.G. 1974. Biomas and primary productivity of birch (Betula pubescens s. lat.) in south-west Greenland. - J. Ecol. 62: 821-830.
Etherington, J.R. 1982. Environment and Plant Ecolgy. - John Wiley & Sons. Chichester. England.
Evans, L.S. 1984. Botanical aspects of acidic precipitation. - Bot. Rev. 50: 449-490.
Ewald, J. 2000. The influence of coniferous canopies on understorey vegetation and soils in mountain forests of the northern Calcareous Alps. - Appl. Veg. Sci. 3: 123-134.
Falkengren-Grerup, U. 1986. Soil acidification and vegetation changes in deciduous forest in southern Sweden. - Oecologia 70: 339-347.
Falkengren-Grerup, U. & Lakkenborg-Kristensen, H. 1994. Importance of ammonium and nitrate to the performance of herb-layer species from decidous forests in southern Sweden. - Environm. exp. Bot. 34: 31-38.
Fenstad, G.U., Walløe, L. & Wille, S.Ø. 1977. Three tests for regression compared by stochastic simulation under normal and heavy tailed distribution of errors. - Scand. J. Statist. 4: 31-34.
Ferrer-Castán, D. & Vetaas, O.R. 2003. Floristic variation, chorological types and diversity: do they correspond at broad and local scales? - Divers. Distrib. Vol. 9. Issue 3: 221-235.
Fitje, A. & Strand, L. 1973. Tremålingslære, ed. 2. - Universitetsforlaget, Oslo.
Fjellberg, A., Nygaard, P.H. & Stabbetorp, O.E. 2007. Structural changes in Collembola populations following replanting of birch with spruce in North Norway. *In:* Effects of afforestation on ecosystems, landscape and rural development, pp. 119-125. Proceeding of the AFFORNORD conference, Reykholt, Iceland, June 18-22, 2005. TemaNord 2007/508.
Fremstad, E. & Elven, R. 1987. Enheter for vegetasjonskartlegging i Norge. - Økoforsk Utredning 1, 1987.
- & Sørensen, O.J. 1989. Floristiske og faunistiske undersøkelser i området Frihetsli-Njunis i Målselv. En konsekvensanalyse. - Norsk Inst. Naturforsk. Oppdragsmelding 3: 1-42.

- 1997. Vegetasjonstyper i Norge. - Norsk Inst. Naturforsk.temahefte 12: 1-279.
Framstad, E (ed.) 2008. Natur i endring. Terrestrisk naturovervåking i 2007: Markvegetasjon, epifytter, smågnagere og fugl. - Norsk Inst. Naturforsk. Rapport 362: 1-116 .
Frisvoll, A.A., Elvebakk, A., Flatberg, K.I. & Økland, R.H. 1995. Sjekkliste over norske mosar. Vitskapleg og norsk namneverk. - Norsk Inst. Naturforsk. Temahefte 4: 1-104.
Førland, E.J. 1993. Nedbørsnormaler, normalperiode 1961-1990. - DNMI Rapp. 39: 1-63.
Gardiner, A.S. 1968. The reputatin of birch for soil improvement. A litterature review. - Forestry Commision Research and development Paper 67. HSMO London.
Gauch, H.G. 1982. Multivariate analysis in community Ecology. Cambrigde University Press. Cambrigde.
Gigon, A. & Rorison, I.H. 1972. The response of ecologically distinct plant species to nitrate and to ammonium nitrogen. - J. Ecol. 60: 93-102.
Glømme, H. 1932. Undersøkelser over ulike humustypers amoniakk- og nitratprodusjon samt faktorer som har innflytelse på disse prosesser. - Meddr norske SkogforsVesen 4: 37-328.
Godal, J. B. & Hauge, K. 1964. Gutulia naturpark. Hovedoppgaver i naturvern. - Skogbruksavdelingen, NLH, Ås. Unpubl.
Grahn, O. 1977. Macrophyte succession in Swedish lakes caused by deposition of airborne acid substances. - Wat. Air. Soil. Pollut. 7: 295-306.
Green, R.N., Trowbridge, R.L. & Klinka, K. 1993. Towards a taxonomic classification of humus forms. - For. Sci. Monogr. 29: 1-49.
Haapasaari, M. 1998. The oligotrophic heath vegetation of northern Fennoscandia and its zonation. - Acta Bot. Fennica 135: 1-219.
Halvorsen, R. 2008. Begrepsapparat for vanntilgang: vannmetning, kildevannspåvirkning og torvdannelse. Naturtyper i Norge. Bakgrunnsdokument 6 (versjon 0.1): 44-48.
Halvorsen, R., Andersen, T., Blom, H.H., Elvebakk, A., Elven, R., Erikstad, L., Gaarder, G., Moen, A., Mortensen, P.B., Norderhaug, A., Nygaard, K., Thorsnes, T., Ødegaard, F. & Norderhaug, K.M. 2008. Naturtyper i Norge – Lokale basisøkokliner. - Naturtyper i Norge Bakgrunnsdokument 4 (versjon 0.1): 1-79 (www.artsdatabanken.no)
Hämet-Ahti, L. 1963. Zonation of the mountain birch forest in northernmost Fennoscandia. - Annls bot. Soc. zool.-bot. fenn. Vanamo 34: 1-127.
Heikkinen, R. 1991. Multivariate analysis of esker vegetation in southern Häme, S Finland. - Annls bot. Fenn. 28: 201-224.
Hesselman, H. 1926. Studier över barrskogens humustäcke, dess egenskaper och beroende av skogsvården. - Meddn St. SkogsförsAnst. 22: 169-552.
- 1937. Om humustäckets beroende av beståndets ålder och sammansättning i den nordiska granskogen av blåbärsrik *Vaccinium*-typ och dess innverkan på skogen föryngring och tilväkst. - Meddn St. SkogsförsAnst. 30: 529-716.
Hill, M.O. 1979. DECORANA - A FORTRAN program for detrended correspondence analysis and reciprocal averaging. Cornell University, Ithaca. New York, USA.
- & Gauch, H.G.J. 1980. Detrended correspondence analysis: an improvedordination technique. - Vegetatio 42: 47-58.
Hylen, G. & Larsson J.Y. 2007. The condition of Norwegian forests. Results from national surveillance 1989-2006. - Oppdragsrapport fra Skog og landskap 09/2007.
Ingelstad, T. 1973. Mineral nutrient requirements of *Vaccinium vitis-idaea* and *Vaccinium myrtillus*. - Physiol. Pl. 29: 239-246.
Kalstad, J. K. 1974. Samene og Dividalen. - In: Vorren, K.-D, pp. 91-98. - Norges nasjonalparker (Øvre Dividal). Luther Forlag, Oslo.
Kielland-Lund, J. 1972. Landskap og vegetasjon. - I: Borgos, G. & Elven, R. 1972. - Norges nasjo-

nalparker 4 (Femundsmarka og Gutulia): 72 - 144.
- 1973. A classification of Scandinavian forest for mapping purposes. - IBP i Norden 11: 173-206.
- 1981. Die Waldgesellschaften SO-Norwegians. - Phytocoenologia 9: 53- 250.
- 1994. Syntaxonomy of Norwegian forest vegetation 1993. - Physical Geography 24: 299-310.

Kause, G.H.M., Arndt, U., Brandt, C.J., Bucher, J., Kenk, G. & Matzner, E. 1986. Forest decline in Europe: development and possible causes. - Wat. Air Soil Pollution 31: 647-668.

Krill, A. G. 1987. Snøhetta berggrunnskart 1519 4, 1:50000. Foreløpig utg. – Norges Geol. Unders. (NGU) Unpubl.

Krog, H., Østhagen, H. & Tønsberg, T. 1994. Lavflora, 2. utg. Norske busk- og bladlav. - Universitetsforlaget, Oslo.

Kruskal, J.B. 1964a. Multidimensional scaling by optimizing goodness of fit to a nonmetric hypothesis. - Psychometrika 29: 1-27.
- 1964b. Nonmetric multidimensional scaling: a numerical method. - Psychometrika 29: 115-129.
- , Young, F.W. & Seery, J.B. 1973. How to use KYST, a very flexible program to do multidimensional scaling and unfolding. Bell Labs. Murray Hill, New Jersey, unpubl.

Kubin, E. 1983. Nutrients in the soil, ground vegetation and tree layer in an old spruce forest in Northern Finland. - Annls bot. Fenn. 20: 361-390.

Kussipalo, J. 1983a. Distribution of vegetation on mesic forest sites in relation to some characteristics of tree stand and soil fertility. - Silva fenn. 17: 403-418.
- 1983b. Distribution of vegetation on mesic forest sites in relation to some characteristics of the tree stand and soil fertility. - Silva fenn. 17: 403-418.
- 1984. Diversity pattern of the forest understorey vegetation in relation to some site characteristics. -Silva fenn. 18: 121-131.
- 1985. An ecological study of upland forest site classification in southern Finland. - Acta for. fenn. 192: 1-77.
- 1988. Dominance pattern with understorey bryophyte vegetation in southern boreal coniferous forest. In: Barkman, J.J. & Sykora K.V. (eds), pp 111-117. Dependent plant communities. - SPB Acad Publ. The Hague.

Laaksonen, K. 1976. The dependence on mean air temperature upon latitude and altitude in Fennoscandia (1921-1950). – Annls Acad. scient. fenn. Ser. A 3. Geol. Geogr. 119:1-19.
- 1979. Effective temperature sums and durations of the vegetative period in Fennoscandia (1921-1950). - Fennia 157: 2: 171-197.

Lahti, T. & Väisänen, R.A. 1987. Ecological gradients of boreal forests in South Finland: an ordination tests of Cajander's forest site type theory. - Vegetatio 68: 145-156.

Larcher, W. 2003. Physiological Plant Ecolgy. - Springer Verlag. Heidelberg. Germany. 1-513.

Lawesson, J.E., Eilertsen, O., Diekmann, M., Reinikainen, A., Gunnlaugsdottir, E., Fosaa, A.M., Carøe, I., Skov, F., Groom, G., Økland, T., Økland, R., Andersen, P.N., & Bakkestuen, V. 2000. A concept for vegetation studies and monitoring in the Nordic countries. - TemaNord 2000: 517. 1-124.

Légaré, S., Bergeron, Y., Leduc, A. & Paré, D. 2001. Comparison of the understory Vegetation in boreal forest types of southwest Quebec. - Can. J. Bot. 79: 1019-1027.

Lid, J. & Lid, D.T. 1994. Norsk flora. 6. Utgåve ved Reidar Elven - Det norske samlaget, Oslo.

Liu, H.Y., Økland, T., Halvorsen, R., Gao, J.X., Liu, Q.R. Eilertsen, O. & Bratli H. 2008. Gradient analyses of forests ground vegetation and its relationships to environmental variables in five subtropical forest areas, S and SW China. - Sommerfeltia (in press).

Løbersli, E. 1989. Terrestrisk naturovervåking i Norge. - Dir. Naturforv. Rapp. 1989: 1-98.
Loucks, O.L. 1962. Ordinating forest communities by means of environmental scalars and phytosociological indices. - Ecological Monographs 32: 137-165.
Malmström, C. 1937. Tönnerssjöhedens försökspark i Halland. Ett bidrag till kännedomen om sydvästra Sveriges skogar, ljunghedar och torvmarker. - Meddn St. SkogsförsAnst. 30: 323-528.
- 1949. Studier över skogstyper och trädslagsfåordelning inom Västerbottens län. - Meddn St. SkogsförsInst. 37: 1-231.
Miehe, G. 1989. Vegetation patterns on Mount Everest as influenced by monsoon and föhn. - Vegetatio 79: 21-32.
Miles, J. 1981. Effect of birch on moorlands. - Institute of Terrestrial Ecology, Cambridge, Great Britain. 1-18.
- Kinnaird, J.W 1979. Grazing: with paticular reference to birch, juniper and Scots pine in the Scottish highlands. - Scottish Forestry 33: 280-289.
- & Young, W.F. 1980. The effects on heathland and moorland soils in Scotland and northern England following colonization by birch (*Betula* spp.). - Bull. Ecol. 11: 233-242.
Miller, H.G. 1984. Nutrient cycles in birchwoods. - Proc. Roy. Soc. Edinburgh 85B: 83-96.
Minchin, P.R. 1987. An evaluation of the relative robustness of techniques for ecological ordination. - Vegetatio 69: 89-107.
- 1990. DECODA Version 2.01. - Dept. Biogeogr. Geomorph., Aust. Natn. Univ., Canberra.
Moen, A. 1990. The plant cover of the boreal uplands of central Norway. - Gunneria 63: 1-451. - 1998. Nasjonalatlas for Norge: Vegetasjon. - Statens kartverk, Hønefoss.
Mork, E. & Heiberg, H.H.H. 1937. Om vegetasjonen i Hirkjølen forsøksområde. - Medd. Norske Skogforsøksvesen 19: 615-684, 1 map, 1 pl.
Munch, J. S. 1974. Nordmennene og Dividalen. In: Vorren, K.-D, pp. 99-104. - Norges nasjonalparker (Øvre Dividal). Luther Forlag, Oslo.
Mylona, Sophia: Historical development of regional sulphur levels in Europe - Some preliminary results. 1993. - Miljøverndepartementet: Fagrapport nr. 42.
Nekola, J.C. & P.S. White. 1999. Distance decay of similarity in biogeography and ecology. J. Biogeogr. 26: 867-878.
Nordhagen, R. 1928. Die Vegetation und Flora des Sylenegebietes. I. Die Vegetation. - Skr. Norske Vidensk. Akad. Mat. Naturv. Kl. 1927: 1-88.
- 1943. Sikilsdalen og Norges fjellbeiter: en plantesosiologisk monografi. - Bergens museums skrifter; 22, Bergen.
Nystuen, J.P. 1979. Elgå, berggrunnsgeologisk kart 1719 II - M 1:50 000. - Norges geol. unders. (NGU) Unubl.
- & Trømborg, D. 1972. Berggrunn, løsavsetninger og landskapsformer. In: Borgos, G. & Elven, R. 1972, pp. 14-25. - Norges nasjonalparker 4 (Femundsmarka og Gutulia): Luther forlag, Oslo.
Odland, A., Bevanger, K., Fremstad, E., Hanssen, O., Reitan, O. & Aagaard, K. 1992. Fjellskog i Sør-Norge: biologi og forvaltning. - Norsk Inst. Naturforsk. Oppdragsmeld. 123: 1-90.
Ogner, G., Opem, M., Remedios, G., Sjøtveit, G. & Sørlie, B. 1991. The chemical analysis program of the Norwegian Forest Research Institute. - NISK, Ås. Unpubl.
Økland, R.H. 1990. Vegetation ecology: theory, methods and applications with reference to Fennoscandia. - Sommerfeltia Suppl. 1: 1-233.
- 1994. Reanalyse av permanente prøveflater i granskog i overvåkingsområdet Solhomfjell 1993. - Utredn. Dir. Naturforv. 1994: 5: 1-37.
- 1995. Population biology of the clonal moss *Hylocomium splendens* in Norwegian boreal spruce forests. I. Demography. - Journal of Ecology 83: 697-712.

- 2000. Population biology of the clonal moss *Hylocomium splendens* in Norwegian boreal spruce forests. 5. Consequences of the vertical position of individual shoot segments. - Oikos 88: 449-469.
- & Bendiksen, E. 1985. The vegetation of the forest-alpine transition in the Grunningsdalen area, Telemark, SE Norway. - Sommerfeltia 2: 1-224.
- & Eilertsen, O. 1993. Vegetation-environment relationships of boreal coniferous forests in the Solhomfjell area, Gjerstad, S Norway. - Sommerfeltia 16: 1- 254.
- & Eilertsen, O. 1994. Canonical correspondence analysis with variation partitioning: some comments and an application. - J. Veg. Sci. 5: 117-126.
- & Eilertsen, O. 1996. Dynamics of understory vegetation in an old-growth 18 boreal coniferous forest, 1988-1993. - J. Veg. Sci. 7: 747-762.
- , Økland, T & Rydgren, K. 2001. Vegetation-environment relationships of boreal spruce swamp forests in Østmarka Nature Reserve, SE Norway. - Sommerfeltia 29: 1-190.
- Bakkestuen, V. 2004. Fine-scale spatial patterns in populations of the clonal moss *Hylocomium splendens* partly reflect structuring processes in the boreal forest floor. - Oikos. 106: 565-575.

Økland, T. 1988. An ecological approach to the investigation of a beech forest in Vestfold, SE Norway. - Nord. J. Bot. 8: 375-407.
- 1990. Vegetational and ecological monitoring of boreal forests in Norway. I. Rausjømarka in Akershus county, SE Norway. - Sommerfeltia 10: 1-52.
- 1993. Vegetasjonsøkologisk overvåking av barskog i Gutulia nasjonalpark. - Norsk Inst. Jord-Skogkartlegging, Ås. Rapp. 6: 1-76.
- 1996. Vegetation-environment relationships of boreal spruce forest in ten monitoring reference areas in Norway. - Sommerfeltia 22: 1-349.
- , Bakkestuen, V., Økland, R.H. & Eilertsen, O. 2001. Vegetasjonsendringer i Nasjonalt nett-verk av flater for intensivovervåking i skog. - Norsk Inst. Jord- Skogkartlegging Rapp. 2001: 1-46.
- , Bakkestuen, V., Økland, R.H. & Eilertsen, O. 2004. Changes in forest understory vegetation in Norway related to long-term soil acidification and climatic change. - J. Veg. Sci. 15: 437-448.

Oksanen, J. 2007. Multivariate analysis of ecological communities in R: vegan tutorial, URL: http://cc.oulu.fi/~jarioksa/opetus/metodi/vegantutor.pdf, pp. 39.

Oksanen, J., Kindt, R., Legendre, P. & O'Hara, B. 2007. Package 'vegan' Version 1.9–13. URL: http://cc.oulu.fi/~jarioksa. -Univ.of Oulu, Oulu, Finland, pp.120.

Olsen, R. 1990. Mikrobielle prosesser i jord sett i forhold til skogens vekst og vitalitet. - Aktuelt Norsk Inst. Skogforsk. 5: 50-61.

Osland, L.M. 1974. Berggrunn. In: Vorren K.-D., pp. 15-20. - Norges nasjonalparker (Øvre Dividal). Luther Forlag, Oslo.

Palmer, M.W. 1993. Putting things in ever better order: the advantages of canonical correspondence analysis. - Ecology 74: 2215-2230.

Parker, K.C. 1988. Environmental relationships and vegetation associates of columnar cacti in the Sonoran desert. - Vegetatio 78: 125-140.

Pavlidis, T. 1982. Algorithms for graphics and image processing. - Springer-Verlag, Berlin.

Pedersen, O. 1988. Biological data program/PC. Version 1.01. Brukerveiledning. - VegeDataConsult, Oslo.

Pearson, K. 1901. On lines and planes of closest fit to systems of points in space. - Phil. Mag., 6. Ser 2: 559-572.

Peidano, M. & Moreno, G. 1989. The genus *Betula* (Betulaceae) in the Sistema Centra (Spain). -

Willdenowia 18: 343-359.
Pigott, C.D. 1983. Regeneration of oak-birch woodland following exclusion of sheep. - J. Ecol. 71: 629-646.
Ponge, J.-F. & Ferdy, J.-B. 1997. Growth of *Fagus sylvatica* saplings inan old-growth forests as affected by soil and light conditions. - J. Veg. Sci. 8: 789-796.
Qian, H., Klinka, K., Økland, R.H., Krestov, P. & Kayahara, G.J. 2003. Comparison of species composition and species density of understorey vegetation in the boreal *Picea mariana* and *Populus tremuloides* stands in British Columbia, Canada. - J. Veg. Sci. 14: 173-184.
Reuss, J.O., Cosby, B.J. & Wright, R.E. 1987. Chemical processes governing soil and water acidification. - Nature 329: 27-32.
Rydgren, K. 1994. Low-alpine vegetation in Gutulia National Park, Engerdal, Hedmark, Norway, and its relation to the environment. - Sommerfeltia 21: 1-47.
Saetre, P. 1998. Decomposition, microbial community structure, and earthworm effects along a birch-spruce soil gradient. - Ecology 79: 834-846.
- , Saetre, L.S., Brandtberg, P.-O., Lundkvist, H. & Bengtsson, J. 1997. Ground vegetation composition and heterogeneity in pure Norway spruce and mixed Norway spruce - birch stand. - Can. J. For. Res. 27: 2034-2042.
Scütt, P. & Cowling, E.B. 1985. Waldsterben, a general decline of forest in Central Europe: Symptoms, development and possible causes. - Pl. Dis 69: 548-558.
Sepponen, P. 1985. The ecological classification of sorted soils of varying genesis in northern Finland. - Communtnes Inst. For. Fenn. 129: 1-77.
Sigmond, E.M.O., Gustavson, M. & Roberts, D. 1984. Berggrunnskart over Norge. - Norges geol. unders.. Målestokk 1:1 mill.
Sirén, G. 1955. The development of spruce forest on raw humus sites in northern Finland and its ecology. - Acta for. fenn. 62: 1-408.
Smith, T.M. & Urban, D.L. 1988. Scale and resolution of forest structural pattern. - Vegetatio 74: 143-150.
Sokal, R.R. & Rohlf, F.J. 1995. - Biometry, 3. ed. Freeman, New York.
Sollid, J.L., Carlson, A.B. & Torp, B. 1980a. Trollheimen-Sunndalsfjella-Oppdal. Kvartærgeologiske kart 1:100000. - Univ. Oslo, Geografisk inst. Unpubl.
- , Carlson, A.B. & Torp, B. 1980b. Kvartærgeologiske kart 1:100000. Kort beskrivelse til kartet. - Norsk Geogr. Tidskr. 34: 177-189.
Stabbetorp, O.E., Bakkestuen, V., Eilertsen, O. & Bendiksen, E. 1999. Terrestrisk naturovervåking. Vegetasjonsøkologiske undersøkelser av boreal bjørkeskog i Lund, Rogaland. - Norsk Inst. Naturforsk. Oppdragsmeld. 609: 1-55.
Stålfelt, M.G. 1937a. Der Gasaustauch der Moose. - Planta 27: 30-60.
- 1937b. Die Bedeutung der Vegetation im Wasserhaushalt des Bodens. - Svenska Skogvårdsfören. Tidskr. 35: 161-195.
Tamm, C.O. 1953. Growth, yield and nutrition in carpets of a forest moss (*Hylocomium splendens*). - Meddn St. SkogsforskInst. 43: 1: 1-140.
- 1959. Stuclier over kliinatets huiniclitet i Sverige. - Kungl slrogshogsk slir. 32: 1-49.
- 1976. Acid precipitation: biological effects in soil and on forest vegetation. - Ambio 5: 235-238.
- 1991. Nitrogen in terrestrial ecosystems. Questions of productivity, vegetational changes, and ecosystem stability. - Ecol. Stud. 81: 1-116.
Tamm, O. 1959. Studier över klimaets humiditet i Sverige. - K. Skogshögsk. Skr. 32: 1-48.
Taylor, B.R., Carleton, T.J., & Adams, P. 1987. Understorey vegetation change in a *Picea mariana* chronosequence. - Vegetatio 73: 63-72.

Tonteri, T., Mikkola, K. & Lahti, T. 1990. Compositional gradients in the forest vegetation of Finland. - J. Veg. Sci. 1: 691-698.

Tørseth, K. & Semb, A. 1997. Deposition of major inorganic compounds in Norway 1992-1996. - Norsk Inst. Vannforsk. Rapp. 1997: 1-44.

Ulrich, B., Mayer, R. & Khanna, P.K. 1979. Deposition von Luftverunreinigungen und ihre Auswirkungen im Waldekosystem im Solling. - Schr. forst. Fak. Univ. Göttingen 58: 1-291.

Varskog, P. 1995. A study of the chemical composition of Norwegian forest soils with relation to climatic, pedological and edaphic factors. - Dr scient. Thesis, Univ. Trondheim, Trondheim.

Venables, W. & Ripley, B. 2002. Modern Applied Statistics with S-Plus. - Springer, New York, USA.

Vetaas, O.R. 1992. Gradients in field-layer vegetation on an arid misty mountain plateau in the Sudan. - J. Veg. Sci. 3: 527-534.

Vevle, O. 1986. Norske vegetasjonstypar. 3rd ed. - Nistås Forlag, Bø.

Vorren, K.-D. & Engelskjøn, T. 1974. Vegetasjon og flora. - Norges nasjonalparker (Øvre Dividal): 38-69.

Walter, H. & Walter, E. 1953. Einige allgemeine Ergebnisse unserer Forschungsreise nach Südwestafrika 1952/53: Das Gesetz der relativen Standortskonstanz; das Wesen der Pflanzengemeinschaften. - Berichte der Deutschen Botanischen Gesellschaft 66: 228-236.

Wielgolaski, F.E. 1997. Fennoscandian tundra. In: Wielgolaski F.E. (ed.), pp. 227-283. Ecosystems of the world 3. Polar and alpine tundra. - Elsevier, Amsterdam.

Wittich, W. 1961. Der Einfluß der Baumart auf den Bodenzustand. - Allg. Forst-Z. 16: 41-45.

Wittig, R. & Neite, H. 1985. Acid indicators around the trunk base of Fagus sylvatica in limestone and loess beechwoods: distribution pattern and phytosociological problems. - Vegetatio 64: 113-119.

Wold, O. 1989. Botaniske undersøkelser i Gutulia nasjonalpark 1988. - Fylkesmannen i Hedmark, Miljøvernavd. Rapp. 29: 1-32.

Aarrestad P.A. 2002. Vegetation-environment relationships of broad-leaved deciduous forests in Hordaland county, western Norway. - Ilicifolia 3: 1-90.

- , Bakkestuen, V., Stabbetorp, O.E. & Wilmann B. 2008. Vegetasjonsøkologiske undersøkelser av boreal bjørkeskog i Møsvatn 2007. In: Framstad, E (ed.) 2008. pp. 16-27. Natur i endring. Terrestrisk naturovervåking i 2007: Markvegetasjon, epifytter, smågnagere og fugl. - NINA Rapport 362.

Aas, Ø. 1989. Skoglige forhold i Gutulia nasjonalpark og i utvidelsesalternativene. - Fylkesmannen i Hedmark, Miljøvernavd. Rapp. 23: 1-41.

Aas, W., Tørseth, K., Solberg, S., Berg, T., Manø, S. & Yttri, K.E. 2002. Overvåking av langtransportert forurenset luft og nedbør. Atmosfærisk tilførsel, 2001. - St. Progm. Forurensn. Overvåking Rapp. 847: 1-156.